

Substitution Patterns
in and over Polymer Chains –
New Approaches for
Carboxymethyl Cellulose

Von der Fakultät für Lebenswissenschaften
der Technischen Universität Carolo-Wilhelmina

zu Braunschweig

zur Erlangung des Grades einer
Doktorin der Naturwissenschaften

(Dr. rer. nat.)

genehmigte

D i s s e r t a t i o n

von

Anne Adden

aus

Hannover

1. Referentin:	Professor Dr. Petra Mischnick
2. Referent:	Professor Dr. Henning Menzel
eingereicht am:	17.08.2009
mündliche Prüfung (Disputation) am:	04.12.2009

Druckjahr 2009

Acknowledgements - Danksagung

Die vorliegende Arbeit wurde von November 2005 bis Mai 2009 am Institut für Lebensmittelchemie der Technischen Universität Braunschweig im Arbeitskreis von **Prof. Dr. Petra Mischnick** angefertigt. Ich möchte ihr an dieser Stelle ganz herzlich für ihr Interesse, ihre Diskussionsbereitschaft und Unterstützung, die Möglichkeit an Tagungen teilzunehmen und die gute Arbeitsatmosphäre danken.

Prof. Dr. Henning Menzel danke ich für die Anfertigung des Zweitgutachtens und **Prof. Dr. Stefan Schulz** für den Prüfungsvorsitz.

Dr. Manfred Nimtz (HZI) und seinen Mitarbeiter/innen danke ich für das Aufnehmen von zahlreichen MALDI-TOF Massenspektren.

Prof. Dr. Bodo Saake (von-Thünen-Institut) und seinem Arbeitskreis danke ich für die HPAEC-Messungen und ganz besonders für die herzliche Gastfreundschaft.

Ich möchte auch **Dr. André Henrion** und **Rüdiger Ohlendorf** (PTB) für die Möglichkeit der CE-MS-Messungen, die Unterstützung und die nette Arbeitsatmosphäre danken.

Mein besonderer Dank gilt **Silke Lehmann**: nicht nur für Deine Beiträge zu dieser Arbeit und Deine große Hilfsbereitschaft, sondern vor allem für die sonnige Stimmung, den Trost bei Frust und die schöne Zeit!

Darüber hinaus danke ich auch **Annika Ulbricht** und **Tim Orth** für ihre Beiträge, die tolle Stimmung im Labor und die vielen Kekse.

Ich danke meinen Kolleginnen und Kollegen aus dem **Institut** für das gute Arbeitsklima und die Hilfsbereitschaft bei großen und kleinen Laborproblemen. Meinem **Arbeitskreis** danke ich für Rat und tatkräftige Unterstützung bei jeglichen Sorgen und natürlich für Sekt, Kuchen, Kaffee, Heidepark, Zoo...einfach die schöne Zeit mit Euch!

Meinen **Eltern** und meinem **Bruder** danke ich für Eure Unterstützung, dass Ihr mir immer den Rücken gestärkt habt und stets ein offenes Ohr habt. Meinen Freunden und meiner Familie danke ich für Ablenkung und Trost in stressigen Zeiten. Besonders meinem **Mann Roland** möchte ich dafür danken, dass Du immer für mich da bist und mir bei allen kleinen und großen Problemen zur Seite stehst – auch bei dieser Arbeit.

Content

1	Introduction	1
1.1	Cellulose	2
1.2	Cellulose ethers.....	5
1.3	Carboxymethyl cellulose (CMC).....	8
1.3.1	Applications	8
1.3.2	Synthesis	9
1.3.3	Properties of CMC in aqueous solution	11
1.4	Analysis of the substituent distribution	13
1.5	The substitution pattern in the glucosyl unit	15
1.6	Mathematical models	16
1.7	The substitution pattern along the polymer backbone	19
1.8	Analytical techniques in carbohydrate chemistry.....	22
1.8.1	Capillary Electrophoresis (CE).....	23
1.8.2	High pH Anionexchange Chromatography (HPAEC)	28
1.8.3	Gas Liquid Chromatography (GLC).....	30
1.8.4	Mass spectrometry (MS).....	31
2	Scope of the thesis.....	37
3	Monomer analysis of CMC.....	38
3.1	Complete acidic hydrolysis.....	38
3.2	CE-UV	40
3.3	HPAEC-PAD	47
3.4	GLC-FID after reduction to HEC.....	54
3.5	Comparison of the methods for monomer analysis	59
3.6	Comparison of the monomer distribution with statistical models	61
4	New approaches in oligomer analysis for CMC.....	68
4.1	Formation of chemically uniform products after degradation	68
4.1.1	Acetylation, propionylation, butyrylation of CMC after methanolysis	71
4.1.2	Methoxyacetylation after d_4 -methanolysis	80
4.1.3	Variations of the acylation process	86
4.2	Influences during MS measurement.....	88
4.2.1	Variations of the solvent	88
4.2.2	Fractionation by column chromatography.....	88
4.3	Accessibility during degradation: influence on the oligomer yield.....	94
4.3.1	Methoxyacetylation after hydrolysis.....	94
4.3.2	Investigation of the oligomer yield by LC-ELSD	97
4.3.3	Accessibility of CMC during methanolysis	99
4.4	Introduction of a permanently charged tag.....	104
4.4.1	Influence on the response in MS	104
4.4.2	Application to CMC hydrolyzates.....	109
5	Kinetic studies of the partial degradation of CMC.....	116
5.1	Kinetics of hydrolysis.....	119
5.1.1	Development of a CE-method for end group analysis	120
5.1.2	Composition of partially hydrolyzed CMC	122
5.1.3	Kinetics of the partial degradation	126
5.2	Kinetics of methanolysis	133
5.2.1	Time course study of methanolysis	134
5.2.2	Time course study of methanolysis with removal of DP >20	138

6	Summary	145
7	Zusammenfassung.....	149
8	Experimental.....	153
8.1	Chemicals	153
8.2	Instrumentation	155
8.2.1	Capillary Electrophoresis	155
8.2.2	ESI-Ion Trap-Mass Spectrometer	155
8.2.3	MALDI-TOF-MS (Helmholtz centre for Infection research, HZI)	156
8.2.4	HPLC-ELSD	156
8.2.5	GLC-FID	157
8.2.6	GLC-MS	157
8.2.7	HPAEC-PAD	157
8.2.8	ATR-IR	158
8.2.9	¹ H-NMR	159
8.2.10	Column chromatography	159
8.2.11	Ion exchange (triethylammonia salt)	159
8.2.12	Heating block	159
8.2.13	Lyophilization	159
8.3	Methods	160
8.3.1	Ion exchange to triethylammonium-(TEA)-CMC ^[79]	160
8.3.2	Hydrolysis	160
8.3.3	Reductive amination ^[109]	162
8.3.4	Labeling with Girard'sT reagent	162
8.3.5	Methanolysis	162
8.3.6	CMC monomer analysis with GLC-FID after reduction to HEC	163
8.3.7	Acetylation, propionylation, butyrylation	164
8.3.8	Methoxyacetylation	165
8.3.9	Cellooligomer standards for LC-ELSD	168
8.3.10	Methoxyacetylation after hydrolysis	169
8.3.11	Fractionation	171
8.3.12	Time course study of methanolysis	172
9	References	174
10	Appendix	185

Abbreviations and Acronyms

ABA	4-aminobenzoic acid
ABN	4-aminobenzonitrile
Ac	acetyl-
AGU	anhydro glucose unit
ANTS	8-aminonaphtalene-1,3,6-trisulfonic acid
aq	aqueous
ATR-IR	Attenuated Total Reflection Infrared Spectroscopy
au	absorbtion units
BGE	background electrolyte
CE	Capillary Electrophoresis
CEC	carboxyethyl cellulose
CHCA	α -cyano-4-hydroxycinnaminic acid
α_i	molar fraction of <i>i</i> -fold substituted AGU
CID	Collision Induced Dissociation
CMC	carboxymethyl cellulose
CMS	carboxymethyl starch
CRM	Charge Residue Model
CZE	Capillary Zone Electrophoresis
DAD	Diode Array Detector
DEAE	2-diethylaminoethyl
DMAc	<i>N,N</i> -dimethylacetamide
DMF	<i>N,N</i> -dimethylformamide
DMSO	dimethyl sulfoxide
DP	Degree of Polymerization
DS	Degree of Substitution
ECR	Effective Carbon Response
EDC	1-ethyl-3-(3-dimethyl-aminopropyl) carbodiimide
ELSD	Evaporative Light Scattering Detector
EOF	Electroosmotic Flow
eq	equivalents
ESI	Electrospray Ionization
FID	Flame Ionization Detector
Fig.	figure

FTIR	Fourier Transform Infrared Spectroscopy
GLC	Gas Liquid Chromatography
glc	glucose
H-CMC	carboxymethyl cellulose, free acid form
HEC	hydroxyethyl cellulose
HPAEC	High pH Anion Exchange Chromatography
HPC	hydroxypropyl cellulose
HPLC	High-performance Liquid Chromatography
HPMC	hydroxypropylmethyl cellulose
I.D.	internal diameter
IEM	Ion Evaporation Model
IR	Infrared Spectroscopy
IT	Ion Trap
m/z	mass to charge ratio
mal	maltose
MALDI	Matrix-Assisted Laser Desorption/Ionization
MC	methyl cellulose
MCA	mono-chloroacetic acid
Me	methyl-
MEKC	Micellar Electrokinetic Chromatography
MS	Mass Spectrometry
MWCO	molecular weight cut-off
NMR	Nuclear Magnetic Resonance
O.D.	outside diameter
OHP	Outer Helmholtz Plane
p.s.i.	pounds per square inch
PAD	Pulsed Amperometric Detection
PEG	polyethylene glycol
QqQ	triple quadrupole mass analyzer
r.t.	room temperature
SEC	Size Exclusion Chromatography
SEM	Scanning Electron Microscopy
s_i	Mol fraction of an AGU substituted in position(s) i
T	temperature

t	time
Tab.	table
TEA	triethylamine
TFA	trifluoroacetic acid
THF	tetrahydrofuran
TLC	Thin Layer Chromatography
TMSH	trimethylsulfonium hydroxide
TOF	Time-of-Flight
tol	<i>p</i> -toluidine
UV	ultra violet
x_i	partial DS-value in position <i>i</i>
xyl	xylose
ZZuIV	Zusatzstoff-Zulassungsverordnung
δ	bending vibration
ν	valency vibration

1 Introduction

Cellulose is the most abundant biopolymer on earth, produced by plants to be the structural basis of their cell wall. The importance of cellulose-based materials in the world economy is well known, about 10^{11} to 10^{12} tons of these are produced annually ^[1].

We are in contact with this glucose polymer not only through textiles and paper, but also through an increasing variety of application. The application of cellulose itself is limited due to its insolubility in water, but its water soluble derivatives, in particular cellulose ethers, play an important role in our daily life that we often are not aware of. They are used as thickening agents in toothpaste, as stabilizers in ice-cream, as retardants in building applications like plasters and paints, as film formers, and drug-delivery pharmaceuticals, to name just a few. In many cases the amount of cellulose ether required is only between 0.02 and 2 %, but this small level is often crucial for the properties of the product ^[2].

Furthermore, they are renewable and biodegradable, leading to less strain in the environment. Environmental requirements have become of great interest in today's society with the need to ease the consumption of petroleum-based polymers.

For its application, it is necessary to control the physicochemical properties of modified cellulose, such as the water solubility, thickening ability or gelation behaviour. Amongst others, these properties are determined by the manufacturing process. Since this may vary and cellulose is a natural product, the correlation between manufacturing and final properties is not entirely understood. There is thus a great interest in the development of new pathways for the analysis of cellulose derivatives.

Cellulose structure, derivatization reactions, and possible applications of the obtained cellulose ethers are briefly described in the following chapters 1.1 to 1.4. The state of instrumental analysis for polysaccharides in general and cellulose ethers in particular is outlined in chapter 1.8.

1.1 Cellulose

Cellulose was first described by *Payen* as a material being resistant to the extraction of plants with water, ethanol or ether. In elemental analysis he found the composition of 44.4 % C and 6.2 % H, and thus concluded the formula $(C_6H_{10}O_5)_n$ and the isomerism to starch in 1842 ^[3].

Cellulose consists of D-Glucose, forming β -(1 \rightarrow 4) glucopyranosidic linked chains by condensation. Through rotation of every second anhydroglucosyl unit (AGU) for about 180 °, cellobiose as elementary repeating unit (Fig. 1-1) is formed. This allows the glucan chain to assume a flat, ribbon-like structure.

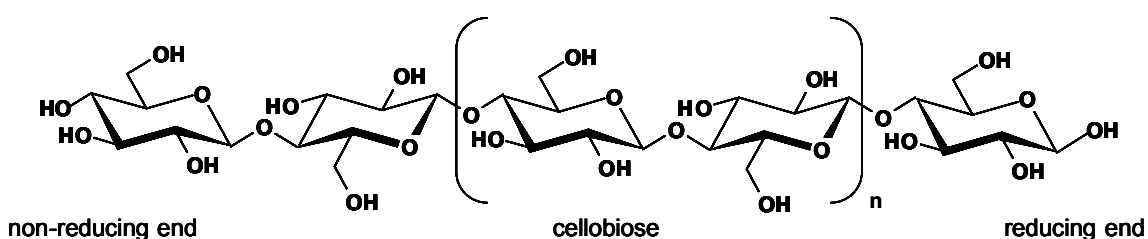


Fig. 1-1 Molecular structure of cellulose

The concept that cellulose is a linear macromolecule of anhydroglucosyl units could be verified in the late 1920s. Its structure has mainly been cleared by *Staudinger* ^[4], the chain-like constitution was discussed during the same time both by *Freudenberg* ^[5] and *Herzog and Jancke* ^[6,7].

Each AGU comprises three free hydroxyl groups that can undergo further reaction: at position O-2, O-3, and O-6 (Fig. 1-2). Due to the high molecular mass of cellulose, end groups are usually neglected as reaction sites. Cellulose is a high-molecular mixture of chains with different lengths with an average degree of polymerization (DP) between 1000 and 14000 AGU (M_w of 160 to 2400 kDa), depending on source and pretreatment.

In the 1960s and 70s, X-ray crystallography and NMR-studies proved that the conformation of each glucosyl unit is the thermodynamically more stable 4C_1 ^[8-10]. At this conformation, all hydroxyl groups are ordered equatorial thus minimizing their interaction (Fig. 1-2).

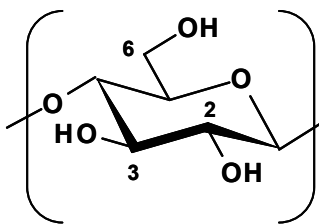


Fig. 1-2 Reaction sites in the anhydroglucosyl unit (AGU): O-2, O-3, and O-6

Native cellulose consists of crystalline and amorphous regions, leading to a structure that can be considered as fringed fibril ^[11-13] as shown in Fig. 1-3.

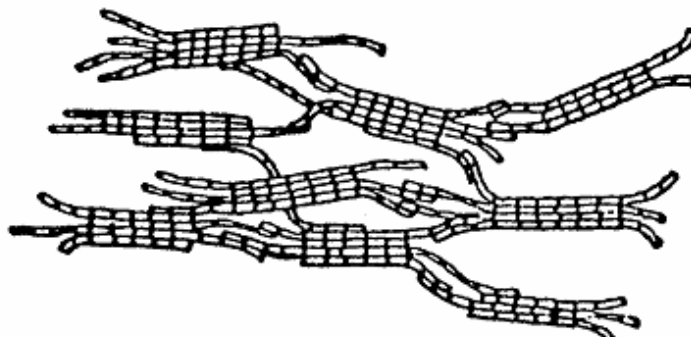


Fig. 1-3 Fringed fibril structure of native cellulose ^[13]

Depending on its source, the crystallinity of native cellulose varies between 50 and 90 % ^[14]. Two crystalline phases co-exist on the molecular level, the tricline I_{α} - and the monocline I_{β} -cellulose, with the latter one being thermodynamically more stable ^[15,16]. The orientation of the polymer chains in the unit cell is parallel, i.e., the reducing ends on one, the non-reducing ends on the other side ^[17] (Fig. 1-4). The chains ordered with the grain form the b-axes. In a-axes direction, intermolecular hydrogen bonds occur while in c-axes direction, hydrophobic interactions exist. Inter- and intramolecular hydrogen bonds are primarily formed between the hydroxyl group on C-3 and the pyranose ring oxygen of the adjacent AGU, but also between O-2 and O-6 of the directly neighboured monomer ^[18,19] (Fig. 1-4). These hydrogen bonds are formed exclusively within a layer of the cellulose unit cell, but not amongst the layers and they are responsible for the rigidity of the cellulose molecule.

Cellulose is the structural basis of the plant cell wall and its principal component. The purity of cellulose depends on its source and can vary significantly from the rather pure form in cotton (95 %) to the more complex mixture in wooden plants, where it

has a mass amount of about 40 to 50 % and is accompanied by other polysaccharides in the cell wall.

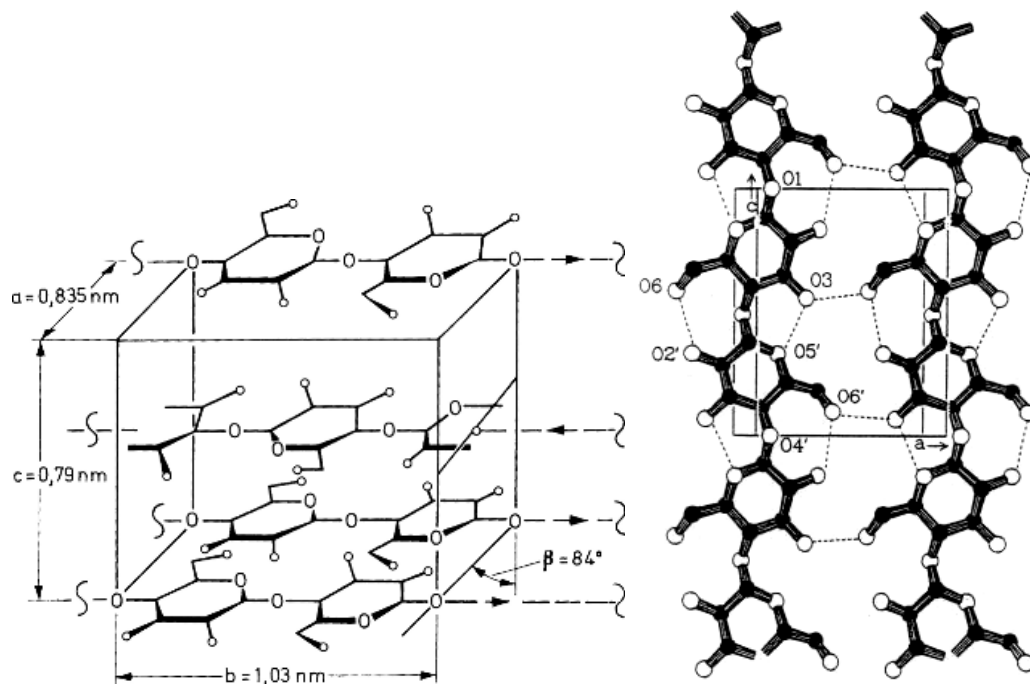


Fig. 1-4 Left: Unit cell of I_{β} -cellulose ^[20]; Right: Structure of cellulose I, intra- and intermolecular hydrogen bonds are indicated as dashed lines

Hemicelluloses are cell wall polysaccharides that are not solubilized by hot water, but by aqueous alkali ^[21].

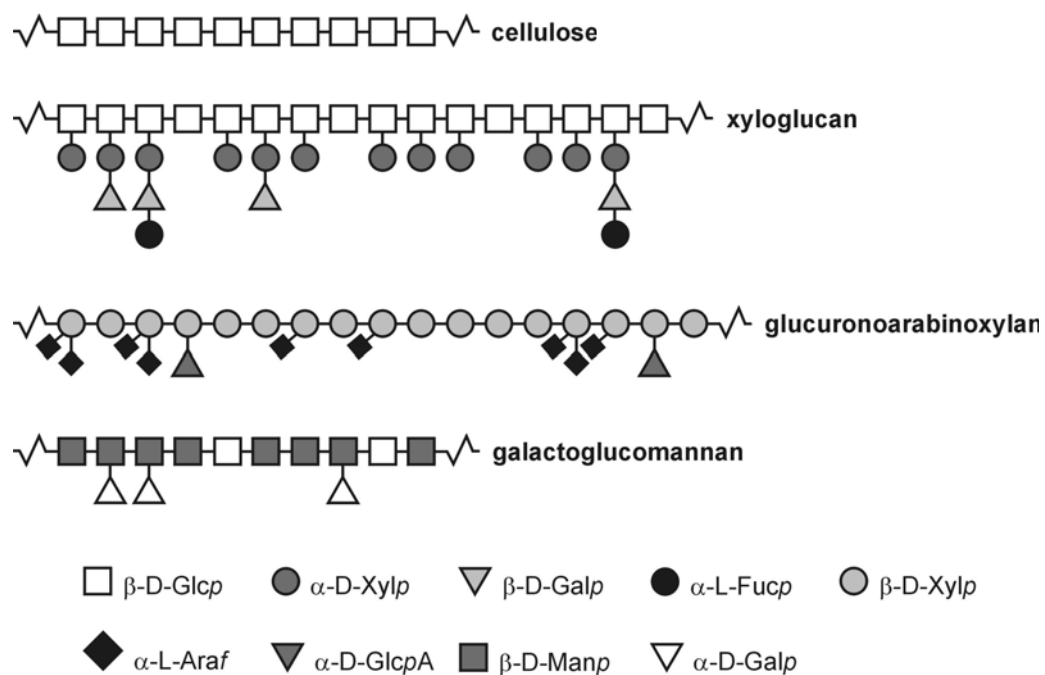


Fig. 1-5 Schematic structures of cellulose and hemicelluloses ^[22]

They are structurally homologous to cellulose in the way, that they also have a backbone composed of β -(1 \rightarrow 4)-linked pyranosyl residues of glucose, mannose, or xylose (Fig. 1-5) but unlike cellulose they are usually branched ^[22]. The structural similarity between cellulose and hemicelluloses facilitates a strong, non-covalent association of the hemicellulose- with cellulose-microfibrils. The amounts of hemicelluloses and lignin in the wooden cell wall range between 25 and 30 %, respectively ^[23]. For further use in industrial applications, the wooden matrix needs to be broken up in a pulping process that also degrades and dissolves the accompanying lignin and hemicelluloses ^[24]. Two processes are commonly used for pulping: the sulfate- and the sulfite-method. Both methods operate with high pressure (5-10 bar) and high temperature (140-180°C). During the sulfite-process, hydrogensulfite solution is used; its pH values may vary between 2 and 11. Due to those harsh conditions a degradation of the chains occurs, whether by acid hydrolysis or by alkaline “peeling”-reactions. Alkaline chain degradation ends with the formation of carboxylic end groups ^[25,26]. The amount of carbonyl- and carboxyl groups resulting from the pre-treatment in paper pulp has an influence on the stability of the resulting paper and strongly varies. Up to 1800 $\mu\text{mol/mol}$ cellulose have been found in paper pulp. *Potthast* and *Rosenau* developed very sensitive methods enabling quantification of even low amounts of carbonyl- and carboxyl groups by fluorescence labeling ^[27-30].

Commercial purified cellulose supplies an annual world consumption of about 150 million tons of fibrous raw material. Thereof, 100 million tons derived mostly from pulped wood, are converted to paper; about 12 million tons, mostly from cotton, are used for textiles and 7 million tons are chemical-grade cellulose ^[31]. In 2003, about 3 million tons were used for chemical modification resulting in functional polysaccharides applied for various purposes ^[32].

1.2 Cellulose ethers

The manufacture of cellulose ethers was first published by *Suida* ^[33] in 1905 and the first patents relating to their industrial production were issued in 1918 ^[34]. In the 1920s and 30s, carboxymethyl cellulose (CMC) was the first cellulose ether to gain economic significance, followed by methyl celluloses (MC) and hydroxyethyl cellulose (HEC). These three product categories and their mixed derivatives such as

methylhydroxyethyl (MHEC) or methylhydroxypropyl cellulose (MHPC) still dominate the market today ^[2].

The three free hydroxyl groups in the cellulose AGU, which vary in their reactivity, can be etherified which is a polymer-analogous reaction. Thereby, the origin of the used cellulose and its quality are crucial in regard to the ultimate properties of the product as they determine amongst others the average chain length, hence the viscosity yield of the final cellulose ether. Therefore, many different types of cellulose obtained from wood pulp or cotton linters are used. The chain length is reduced due to the chemical and thermal stresses during the manufacturing process.

Before etherification, inter- and intramolecular hydrogen bonds need to be broken. Therefore, cellulose is treated usually with sodium hydroxide solution (caustic soda) to obtain a sufficiently swollen material that is accessible for further reactions, known as alkali cellulose or soda cellulose. During this activation process, several properties of the end product are predetermined, since the degree of swelling and the homogeneity of the activation influence the distribution of the substituents introduced in the next step of cellulose ether production.

After activation, the etherifying reagent is added. In principle, any etherification known in the context of low-molecular alcohols could be applied ^[35].

In industrial production two basic types are established: reactions that consume sodium hydroxide solution (Williamson ether synthesis) and alkali-catalyzed additions of epoxides (alkoxylation), the reaction schemes are shown in Fig. 1-6.

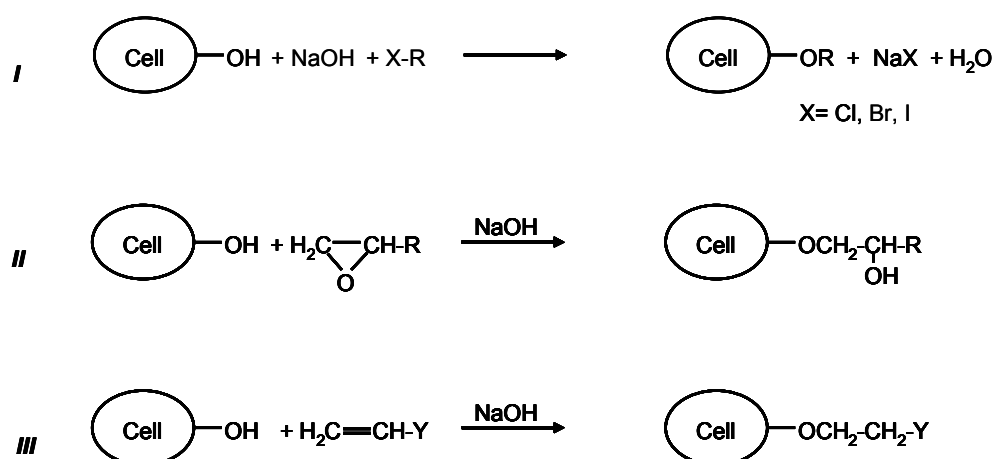


Fig. 1-6 Basic reactions in cellulose etherification; I: alkali consuming Williamson Etherification, II: alkali catalyzed alkoxylation, III: alkali catalyzed addition
Y = electron withdrawing group

The alkali catalyzed addition to activated double bonds, e.g. acrylonitrile, technically does not play an important role ^[2].

On laboratory scale, several other cellulose ether preparations are reported in literature, such as homogeneous etherification in DMAc/ LiCl ^[36,37].

Cellulose ethers are nontoxic, white to yellowish powders or granules and most of them are water-soluble.

The most important properties of cellulose ethers such as thickening of aqueous solutions, stabilization of suspensions or emulsions, water retention, film formation or adhesiveness determine their applications. Further special properties include thermogelation, surfactant action, foam stabilization, or thixotropy. Tab. 1-1 shows the common industrial cellulose ethers and their main applications.

In pharmaceutical application, hydrophilic swellable polymers are widely used to control the release of drugs from matrix formulations ^[38,39]. A zero-order release of the active ingredient is desired as it enables a constant therapy and less substance is needed. Cellulose ethers such as MC, hydroxypropylmethyl cellulose (HPMC), hydroxypropyl cellulose (HPC) and CMC have gained popularity in the formulation of oral hydrophilic matrices due to their swelling properties. Additionally, cellulose ethers have good compression characteristics such that they can be directly compressed to form sustained release swellable matrices ^[40].

Tab. 1-1 Major fields of application for common industrial cellulose ethers ^[2]

carboxymethyl cellulose	methyl cellulose, hydroxyalkyl methyl cellulose	hydroxyethyl cellulose	hydroxypropyl cellulose
paper	tile adhesives	latex paints	adhesives
detergents	plasters/ renders	adhesives	ceramics
drilling for oil and gas	pharma/ cosmetics	building materials	cosmetics
pharma	joint compounds	cosmetics	encapsulation
cosmetics	wallpaper paste	drilling for oil and gas	food
textile industry	polymerization	agriculture	household goods
food	food	paper	printing inks
coatings	latex paints	synthetic resins	polymerization
encapsulation	cement extrusion	textile industry	films

1.3 Carboxymethyl cellulose (CMC)

With a production of approx. 230 000 tons p.a., CMC is the economically most important cellulose ether^[2]. Commercial CMCs are produced with a degree of substitution (DS) between 0.2 and 1.5. The structure is displayed in Fig. 1-7.

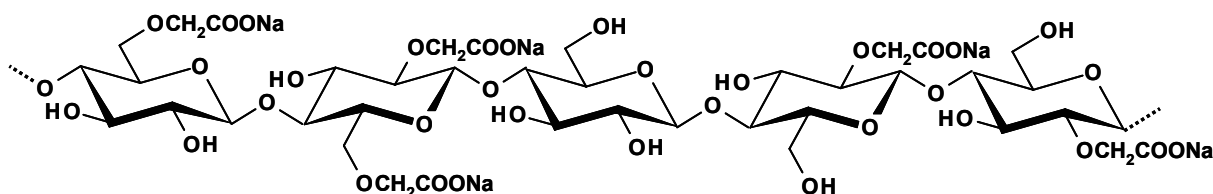


Fig. 1-7 Molecular structure of carboxymethyl cellulose (Na salt, NaCMC)

1.3.1 Applications

CMC is applied in various levels of purity. “Unpurified” CMC, used for technical applications up to “highly purified” CMC for pharmaceutical- and food-grade applications are commercially available (Tab. 1-2).

Tab. 1-2 Carboxymethyl cellulose (CMC) grades and typical applications^[41]

Quality	Examples of application areas	Content of CMC [%]	Content of salts [%]
technical	detergents, mining floating	< 75	> 25
semi-purified	oil and gas drilling muds	75 – 85	15 – 25
purified	paper coating, textile sizing and printing, ceramic glazing	> 98	< 2
extra purified (cellulose gum)	food, toothpaste, pharmaceuticals	> 99.5	< 0.5

In its initial application, CMC is used as soil carrier and redeposition inhibitor in detergents as anionic dirt particles are repelled by the anionic charges of the dissociated CM-group. It is used in deep-well drilling as flotation aid in drilling mud. Purified products are used in surface coatings and e.g. in paper industry due to the affinity of CMC to cellulose for coatings and pulp sizing to improve fiber retention, filler/pigment/dye yield as well as paper strength. CMC also improves the printability and smoothness of paper. Together with gelatine CMC is used as a coacervate to encapsulate ink in the production of non-carbon copy papers.

Building applications use its high water retention. CMC stabilizes e.g. aqueous solutions of clay and helps control adhesion by providing bonding strength and improves workability.

In cosmetics and pharmaceutical industries extra purified grades are used for instance as fat-free ointment base or as tablet filling matrix. Mixed esters of CMC like CMC acetate butyrate (CMCAB) showed zero-order release of the active component when used as filling matrix for drug-delivery agents ^[42].

In food-grade purity, NaCMC is commonly known as “cellulose gum” or as food additive E 466. In Europe, its use is regulated by law. By the order EG 178/2002 of the Parliament and the Council of Europe the regulations for food, animal feed, and food contact materials, and consumer products in the European Union are defined. The German implementation of this European regulation is the “Lebensmittel- und Futtermittelgesetzbuch, LFGB”. Based on the LFGB, the “Zusatzstoff-Zulassung-Verordnung (ZZuIV)” regulates the use of food additives hence the use of CMC. In annex 4 to §§ 5.1 and 7 ZZuIV the terms for the application of CMC in food are regulated. Though no maximum permissible quantities are named (“quantum satis”), its use is restricted to certain applications. An addition of CMC is forbidden e.g. for honey, butter or minced meat.

In food applications, CMC improves consistency, and emulsion stability and controls and provides e.g. freeze-thaw stability of deep-frozen products. CMC is neither digested nor resorbed in the human intestinal tract ^[43].

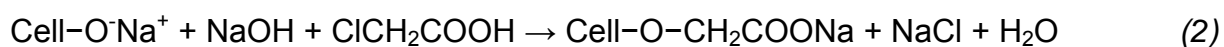
1.3.2 Synthesis

Cellulose derivatization in industrial scale is a heterogeneous process. CMC is produced in a Williamson ether synthesis from alkali cellulose with monochloroacetic acid (MCA) or its sodium salt (NaMCA) in an aqueous or aqueous-alcoholic medium (slurry).

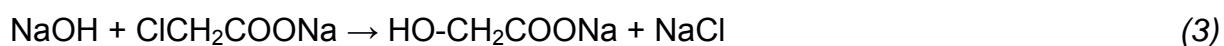
In practice, the manufacture of CMC involves two reaction steps. First, cellulose is treated with NaOH (1). This activation (mercerisation) is of immense importance, as it modifies and widens the crystalline structure of cellulose. The hydrogen bonds are partially broken and the AGUs become more easily accessible to the nucleophile.



This so-called alkali cellulose is now accessible for MCA, which is added in the second step (2)



As a side reaction, hydrolysis of MCA occurs (3), forming glycolate and sodium chloride and hydrochloric acid, respectively.



The first continuous process for carboxymethylation was used by Wyandotte Chem. Corp. in 1947, but it had no washing stage and was therefore only suitable for unpurified CMC ^[44]. In current CMC production, cellulose is processed batch wise either as a suspension (for a low mass fraction of cellulose) or in mixers as slurry (for high mass fraction). Both processes use short-chain alcohols as reactand-transfer and heat-exchanging media and as suspending agents, respectively. For high mass fraction processes, ethanol is usually used as slurry medium, whereas isopropyl alcohol is used in suspension-type processes ^[41,45].

Carboxymethylation is exothermic and takes place between 50 °C and the boiling point of the slurry or suspension medium under appropriate system pressure. The reagent efficiency is between 65 % and 80 %. Depending on the required purity, the product is washed with alcohol-water mixtures, preferably with the same alcohol used in synthesis. Before drying, suspension agents and washing liquids are collected and reprocessed either by distillation and extraction or membrane processes ^[2].

The use of ethanol during the mercerisation stage causes a homogeneous system of sodium hydroxide, water, and ethanol whereas by the use of isopropanol a non-homogeneous system occurs, forming a layer around the fibre composed of a highly concentrated sodium hydroxide water phase, caused by the low solubility of sodium hydroxide in unpolar systems ^[46]. The sodium hydroxide concentration is therefore high around the fibre. The use of isopropanol in CMC synthesis is reported to generate less sodium glycolate, as the less polar solvent provides an environment for MCA whereas NaOH is enriched in the aqueous phase ^[35].

Various other solvent systems, like acetone, benzene and LiCl/ DMAc (LiCl / *N,N*-dimethylacetamide) show cellulose dissolving properties ^[47-49], but those are usually only used in laboratory scale.

Even a clear solution is not a sufficient condition for a homogenous reaction, as cellulose is not necessarily molecular dispersed. It may still contain aggregates of ordered cellulose molecules ^[11-13]. These aggregates, so-called fringed micelles/fibrils, consist of aligned chains forming a compact core, thus do not interact with the solvent, and of solvated amorphous outer chains.

In 1995, *Fink et al.* ^[50] studied the influence of the surrounding alkali concentration on the cellulose state using X-ray and solid state ¹³C-NMR. They observed that in aqueous alkaline systems phase transitions occur above 10 % NaOH, while below this level the original crystalline structure is preserved. In 2003, *Dapía et al.* ^[51] presented their study on CMC preparation from pulp of *Eukalyptus glubulus*. They found that concentrations of NaOH and MCA strongly affected the DS of the resulting CMC and concluded that the MCA concentration should not be too high while the NaOH concentration could be very high. These results do not agree with those obtained by *Stigsson et al.*, who concluded an optimum in NaOH concentration.

1.3.3 Properties of CMC in aqueous solution

CMC swells in water and is alkali soluble even at a low degree of substitution. With pK_a -values of 4-5 (depending on DS) CMC is weakly acidic. *Trivedi et al.* ^[52] studied the effects of polymer concentration, charge density (DS) and size of the counterions on the dissociation constant of CMC potentiometrically. Consequently, the solubility of CMC depends on pH. Depending on its DS, CMC precipitates at low pH values due to intermolecular hydrogen bond formation between the undissociated carboxymethyl groups (Fig. 1-8).

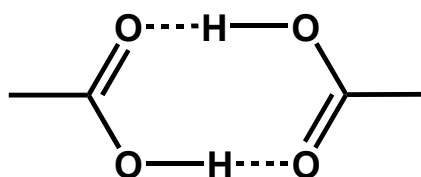


Fig. 1-8 Scheme of H-bond formation between two carboxylic acid groups at low pH-values

These H-bonds are very strong. With 1.64 Å the length of H \cdots O between two acetic acid molecules is in the range of the covalent C-OH bond (1.33 Å) ^[53]. At DS values of 0.3 - 0.5, precipitation occurs at pH-values below 3, higher substituted CMC with DS values between 0.7 and 0.9 precipitates at pH < 1. With rising pH, the amount of carboxylate and thus repulsion increases. At pH > 12, the repulsion between the negatively charged CM-groups decreases due to the presence of alkali-metal cations like sodium. Consequently, the CMC molecules form a coil resulting in a drop of viscosity. Heavy-metal salts like Cu²⁺, Ag⁺ or Pb²⁺ and trivalent cations such as Al³⁺, Fe³⁺ or Cr³⁺ may form insoluble salts or complexes and hence CMC precipitates. With divalent cations (e.g. Ca²⁺) these effects depend largely on the substituent to salt ratio ^[54].

In neutral solutions, molecular dispersed molecules are arranged in uncoiled linear structures, but CMC may also form aggregates in aqueous solution. *Burchard* intensively studied the behaviour of cellulose ^[55] and its aliphatic ethers ^[56] in solution. He suggests that the crystalline sections in cellulose are not fully destroyed but form a bundle of aggregated chains with dangling outer chains. These outer chains bind water molecules extensively. Already in 1961, *Francis* ^[57] suggested that residual crystalline cellulose sections are responsible for aggregation and discrete gel particle formation in aqueous CMC solutions according to the fringed micelle model.

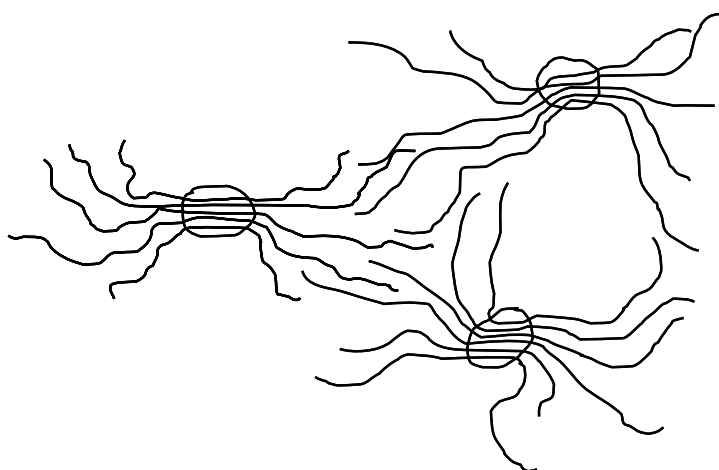


Fig. 1-9 Aggregate formation of CMC in aqueous media according to the fringed fibril model ^[57,58]

In 2005, *Liebert et al.* ^[58] visualized these superstructures in aqueous CMC solutions by atomic force microscopy (AFM). For their measurements they dried aqueous solutions with 1 to 10 µg/ mL statistically substituted CMC on freshly cleaved mica.

They observed various aggregates that correspond to the fringed micellar model with a total size of 200 to 350 nm. According to the authors, the compact cores were in the range of 60 to 100 nm and outer chains with up to 150 nm were observed. For block-like substituted CMC, they did not find separated fringed micelles but an extended network with domain-like areas.

1.4 Analysis of the substituent distribution

The distribution of the CM-groups both in the glucosyl unit as well as over the whole polymer is crucial with respect to structure-property relationships of CMC. Due to the high molecular mass of the starting material cellulose, terminal residues are usually neglected and only positions C-2, C-3, and C-6 of the AGU are considered. Therefore, carboxymethylation as a polymer-analogous reaction (Fig. 1-10) leads to eight possible substitution patterns.

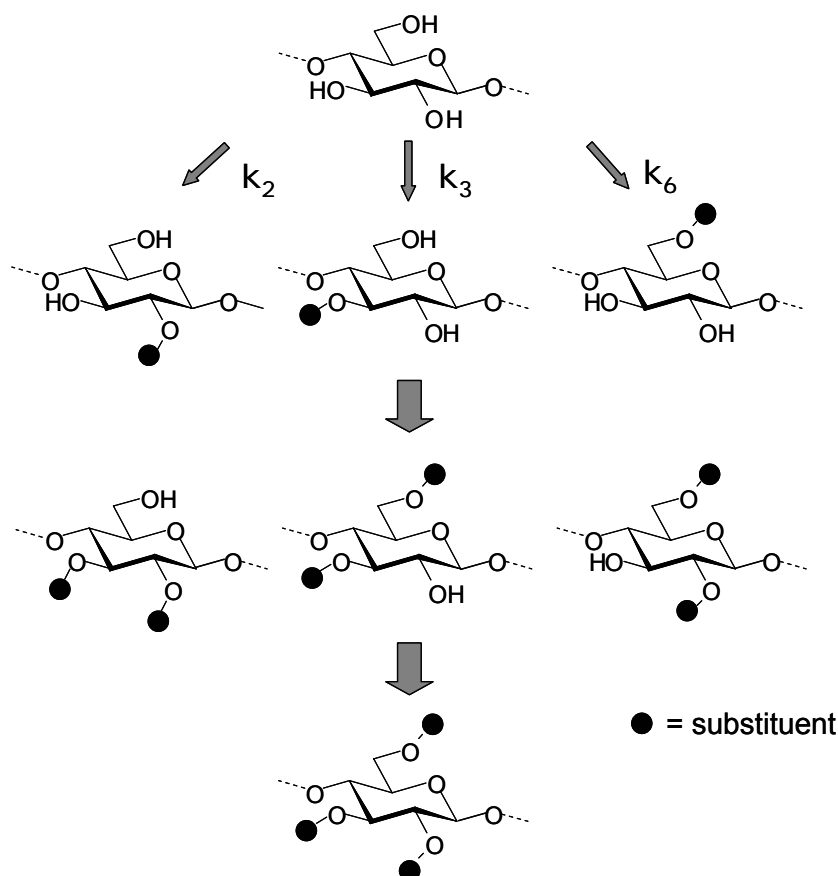


Fig. 1-10 Scheme of cellulose derivatization as a polymer-analogous reaction, substituent is $-\text{CH}_2\text{COONa}$ in case of NaCMC

The kinetic of carboxymethylation has been studied by various groups. *Salmi et al.* ^[59] observed that consumption of MCA by side reactions had no rate-controlling

influence. They calculated first order behavior for the entire process, which indicated that etherification was controlled by diffusion.

In 1998, *Olaru et al.*^[48] described carboxymethylation as two parallel first order reactions. Thereby, the fast initial reaction is due to reactions in less ordered regions of the original cellulose. *Hedlund and Germgård*^[60] investigated the kinetics of etherification with MCA in 2007, using nine commercially available pulps from different origins. They found the etherification rate depending on the molar MCA to AGU ratios.

Tab. 1-3 Comparison of relative rate constants of different CMC samples

Author, year	Method	k_2	k_3	k_6	Influence of substituted adjacent groups
Baar et al., 1994 ^[61]	¹³ C-NMR after ultrasonic degradation	3.0	1.0	2.1	no influence
Kragten et al., 1992 ^[62]	HPAEC after acidic (HClO ₄) degradation	1.8	1.0	1.3	(not investigated)
Zeller et al., 1991 ^[63]	GLC after methylation and reductive cleavage	2.4	1.0	1.8	(not investigated)
Abdel-Malik and Yalpani, 1990 ^[64]	¹ H- and ¹³ C-NMR of undegraded CMC	2.1	1.0	1.5	(not investigated)
Niemelä and Sjöström, 1989 ^[65]	GLC after acidic (HCl) degradation, trimethylsilyl derivatization	3.1	1.0	2.6	no influence
Reuben and Connor, 1983 ^[66]	¹³ C-NMR after acidic (HClO ₄) degradation	2.1	1.0	1.6	no influence
Ho and Klosiewicz, 1980 ^[67]	¹ H-NMR after acidic (H ₂ SO ₄) degradation	2.0	1.0	1.5	(not investigated)
Buytenhuys and Bonn, 1977 ^[68]	Gas Liquid Chromatography	2.5 ^a	1.0	1.8	no influence
		4.6 ^b	1.0	3.6	no influence
Croon and Purves, 1959 ^[69]	paper chromatography and electrophoresis after hydrolysis, methanolysis, and reduction (LiAlH ₄)	2.0	1.0	2.5	strong influence
Timell and Spurlin, 1952 ^[70]	tosylation-ionidation and tritylation/ periodate-HCOH	1	1	2	no influence

molar ratio of water to cellulose during synthesis: a: 7 : 1; b: 14 : 1 at equal base concentrations

Tab. 1-3 shows an overview of published relative rate constants k_2 , k_3 , and k_6 for carboxymethylation and whether an influence of substituted vicinal OH-groups could be observed, determined by different analytical methods of various CMC samples. The determination of the relative rate constants is one of the aims of monomer analysis.

1.5 The substitution pattern in the glucosyl unit

Important parameters can be received from the analysis of the monomer composition^[71] after complete degradation of the cellulose ether:

DS (degree of substitution) average of substituted hydroxyl groups in the AGU (between 0 and 3)

s_i amount (mol fraction) of the monomer of a certain substitution pattern

x_i partial DS in position i , e.g. x_3 is the partial DS of position C-3

c_i mol fractions of un-, mono-, di- and tri- substituted monomers,
e.g. $c_1 = \text{monosubstituted} = s_2 + s_3 + s_6$

The s_i - and c_i - values can be obtained experimentally, c_i and are interrelated as follows:

$$c_0 = s_0 \quad (1)$$

$$c_1 = s_2 + s_3 + s_6 \quad (2)$$

$$c_2 = s_{23} + s_{26} + s_{36} \quad (3)$$

$$c_3 = s_{236} \quad (4)$$

The relation between s_i -and x_i is:

$$x_2 = s_2 + s_{23} + s_{26} + s_{236} \quad (5)$$

$$x_3 = s_3 + s_{23} + s_{36} + s_{236} \quad (6)$$

$$x_6 = s_6 + s_{26} + s_{36} + s_{236} \quad (7)$$

The DS can be calculated as follows:

$$DS = 0 \cdot c_0 + 1 \cdot c_1 + 2 \cdot c_2 + 3 \cdot c_3 \quad (8)$$

$$DS = x_2 + x_3 + x_6 \quad (9)$$

As can be seen, already at this level of substituent distribution in the AGU the relatively simple carboxymethylation leads to a complex mixture of products which can be described by a variety of parameters.

1.6 Mathematical models

One way to interpret the analytical results is to compare them with a mathematical model for random distribution. The first and until now most commonly used statistical model to describe the processes during etherification was published by *Spurlin* in 1939 ^[71]. In 1986, *Reuben* ^[72] proposed a refined model based on the one by *Spurlin*.

Assuming that only positions C-2, C-3 and C-6 in each AGU of the cellulose molecule are substituted, *Spurlin* developed a statistical model to describe the substitution pattern of cellulose derivatives, hence the reaction kinetics during the reaction. First, he made several simplifying assumptions:

- Etherification is a pseudo-first-order process and the relative rate constants remain constant during the course of reaction.
- All hydroxyl groups are equally accessible during the reaction.
- There is no influence of the OH-groups on each other.
- The cellulose chain is sufficiently long for the end groups to be neglected.
- Other structural variations (e.g. partial oxidation) may be neglected.

Reuben included an influence of the vicinal hydroxyl groups in positions C-2 and C-3 in his model, this was already postulated by *Ott et al.* in 1963 ^[73]. He proposed two models: the first one assumes that k_2 remains constant during the reaction independent of position 3. The reactivity of position 3 though changes with a substitution of C-2 from $k_3 \rightarrow k_3'$. The second model corresponds with *Spurlin's* assumptions including additionally to k_3' an interrelation of a primary substitution in position C-3 on the reactivity of position C-2 ($k_2 \rightarrow k_2'$). This model can be neglected in practice ^[72].

For the *Spurlin*-model ^[71], the theoretical s_i -values are calculated as follows:

$$s_{0(\text{Spurlin})} = p_2 \cdot p_3 \cdot p_6 \quad (10)$$

$$s_{2(\text{Spurlin})} = x_2 \cdot p_3 \cdot p_6 \quad (11)$$

$$s_{3(\text{Spurlin})} = p_2 \cdot x_3 \cdot p_6 \quad (12)$$

$$s_{6(\text{Spurlin})} = p_2 \cdot p_3 \cdot x_6 \quad (13)$$

$$s_{23(\text{Spurlin})} = x_2 \cdot x_3 \cdot p_6 \quad (14)$$

$$s_{26(\text{Spurlin})} = x_2 \cdot p_3 \cdot x_6 \quad (15)$$

$$s_{36(\text{Spurlin})} = p_2 \cdot x_3 \cdot x_6 \quad (16)$$

$$s_{236(\text{Spurlin})} = x_2 \cdot x_3 \cdot x_6 \quad (17)$$

For the model from *Reuben* ^[66], p_2 and p_3 can be calculated according to *Spurlin*, but for p_3 the influence of a prior substitution on position C-2 is taken into account. So p_3 is calculated by:

$$p_{3(\text{Reuben})} = 1 - x_3 = (1 - x_2 + s_0 + s_6 - s_3 - s_{36})/2 \cdot (1 - x_2) \quad (18)$$

Consequently, the theoretical s_i -values for this model ^[66] are evaluated by following equations:

$$s_{0(\text{Reuben})} = p_2 \cdot p_{3(\text{Reuben})} \cdot p_6 \quad (19)$$

$$s_{2(\text{Reuben})} = p_6 \cdot (s_2 + s_{26}) \quad (20)$$

$$s_{3(\text{Reuben})} = p_2 \cdot p_6 \cdot (1 - p_{3(\text{Reuben})}) \quad (21)$$

$$s_{6(\text{Reuben})} = p_2 \cdot p_{3(\text{Reuben})} \cdot x_6 \quad (22)$$

$$s_{23(\text{Reuben})} = p_6 (1 - p_2 \cdot p_{3(\text{Reuben})} - s_2 - s_{26} - p_2 (1 - p_{3(\text{Reuben})})) \quad (23)$$

$$s_{26(\text{Reuben})} = x_6 \cdot (s_2 + s_{26}) \quad (24)$$

$$s_{36(\text{Reuben})} = p_2 \cdot (1 - p_{3(\text{Reuben})}) \cdot x_6 \quad (25)$$

$$s_{236(\text{Reuben})} = x_6 \cdot (1 - p_2 \cdot p_{3(\text{Reuben})} - s_2 - s_{26} - p_2 (1 - p_{3(\text{Reuben})})) \quad (26)$$

An average heterogeneity parameter H can be calculated from the single deviations Δs_i between the experimental and theoretical s_i -values ^[74]. This parameter shows the extent of the deviation between the statistical model and the sample. As H only

indicates the average deviation of a model with the experimental data, it is helpful to compare the distinct s_i -values as well to get a better impression of the type of deviation.

$$H = \sqrt{\sum (\Delta s_i)^2} \quad (27)$$

Based on the Spurlin model, the theoretical course of the reaction can be plotted to estimate the monomer composition at a distinct DS. Therefore, the experimentally obtained k -values are normalized to 1

$$k_{i(norm)} = \frac{k_i}{k_2 + k_3 + k_6} \quad (28)$$

and used to evaluate x_i -values over the whole reaction by the equation:

$$x_i = 1 - e^{-k_i \cdot B} \quad (29)$$

For the previously described factor B (proportional to the reaction time) variable values are chosen between 0 and ∞ to plot a reaction course.

If a set of CMCs was produced under the same or similar reaction conditions, the individual s -, c - and x -values for each sample should agree with the curves based on the k -values.

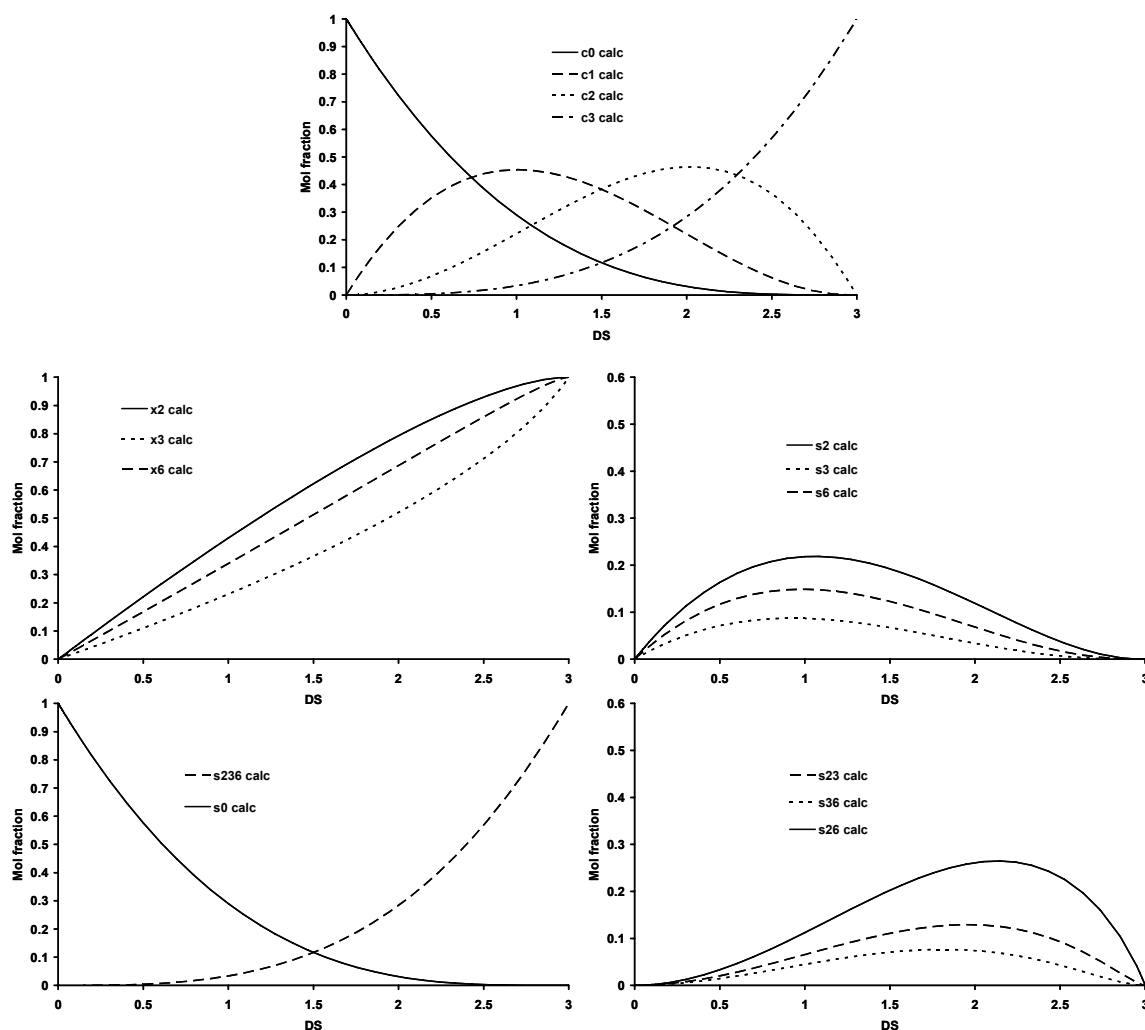


Fig. 1-11 Exemplary plot of reaction courses to estimate the molar monomer distribution (s_i - and c_i -values) and partial DS-values (x_i -values) for a distinct DS, based on the experimentally obtained k -values by *Reuben and Connor*^[66]

In Fig. 1-11 exemplary reaction courses are displayed, calculated based on the previously described model and the k -values obtained by Reuben and Connor^[66] from Tab. 1-3. These relations are applied on the CMCs investigated within this work in chapter 3.6, Fig. 3-18.

1.7 The substitution pattern along the polymer backbone

The analysis of the substitution pattern along and over the polymer chains is a very challenging part in the characterization of cellulose ethers. It is desirable to develop new methods for the analysis of oligomeric sequences, as the distribution of

the substituents along the backbone plays a key role in structure-property relationships.

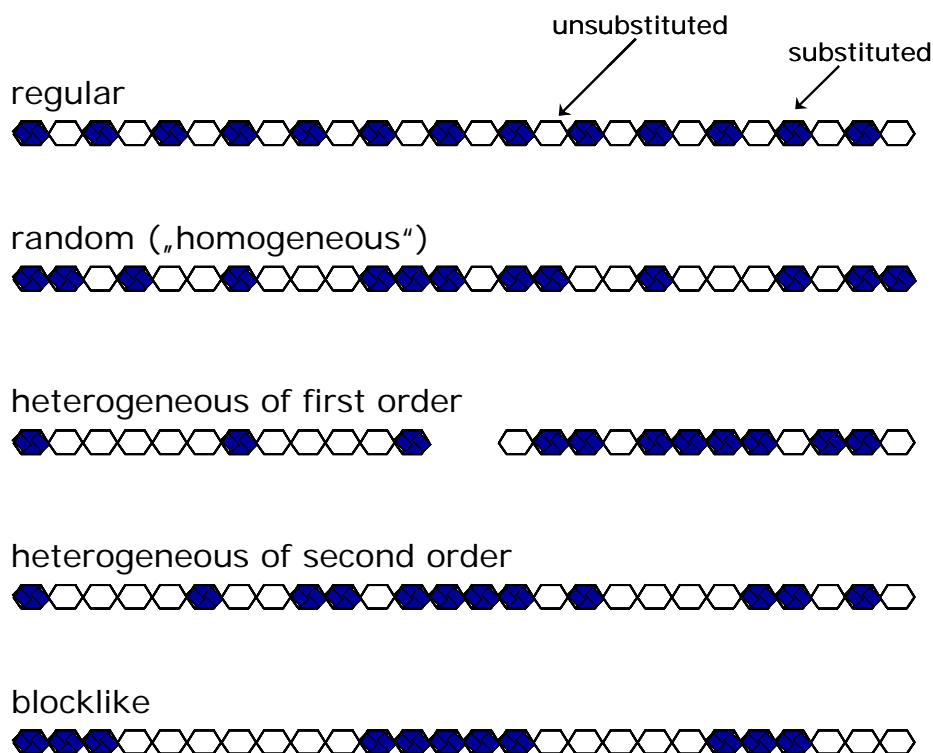


Fig. 1-12 Schematic presentation of types of the substitution pattern along and over the polymer chains ^[75]

Fig. 1-12 displays the possibilities of different distributions of substituents along and over the cellulose chains. Even at the same DS- and s_i -values, the distribution along the backbone offers many different possibilities. As types of distributions, a completely regular pattern, a random distribution (often referred to as homogeneous since expected from homogeneous reactions), then a more heterogeneous and a blocklike pattern are illustrated in Fig. 1-12.

Heterogeneity among the chains is of first order, within one chain of second order ^[75]. A random distribution is the result of an equal accessibility of all AGUs during etherification and is used as reference. If the accessibility is different, e.g. due to inert crystalline regions in the native cellulose, a more heterogeneous substitution pattern in comparison to a random distribution results. The reactivity of monomers might also change during the reaction. This would happen if the local reactivity was enhanced after primary substitutions changed accessibility of adjacent AGUs. The reactivity may decrease due to sterical effects or electrostatic repulsion which would result in a more regular pattern ^[76].

Comparing the experimentally obtained distribution with a random one allows interpreting the extent and type of deviation. In contrast, after complete degradation, the direct information about the former adjacent AGU is lost.

Approaches to gain more information on the polymer level are based on a partial degradation of the molecule to get sequences that are applicable for mass spectrometry (MS), followed by a statistical evaluation. Important for this kind of analysis is the assumption that during etherification the influence of a primary substitution affects only a very short sequence of adjacent AGUs. Therefore, even small oligomers (> DP 3) represent the substituent distribution of neighbored AGUs of the entire polymer. A limitation is though that it is not possible to differentiate between heterogeneities of first (over the chains) and second order (within the chains) ^[74,77].

To enable the determination of the substitution pattern, various conditions need to be fulfilled:

- First, the partial degradation process needs to proceed randomly, producing an oligomeric mixture in which each DP represents the average composition of the entire polymer. This was achieved for methyl cellulose (MC) by perdeuteromethylation of the free hydroxyl groups with d_3 -methyl iodide as nucleophile ^[74,77], resulting in a chemically uniform product without significant differences in the stabilities of the glucosidic linkages. The original methyl pattern is saved by the use of the isotopic analogon of the methylgroup allowing a differentiation due to the mass difference in MS.
- A second requirement for this type of analysis is to exclude discrimination with respect to the chemical composition (DS, substitution pattern) in the mixture by instrumental settings. The signal intensities of a mass spectrum usually do not represent the ratios of the mixtures' components. Depending on their size, polarity, basicity, and stereochemistry, some molecules can form adducts (e.g. sodium adducts) and hence be ionized more easily than others.

For MC, perdeuteromethylation is sufficient to overcome both bias causing influences: the differences in the stabilities of the glucosidic linkages during partial degradation as well as discriminating effects during measurement in MS. This strategy could theoretically also be applied to ethyl cellulose (EC) or other non-ionic derivatives that can be transformed into chemically uniform and isotopically labeled

derivatives. Acetates ^[78], sulfates ^[79], or other labile substituents ^[75] that can be converted to methyl-/deuteromethyl-oligomers could also be investigated by this strategy.

Adden et al. showed that the bias observed when investigating hydroxyalkyl ethers such as HEC ^[80], HEMC ^[81] and HPMC ^[82] in MALDI-TOF-MS could be successfully overcome by the introduction of a permanently charged quaternary ammonium group by reductive amination and subsequent permethylation, a strategy already introduced by *Heinrich* in 1999 ^[83]. To favor random cleavage and to inhibit intramolecular acetal formation of 2-O-hydroxyalkyl residues during partial hydrolysis, hydroxylalkyl ethers were also perdeuteromethylated as first step in sample preparation.

During previous studies in our group complete alkylation of CMC could not be achieved by the common methods. As a complete alkylation is crucial for the methods described above, these were not applicable to CMC. Therefore, alternative sample preparation procedures had to be developed.

1.8 Analytical techniques in carbohydrate chemistry

The heterogeneity of poly- and oligosaccharides in molecular weight, primary sequence and branching, linkage, the variety of sugar structural isomers, the different substitution pattern in derivatives, and the lack of active functional or chromophore/ fluorophore groups is a challenge in carbohydrate separation and analysis.

A number of analytical methods have been applied to carbohydrates in general. They include paper ^[69,84] and thin layer chromatography (TLC) ^[85], gas liquid chromatography (GLC), high performance liquid chromatography (HPLC) ^[86], high pH-anion exchange chromatography (HPAEC) ^[87,88], supercritical fluid chromatography ^[89], affinity chromatography ^[90], polyacrylamide slab gel ^[91], thin layer ^[92], and capillary electrophoresis (CE) ^[93-95] as separation and mass spectrometry and nuclear magnetic resonance spectroscopy (NMR) as structural characterization techniques.

The techniques used within this thesis and those common in cellulose and starch ether analysis are described in the following chapters.

1.8.1 Capillary Electrophoresis (CE)

Electrophoresis describes the motion of dispersed particles carrying an electric surface charge relative to a fluid under the influence of an electric field that is space uniform.

Capillary zone electrophoresis (CZE) is the simplest and most commonly utilized form of CE and was also used in this work. Fused-silica capillaries employed in CE typically have an internal diameter (ID) of 20 to 100 μm and an outside diameter (OD) of 375 μm . Often used are lengths of 20 -100 cm and the capillary is coated with polyimide to increase the flexibility (Fig. 1-14). To perform capillary zone electrophoretic separation, the capillary is filled with an appropriate buffer at the desired pH-value.

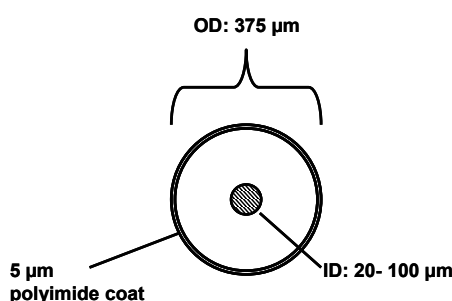


Fig. 1-13 Diagram of the inner surface of a fused-silica capillary

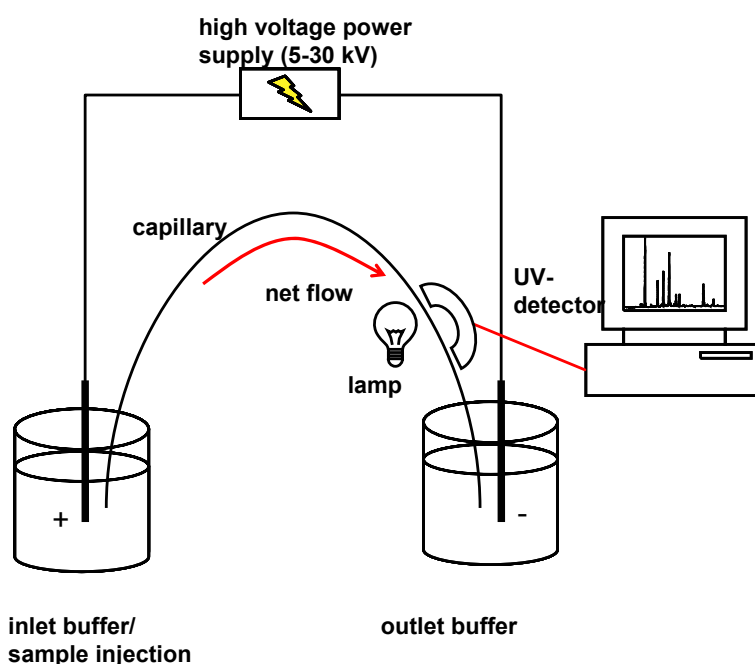


Fig. 1-14 General schematic of a CE instrument with UV-detector (lamp e.g. D_2 or Hg). A “window” is created by removal of the polyimide coating to make online detection possible. The capillary is thermostated, e.g. by air or a liquid cooling agent to gain constant temperatures.

Basis components of a CE instrument include a high voltage supply (0-30 kV), the polyimide coated capillary described above, two buffer reservoirs that can accommodate both the capillary and the Pt-electrodes connected to the power supply, and a detector (e.g. UV-detector or MS). The “normal” polarity is considered to be inlet (+) → detector → outlet (-) as shown in Fig. 1-14. A charged molecule in solution becomes mobile when placed in an electric field ^[96]. The velocity v_i , acquired by the solute under the influence of the applied voltage H is the product of μ_{app} , the apparent solute mobility and the applied field E . E is the applied voltage H divided through its length, L ($E = H/L$).

So the velocity is the distance traveled during the time of electric field application

$$v_i = \mu_{app} \cdot E \quad (30)$$

while μ_{app} is a property of the molecule, proportional to its charge and reciprocal to the frictional forces acting upon it in solution. The electrical force F_{el} can be given by

$$F_{el} = q \cdot E \quad (31)$$

and the frictional force F_{fr} on a spherical ion is

$$F_{fr} = -6\pi \cdot \eta \cdot r \cdot v_i \quad (32)$$

During electrophoresis a steady state is attained, when both forces are equal but in opposite directions.

$$q \cdot E_r = -6\pi \cdot \eta \cdot r \cdot v_i \quad (33)$$

Consequently, the mobility can be described by:

$$\mu_{app} = \frac{q}{6\pi \cdot \eta \cdot r} \quad (34)$$

From this equation it is evident that the mobility of an analyte molecule depends on both, size and charge.

Silica has an amorphous nature and various silanol groups with a pK_a -range of 4-6. Therefore, their ionization behavior is determined by the buffer pH. Deprotonated silanol groups at the capillary wall attract cations from the buffer solution. The ionic layer formed has a positive charge density decreasing as the distance from the wall increases. The double layer formed closest to the surface is referred to as *Inner Helmholtz* or *Stern Layer* and is essentially static. The *Outer Helmholtz Plane (OHP)* distal to the *Stern Layer* is less ordered (Fig. 1-15). In the *Stern Layer*, the decrease of the positive charge density is linear, while it is exponential in the diffuse OHP. This exponential decrease is responsible for the electric potential in the ionic double layer referred to as ζ -potential.

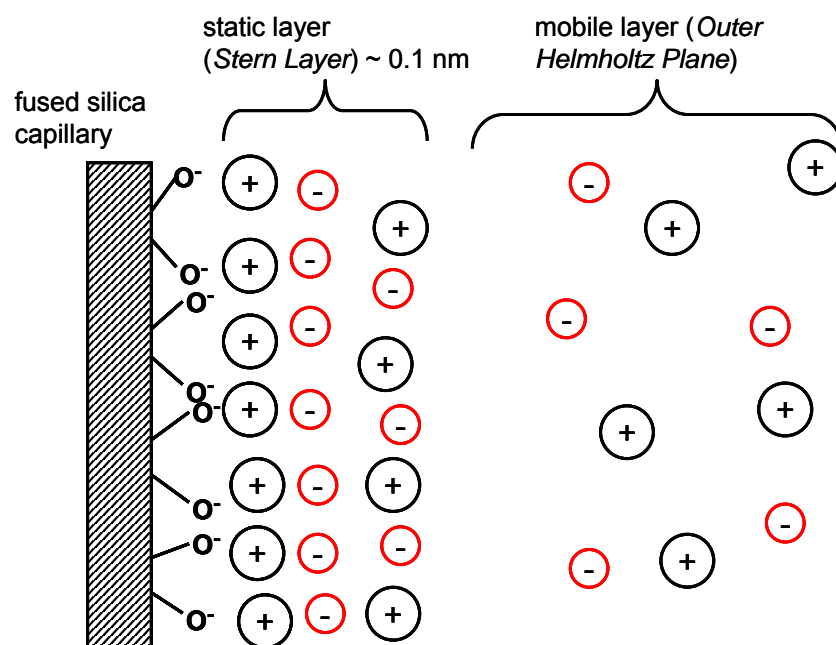


Fig. 1-15 Illustration of the double-ionic layer formed in bare silica capillaries due to deprotonation of silanol groups, critical in generating electroosmotic flow (EOF) according to ^[97]

When an electric field is applied, the hydrated cations of the OHP migrate in the direction of the cathode. Since they are clustered in the ionic layer, the entire buffer solution, even the anions, is pulled towards the cathode due to the hydrogen bonds of the hydration. This so-called Electroosmotic Flow (EOF) drives all components in the capillary towards the cathode, so it has to be considered when determining the electrophoretic mobility of an analyte molecule. The velocity of the EOF depends on the ζ -potential and can be experimentally determined by a neutral reference marker. Borate buffers enable to separate regiosomeric polyhydroxy compounds including carbohydrates as they can reversibly form anionic complexes with borate ^[98]. Borate

complexes are more stable with *cis*- than with *trans*- oriented hydroxyl groups and with 1,2-diols more than with 1,3-diols. Furthermore, cyclic forms of sugars (e.g. aldoses), react less efficiently with tetrahydroxyborate than acyclic ones (alditols). A higher number of hydroxyl groups in the analyte increases the strength of borate complexation^[94]. The carbohydrate-borate complex formation is largely influenced by the presence of substituents in the analyte molecule, their charges, and locations. Generally, a decrease of the stability of the borate ester is observed as a result of Coulombic repulsion between a negatively charged substituent (e.g. COO⁻) and borate moieties^[99]. Due to their ability to separate even diastereomeric polyols, borate buffer systems are very popular in carbohydrate analysis. Other common buffer systems used are phosphates (pH 3 and 9), mixed phosphate/borate systems, or acetates^[97,100].

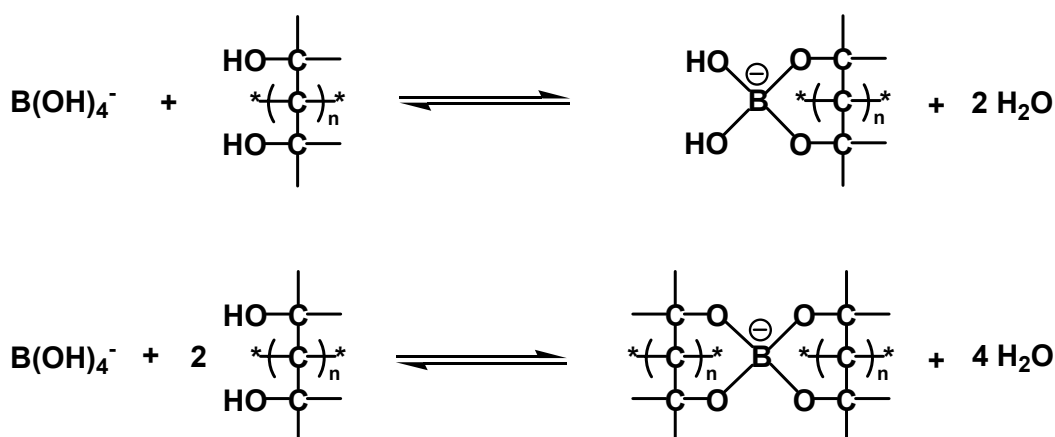


Fig. 1-16 Complex formation between borate and polyols, $n=0$ or 1. Top: Formation of a monocomplex. Bottom: Formation of a dicomplex or spirane

Derivatization of carbohydrates to render a chromophore group and/ or charge was demonstrated by *Honda et al.* in 1989^[101]. Since then, various derivatization strategies have been developed, most of them are reductive aminations, e.g. with 2-aminopyridine, 4-aminobenzoate, 4-aminobenzonitrile (ABN), 8-amino-naphthalene-1,3,6-trisulfonic acid (ANTS), to name just a few^[102,103]. The mechanism of labeling the carbonyl group of the sugar with an aminocompound by reductive amination is displayed in Fig. 1-17. Alternatively to labeling indirect UV or fluorescence detection with an absorbing substance such as benzoic or picric acid added to the background electrolyte (BGE). *Bazzanella and Bächmann*^[104] used copper(II)sulphate in aqueous ammonia (pH 12) to determine sugars and amino acids as their copper amino complexes.

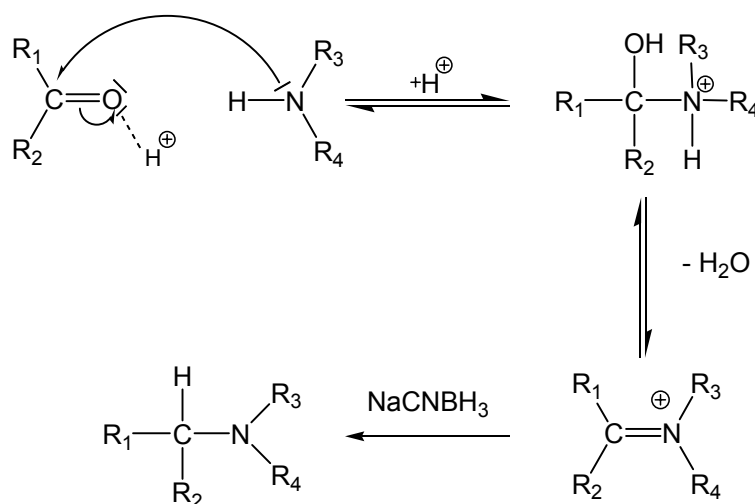


Fig. 1-17 Acid catalyzed reductive amination of carbohydrates.

There are some publications using direct detection for carbohydrates without prior derivatization with a chromophore or fluorophore at very small wavelengths. Carbohydrates have a very low UV absorbance due to the small proportion of the carbonyl- (or open-chain-) form in aqueous solution. But *Hoffstetter et al.* ^[105] found that the absorbance at very low wavelengths (195 nm) was enhanced significantly by adding borate, probably since borate complexation shifts the equilibrium from the cyclic to the open-chain-form. *Oudhoff et al.* ^[106] used the absorbance of CMC at 196 nm for the detection of underivatized CMC samples in 2004. Their aim was to determine the DS and the DS distribution of underivatized and undegraded CMCs^[107]. They determined the electrophoretic mobilities of five CMC samples with DS values between 0.60 and 1.64 with molar masses in the range of 200 and 400 kDa. To enhance the moderate sensitivity, they used wide capillaries (I.D. 75 µm) and injected relatively large sample amounts (1 g/L). They found that especially at higher DS values the mobility as a function of DS is non-linear and a linear connection was considered only for DS values below 1. This method has the advantage to save the time for derivatization and degradation to determine the DS, but the small linear range of the mobilities and the low sensitivity makes it insufficient for a wide application. As the native polymer was analyzed, no information about the substitution pattern of the AGU was obtained.

A further disadvantage is that selectivity decreases with decreasing wavelength, 190 nm was the lower limit of the instrument used within this thesis.

In 2001, *Lazik et al.* ^[108] introduced CE for the separation of CMC hydrolyzates. The corresponding monomers were tagged with UV-active ABN by reductive amination. To assign the peaks to the carboxymethylated monomers, they were compared with

standard substances obtained from regioselectively carboxymethylated celluloses. The results were compared with those obtained by HPAEC ^[62]. With this method, it was possible to determine the complete monomer composition of CMC hydrolyzates. The monomer analysis of the four CMC samples investigated within this thesis is based on this work (see 3.2). This method was applied in 2004 by *Tüting et al.* ^[109] on the structural analysis of CMS. *Faustmann* ^[110] used CE-MEKC for the structural analysis of amphiphilic starch hydrolyzates.

Besides UV-Vis, MS is important as detection and identification method for carbohydrate analysis ^[95]. CE-MS was used for the characterization of heparins. The disaccharides composition after complete enzymatic degradation ^[111,112] as well as heparin oligomers ^[113] and the whole polymer ^[114] could be investigated by CE-MS. *Larsson et al.* ^[115] could apply on-line CE-ESI-MS for the analysis of ANTS-derivatized maize starch oligosaccharides. *Gennaro et al.* ^[116] combined on-line multiple stage ESI-Ion Trap-MS up to MS⁵ to obtain structural information on several oligosaccharide mixtures after derivatization with ANTS.

1.8.2 High pH Anionexchange Chromatography (HPAEC)

High pH (also: performance) anionexchange chromatography with pulsed amperometric detection (HPAEC-PAD) was introduced in carbohydrate chemistry in the mid 1980s ^[117,118]. Stationary phases commonly used consist of spheres functionalized with quarternary ammonia groups. NaOH solutions are usually employed as mobile phase. Sodium acetate is used as co-eluent for oligosaccharides and to displace carbonate ions (from the eluent) from the cationic stationary phase ^[119]. The very high pH values > 12 used in HPAEC promote the formation of the enolate anion, so carbohydrates can be separated according to the pK_a values of their hydroxyl groups. A monosaccharide molecule possesses several potentially ionizable hydroxyl groups with an order of acidity of 1-OH > 2-OH ≥ 6-OH > 3-OH ≈ 4-OH ^[120]. The retention times are reciprocal to the pK_a values and increase with chain length. Acidic compounds are retained even more strongly. Stereochemistry is important for the coordination with the stationary phase as well, hence influences retention behavior. This way it is possible to separate diastereomers, one of the general challenges in carbohydrate chemistry ^[87]. PAD is the most common detection technique for carbohydrates. It is convenient, as it does not require any pre- or postcolumn derivatization. PAD is based on the measurement

of the anodic current caused by oxidation of the analyte at a gold, carbon or platinum electrode. Electro-oxidation as a heterogeneous detection suffers from the fouling of the electrode surface by intermediate oxidation products or elution impurities causing a rapid decrease in sensitivity. This problem is overcome by employing a triple stage waveform with anodic and cathodic polarization of the working electrode (Fig. 1-18). It starts with a detection potential (E_1) at which the analytes are detected by oxidation of the hydroxyl groups. To minimize background signals from double-layer charging, a time delay for the detector is introduced allowing the charging to decline before the measurement of the current occurs. After this sequence a high positive potential is applied to clean the electrode surface by full oxidation (E_2). Finally, the electrode surface is regenerated by a negative potential strong enough to reduce the previously formed gold oxide film (E_3).

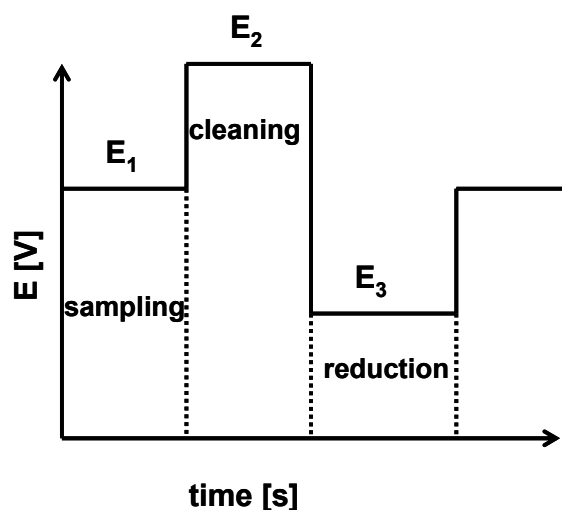


Fig. 1-18 Waveform used in pulsed amperometric detection (PAD): E_1 : sampling, E_2 : cleaning, E_3 : reduction

The great problem in PAD is that the molar response (unlike for UV-, radio- or fluorescent labeled oligosaccharides) is different for each compound. This can be overcome by a calibration with applicable standards, but especially in oligosaccharide analysis, reference compounds are often unavailable in the required purity. Therefore, only a “relative quantification” can be obtained. Another problem is epimerization caused by the strongly alkaline conditions in HPAEC ^[119]. So in 100 mM NaOH the equilibrium between GlcNAc and ManNAc is reached within an hour, so large saccharides containing GlcNAc or GalNAc suffer from epimerization and degradation due to β -elimination. This problem can partly be overcome by

reducing the oligosaccharides in advance ^[121,122], though then the most acidic group is lost and retention as well as detection sensitivity decreases.

HPAEC-PAD was used in the analysis of cellulose and starch and its derivatives by various groups, partly after enzymatic degradation ^[123,124]. In 1992, *Kragten et al.* ^[62] could determine the molar response factors for O-CM-glucoses by collecting the fractions of a CMC hydrolyzate and establishing the monomer composition by ¹H-NMR. They found that CM-substitution decreased the response relative to glucose. *Heinrich and Mischnick* ^[125] used HPAEC-PAD in 1996 to investigate the substituent distribution of MC monomers after complete hydrolysis with TFA and assigned the peaks and determined the molar response factors using synthesized standards. They observed that the detector response relative to glucose decreases with methyl substitution and also found overlapping of 3,6-O-methyl glucose with a side product probably HMF, resulting in too high amounts of this monomer.

1.8.3 Gas Liquid Chromatography (GLC)

Gas Liquid Chromatography coupled with Flame Ionization Detection (GLC-FID) is a very common analytical technique due to its high separation efficiency and wide linear detection range. As it requires volatile and thermally stable analytes it is not applicable for cellulose and its derivatives without derivatization. An appropriate pre-treatment for non-ionic cellulose ethers such as MC or HEC follows the step of methylation analysis (partially methylated alditol acetates) according to *Björndal* ^[126,127]. First, free hydroxyl groups of the cellulose derivatives are alkylated, e.g. with methyl iodide. Permethylation is often performed according to *Ciucanu and Kerek* ^[128], using solid NaOH suspended in DMSO to deprotonate the OH-groups or according to the method of *Hakomori* ^[129] that in a modified version uses lithium dimethylsilyl as base. This step is important for hydroxyalkyl derivatives such as HEC or HE-starch to avoid side reactions like intramolecular acetal formation ^[130] or the formation of anhydro sugars. Complete degradation is achieved by acidic hydrolysis. The reduction of the received α - and β -glucose derivatives with sodium borohydride (NaBH_4) yields alditols and hence minimizes the number of peaks in the chromatogram. Finally, the released hydroxyl groups at positions C-1, C-4, and C-5 are acetylated to achieve volatile analytes, e.g. using acetic anhydride and pyridine. This method has been successfully applied to various non-ionic cellulose ethers like MC, MHEC ^[81], MHPC ^[82] etc.

As CM-groups are partly reduced as well during this procedure yielding hydroxyethyl groups, lactones can be formed. So this method is not appropriate for CMC. *Ukai et al.* ^[131] performed reduction of CM-glucans to HE-, activating CM-glucose with 1-ethyl-3-(3-dimethylaminopropyl)carbodiimide ^[132,133]. Alternatively, CMC monomers have been investigated after acid hydrolysis as their trimethylsilyl derivatives ^[65,134]. In 1982, *Rolf and Gray* ^[135] introduced reductive cleavage as alternative degradation method for cellulose and starch derivatives. Promoted by a Lewis acid as TMF triflate the glucosidic bonds are cleaved and the carboxonium ion is directly reduced with triethylsilane to the corresponding anhydroglucose. Products can be analyzed by GLC-MS after acetylation. *Zeller et al.* ^[63] determined the positions of O-CM-groups of commercially available CMCs by GLC-FID after methylation and reductive cleavage, using the effective carbon-response (ECR) method to correct the peak areas ^[136-139]. The drawback of this method is that it requires permethylation, which was performed with lithium methylsulfinyl carbanion as base ^[140,141], but is often difficult to achieve. The advantage is that reductive cleavage conditions in contrast to aqueous acid hydrolysis tolerate esters, which makes this method applicable for such derivatives.

1.8.4 Mass spectrometry (MS)

The analysis of large biomolecules by MS has profited significantly from the progress of soft ionization techniques like Electrospray Ionization (ESI) or Matrix-Assisted Laser Desorption/Ionization (MALDI). Traditionally MS techniques have been of limited use for the investigation of high mass species until fast atom bombardment (FAB) was developed in the early 1980s by *Barber et al.* ^[142].

In soft ionization techniques usually fragmentation neither occurs during nor after the ionization or fragments are not observed as in MALDI-TOF-MS. Therefore, either molecular ions ($[M]^+$, $[M]^-$) or pseudomolecular ions ($[M + n H]^n+$, $[M + Na]^+$, $[M - H]^-$ etc.) are detected.

Ion formation in ESI can be divided into three steps: first, an electrically charged spray is created ^[143,144], followed by a dramatic size reduction of the droplets and finally the liberation of fully desolvated ions (Fig. 1-19). As soon as the electrostatic repulsion of the ions in the microdroplets of the electrospray exceeds the force of surface tension, disintegration of the droplet will occur ^[145]. Recent work showed that the droplets do not explode in a so-called *Coulomb Explosion*, but eject a series of

much smaller microdroplets from an elongated end. Thus, the charge density on their surface is not homogeneous, but significantly increased in the region of sharper curvature. This process, referred to as *Droplet Jet Fission*, resembles the jet ejection from the so-called *Taylor Cone* and has been proven by flash microphotography^[146,147]. The final formation of ions from the disintegrated droplets is not yet clarified and still debated, while two models co-exist: The Charged-Residue Model (CRM)^[148] assumes that the complete desolvation of ions occurs by successive loss of all solvent molecules from droplets that are sufficiently small enough to contain just one analyte molecule in the end of a cascade of disintegration of the droplets (originally referred to as Coulomb Explosions). Finally, the charges of these ultimate droplets are transferred onto the molecule. The CRM model is supported by the fact that this way, even very large molecules like proteins can yield singly charged ions.

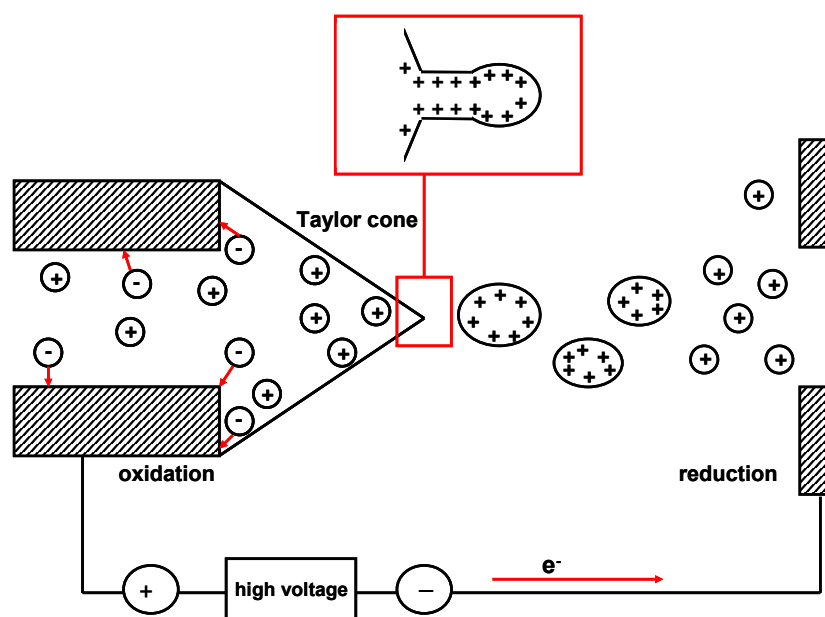


Fig. 1-19 Scheme of *Taylor Cone* formation (positive ion mode), ejection of a jet, and its disintegration into a fine spray.

The Ion Evaporation Model(IEM)^[149] describes the formation of desolvated ions as direct evaporation from the surface of highly charged microdroplets. It corresponds to the observation, that the number of charges is related to the part of the surface of the microdroplet that can be covered by a molecule. As the radius diminishes, molecule size and number of droplet charges remain constant, thus the increasing charge density brings more charges to the molecule. Therefore, planar molecules exhibit higher average charge than spheric ones^[150].

In Laser Desorption/Ionization, laser radiation is applied to generate isolated, intact ionized analyte molecules in the gas phase. Commonly used are nitrogen lasers with a wavelength of 337 nm and a pulse width of less than 1 nsec. Its application for higher masses was achieved by the idea to embed the low concentrated analyte into a highly absorbing matrix ^[151,152], thus MALDI-MS was created. Among the ability to absorb at the laser's wavelength hence causing heating and phase transition, matrices cause co-desorption of the analyte. They need to be stable in vacuum and have to embed and isolate the analyte completely, e.g. by co-crystallization, minimizing analyte-analyte interactions. Fig. 1-20 shows an overview of matrices commonly used in carbohydrate analysis.

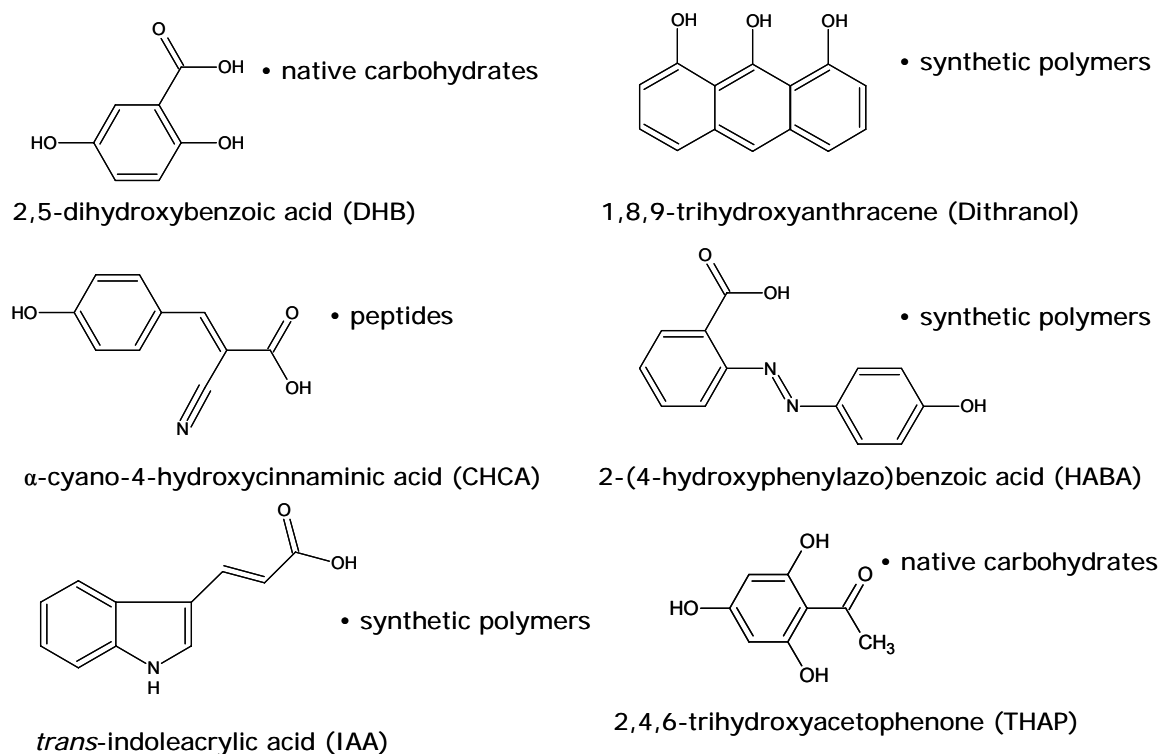


Fig. 1-20 Structures and applications of commonly used MALDI matrices

Despite the numerous applications of MALDI, the mechanisms of desorption and ionization are not yet fully understood. In 2003, *Karas and Krüger* ^[153] introduced the cluster ionization mechanism to explain ion formation in MALDI. They stated that ions are generated from high mass precursors in the gas phase consisting of analyte and matrix molecules.

The Quadrupole Ion Trap (IT) ^[154] consists of two hyperbolic electrodes and a ring electrode which are electrically connected. A dipolar alternating current (AC) and radio frequency (RF) potentials are applied between them. The mass separating

principle of the IT is to create stable trajectories for ions within a certain m/z -range “trapping” them this way. Unwanted ions are removed by letting them collide with the walls due to their unstable trajectories. Fragmentation occurs by collision of the background gas (He) with the analyte ion (collision induced dissociation, CID). The fragment ions are accumulated and can be fragmented again before they are released from the trap and detected (Fig. 1-21). Although theoretically MS^n experiments could be performed with an IT, decreasing sensitivity and stability of the ions against further fragmentation are limitations in practise.

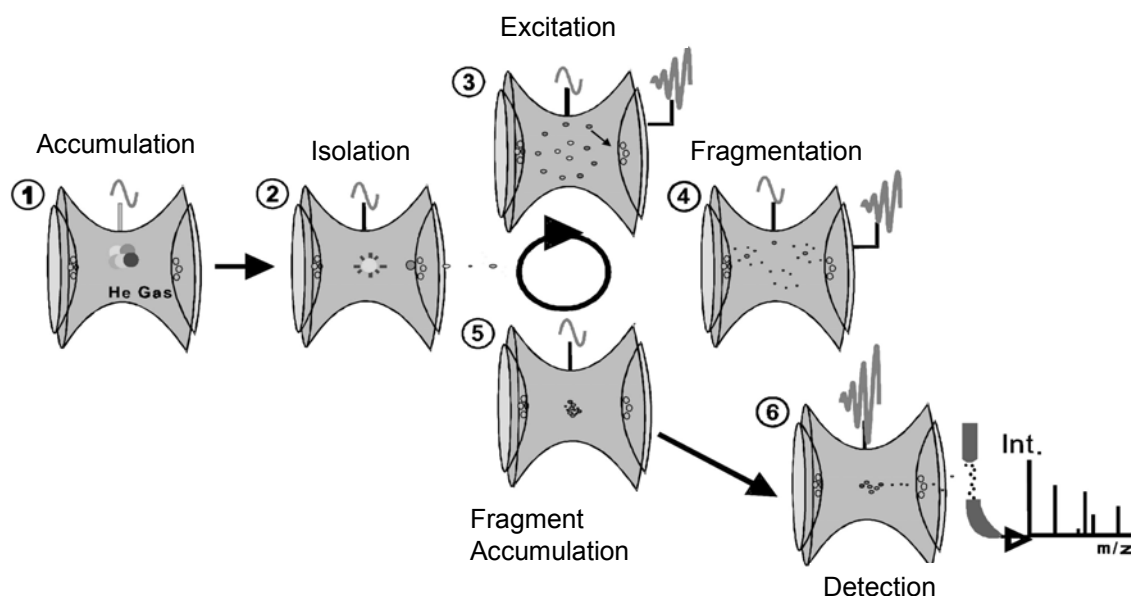


Fig. 1-21 Steps of collision induced dissociation (CID) in the Ion Trap (Bruker Daltonics)

TOF analyzers use the fact that m/z -values can be determined by measuring the velocity of the analyte ion after accelerating it to a defined kinetic energy. At a fixed kinetic energy smaller ions travel at higher speed than larger ones and consequently reach the detector earlier after passing the field-free drifting region L (Fig. 1-22). Nevertheless, two ions of the same mass and charge can show differences in flight time resulting in low mass resolution. These differences are mainly caused by dispersity of energies and initial direction of the ions. The most effective way to reduce this initial energy spread is by reflecting^[155] the ions under a small angle onto the detector. The short pulsed laser used in MALDI in combination with the ability to focus on small spot sizes in relation to the other dimensions of the ion source, result in ion generation comparable to a point source in space and time. These conditions are ideal for TOF analyzers making MALDI-TOF such a common combination^[156].

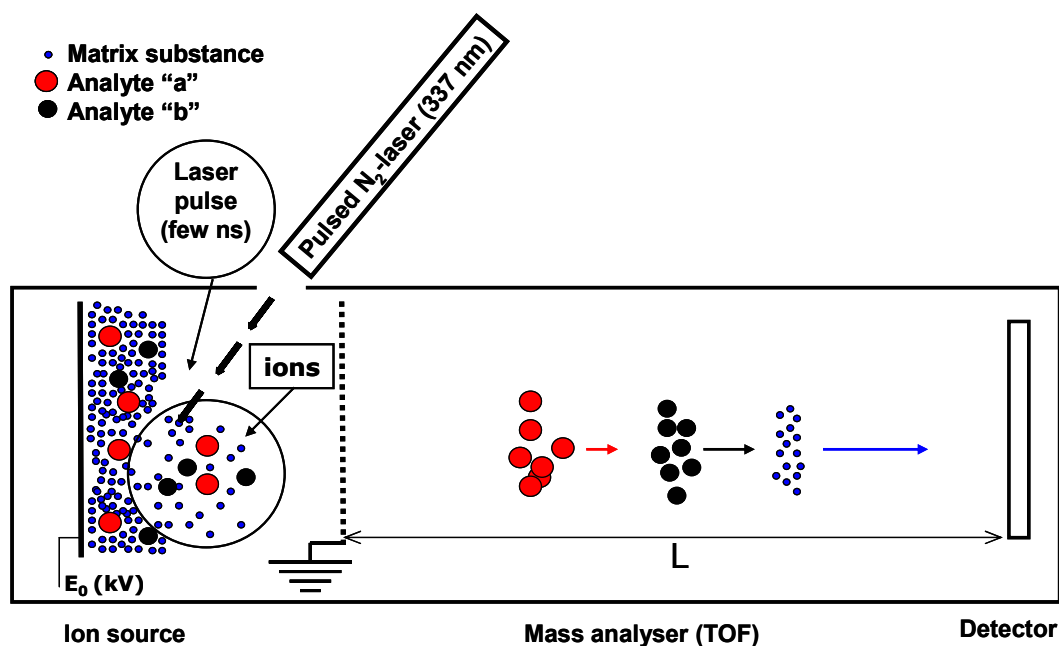


Fig. 1-22 Schematic of a linear MALDI-TOF Mass Analyzer

In carbohydrate analysis, ESI-^[157-160] and MALDI-MS^[161-164] are mostly used to determine the primary structure of oligosaccharides for gaining information about sequence and branching, linkage type and monosaccharide substitution patterns by fragmentation of selected ions^[165]. Tandem mass spectrometry is a valuable tool to characterize the structure of carbohydrates. A nomenclature for fragments of oligosaccharides was described by *Domon and Costello*^[166] in 1988. Due to the relatively poor signal intensities of underivatized carbohydrates, Girard's reagent T (introduced by *Naven and Harvey* in 1996^[167]) and glycidyltrimethylammonium chloride as charged tags were used by *Gouw et al.*^[168] enhancing the response in MALDI-TOF for small oligosaccharides. Besides intensity enhancement, labeling also influences fragmentation pathways thus offering additional structural information. *Harvey* intensively studied fragmentation of negatively charged oligosaccharides^[169-171].

For MS, polysaccharides must be partially degraded before analysis to gain oligosaccharides. *Tüting et al.* deduced on the effect of various synthetic procedures on the substituent distribution in cationic starch granules from the results obtained by ESI-MS² of enzymatically degraded samples^[172]. In 2004, *Tüting et al.*^[173] investigated how the substituent distribution of regioselectively O-methylated maltooligosaccharides influences the fragment ion pattern. *Adden and Mischnick*^[174] continued this study in 2005 and developed a quantitative method to use the fragments for the determination of the complete substitution pattern in the AGU of

both α - and β -(1 \rightarrow 4) linked glucose polymers. Their method is based on perdeuteromethylation of the free hydroxylgroups of O-methyl celluloses and amyloses. This step is followed by partial hydrolysis, tandem MS analysis and finally calculation of the distribution. The method requires MS² and MS³ data from both sodium and lithium adducts to obtain sufficient information for the evaluation.

Momcilovic et al. reported on an optimization of sample preparation for enzymatically degraded MC^[175] and CMC^[176] for MALDI-TOF analysis in 2003. They investigated different matrices and solvents and their combinations. In 2005, they reported on using MALDI-TOF and ESI-IT tandem MS to analyze acidic and enzymatically hydrolyzed cellulose ethers^[177,178] by coupling the reducing end with dimethylamine (DMA) forming a *Schiff base* and estimated the substituent distribution from the fragmentation pattern. Their approach is not quantitative due to the free hydroxyl groups, but it showed that the combination of DMA derivatization and tandem MS is a useful tool to gain information about enzyme selectivity. DMA enhanced the response significantly.

2 Scope of the thesis

The aim of this work is to determine the distribution of glucosyl units and its mono- to tri-O-carboxymethylated derivatives in the cellulose chain. Therefore, a strategy introduced by *Arisz et al.* ^[74] and by *Mischnick and Kühn* ^[77] for methyl ethers, and modified and applied to other types of derivatives in the last decade was followed. This so-called “oligomer analysis” comprises a random degradation of the polymer to oligomeric sequences and the quantitative mass spectrometric analysis of the substituent distribution within a certain DP (mainly 2, 3 and 4) after appropriate sample preparation ^[179]. The application of this strategy to CMC has to overcome some basic problems, such as the possible influence of substituents on the hydrolytic stability of the glucosidic linkages and the influence of the chemical structure (i.e. the various numbers of substituents and of the molecular mass) on ion yields and sensitivity in ESI-IT- as well as in MALDI-TOF-MS. Preliminary studies in our group on CM-glucoses and on CM-cellooligosaccharides by other groups showed that carboxymethyl groups enhance the response compared to unsubstituted glucosides ^[176]. Therefore, the DS is overestimated, an effect which can be partially overcome by dilution and which becomes less pronounced with increasing DP. In MALDI-TOF-MS analysis we observed less discrimination compared to ESI-IT-MS when investigating hydroxyalkyl oligosaccharides ^[81], but the ionization yield will also be influenced by structure and molecular mass.

Therefore, the following strategy should be applied within this thesis:

Monomer analysis: The determination of the CM-group distribution in the AGU is the basis for the interpretation of the substitution pattern on higher structural levels.

Partial degradation: Partial methanolysis and partial hydrolysis should be investigated with respect to their randomness and efforts should be made to improve the solution state of CMC in the reaction media to eliminate bias by uneven accessibility.

Mass spectrometry: To eliminate discriminating influences during ionization, analytes as chemically uniform as possible should be prepared.

3 Monomer analysis of CMC

Sample material (Tab. 3-1) was provided by Dow Wolff Cellulosics (DWC). The average DS (determined by titration) and the NaCl content were determined by DWC. The water content was determined gravimetrically (80 °C, 8 h).

Tab. 3-1 DS values, dry mass and NaCl content of the investigated CMC samples provided by DWC

	DS (DWC)	dry mass [w %]	NaCl [%] (DWC)
CMC 1	0.86	88.8	< 0.05
CMC 2	0.84	89.1	< 0.05
CMC 3	0.92	90.6	< 0.05
CMC 4	0.99	89.6	< 0.05

The monomer distribution of the four samples was determined after complete acid hydrolysis by CE-UV^[180,181] (chapter 3.2), HPAEC-PAD^[62,108,182,183] (chapter 3.3), and GLC-FID after reduction to HEC (chapter 3.4). The applied methods are discussed in comparison (chapter 3.5) and the monomer distribution is compared with statistical models to gain information on the relative reaction rates of carboxymethylation (chapter 3.6).

3.1 Complete acidic hydrolysis

The complete degradation of the polymer derivative to monomers is the central but also critical step in monomer analysis. A possible pathway is the hydrolytic cleavage of the glycosidic bonds, as they are less stable than the ether linkages of substituents and therefore no loss of the substituent is observed. Side reactions like the formation of hydroxymethyl furfural (HMF) or of reversion products may cause systematical errors. Acid catalyzed hydrolysis can be performed e.g. with sulfuric acid (H₂SO₄)^[184] or hydrochloric acid (HCl). TFA is a common hydrolyzing agent for methyl ethers of cellulose or starch^[74,77], but by ¹³C-NMR spectroscopy *Heinze*^[185] found that it was not appropriate to achieve a complete hydrolysis of CMC.

Kasulke et al.^[186] compared the hydrolysis of CMC and carboxyethyl cellulose (CEC) with sulfuric and trifluoroacetic acid (TFA). They investigated samples with DS values

between 0.63 and 1.36 (CMC) and 0.2 (CEC), respectively, and afterwards determined the amount of glucose enzymatically. Based on the statistical models from *Spurlin* ^[71] they calculated the theoretical yield of glucose (c_0) applying the ratios of $k_2 : k_3 : k_6$ 2.14 : 1.00 : 1.58 determined by Reuben ^[66]. For both acids, they found yields of 90 to 98 % monomers this way, but as only glucose could be determined directly and none of the substituted monomers these conclusions are of limited significance. As shown in Tab. 1-3 it is not possible to apply relative rate constants of other CMCs as they depend on the synthesis parameters and vary.

Well known for CMC is hydrolysis with perchloric acid, HClO_4 ^[62,66]. *Saake et al.* ^[183] found that the yield of O-CM-glucosides depends both on DS of the CMC and on acid. They compared HClO_4 and H_2SO_4 as degrading agents and investigated 10 different CMCs with DS values between 0.7 and 2.7. The monomer distribution was determined by anion exchange chromatography and pulsed amperometric detection (HPAEC-PAD). With increasing DS-values, the yield of O-CM-glucosides decreased for both acids, but the losses were more pronounced for sulphuric acid than for perchloric acid: For DS-values between 0.6 and 2.0 the yields were between 93 and 82 % for HClO_4 and 75 and 53 % for H_2SO_4 . The highest substituted CMC yielded only 58 % (HClO_4) and 30 % (H_2SO_4) monomers, respectively. However, *Saake et al.* did not observe any influence on the relative composition of the monomers, so these losses seemed to be non-specific and did not cause any discrimination. So they showed that perchloric acid hydrolysis is applicable for most CMC samples with industrially relevant DS-values. Therefore, perchloric acid hydrolysis was used throughout this thesis both for partial and total hydrolysis of CMC samples. The perchlorate was removed by precipitation with KOH (8.3.2.1), so neutral hydrolyzates were obtained.

Another degrading method is methanolysis with hydrogen chloride in methanol ^[72]. Methyl glucosides are obtained and thus non-reducing sugar derivatives. Furthermore, the CM-groups become methyl esterified hence nonionic. Methanolysis was also applied as partial degradation method within this work. In this case, HCl is removed by codestillation with methanol. The formation of retro products is more pronounced for methanolic HCl than for perchloric hydrolysis, as HCl is enriched during evaporation, while HClO_4 is neutralized with KOH and removed by filtration. A complete removal by repeated codestillation hence is crucial. Partially degrading

techniques and some aspects on the kinetics of hydrolysis as well as methanolysis are discussed in chapter 5.

3.2 CE-UV

The analysis of the monomers after complete hydrolysis with perchloric acid is performed based on the method developed for carboxymethyl starches^[109,180]. After reductive amination with the UV-active 4-aminobenzonitrile (ABN), the monomers are transformed to their corresponding *N*-*p*-cyanophenyl-1-amino-1-deoxy-*O*-carboxymethyl-D-glucitol derivatives and can be detected by UV-absorbtion (see 8.3.3). Quantitative analysis is based on the assumption that the response is equal for the respective monomers, as each monomer is labeled with a chromophore whose UV-activity is independent of the sugar component (no conjugation between the sugar component and the π -system of the tag)^[180]. An equal response factor could be experimentally proven amongst others for cellobiose, glucose, and xylose. For some of the corresponding CM-derivatives this was previously performed in our group. As analytes that migrate slower also show longer exposure time in the detector window, it is common in CE-UV analysis to divide the peak area by the migration time. A borate buffer is used as background electrolyte (BGE), introducing an additional charge into the molecule (Fig. 3-1).

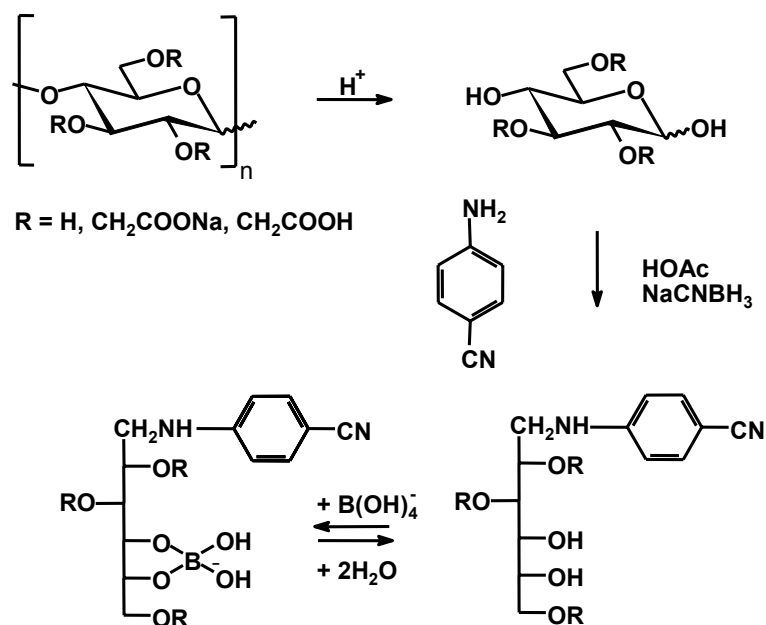


Fig. 3-1 Reductive amination of glucose and derivatives (after complete hydrolysis of CMC) with ABN and formation of the carbohydrate-borate-complex in the BGE

Due to the hindrance of the complex formation by the various substituents, the CM-glucitols are separated from each other. As the borate complex is also more stable with *cis*- than *trans*-diols, mannitols (resulting from hemicelluloses) can be separated from the corresponding glucitols. In this method, UV-detection occurs at the cathode. The anionic analytes are retarded and show longer migration times with increasing average charge. Therefore, *N*-*p*-cyanophenyl-1-amino-1-deoxy-D-glucitol passes the detector first, followed by the mono- and disubstituted monomers. The 2,3,6-tri-O-CM derivative shows the longest migration time (Fig. 3-2).

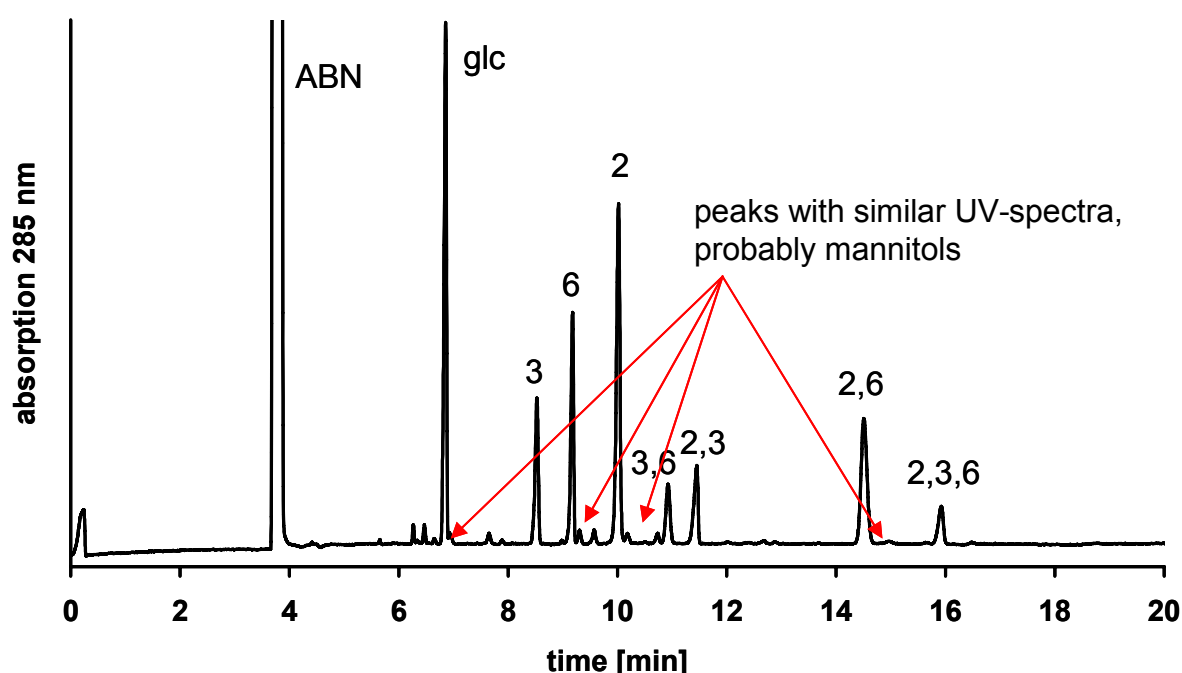


Fig. 3-2 Electropherogram of a total hydrolyzate (17 h, 95 °C, 1.5 M perchloric acid, 8.3.2.1) of CMC 4 (DS 0.99), reductively aminated with ABN (8.3.3), 1-(4-cyanophenyl)amino-1-deoxy-D-glucitols, peaks are assigned according to the positions of CM-substitution
CE-conditions: 175 mM borate buffer, pH 10.5, 28 kV, 25 °C (8.2.1)

Especially the peaks corresponding to the 2,3- and 3,6-di-O-carboxymethyl-D-glucitol derivatives were difficult to separate as they migrated very close to each other. Depending on the measurement parameters (buffer concentration, pH, and temperature); an overlapping of these peaks up to a reversion of the migration order when measured at 30 °C could be observed. At 25 °C, both peaks could be clearly separated but they were difficult to assign to the corresponding monomers as for the current set of samples, the amounts of the two monomers were quite similar. Therefore, the migration order of the peaks was controlled by co-injection of a CMS

hydrolyzate ^[109] (DS: 1.32) with known monomer composition. In this sample the amount of 2,3- is much higher than 3,6-di-O-CM-glucose, so the assignment of the peaks was possible (Fig. 3-3).

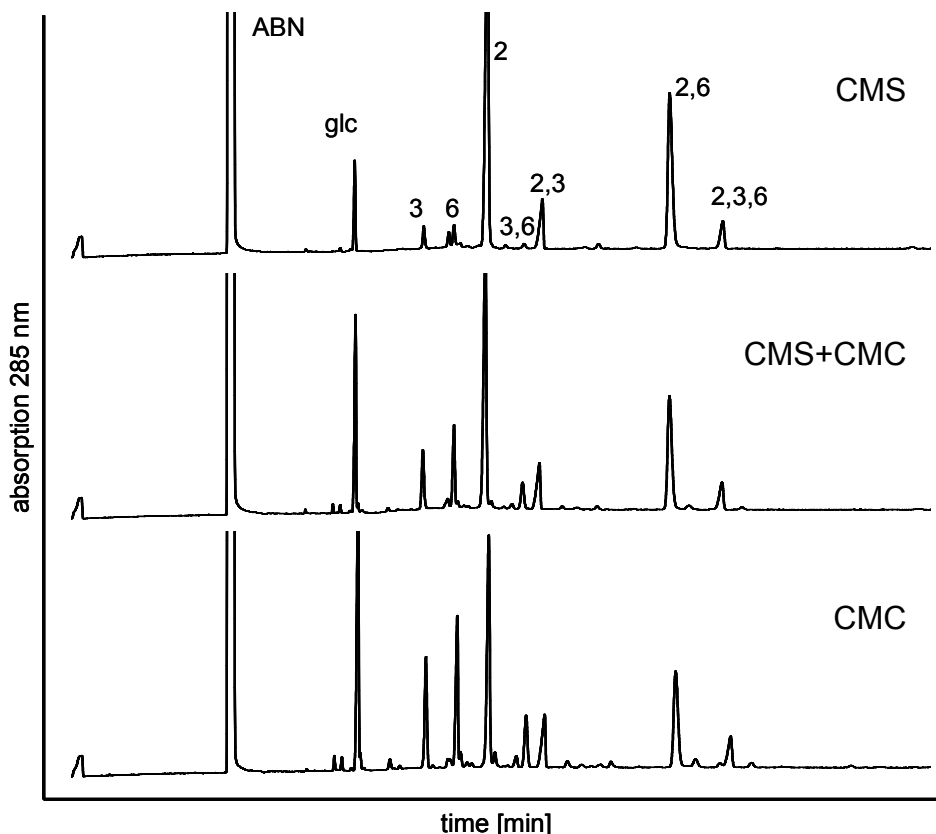


Fig. 3-3 Top: Electropherogram of a total hydrolyzate of CMS (DS 1.32) with known monomer distribution; labeled with ABN; 2,3-O-CM » 3,6-O-CM
Middle: Electropherogram of co-injection of a total hydrolyzate of CMC 4 and CMS, labeled with ABN; peak areas of 2-O- and 2,3-O-CM-glucose are relatively enhanced compared to CMC.
Bottom: Electropherogram of a total hydrolyzate of CMC 4, labeled with ABN
 CE-conditions: 175 mM borate buffer, pH 10.5, 28 kV, 25 °C

At the finally chosen measurement parameters (25 °C, 175 mM borate buffer, pH 10.5, see 8.2.1), the influence of the substituted position on the migration behaviour was multiplicative. This effect is also observed for the alditol acetates in GLC (3.4), although this is a completely different separating mechanism. The migration order for the monosubstituted monomers is $3 > 6 > 2$ accordingly $3,6 > 2,3 > 2,6$ for the disubstituted. In the electropherograms small peaks could be observed that do not correspond to the CM-glucose products (Fig. 3-2). DAD analysis showed that peaks migrating directly after the CM-glucose derivatives correspond to tagged components as well, as the UV-spectra were identical to those of the ABN-labeled CM-glucoses.

These peaks might correspond to hydrolysis products of hemicelluloses, as mannitols migrate slower than glucitols, or to oligomers. Another possible side reaction of CM-derivatives responsible for additional peaks is the formation of lactones. Other side reactions typical for aldoses in acidic media are β -eliminations due to enediol formation and oxosone formation^[187]. These reactions require a free carbonyl group and cannot proceed with already reduced aminated derivatives but during hydrolysis. If these side products such as hydroxymethylfurfural (HMF) have an accessible carbonyl group, they can be aminated hence detected in CE-UV as well but would show a different spectrum in DAD due to conjugation of the π -system. This was the case for the peaks migrating before glucose (around 6 min) and between glucose and 3-O-CM-glucose (8 min), so they probably result such products. An analysis with CE-MS could identify possible side products, but as CE-MS requires volatile buffer systems, a direct application of the borate buffer system is not possible. Volatile buffer systems such as formic acid do not have the ability to separate regioisomers like the borate buffer system hence it would be necessary to develop an appropriate buffer system first. This was not possible within this thesis. The yield of monomers after perchloric acid hydrolysis, determined with xylose as internal standard added directly to the sample before hydrolysis was between 81 and 85 %. This complies with the results obtained by Saake *et al.*^[183] for these hydrolysis conditions.

After hydrolysis (8.3.2.1), perchloric acid was removed by precipitation as potassium perchlorate after addition of aqueous KOH solution until neutrality and filtration. By cooling the sample to 4°C (refrigerator), the solubility of KClO₄ was further decreased; filtration and cooling were repeated until no more precipitation occurred. Nevertheless, weighting after freeze drying showed that still up to a tenfold excess of salt was present. The residue after freeze-drying was dissolved in water and an aliquot was reductively aminated (8.3.3). Perchlorate residues from an insufficient removal of the potassium perchlorate during sample preparation may have an influence on the reproducibility of the CE measurements, as the conductivity of the BGE is changed. Therefore, it was investigated whether this problem could be avoided by dissolving the sample after freeze-drying in methanol instead of water to avoid the dissolution of perchlorate. Therefore, CMC 4 was hydrolyzed and cleaned-up as described. After freeze-drying, the residue was divided. One part was dissolved in methanol, the other one in water before reductive amination. Fig. 3-4

shows the monomer distributions of both parts. The one dissolved in methanol after freeze-drying shows losses of the trisubstituted monomer which is obviously too polar to be dissolved in methanol due to the three CM-groups.

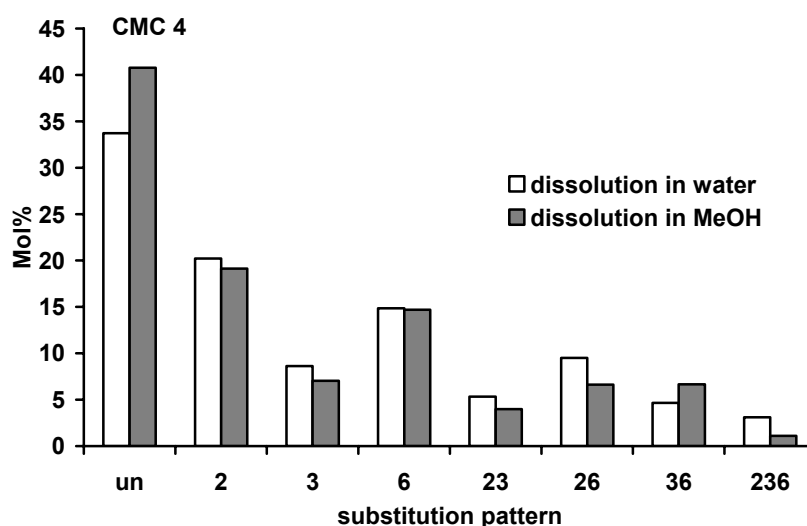


Fig. 3-4 Molar distributions of the CM-monomers obtained after hydrolysis (8.3.2.1) of CMC 4, determined after dissolution of the freeze-dried residue in methanol and water, respectively, reductive amination (8.3.3) and measurement by CE-UV (8.2.1).

So it is necessary to use water as solvent for the sample preparation after freeze-drying. The potassium perchlorate precipitate needs to be removed in advance by repeated cooling and precipitating steps, using as little amounts of cold water during filtration and flushing of the residue as possible to minimize the solubility of KClO_4 . This way, it was possible to get reproducible migration times and to avoid problems resulting from high salt contents.

It was also investigated, whether loss of sample material due to adsorption on the perchlorate precipitate occurred during the repeated filtration. Therefore, the monomer distribution and the yield of four differently prepared samples of CMC 4 were compared. For two samples, respectively, the potassium perchlorate was not additionally washed during filtration, whereas it was washed with cold water for the other two entries. The filtrate of the washing steps was investigated separately. All filtrates were freeze-dried, dissolved in water and filtrated again. The filtration after freeze-drying was investigated as described above. Afterwards, all samples were reductively aminated; xylose was added as internal standard to determine the yields. The total yields of all samples, no matter if flushed with cold water or not, were within

the same range: 83 % for the not washed and 81 % for the washed samples. The amount of monomers in the flushing solutions was too small to be determined. The loss of 2.4 % due to adsorption on the potassium perchlorate is thus not significant. It is more important, that no remarkable effects on certain monomers could be observed, this is crucial to avoid discrimination. Fig. 3-5 shows the molar distributions of the monomers of the flushed, and the not flushed sample, respectively. The average DS values are 0.97 for the flushed, and 0.95 for the not flushed reference, so the difference in the DS is within the experimental error. It can be seen in the graphic that glucose is not influenced by adsorption.

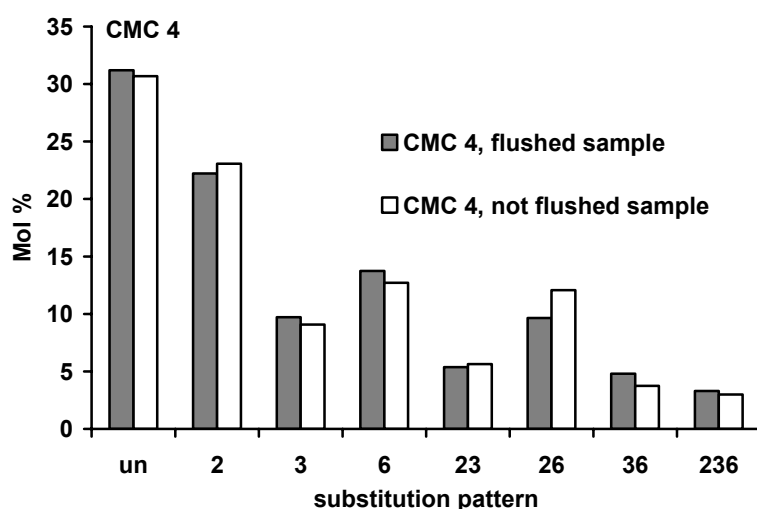


Fig. 3-5 Molar distributions of the monomers after hydrolysis (8.3.2.1) of CMC 4, determined with and without flushing the perchlorate residue during sample preparation, respectively, reductive amination (8.3.3) and measurement by CE-UV (8.2.1). Values are normalized to 100.

Small differences for the relative amounts of the substitution pattern can be seen, but with respect to the experimental set-up, they must not be overinterpreted. As the total yield is not enhanced by washing, and the total loss is only 2.4 %, the adsorptive effects on the CM-monomers are regarded as not significant.

Fig. 3-6 shows the molar distribution of the monomers obtained after complete degradation of the four investigated CMCs 1-4, normalized to 100. With max. ± 1.07 Mol% for 6-O-CM-glucose in CMC 4 the deviation between the double determinations (two different initial weights) is within the range of the standard deviation for this method.

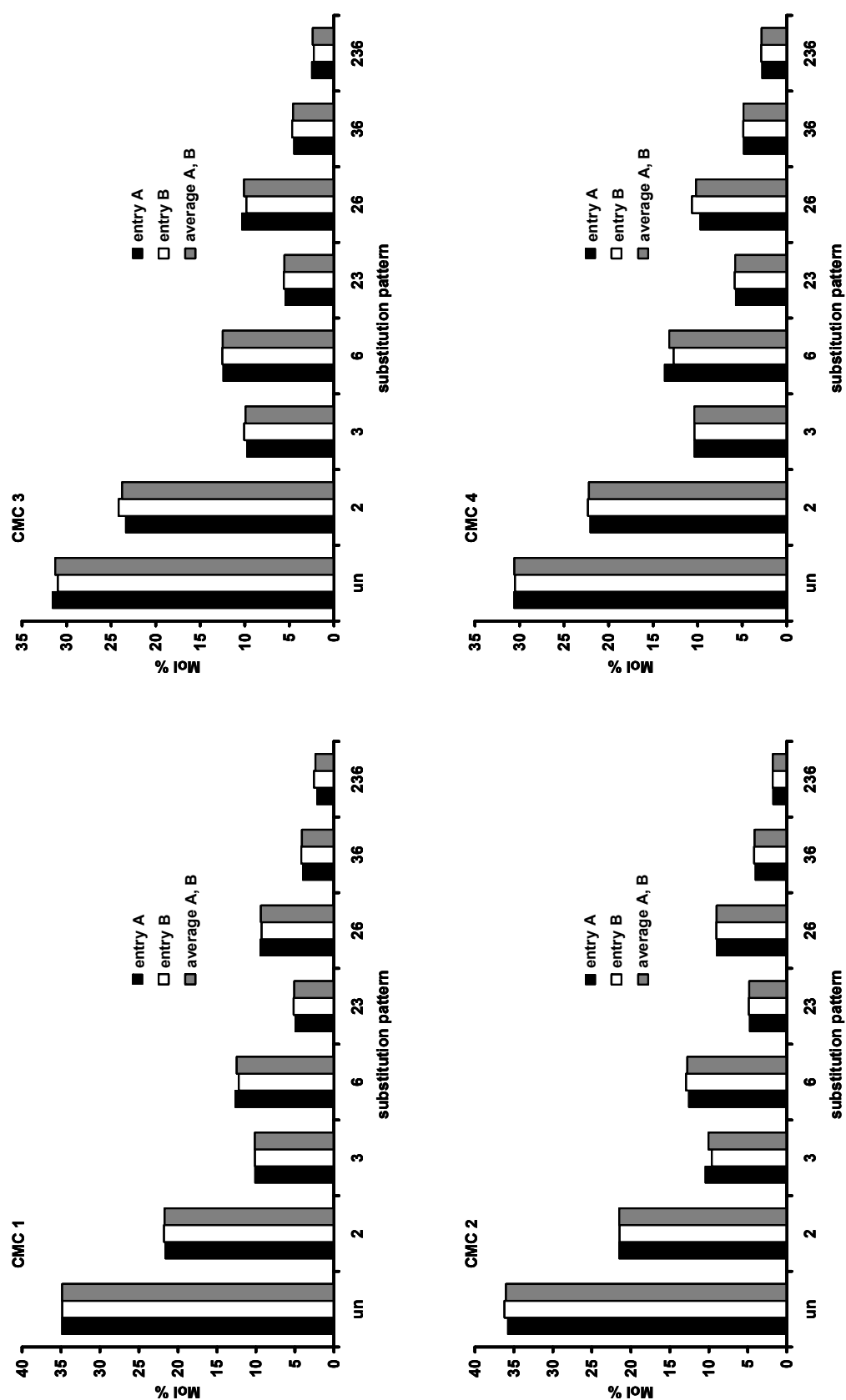


Fig. 3-6 Monomer composition (in Mol %) of CMC 1-4, determined after complete hydrolysis (8.3.2.1), reductive amination (8.3.3), and analysis by CE-UV (3.2). Molar distributions of two entries A and B analysed in parallel and their average are displayed.

Depending on the DS, the amount of glucose varies between 36 Mol % (CMC 2, DS 0.85) and 30 Mol % (CMC 4, DS 0.96). Displayed in Tab. 3-2 are the average s_i values of the CMC samples, the DS values and the monomer yield. With only about 2 % deviation, the DS values determined with CE-UV agree very well with those determined by DWC by titration. The amount of 2,3-di-O-CM-glucose is higher than of 3,6-di-O-CM-glucose, this complies with the partial DS values x_i .

Tab. 3-2 Molar distributions of the monomers released by complete hydrolysis of CMCs 1-4. Average values of duplicate determination. Monomer yield (Mol %, based on dry mass) was determined with xylose as internal standard

	CMC 1	CMC 2	CMC 3	CMC 4
s_0	34.86	36.01	31.28	30.56
s_2	21.70	21.48	23.76	22.20
s_3	10.12	10.04	9.91	10.37
s_6	12.44	12.76	12.47	13.21
s_{23}	5.07	4.81	5.55	5.79
s_{26}	9.36	9.01	10.08	10.19
s_{36}	4.09	4.11	4.58	4.86
s_{236}	2.36	1.78	2.38	2.82
c_0	34.86	36.01	31.28	30.56
c_1	44.27	44.28	46.14	45.78
c_2	18.52	17.93	20.20	20.84
c_3	2.36	1.78	2.38	2.82
x_2	0.38	0.37	0.42	0.41
x_3	0.22	0.21	0.22	0.24
x_6	0.28	0.28	0.30	0.31
DS	0.88	0.85	0.94	0.96
DS (DWC)	0.86	0.84	0.95	0.99
yield [Mol %]	81	84	83	85

3.3 HPAEC-PAD

The analysis of the four CMC samples with HPAEC-PAD including the sample preparation (perchloric acid hydrolysis) was performed in cooperation with Dr. Bodo Saake at the former Bundesanstalt für Holzforschung (BfH) (now van Thünen-Institut) in Hamburg, Germany.

The separation mechanism in HPAEC is based on the different affinities of the analytes to the quaternary ammonia groups of the weakly basic anion exchange material due to their different pK_a -values. Strongly basic eluents such as 100 mM

NaOH are used at the applied method ^[108,188] (8.2.7). The elution order in CMC monomer analysis is shown in Fig. 3-7.

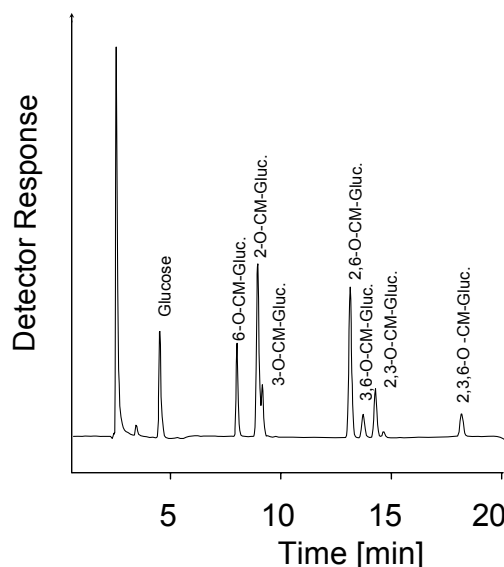


Fig. 3-7 HPAE chromatogram of a perchloric acid hydrolyzate of a CMC (DS 1.7) ^[183]

The affinity to the exchanger material depends on the charge of the analyte molecule and on its constitution, so it is possible to separate the regioisomers.

In Pulsed Amperometric Detection (PAD), analytes are oxidized according to their redox potential on a gold electrode; working electrode at the applied system is an AgCl-electrode. The detector response highly depends on the number of free hydroxyl groups in the analyte molecule, so glucose is displayed more intensely than the trisubstituted monomer. The response factors published by *Kragten et al.* ^[62] (Tab. 3-3) cannot be applied as the relative response depends on the state of the detector and is not linear ^[183]. Thus a calibration with standard substances is necessary. Standards of the mono- and disubstituted monomers were isolated from a CMC hydrolyzate by *Saake et al.* and their quantitative compositions were determined by ¹³C-NMR-spectroscopy ^[183]. These standards were used to evaluate the response factors at different potentials for the PAD. It could be observed that the PAD response depended on the concentration, very significantly for glucose and 6-O-CM-glucose. This dependence was less remarkable for the di- and trisubstituted monomers, as their responses were very small. Furthermore, the response factors decreased significantly with increasing substitution and also depended on the position of the CM-group. 6-O-CM-glucose and glucose were displayed more than twice as intense as 2-O-CM-glucose.

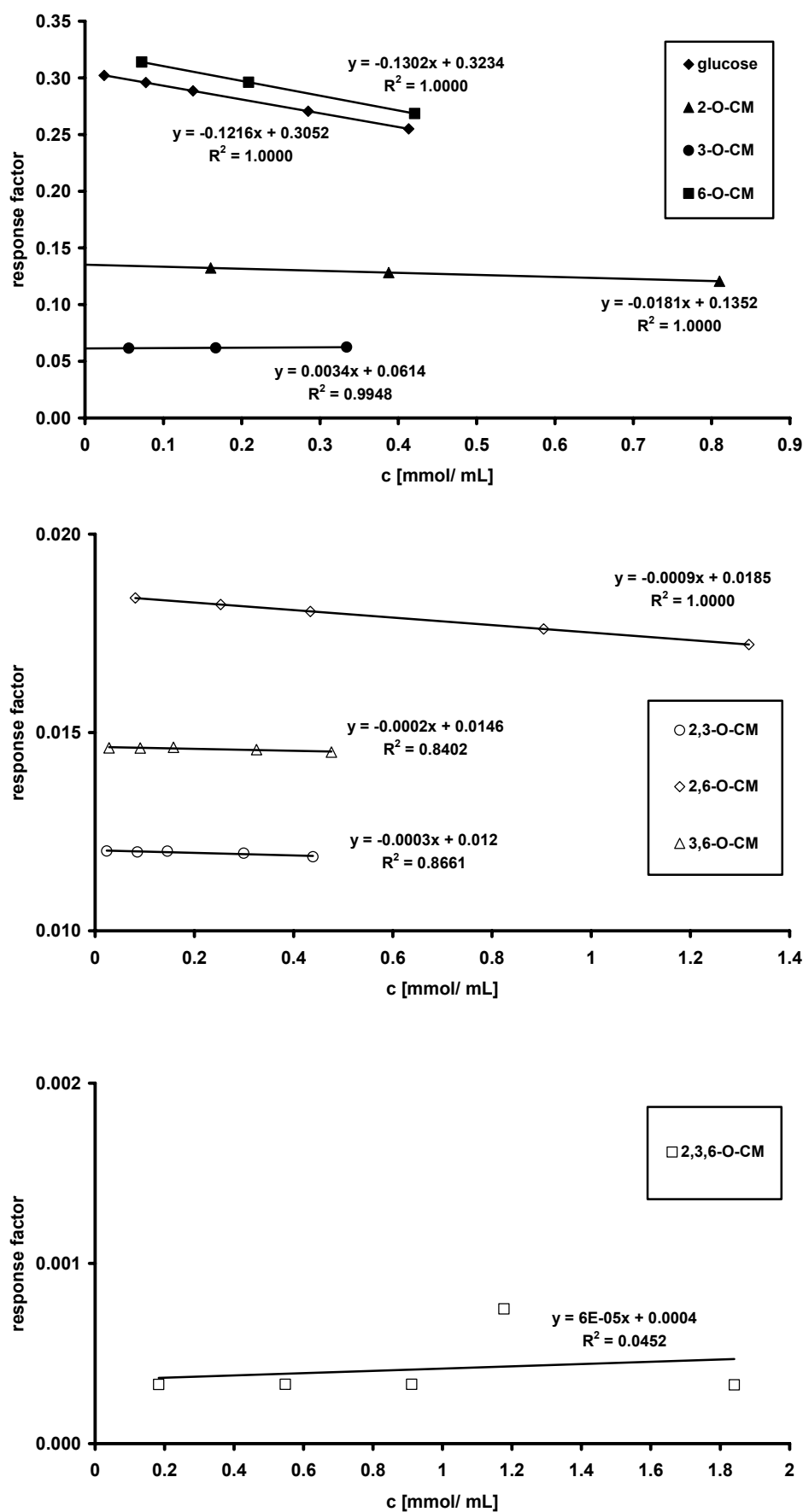


Fig. 3-8 Molar response factors for CMC hydrolysis products in PAD (0.1 V, conditions see 8.2.7) in dependence on the analyte concentration

The disubstituted components show only a tenth part of the intensity of the monosubstituted monomers and glucose was detected factor 1000 more intensively than 2,3,6-O-CM-glucose (Fig. 3-8). With response factors that high, even relatively small difference in integration lead to significant bias. The concentration dependence of the response factors is also a problem.

The response factors for the di- and trisubstituted monomers of the actual measurement differ significantly from those published by *Horner*, although except for the potential all parameters of the analysis were applied. For the analysis within this work, 0.1 V were applied to minimize the fouling of the electrode, but the variation of the potential (0.05 V as used by *Horner*) has only little influence and does not minimize the concentration dependence. The average response factors determined within this work are displayed in Tab. 3-3 compared to those published by *Kragten et al.* ^[62] and *Horner* ^[188] for a CMC with a DS of 1.2.

The various data agree only in the order of the detector response of $6 > 2 > 3$, the reasons for this great deviation could not be clarified.

Tab. 3-3 Molar response factors for CM-glucoses relative to glucose compared to those determined by *Horner* for a CMC hydrolyzate with DS 1.2 ^[188]

Monomer	PAD-response (0.1 V), applied for this analysis	PAD-response, (0.05 V)	PAD-response <i>Kragten et al.</i> ^[62]	PAD-response for a CMC with DS 1.2 <i>Horner</i> ^[188]
glucose	1.00	1.00	1.00	1.00
2-O-CM-glucose	0.45	0.45	0.71	0.67
3-O-CM-glucose	0.22	0.19	0.37	0.18
6-O-CM-glucose	1.03	0.81	0.77	0.80
2,3-O-CM-glucose	0.04	0.06	0.26	0.17
2,6-O-CM-glucose	0.06	0.09	0.38	0.35
3,6-O-CM-glucose	0.05	0.06	0.24	0.15
2,3,6-O-CM-glucose	0.001	0.007	0.20	0.03

First, the same hydrolyzates as for CE-analysis were measured, but in these samples (5 mg CMC/ mL) the amount of the trisubstituted monomer was underneath the detection limit. Therefore, perchloric acid hydrolysis had to be repeated with a higher initial weight (20 mg/ mL). The sample preparation varied from the procedure performed in CE analysis. Applying the method from *Horner*^[188], perchloric acid hydrolysis was performed only for 1 h at 120 °C (8.3.2.2, method B). The peaks of 2- and 3-O-CM-glucose were not baseline separated, this problem was already observed by *Saake et al.*^[183]. Due to the detector response the intensity of the peaks according to the disubstituted compounds was extremely small in comparison to those for glucose and the monosubstituted monomers. The four investigated CMC samples all have DS values ≈ 1 , so in contrary to the hydrolyzate of a CMC with a DS of 1.7 that is displayed in Fig. 3-7, not all monomers could be detected at one sample concentration. The amounts of glucose as well as mono- and disubstituted glucose were determined from a 1 : 10 diluted sample, while 2,3,6-tri-O-CM-glucose was determined from the original sample.

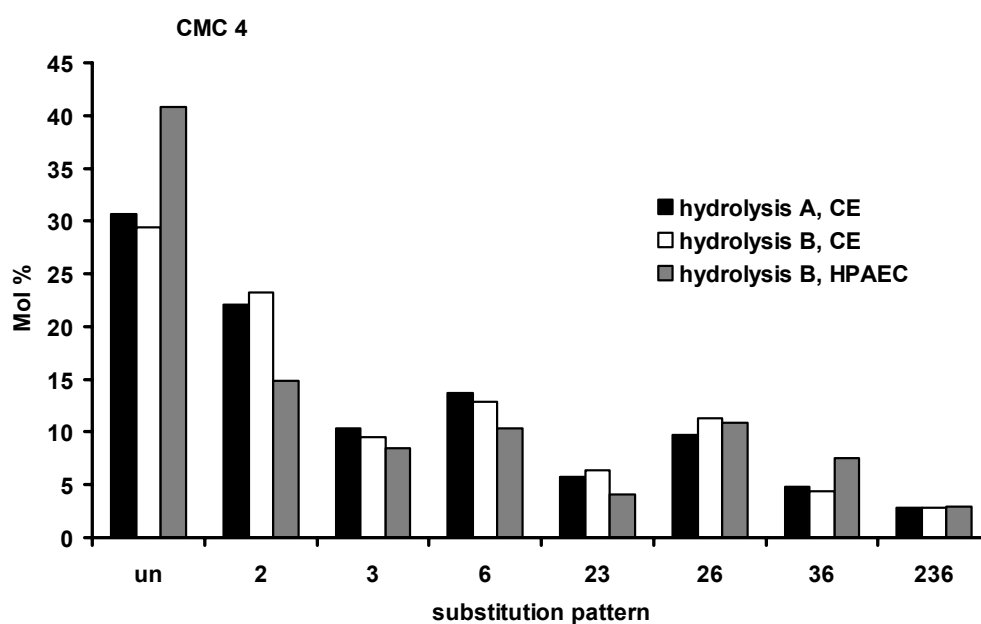


Fig. 3-9 Monomer composition (Mol %) of CMC 4, determined after hydrolysis A (8.3.2.1) and B (8.3.2.2), and measurement by CE-UV (labelling with ABN) and HPAEC-PAD, respectively

By external calibration with the standards (five point calibration curve) quantification of the monomeric compounds and determination of their yields were possible. The

total yield of the monomers was between 47 % (CMC 4) and 60 % (CMC 1-3). This is more than 20 % lower than found in CE analysis (8.3.2.1, method A).

To estimate the influence of the different hydrolysis conditions, the hydrolyzates from method B were reductively aminated and measured by CE-UV. Fig. 3-9 shows the monomer compositions of CMC 4. The deviation between the results obtained by HPAEC and CE of the same hydrolyzate is much higher than between the different hydrolyzates measured by CE-UV. So the influence of the varied hydrolysis conditions is not that significant as the instrumental set-up. Fig. 3-10 shows the molar compositions of the monomers from CMC 1-4, normalized to 100 %. The amount of glucose predominates with over 40 % significantly. The standard deviation between the two investigated entries A and B is with max. 3 % very low. Tab. 3-4 shows the average s_i -values of the CMCs 1 to 4, their DS values and their monomer yield. The DS values obtained by HPEAC are about 10 % lower than the ones determined by titration by DWC and by CE-UV (Tab. 3-2). The amount of 3,6-di-O-CM-glucose is apparently higher than 2,3-di-O-CM-glucose, although based on the partial DS values x_i an order of $2,6 > 2,3 > 3,6$ is expected and observed in CE-UV.

Tab. 3-4 Molar distributions of the monomers after complete hydrolysis of CMCs 1-4. Average values of duplicate determination. Monomer yield (Mol %, based on dry mass) was determined with standard substances ^[183] (external five point calibration)

	CMC 1	CMC 2	CMC 3	CMC 4
s_0	45.04	47.00	40.68	40.85
s_2	14.66	14.15	16.50	14.91
s_3	8.61	8.34	8.32	8.74
s_6	9.79	9.65	10.04	10.34
s_{23}	4.04	4.10	3.79	4.15
s_{26}	9.42	9.26	11.41	10.85
s_{36}	6.38	5.57	6.73	7.51
s_{236}	2.07	1.94	2.54	2.65
c_0	45.04	47.00	40.68	40.85
c_1	33.06	32.14	34.86	33.98
c_2	19.84	18.92	21.92	22.52
c_3	2.07	1.94	2.54	2.65
x_2	0.30	0.29	0.34	0.33
x_3	0.21	0.20	0.21	0.23
x_6	0.28	0.26	0.31	0.31
DS	0.79	0.76	0.86	0.87
DS (DWC)	0.86	0.84	0.95	0.99
yield [Mol %]	61	58	61	47

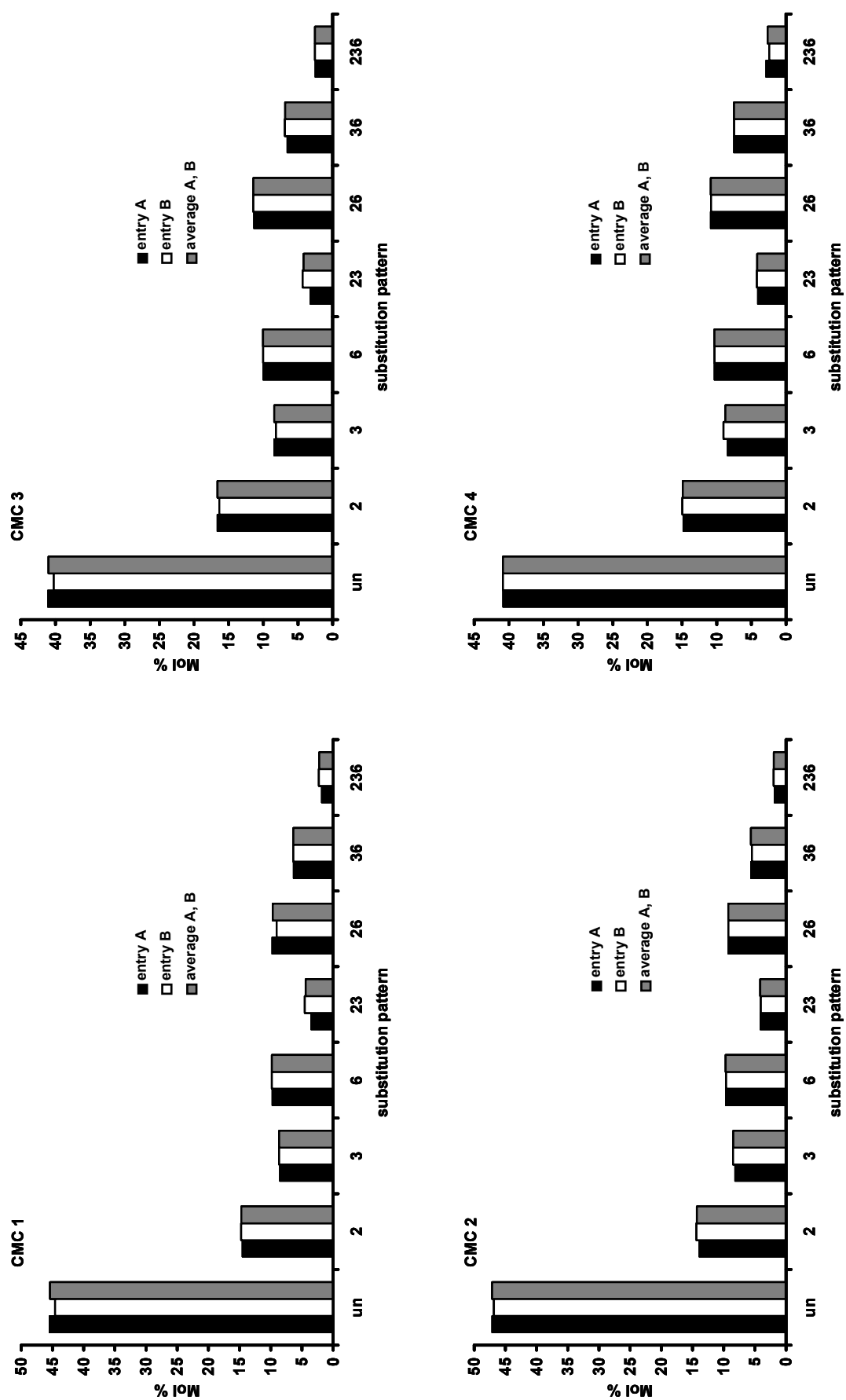


Fig. 3-10 Monomer composition (in Mol %) of CMC 1-4, determined after complete hydrolysis (8.3.2.2) and analysis by HPAEC-PAD (8.2.7). Monomer distributions of two entries A and B analysed in parallel and their average are displayed.

3.4 GLC-FID after reduction to HEC

Another approach in the determination of the distribution of the CM-groups in CMC described by *Ukai et al.* [131] is the analysis after reduction to hydroxyethyl (HE)-groups. This method might also be an interesting way for oligomer analysis, as the obtained HEC could be analyzed using MALDI-TOF-MS according to the method developed for HEMC [81]. Therefore, it is necessary that the reduction is quantitative; this is tested by IR-spectroscopy and GLC-FID.

The reduction of CMC to HEC was carried out by the method used by *Taylor* and co-workers for the reduction of the CM-groups of uronic acid residues in polysaccharides [132,133].

The reduction proceeds in two steps. First, CMC reacts with 1-ethyl-3-(3-dimethylaminopropyl) carbodiimide (EDC) at pH 4.75 to activate the CM-group. During the addition of NaBH_4 , pH is held constant at 7.00 with 4 mM aqueous HCl for reduction (Fig. 3-11). Finally, the reaction mixture is cleaned-up by dialysis over night.

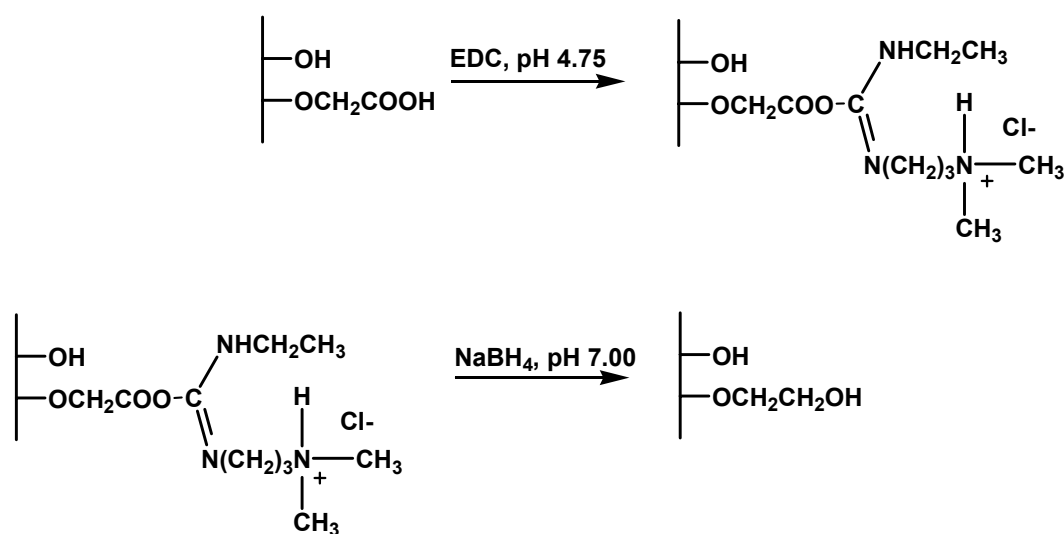


Fig. 3-11 Reduction of a carboxymethyl to a hydroxyethyl-group after activation with EDC

The reduction was repeated two times in a first series, and four times in a second set. The reduction progress was controlled by ATR-IR measurements, (decrease of the carbonyl valency vibration at 1590 cm^{-1}). Representative for the other three CMC samples the ATR-IR spectra of CMC 1 after two and four times of reduction are displayed in Fig. 3-12, compared to the original NaCMC and a HEC. Already after two reduction steps, the carbonyl absorption had decreased significantly. Two more reductions resulted in further improvement. The yield after four reduction steps was between 60 (CMC 1, 2, and 4) and 70 weight% (CMC 2, see 8.3.6.1). According to

the IR spectra in Fig. 3-12 a relatively high conversion rate could be concluded from the decrease of carbonyl band.

The reduced CMC (HEC) was further treated for analysis by GLC-FID. It was permethylated ^[129], then hydrolyzed, reduced and acetylated to get volatile analytes. The reduction to glucitols reduced the number of products since no α - or β -anomers are obtained. By the use of NaBD₄ as reducing agent the reducing end is marked, this allows the differentiation between the reducing and the non-reducing end in GLC-MS (Fig. 3-13).

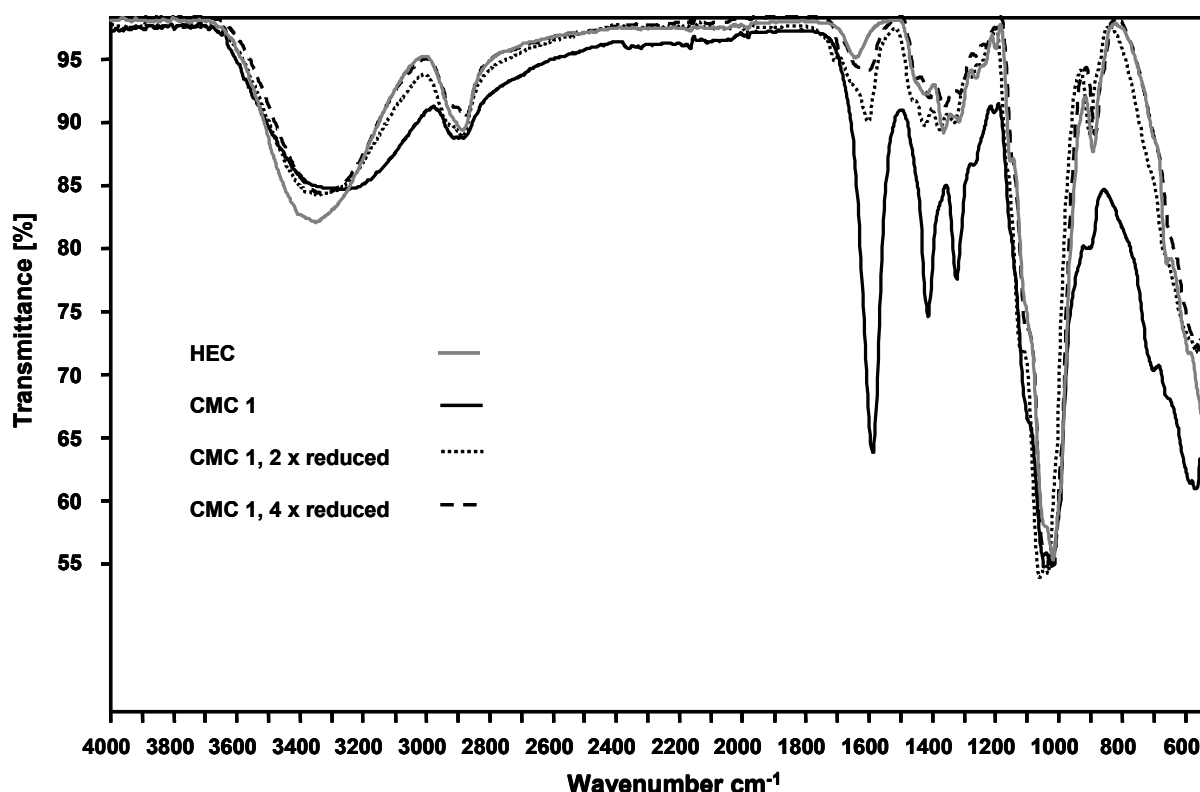


Fig. 3-12 ATR-IR spectra of CMC 1: underivatized and reduced twice and four times, respectively. HEC is displayed as reference.

The alditol acetates of CMC 1 to 4 were investigated by GLC-FID, the peaks were assigned by GLC-MS. The response factors for FID were evaluated based on the ECR-concept which takes the dependence of the molar response on the number and vicinity of carbon atoms into account ^[139,189,190]. ECR values are listed in the appendix (12.1). Fig. 3-14 shows the resulting chromatogram of CMC 1. In the chromatogram the peaks around 20 min could be assigned to incompletely methylated monomers, but no peak corresponding to the former 2,3,6-tri-O-CM-monomer was found. Several additional peaks that could not be assigned by GLC-MS were observed, so

the results of the ATR-IR spectra that the reduction of the CM- to HE-groups was not complete, were supported.

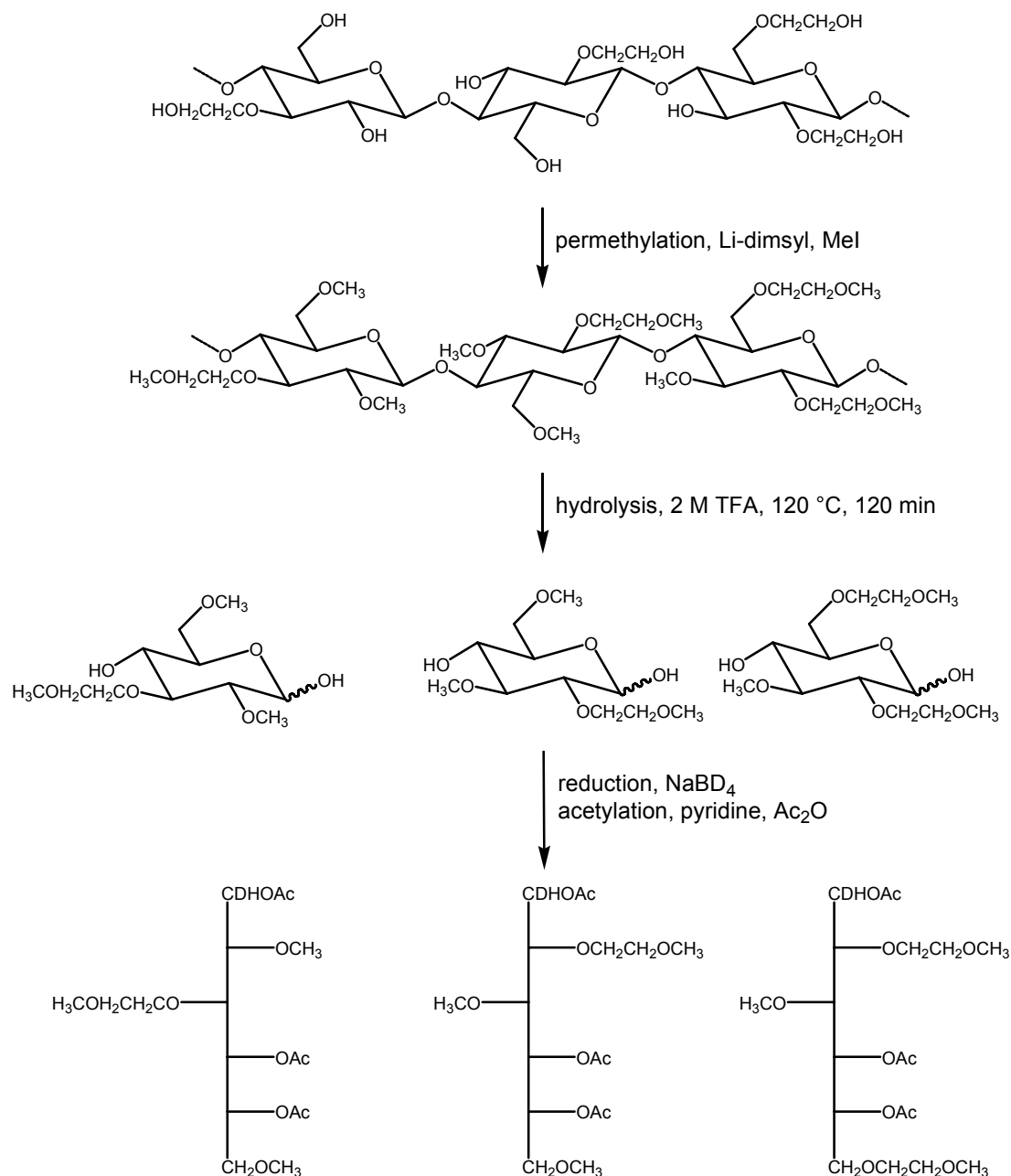


Fig. 3-13 Formation of the corresponding alditol acetates from CMC after reduction to HEC for GLC analysis.

Fig. 3-15 shows the molar distributions of the HE-monomers determined by GLC-FID. It can be seen that the unsubstituted monomer is with over 42 % significantly overestimated. Consequently, the obtained average DS-values are too low compared to those obtained by titration or CE-UV (Tab. 3-5).

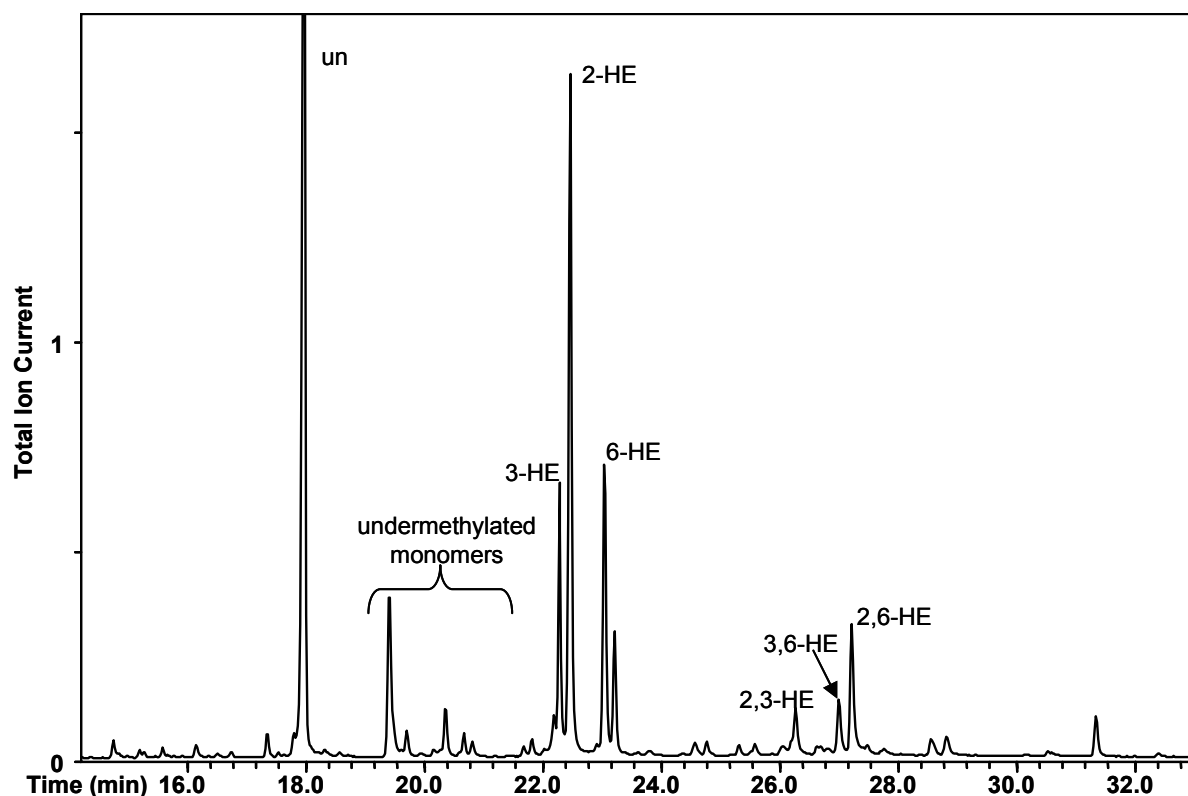


Fig. 3-14 Gas liquid chromatogram (MS) of CMC 1 after reduction of the CM-groups to HE-groups, hydrolysis, and derivatization to alditol acetates, peaks are assigned after MS analysis (see appendix 12.1).

Tab. 3-5 Molar distributions [Mol%] of the monomers released after complete hydrolysis of the four investigated CMCs 1-4 after reduction to HEC, normalized to 100. Monomers were converted to the corresponding alditol acetates. Correction factors for the FID are calculated based on the ECR-concept.

	CMC 1	CMC 2	CMC 3	CMC 4
s_0	42.04	44.05	43.36	44.71
s_2	22.50	23.34	24.09	26.58
s_3	10.00	11.01	10.64	11.96
s_6	9.76	9.21	9.57	8.25
s_{23}	3.84	3.22	3.54	1.24
s_{26}	8.70	6.74	6.20	4.64
s_{36}	3.17	2.43	2.61	2.62
s_{236}	0.00	0.00	0.00	0.00
c_0	42.04	44.05	43.36	44.71
c_1	42.26	43.56	44.30	46.79
c_2	15.71	12.39	12.35	8.50
c_3	0.00	0.00	0.00	0.00
x_2	0.35	0.33	0.34	0.32
x_3	0.17	0.17	0.17	0.16
x_6	0.22	0.18	0.18	0.16
DS	0.74	0.68	0.69	0.64
DS (DWC)	0.86	0.84	0.95	0.99

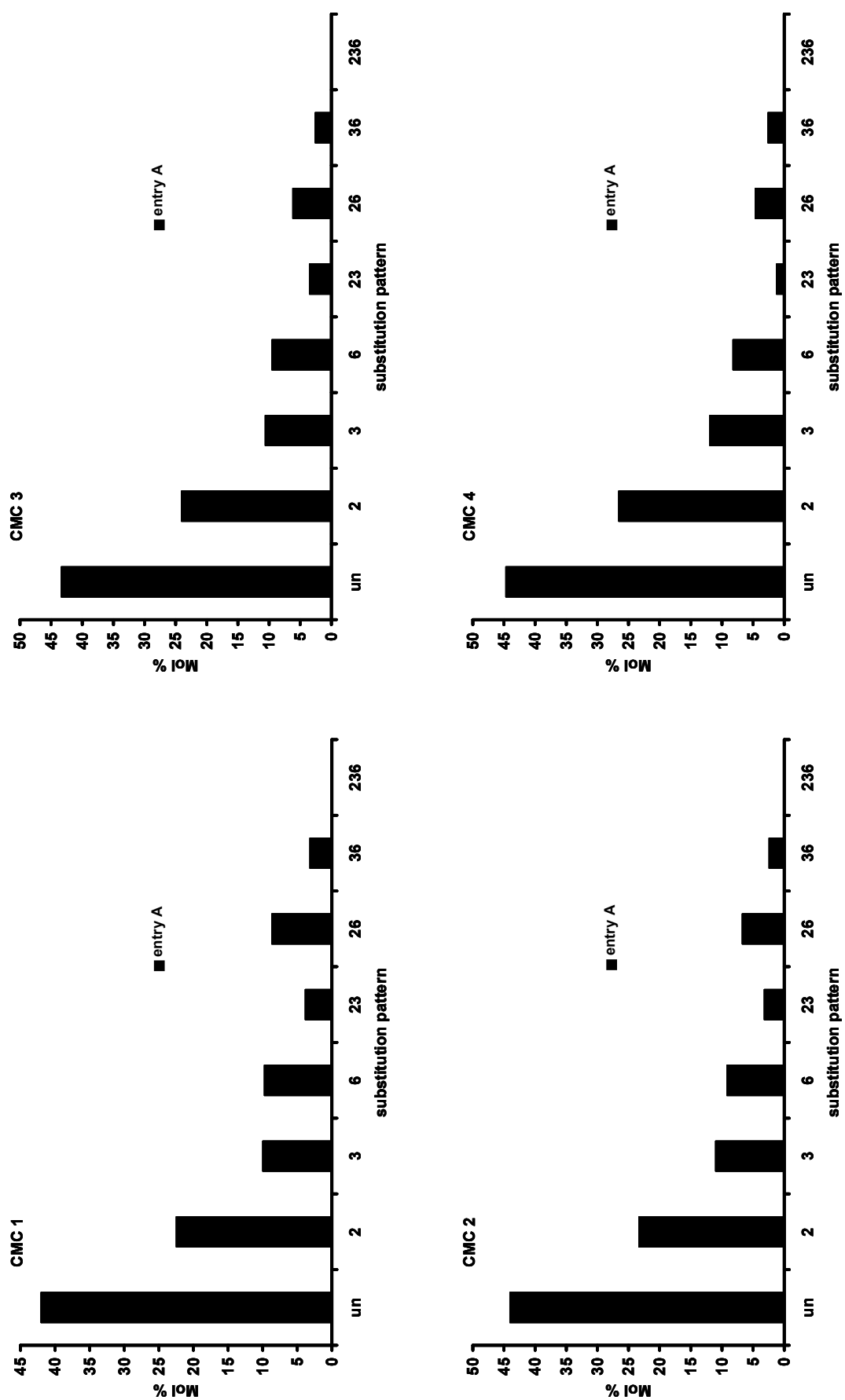


Fig. 3-15 Monomer composition (in Mol %) of CMC 1-4, determined by GLC-FID after reduction to HEC, complete hydrolysis (TFA, 120 °C, 20 min), and conversion to the corresponding alditolacetates. Response factors for FID are estimated based on the ECR concept.

The amount of 2,3-di-O-CM-glucose is higher than 3,6-di-O-CM-glucose, this complies with the partial DS values x_i and the CE-UV results.

Since the degree of reduction is not 100% and the exact stage of reduction cannot be determined quantitatively, no yields for the conversion to monomers can be calculated.

3.5 Comparison of the methods for monomer analysis

The monomer compositions (average values) of the four CMC samples determined by the three methods are shown in Fig. 2-19.

The analysis by GLC-FID after reduction to a HEC is very time-consuming and elaborate, and the reduction is not complete even after four repetitions. The yield after a four fold reduction is with 65 weight% relatively poor. Due to the fact that the trisubstituted monomer cannot be detected by GLC-FID, the average DS-values are too low and deviate by -14 % for CMC 1, -19 % for CMC 2, -27 % for CMC 3, and even -35 % for CMC 4 from the titration values. Due to the incomplete reduction and thus discrimination of higher substituted glucose, this method is not applicable and the results are not valid.

The analysis by HPAEC-PAD is fast and easy to perform. The deviation between the double determinations is very low and the retention times are reproducible. The monomer yield is with 60 % relatively low, which is in disagreement with the yield published for this kind of analysis (85 %) ^[183]. The different hydrolysis conditions though did not have an influence. The obtained DS-values deviate from those determined by DWC by titration - 8% for CMC 1, -10 % for CMC 2, -10 % for CMC 3, and -12 % for CMC 4. As the deviation from the average DS is relatively constant, there is no evidence for the suppression of individual monomers, at it is the case in GLC-FID. The response factors for the monomers differ significantly from those obtained by *Horner* ^[188] and *Kragten et al.* ^[62] and up to factor 1000 between the individual monomers. As the response in PAD was found to depend on the analyte concentration, the results are regarded as not valid.

CE-UV is quite time consuming in comparison with HPAEC, due to the removal of the perchlorate. The monomer yield for the longer hydrolysis (17 h) is with 80-85 % good.

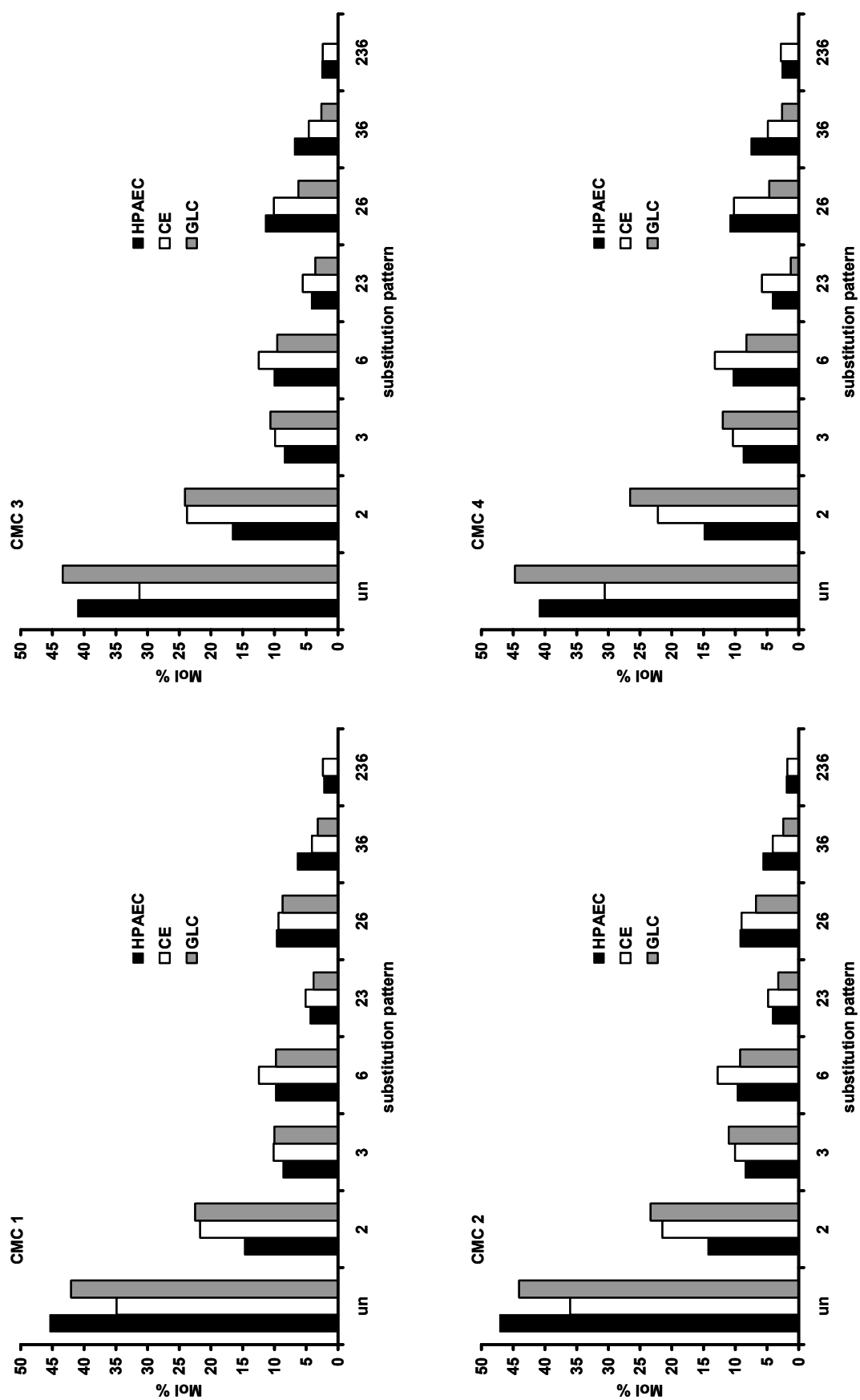


Fig. 3-16 Comparison of the monomer compositions (in Mol %) of CMC 1-4, by CE-UV (3.2), HPAEC-PAD (3.3), and GLC-FID after reduction (3.4).

CE-UV has the advantage that no calibration with standard substances is necessary as the relative molar response for tagged analytes is 1 independent of the substituent pattern. The standard deviation is very low and the migration times are reproducible. The average DS-values differ from those obtained by titration by +2 % for CMC 1, +1 % for CMC 2, -1 % for CMC 3, and - 3% for CMC 4. So from the three applied methods, the results obtained by CE-UV show the best agreement with the results from titration.

3.6 Comparison of the monomer distribution with statistical models

Tab. 3-6 shows the monomer composition obtained by CE-UV (see chapter 3.2) in comparison with the values calculated based on the models of Spurlin^[71] and Reuben^[66] (see chapter 1.6) and their deviation from the experimentally results. The heterogeneity parameter H_1 for the Spurlin-model is about 2 for all investigated CMCs, and thus in agreement with the model assumptions within experimental error (Tab. 1-3). The model from Reuben shows a slightly lower deviation with H_1 -values of max. 1.6, but this does not allow conclusions with respect to an influence of a primary substitution of position C-2 on reactivity in position C-3. The present CMCs reacted with a relative reactivity of $2 > 6 > 3$ during etherification.

Reactive rate constants k for the individual positions can be evaluated according to Spurlin^[71] from the experimentally obtained data by the simplified equation

$$-\ln(1-x) = k \quad (35)$$

The results are shown in Tab. 3-7.

According to Reuben^[191], the reactive rate constants can also be calculated by plotting $-\ln[p]$ against $-\ln[s_0]$ with k as slope. Based on the relation

$$p_i = e^{-Bk_i} \quad (36)$$

$$-\ln[p_i] = Bk_i \quad (37)$$

Tab. 3-6 Monomer composition of CMC 1 to 4 determined by CE-UV (average values of double determination), the substitution pattern based on the models by Spurlin and Reuben, and their deviation from the experimentally obtained data (Δ). All values in Mol%.

	CMC 1					CMC 2				
	CE	Spurlin	Δ	Reuben	Δ	CE	Spurlin	Δ	Reuben	Δ
s_0	34.86	34.58	0.27	33.94	0.92	36.01	36.07	-0.06	35.28	0.73
s_2	21.70	21.64	0.06	22.29	-0.58	21.48	21.26	0.22	22.06	-0.57
s_3	10.12	9.55	0.57	10.20	-0.08	10.04	9.44	0.60	10.23	-0.20
s_6	12.44	13.62	-1.17	13.36	-0.92	12.76	13.79	-1.03	13.49	-0.73
s_{23}	5.07	5.98	-0.90	5.33	-0.26	4.81	5.57	-0.75	4.77	0.04
s_{26}	9.36	8.52	0.84	8.77	0.58	9.01	8.13	0.88	8.43	0.57
s_{36}	4.09	3.76	0.33	4.01	0.08	4.11	3.61	0.50	3.91	0.20
s_{236}	2.36	2.35	0.01	2.10	0.26	1.78	2.13	-0.34	1.82	-0.04
c_0	34.86	34.58	0.27	33.94	0.92	36.01	36.07	-0.06	35.28	0.73
c_1	44.27	44.81	-0.54	45.84	-1.58	44.28	44.50	-0.22	45.78	-1.50
c_2	18.52	18.26	0.26	18.12	0.40	17.93	17.31	0.62	17.12	0.81
c_3	2.36	2.35	0.01	2.10	0.26	1.78	2.13	-0.34	1.82	-0.04
H_1	1.84				1.59	1.78				1.34
x_2	0.38					0.37				
x_3	0.22					0.21				
x_6	0.28					0.28				
DS (CE)	0.88					0.85				
DS (DWC)	0.86					0.84				
	CMC 3					CMC 4				
	CE	Spurlin	Δ	Reuben	Δ	CE	Spurlin	Δ	Reuben	Δ
s_0	31.28	31.85	-0.57	30.84	0.44	30.56	30.97	-0.41	30.16	0.39
s_2	23.76	22.84	0.92	23.86	-0.09	22.20	21.52	0.68	22.32	-0.12
s_3	9.91	9.20	0.71	10.21	-0.30	10.37	9.70	0.67	10.50	-0.13
s_6	12.47	13.33	-0.86	12.91	-0.44	13.21	13.96	-0.76	13.60	-0.39
s_{23}	5.55	6.60	-1.05	5.59	-0.04	5.79	6.74	-0.95	5.94	-0.14
s_{26}	10.08	9.56	0.52	9.98	0.09	10.19	9.70	0.48	10.06	0.12
s_{36}	4.58	3.85	0.73	4.28	0.30	4.86	4.37	0.49	4.73	0.13
s_{236}	2.38	2.76	-0.38	2.34	0.04	2.82	3.04	-0.22	2.68	0.14
c_0	31.28	31.85	-0.57	30.84	0.44	30.56	30.97	-0.41	30.16	0.39
c_1	46.14	45.38	0.77	46.98	-0.84	45.78	45.18	0.60	46.42	-0.65
c_2	20.20	20.01	0.19	19.85	0.36	20.84	20.82	0.03	20.74	0.11
c_3	2.38	2.76	-0.38	2.34	0.04	2.82	3.04	-0.22	2.68	0.14
H_1	2.11				0.77	1.75				0.65
x_2	0.42					0.41				
x_3	0.22					0.24				
x_6	0.30					0.31				
DS (CE)	0.94					0.96				
DS (DWC)	0.92					0.99				

Tab. 3-7 Reactive rate constants of CMC 1 to 4 for the positions C-2, C-3, and C-6, normalized to 1 ($k_i/(k_2+k_3+k_6)$)

	k_2	k_3	k_6
CMC 1	0.46	0.23	0.31
CMC 2	0.45	0.23	0.32
CMC 3	0.47	0.22	0.31
CMC 4	0.45	0.23	0.32

and the relation between B , s and p

$$s_0 = p_2 \cdot p_3 \cdot p_6 \quad (38)$$

$$s_0 = e^{-Bk_2} \cdot e^{-Bk_3} \cdot e^{-Bk_6} \quad (39)$$

$$s_0 = e^{-Bk_2} \cdot e^{-Bk_3} \cdot e^{-Bk_6} \quad (40)$$

$$-\ln[s_0] = Bk_2 + Bk_3 + Bk_6 \quad (41)$$

$$B = \frac{1}{k_2 + k_3 + k_6} \cdot -\ln[s_0] \quad (41)$$

the following equation is used to determine k :

$$-\ln[p_i] = \frac{k_i}{k_2 + k_3 + k_6} \cdot -\ln[s_0] \quad (42)$$

The values for $-\ln[1-x_i]$ ($=-\ln[p_i]$) and $-\ln[s_0]$ for the set of CMC 1 to 4 are listed in Tab. 3-8.

Tab. 3-8 Values for $-\ln(1-x_i)$ and $-\ln(s_0)$ for CMC 1 to 4.

	$-\ln(1-x_2)$	$-\ln(1-x_3)$	$-\ln(1-x_6)$	$-\ln(s_0)$
CMC 1	0.49	0.24	0.33	1.05
CMC 2	0.46	0.23	0.32	1.02
CMC 3	0.54	0.25	0.35	1.16
CMC 4	0.53	0.27	0.37	1.18

Fig. 3-17 shows the plot of $-\ln(1-x_i)$ against $-\ln(s_0)$ for CMC 1 to 4. The slopes of the linear regressions are the k -values for this set of CMCs.

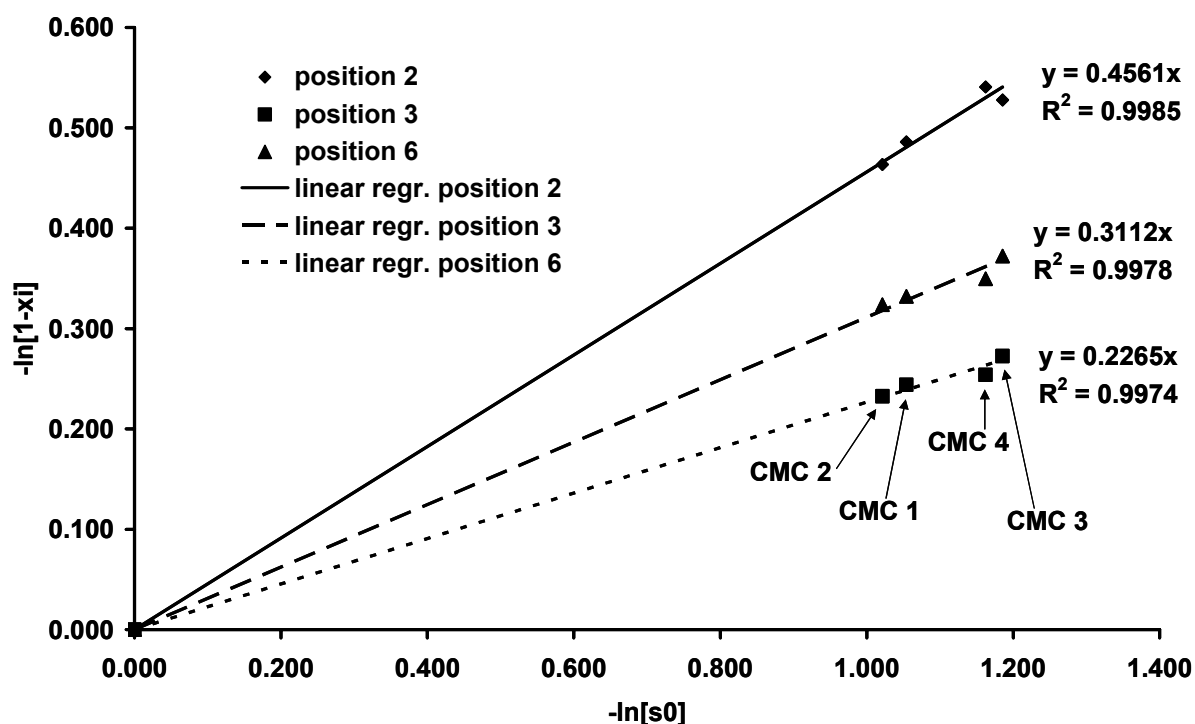


Fig. 3-17 Plot of $-\ln(1-x_i)$ and $-\ln(s_0)$ for CMC 1-4. The slopes of linear regressions are the k -values for the individual OH-positions determined for the four CMCs.

As can be seen, the regression coefficients show a good agreement between the linear regressions and the values from CMC 1 to 4.

So it can be concluded that the reactive rate constants are equal for the present set of samples, as is already obvious from Tab. 3-7. The averaged k -values determined from the whole set of samples plotted in Fig. 3-17 are used to envisualize the differences in the reactivities of the individual CMCs, as it is described in chapter 1.6. For this model, the slopes of the linear regressions of Fig. 3-17 are normalized to 1, as only the relative ratios of the reactive rate constants to each other are considered (Tab. 3-9). The obtained k -values are in agreement with those published by other groups for CMC, displayed in Tab. 1-3.

Tab. 3-9 Averaged reactive rate constants for the positions C-2, C-3, and C-6, determined for the set of CMCs 1 to 4 according to Fig. 3-17, normalized to 1

	$k_i/(k_2+k_3+k_6)$	k_i/k_2	k_i/k_3	k_i/k_6
position 2	0.46	1.00	2.01	1.47
position 3	0.23	0.50	1.00	0.73
position 6	0.31	0.69	1.37	1.00

With this set of k -values, the following plots in Fig. 3-18 to Fig. 3-22 are formed, showing the corresponding monomer composition [Mol%] to a certain DS for the etherification of CMC 1 to 4. The values resulting from CMC 1 to 4 are marked. The agreement of the individual results to the lines based on the averaged k -values shows the very similar reactivities of the four CMCs.

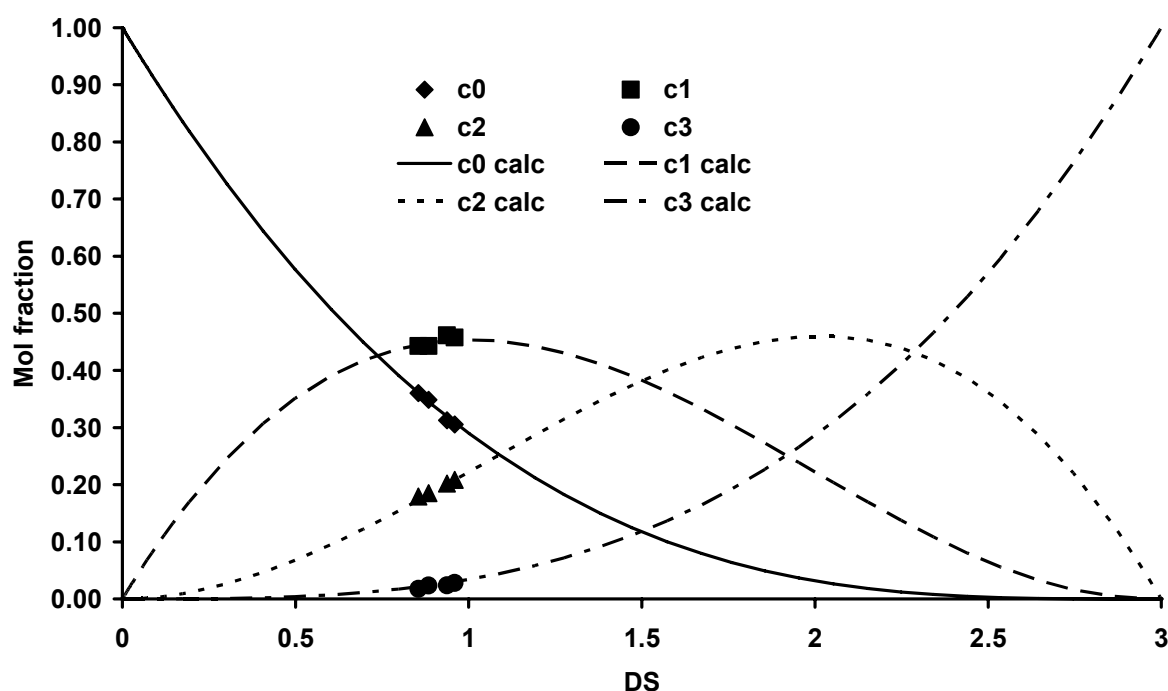


Fig. 3-18 Experimentally obtained c -values for CMC 1 to 4 by CE-UV and calculated c -values for the course of etherification, evaluated according 1.6

Fig. 3-19 shows the plot for the x -values. They are key input values of the model and therefore of the calculated values. Strong deviations in this plot would indicate that not all samples included follow the same reaction rates.

Fig. 3-18 gives an overview about the distribution of un-, mono-, di- and trisubstituted units depending on DS with a very good agreement of the model with the experimental data. Deviations from the model increase somewhat for the monomers which are less contributing to the entire polymer (s_3 , s_6 , s_{23} and s_{36} , Fig. 3-21 and Fig. 3-22).

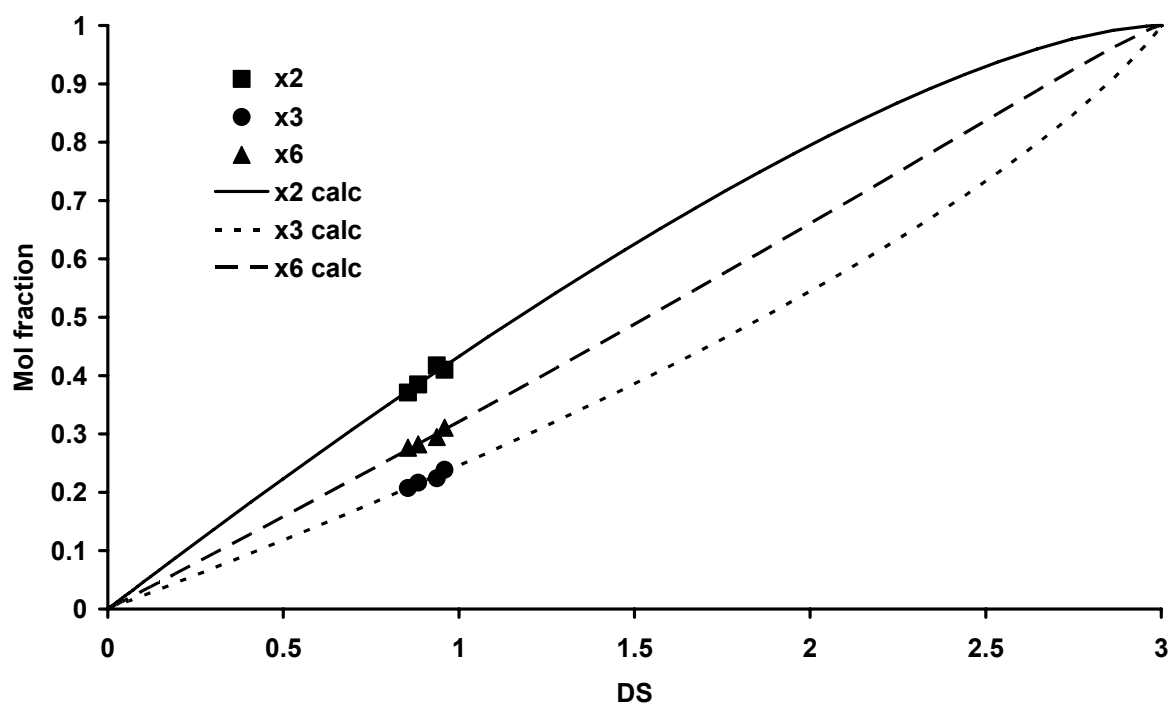


Fig. 3-19 Experimentally obtained x-values for CMC 1 to 4 by CE-UV and calculated x-values for the course of etherification, evaluated according 1.6

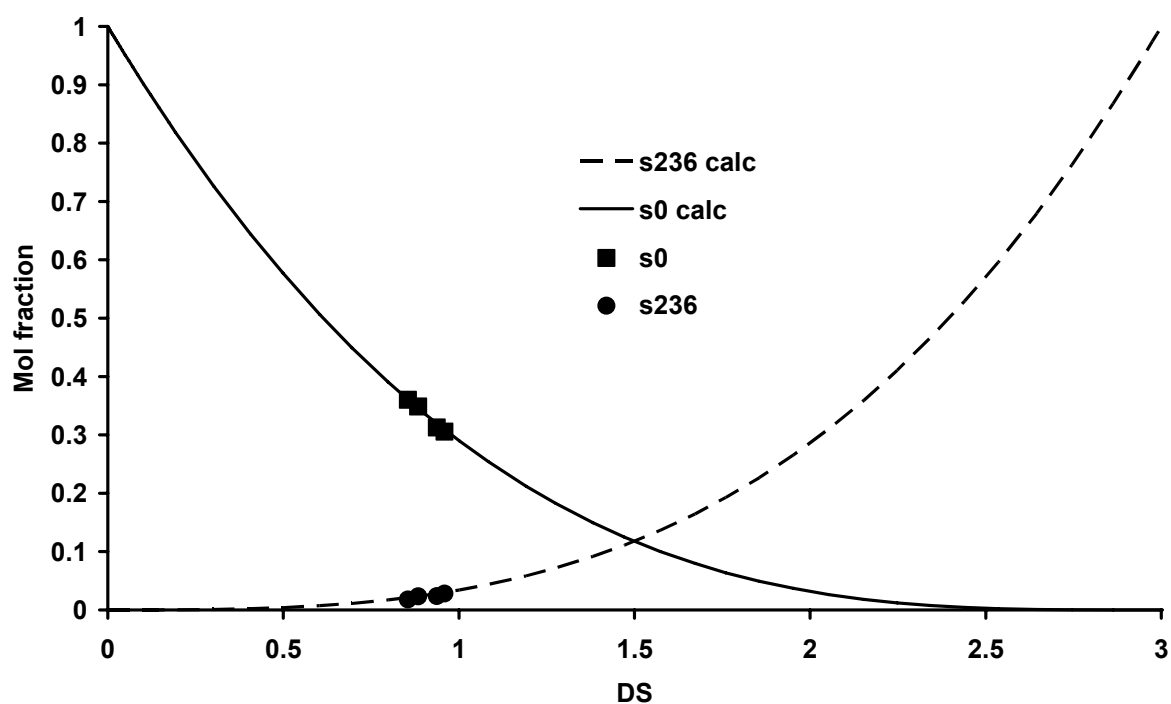


Fig. 3-20 Experimentally obtained s-values for CMC 1 to 4 by CE-UV and calculated s-values for the un- and trisubstituted monomers for the course of etherification, evaluated according 1.6

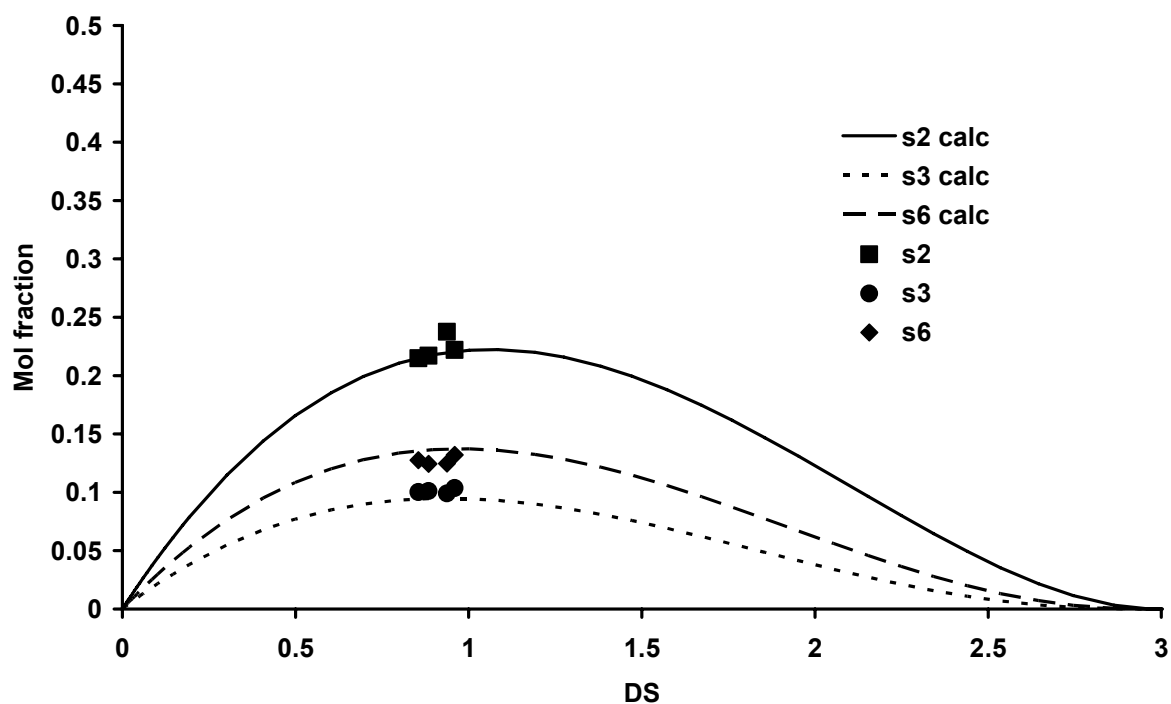


Fig. 3-21 Experimentally obtained s-values for CMC 1 to 4 by CE-UV and calculated s-values for the monosubstituted monomers for the course of etherification, evaluated according 1.6

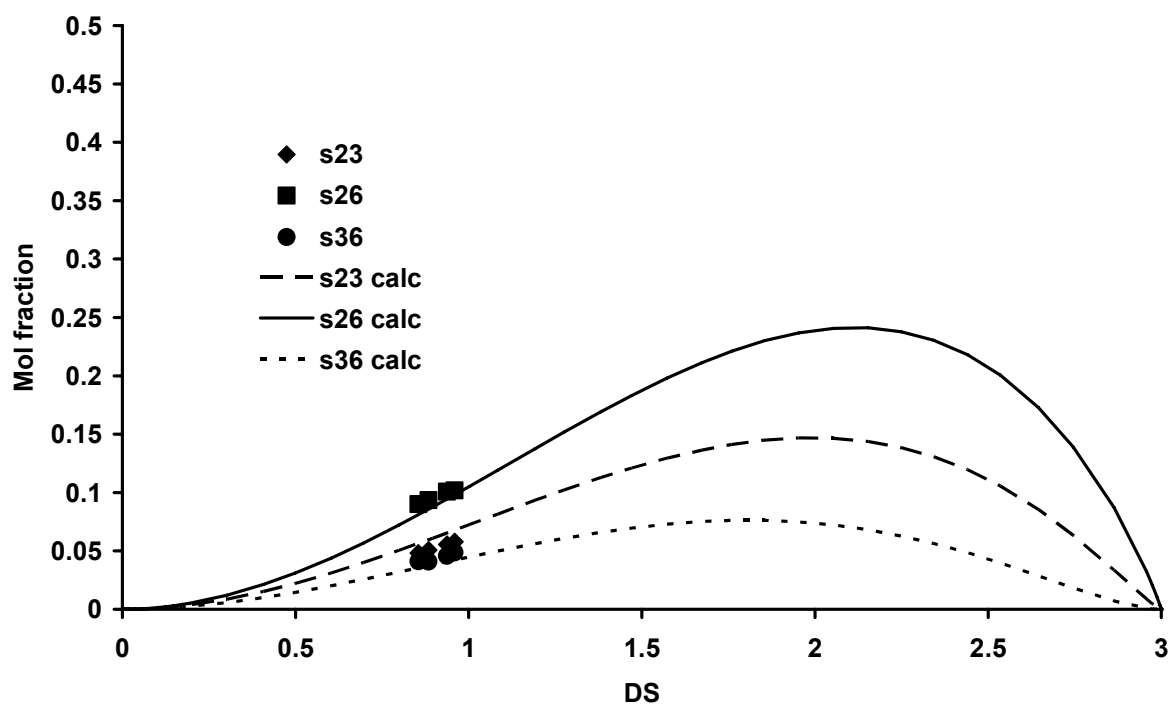


Fig. 3-22 Experimentally obtained s-values for CMC 1 to 4 by CE-UV and calculated s-values for the disubstituted monomers for the course of etherification, evaluated according 1.6

4 New approaches in oligomer analysis for CMC

Besides the analysis of the monomers, oligomer analysis is important to gain information about the distribution of the substituents over the polymer backbone. The aim of this work was to develop a method for the oligomer analysis of CMC based on the method for aliphatic ethers such as HEC^[80] or HEMC^[81]. The strategy introduced by *Arisz et al.*^[74] and by *Mischnick and Kühn*^[77] for methyl ethers in the mid nineties comprises a random degradation of the polymer to oligomeric sequences, the quantitative mass spectrometric analysis of the substituent distribution within a certain DP (mainly 2, 3 and 4) after appropriate sample preparation, and statistical evaluation. Application of this strategy to CMC has to overcome some basic problems: influence of chemical structure, i.e. the various numbers of substituents, and of the molecular mass on ion yields and relative sensitivities in mass spectrometry and the probable influence of substituents on the hydrolytic stability of glucosidic linkages. Preliminary studies in our group on CM-glucoses and of CM-cellooligosaccharides have shown that CM-substitution enhances the response in mass spectrometry. Therefore, the DS is overestimated in ESI-MS, an effect which can be partly overcome by dilution and which becomes less pronounced with increasing DP. The aim was to create products as chemically uniform as possible to minimize these effects by substituting the free hydroxyl groups.

4.1 Formation of chemically uniform products after degradation

In a first approach, partial degradation of CMC was performed by methanolysis. The advantage of methanolysis is the formation of CM-methyl esters and methyl glycosides, thus neutral products. This is of advantage for further derivatization steps and the sample clean-up process. In addition, a mixture of sodium salt and free acid in mass spectrometry is avoided, thus the complexity of the positive mode mass spectra (Fig. 4-1) is reduced. A drawback of methanolysis is the heterogeneity of this process: CMC is not soluble in methanol. Thus methanolysis is a potential source for discrimination. To avoid the formation of supramolecular structures during the degradation, a concentration of 2 mg CMC/ mL methanolic HCl

was chosen. After the removal of HCl by repeated co-distillation the sample is filled up to 1 mL with methanol before measurement (see 8.3.5)

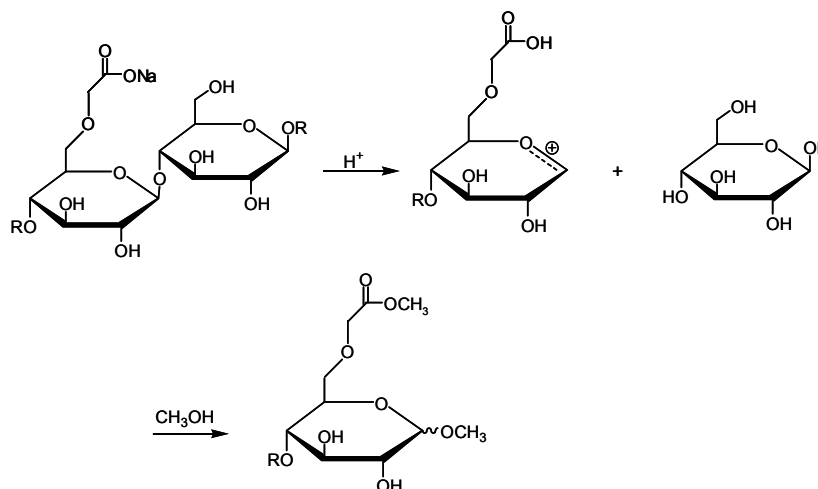


Fig. 4-1 Schematic of methanolysis, formation of the neutral methyl glucosides and methyl O-methoxycarbonyl celooligosaccharides

Fig. 4-2 shows the ESI-IT-mass spectrum of partially methanolized CMC 1, the m/z -values correspond to $[M + Na]^+$ of the oligomers up to DP 3. Unsubstituted compounds are discriminated: No peaks corresponding to the unsubstituted monomer (217 m/z) or unsubstituted dimer (379 m/z) could be detected. Therefore, DS-values evaluated from this data are overestimated.

In Fig. 4-3, the experimentally obtained data for DP 2 from the methanolizates of CMC 1 (2 mg/mL) in three states of dilution are compared with a statistical distribution based on Bernoulli statistics from the CE data of the monomer analysis. For the evaluations, the areas of $[M]$, $[M+1]$, (and $[M+2]$ when of sufficient intensity) were considered. The DS for DP 2 (1.54) deviates + 75 % from the DS by monomer analysis with CE-UV (0.88). For DP 3, (DS 1.31) the deviation is + 49 %. Therefore, the deviation from the statistical data is too high to be interpreted with respect to a possible heterogeneity.

Dilution has a somewhat positive effect: in the 10fold dilution, the DS for DP 2 is 1.47 (DP 3: 1.28) and in the 100fold dilution it is 1.39 (DP 3: 1.27), which is still 67 % (DP 3: 45 %) and 58 % (DP 3: 44 %) too high. A derivatization step is necessary to eliminate effects such as different ion complexation abilities and polarities. Previous investigations showed that it is very difficult to achieve peretherification of CMC, thus acylation was carried out after a partial degradation of the CMC by methanolysis.

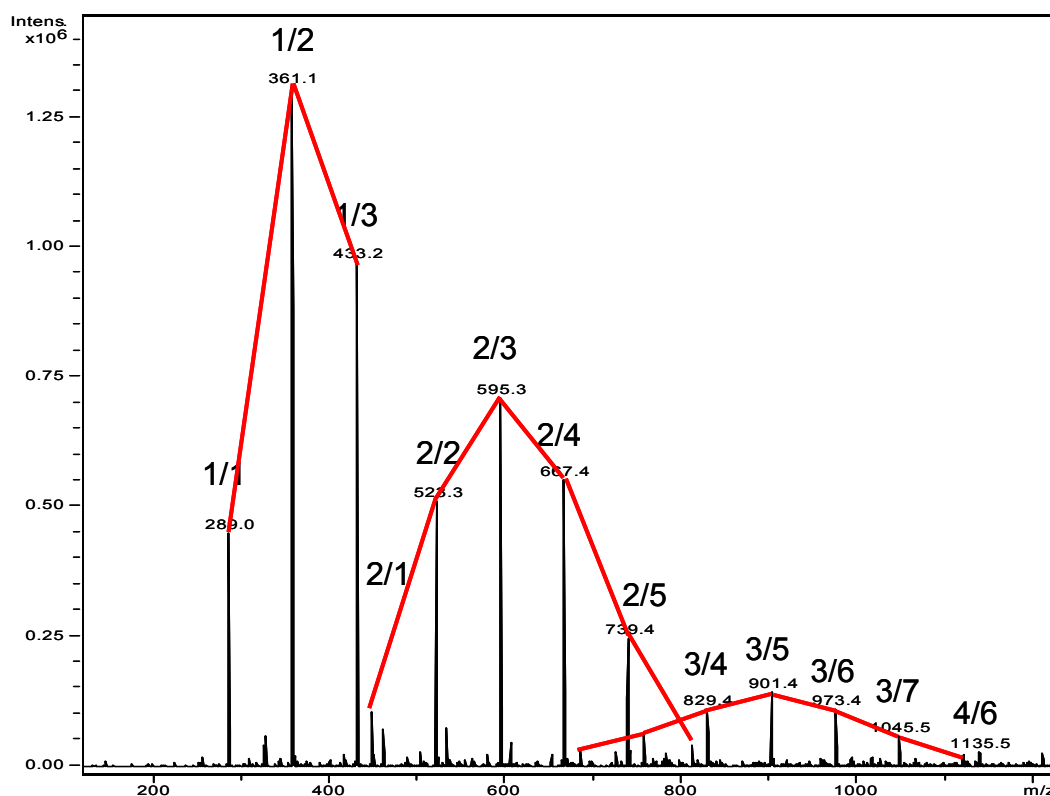


Fig. 4-2 ESI-IT-mass spectrum of the methanolyzate of CMC 1 (0.2 mg/ mL methanol), peaks are assigned according to their DP and the number of CM-groups: DP/n(CM), $[M + Na]^+$

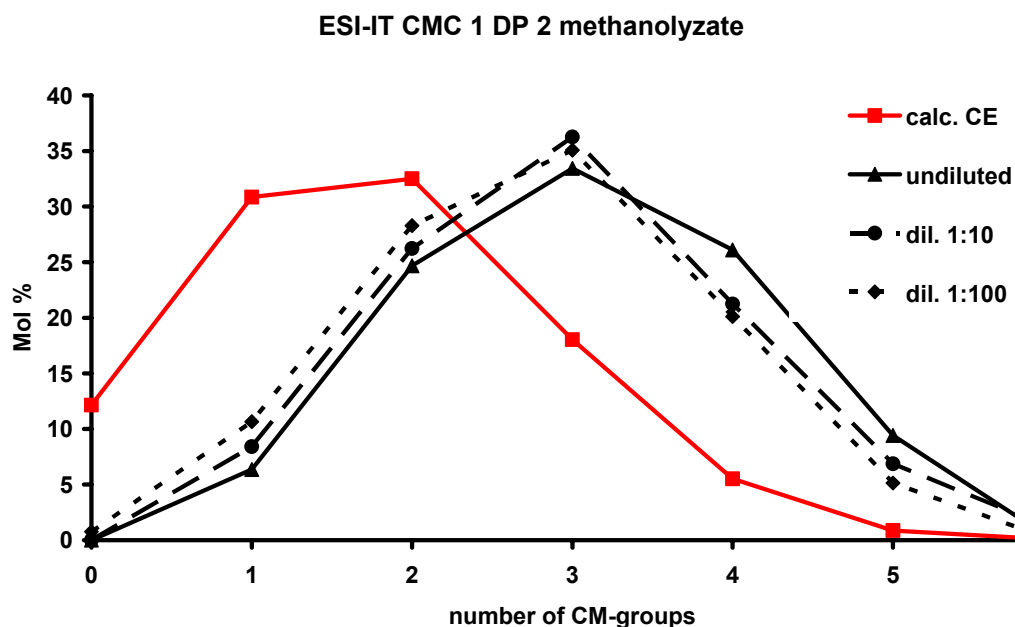


Fig. 4-3 Distribution of the CM-groups of DP 2 obtained by ESI-IT-MS of methanolyzates of CMC 1 (2 mg/mL) in three stages of dilution (undiluted, 1:10, and 1:100 diluted with methanol). Experimentally obtained data is compared with the statistical distribution calculated by Bernoulli statistics from monomer analysis by CE-UV (calc. CE, 8.3.2.1, 8.3.3).

4.1.1 Acetylation, propionylation, butyrylation of CMC after methanolysis

With this series of homologous acylation reactions after methanolysis, two parameters should be tuned for MS analysis: the polarity of the analytes and the molecular mass. The mass difference/substituent for methoxycarbonyl and acyl is 30 for acetates, 16 for propionates and only 2 for butyrates (Fig. 4-4) while the polarity is highest for acetates and lowest for butyrates.

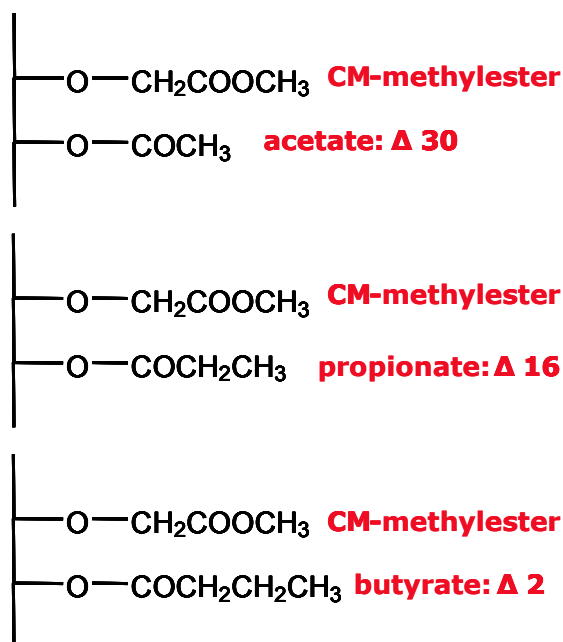


Fig. 4-4 Mass differences between the methyl O-methoxycarbonyl- and O-acyl groups

The mass difference influences the ion yield especially in ESI-IT, as the trap is optimized to a certain range of m/z -values. The polarity influences the distribution of the analytes in the droplet during the ionization process in ESI, hence the ionization yield of analytes with a certain polarity (see chapter 1.8.4). The polarity is assumed to be most similar for methoxycarbonyl and propionyl residues. This study of homologous acylation should also give information about the importance of the two parameters polarity and mass difference on the ion yield.

The pyridine catalyzed acylation was performed after methanolysis (2 mg CMC/ mL, see 8.3.6.1, Fig. 4-5), products were extracted with dichloromethane. The reaction yielded yellow to brownish colored samples, an effect that is typical for pyridine catalyzed acylation reactions^[192,193]. Completeness of the acylations was controlled by ATR-IR spectroscopy. The spectra showed sufficient acylations since no hydroxyl absorption at 3400 cm⁻¹ was observed (Fig. 4-6).

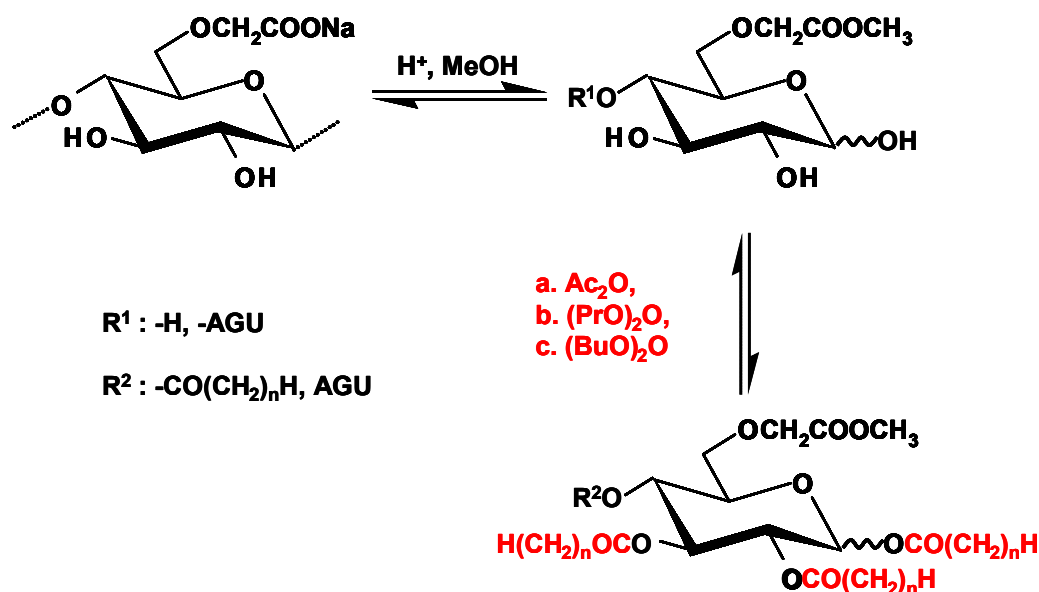


Fig. 4-5 Exemplary reaction scheme of acylation of CMC after methanolysis with the anhydrides of acetic acid, propionic acid, and butyric acid, respectively; a: $n = 1$, b: $n = 2$, c: $n = 3$

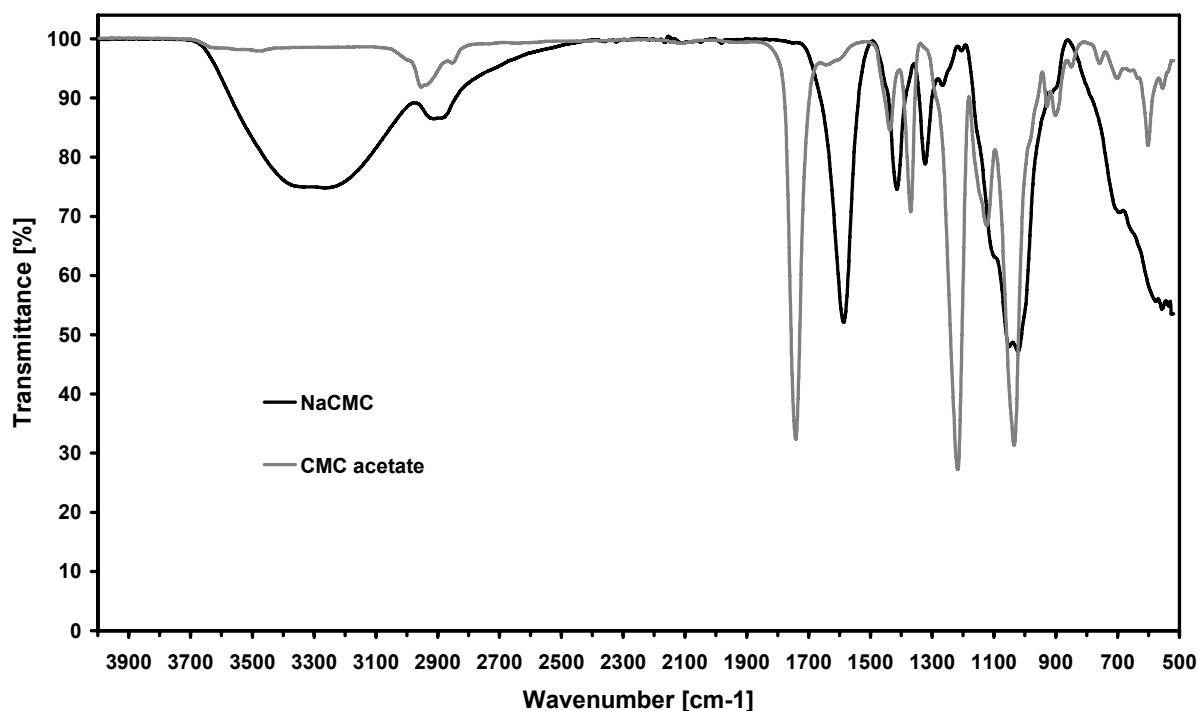


Fig. 4-6 ATR-IR spectrum of CMC 4 before and after acetylation, wavenumbers [cm^{-1}]: 3000-2800: $\nu(\text{C-H})$,w; 1750: $\nu(\text{C=O})$,s, 1400: $\delta(\text{C-H})$,w, 1250: $\nu(\text{C-O-C})$,s;

The carbonyl absorption indicating a deprotonated carboxyl group at 1600 cm^{-1} shifted to 1750 cm^{-1} , which is characteristic for esters. The IR spectra of the propionated and butyrylated samples also showed absorption at 2950 and 2850 cm^{-1} , typical for CH_3 - and CH_2 - valency vibrations.

Before MS-measurement, samples (2 mg/mL dichloromethane) had to be diluted with methanol to enable an appropriate ionization in ESI-IT-MS (variations of the solvent conditions see chapter 4.2.1), they showed appropriate intensity. In the ESI-IT mass spectra of the acetates (Fig. 4-7), peaks according to DP 1 to 3 could be observed, in those of the propionates (Fig. 4-8) and butyrates (Fig. 4-9) only DP 1 and 2. This is a general problem of the IT instrument, as its performance is best for relatively small m/z -values and the obtained mass spectra depend significantly on the chosen instrument parameters. Even with skimmer voltages optimized for DP 3 and 4, no peaks according to higher oligomers could be observed. This indicates a problem due to the degradation process (see chapter 5.2)

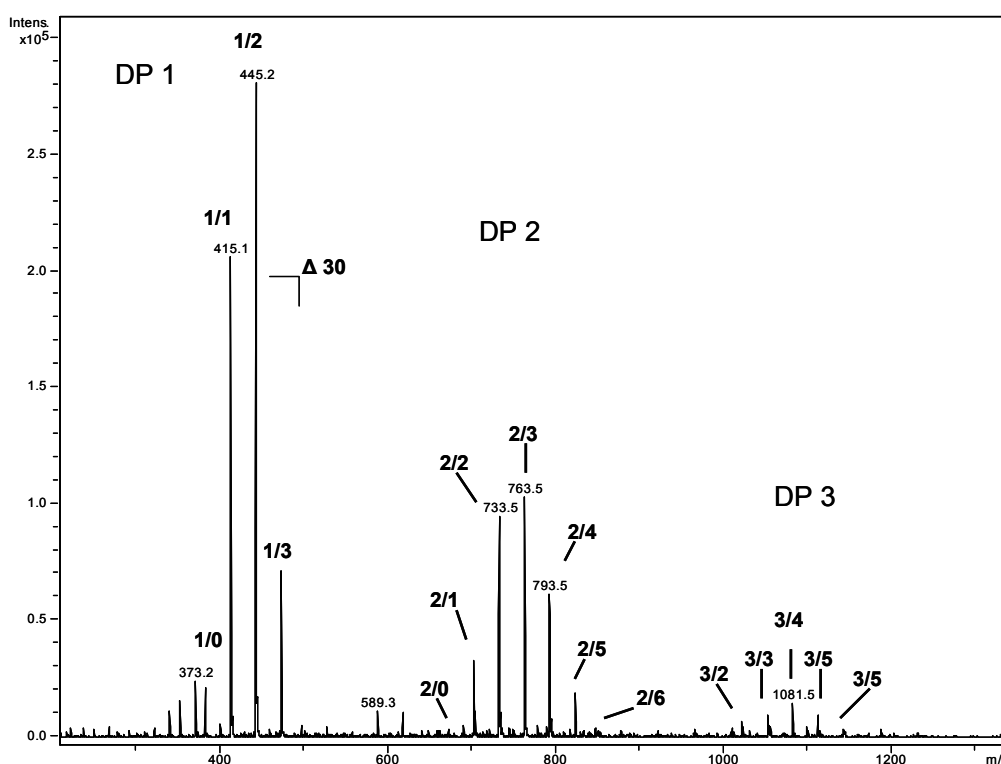


Fig. 4-7 ESI-IT-mass spectrum of the acetylated methanolizate of CMC 1 (0.3 mg/mL), see 8.3.6.1, peaks are assigned DP/n(CM)

The ESI-IT-spectra also confirmed a quantitative acylation, as no peaks corresponding to underacylated compounds could be detected. Even though the samples were colored after acylation, the spectra showed no peaks corresponding to side products such as 2-methyl-3-oxo-pentanoylgroups^[194]. In summary, acylation as derivatizing method has the following advantages: It is fast compared with etherification, it is easy to perform and a complete reaction is very likely due to the IR and ESI-IT-mass spectra. In addition, methyl esters of CM-groups were stable under the reaction and measurement conditions.

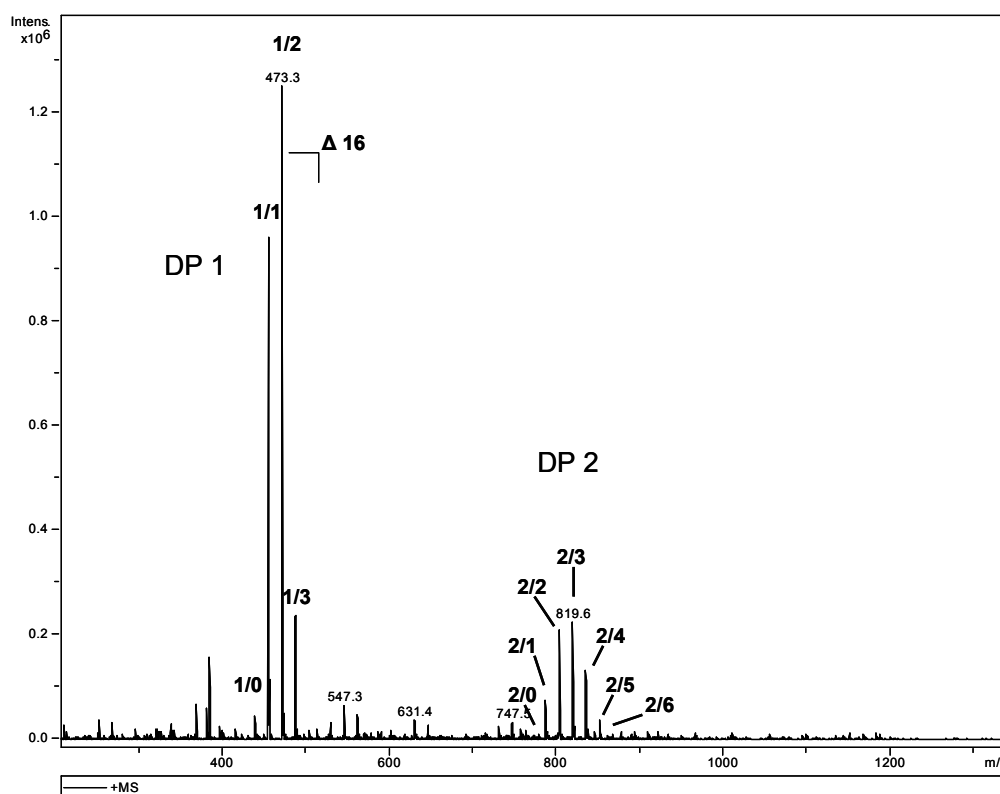


Fig. 4-8 ESI-IT-mass spectrum of the propionylated methanolizate of CMC 1 (0.3 mg/ mL), see 8.3.6.1, peaks are assigned DP/n(CM)

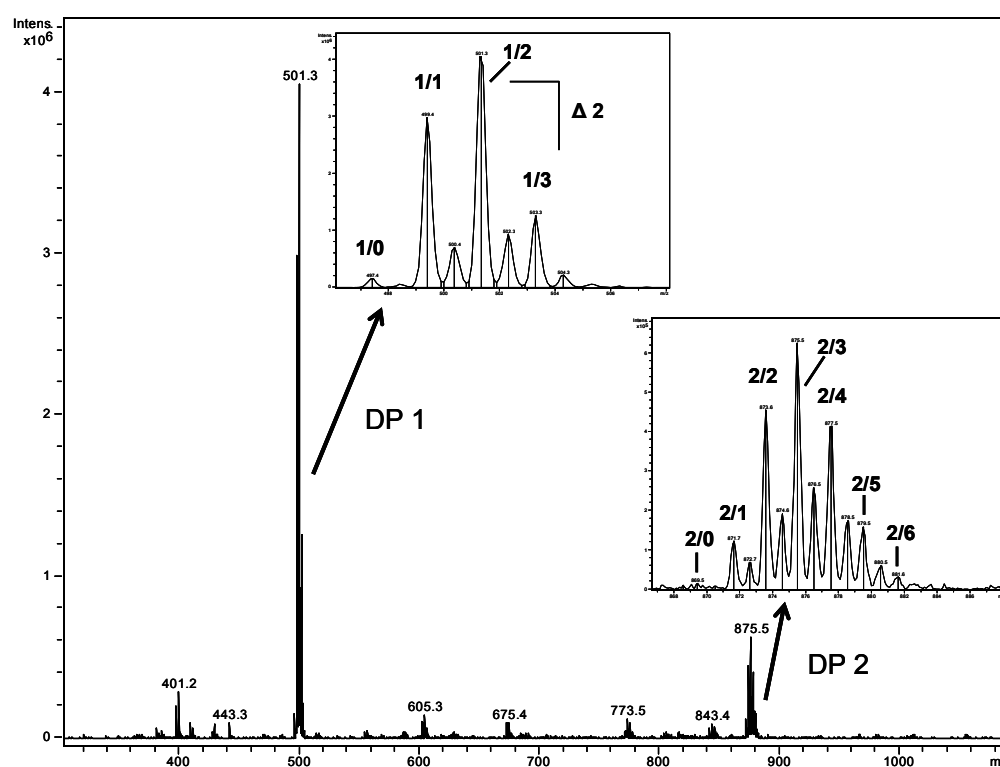


Fig. 4-9 ESI-IT-mass spectrum of the butyrylated methanolizate of CMC 1 (0.3 mg/ mL), see 8.3.6.1, peaks are assigned DP/n(CM)

The experimental results of the four CMCs (see appendix 12.2.1) were compared with the CM-distribution for a certain DP based on the data of the monomer analysis

(CE-UV, 3.2) calculated by Bernoulli statistics (Fig. 4-10). For the evaluations, the areas of [M], [M+1], (and [M+2] when of sufficient intensity) were considered.

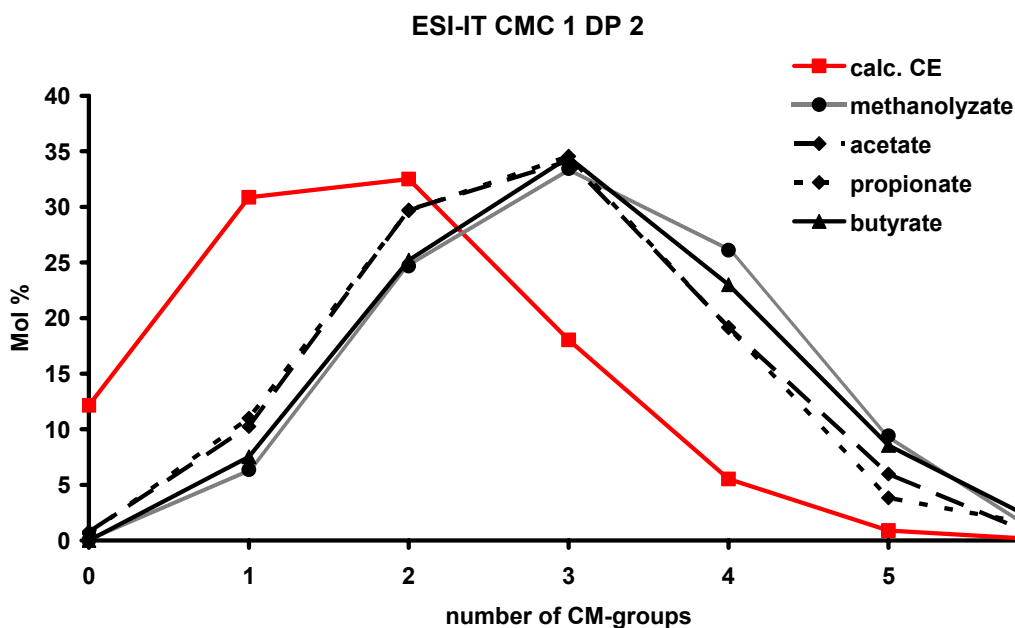


Fig. 4-10 Distribution of the CM-groups of DP 2 obtained by ESI-IT-MS of methanolized CMC 1 after acetylation, propionylation, and butyrylation, 2 mg/ mL respectively (8.3.6.1), samples diluted 1:6 with methanol for measurement. Experimentally obtained data is compared with the statistical distribution calculated by Bernoulli statistics from monomer analysis by CE-UV (calc.CE, 8.3.2.1, 8.3.3).

The average DS-values/ DP 2 for CMC 1 were 1.39 for the acetates, 1.38 for the propionates, and 1.52 for the butyrates. Therefore, the deviations of the methyl-*O*-methoxycarbonyl/*O*-acyl cellooligosaccharides of CMC 1 from the theoretically DS-value determined by CE-UV (0.88) were + 57 % for the acetates, + 57 % for the propionates, and + 73 % for the butyrates for DP 2. So they showed only a minor improvement compared to the CMC methanolizate which was not further derivatized (DS 1.54, deviation + 75 %) shown in Fig. 4-3. However, as mentioned above, the concentration of the sample solution also plays a role in discrimination. Diluting the acylated samples (2 mg/ mL) had a positive effect (Fig. 4-11).

The differences between the 1:100 and 1:1000 diluted samples were not as significant as between the 1:10 and 1:100 dilutions. For CMC 1, the deviations for DP 2 from the DS by CE-UV (0.88) for the 1:1000 dilution were + 41 % for the acetates (DS 1.24), + 32 % for the propionates (DS 1.16), and + 50 % for the butyrates (DS 1.32), and therefore still too high.

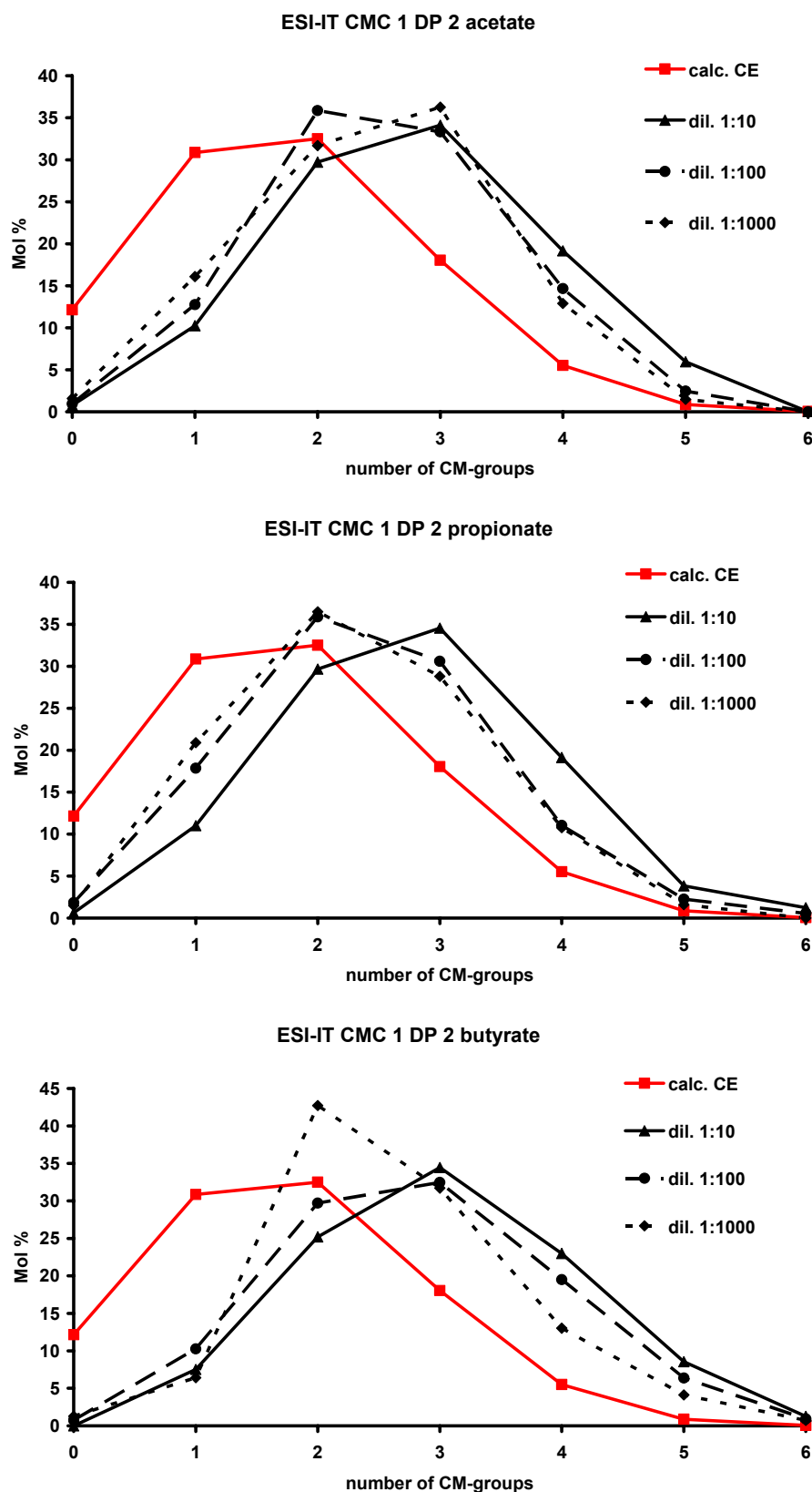


Fig. 4-11 Distribution of the CM-groups of DP 2 obtained after ESI-IT-MS of acetylated (top), propionylated (middle) and butyrylated (bottom, 8.3.7.1) methanolized CMC 1 in three stages of dilution (1:10, 1:100, and 1:1000 diluted with methanol). Experimentally obtained data is compared with the statistical distribution calculated by Bernoulli statistics from monomer analysis by CE-UV (calc. CE, 8.3.2.1, 8.3.3).

In summary, acylation could diminish the discrimination of unsubstituted components in ESI-IT-MS, but these effects were not sufficient for quantitative analysis. The sample dilution to a concentration of about 0.002 mg/ mL with methanol also reduced discrimination. Propionates showed the best abilities to minimize bias, though the difference is less significant to acetates than to butyrates. However, even with propionylation it was not possible to diminish the discrimination in such a way that conclusions to a possible heterogeneity of the investigated CMC were allowed. The observations made with CMC 1 are also representative for the other three samples CMC 2 to 4 (see annex 12.2). So it can be concluded for the substituents that a comparability of polarity and cation complexation properties is more important than of m/z to reduce bias.

To investigate the influence of the ion source and mass analyzer on the bias in mass spectrometry, the four acylated CMC samples were also measured by MALDI-TOF (8.2.3) with α -cyano-4-hydroxycinnaminic acid (CHCA) as matrix. Measurements were performed at the Helmholtz Center for Infection Research (HZI) in Braunschweig in the group of Dr. Manfred Nimtz. The spectra of the acetates, propionates, and butyrates are displayed in Fig. 4-12 to Fig. 4-14. As the lower m/z -limit applied was 500, only $DP \geq 3$ could be measured for the methanolizates. Interestingly, in the MALDI-TOF spectrum of the propionates and more significantly in the one of the butyrates, peaks could be observed that result from a loss of acyl groups, whereas the ATR-IR- and ESI-IT-mass spectra did not indicate underacylation. In Fig. 4-14, representative for the other CMC samples, the resulting patterns are marked. They showed a difference of 70 m/z (and 56 m/z , respectively) to the pattern resulting from the completely butyrylated and propionylated compounds of a certain DP which disagreed with the ESI-IT-mass spectrum of the identical sample (Fig. 4-9). Whether the loss of acyl groups was a result of the ionization process or occurred due to an insufficient stability of the butyryl group during cool storage (the MALDI measurements were performed several weeks after the ESI-IT-measurements) could not be clarified. Deviations of the average DS/ DP 2 of CMC 1 from MALDI-TOF to CE-UV (0.88) were + 53 % for the acetates (DS 1.35), + 27 % for the propionates (DS 1.12), and + 56 % for the butyrates (DS 1.37). The DS for DP 2 of the non-acylated sample could not be evaluated. For DP 3, deviations were + 58 % for the non-acylated methanolizate (DS 1.39), + 47 %

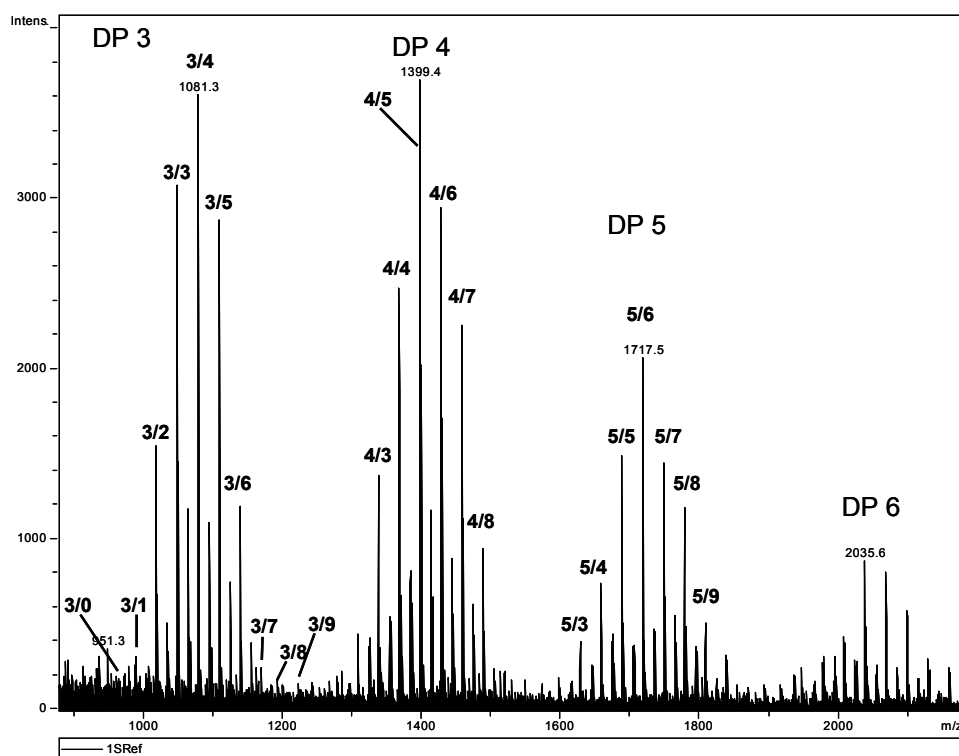


Fig. 4-12 MALDI-TOF-mass spectrum of the acetylated methanolzate of CMC 1 (2 mg/ mL, 8.3.5.3, 8.3.7.1), matrix: CHCA (8.2.3), peaks are assigned DP/n(CM)

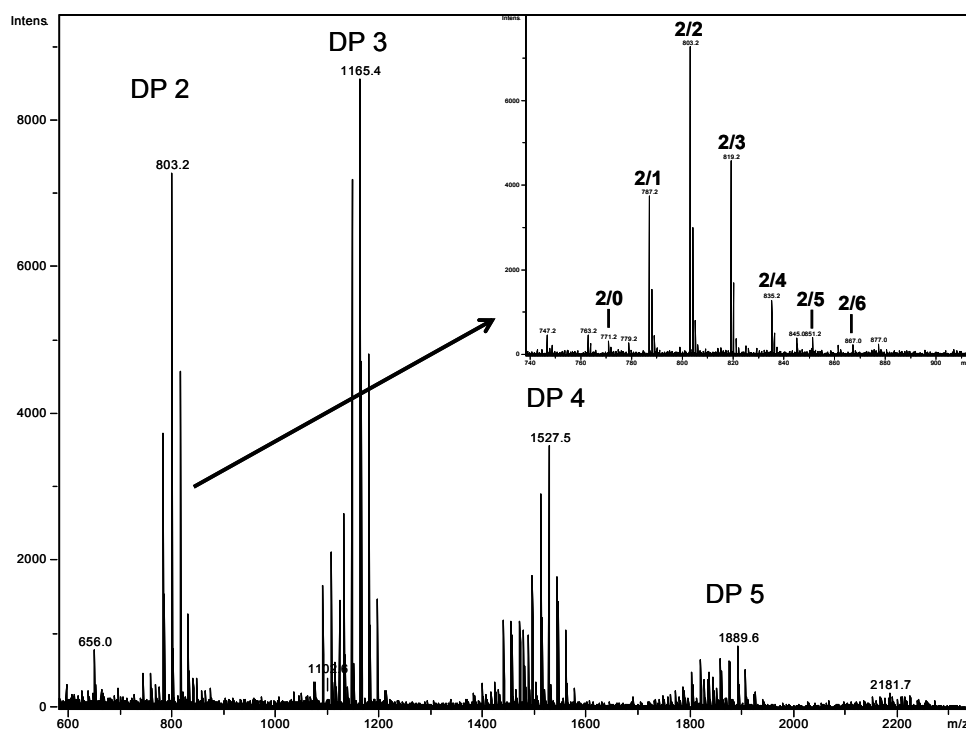


Fig. 4-13 MALDI-TOF-mass spectrum of the propionylated methanolzate of CMC 1 (2 mg/ mL, 8.3.5.3, 8.3.7.1), matrix: CHCA (8.2.3), peaks are assigned DP/n(CM)

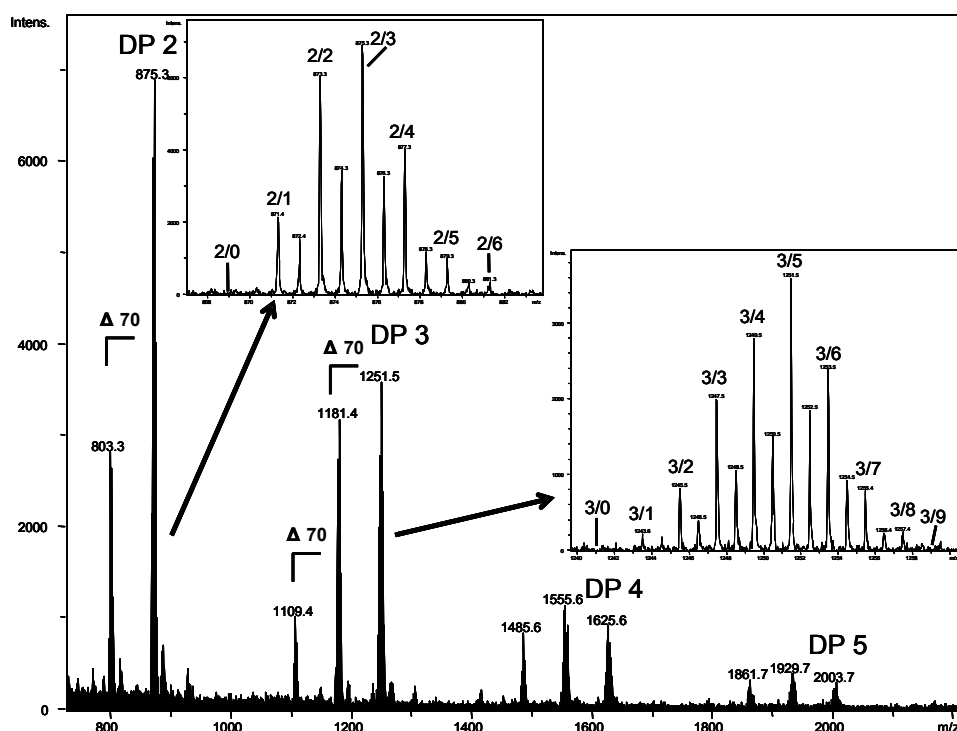


Fig. 4-14 MALDI-TOF-mass spectrum of the butyrylated methanolyzate of CMC 1 (2 mg/ mL, 8.3.5.3, 8.3.7.1), matrix: CHCA (8.2.3), peaks are assigned DP/n(CM)

for the acetates (DS 1.29), + 43 % for the propionates (DS 1.26), and + 72 % for the butyrates (DS 1.51). The deviation from the statistical distribution is shown in Fig. 4-15. The influence of sample dilution on CMC 1 could not be investigated for MALDI-TOF.

As already observed ^[81], in MALDI-TOF-MS less bias occurred than in ESI-IT-MS. With a deviation for the DS of + 27 % for CMC 1, the propionates show the best results out of the three acylating agents for DP 2 (see appendix 12.2).

In summary, a similarity between CM-group and substituent in polarity seems to be more important than the similarity in mass. Decreasing polarity also influences the solubility in methanol and the miscibility with CHCA, respectively, and therefore the sample preparation, which must be considered as further source of discrimination. Comparing methoxycarbonyl and acylates, the most important structural difference is the ether oxygen in methoxycarbonyl. Heteroatoms with their non-binding electron pairs are important structural features, in combination with steric demands for cation complexation. The methoxy group of the CM-esters is not balanced by the acylates.

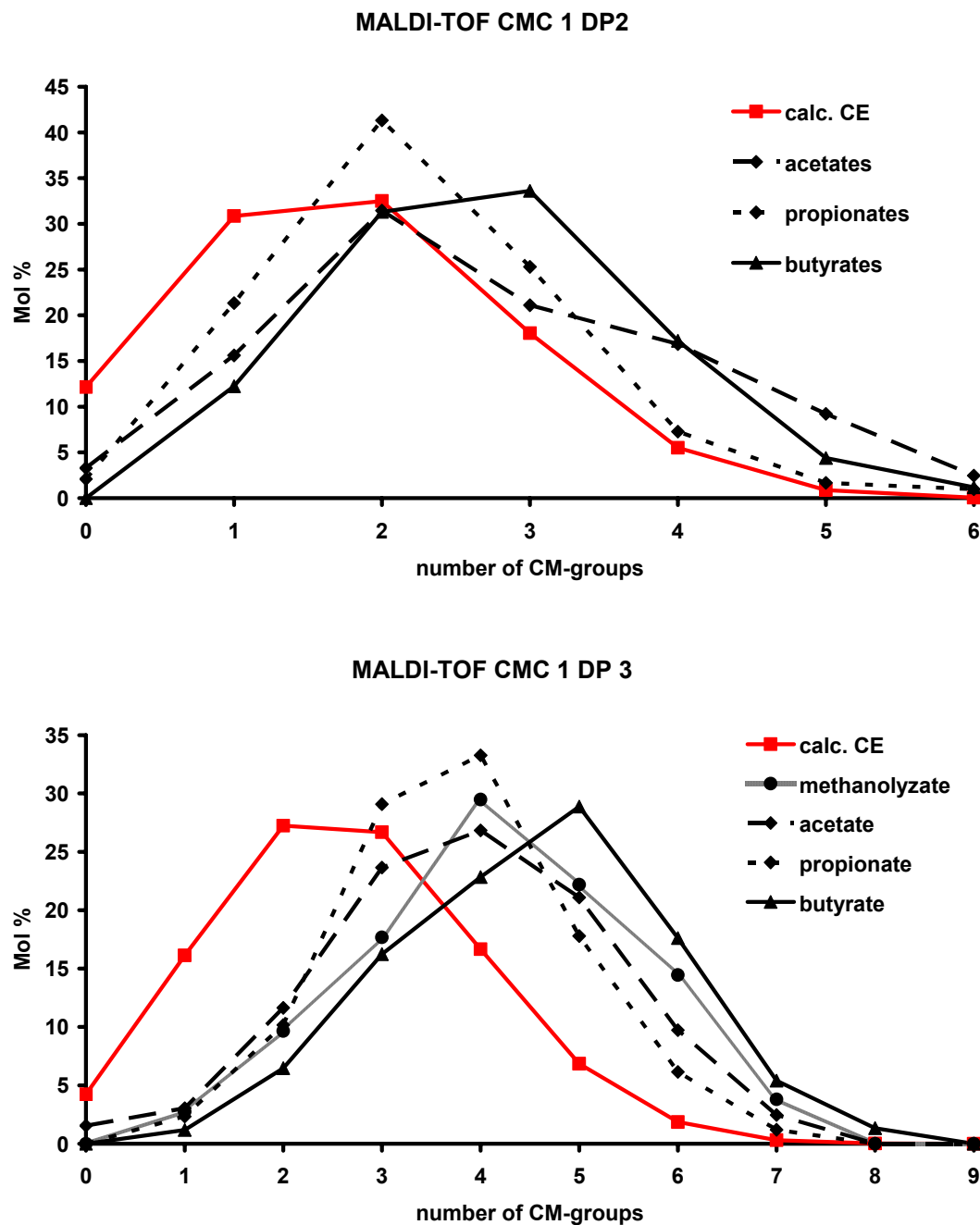


Fig. 4-15 Distribution of the CM-groups of DP 2 (top) and DP 3 (bottom) by MALDI-TOF-MS (matrix: CHCA) of methanolizates after acetylation, propionylation, and butyrylation, respectively (8.3.6.1). Experimentally obtained data is compared with the statistical distribution calculated by Bernoulli statistics from monomer analysis by CE-UV (calc. CE, 8.3.2.1, 8.3.3).

4.1.2 Methoxyacetylation after d_4 -methanolysis

As none of the agents described showed the desired effects, methoxyacetate was chosen as the presumably “ideal” substituent: it is isomeric to the methoxycarbonyl group, i.e. it has the same mass the same structural features

(C=O, OR) as the methylesterified CM-group and therefore should behave similar (Fig. 4-16) during ionization.



Fig. 4-16 Structures of the isomeric methylesterified CM-group (left) and methoxyacetate (right), R: sugar residue

To differentiate these isomeric groups in the mass spectrometer, two options are available: the first possibility is to perform methanolysis with d_4 -methanolic HCl yielding carboxymethyl methyl- d_3 -esters. Second option is an acylation with isotopically labeled d_3 -methoxyacetyl chloride. Methoxyacetate is not available as anhydride but as the corresponding acylchloride, d_3 -methoxyacetyl chloride is not commercially available and needs to be synthesized.

First, the methoxyacetates were prepared according to the procedure described at 8.3.8.1 with pyridine and an excess of acylchloride after methanolysis with d_4 -methanolic HCl to allow a differentiation between CM- and methoxyacetyl residues (Fig. 4-17).

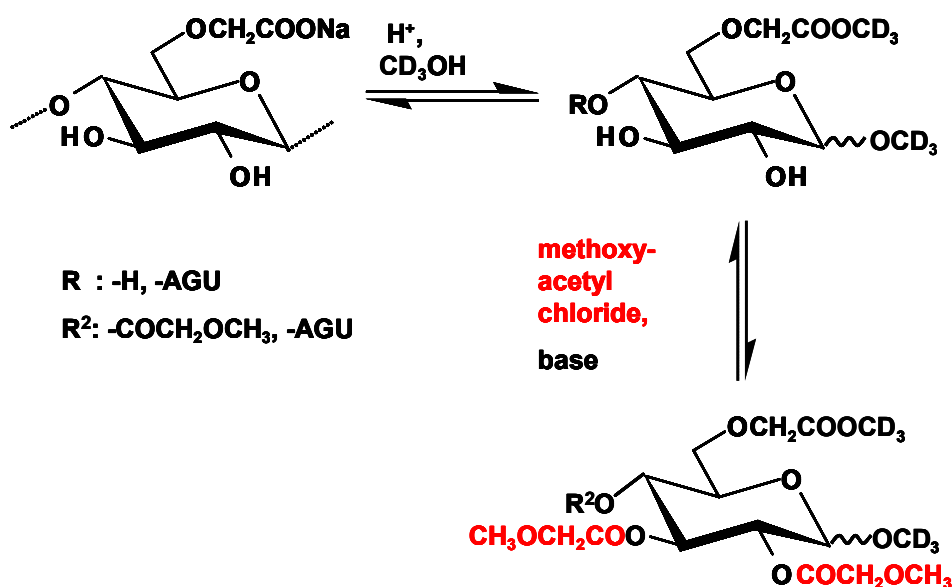


Fig. 4-17 Scheme of methoxyacetylation

As for the other acylating substances, the progress of the reaction was controlled by ATR-IR (Fig. 4-18) and regarded as sufficient. Fig. 4-19 shows the ESI-IT-mass spectrum of the d_4 -methanolizate of CMC 4 after methoxyacetylation. Only DP 1 and 2

could be determined. No peaks that could be assigned to underacylated residues could be observed, neither any peak that could be assigned to other kind of side products.

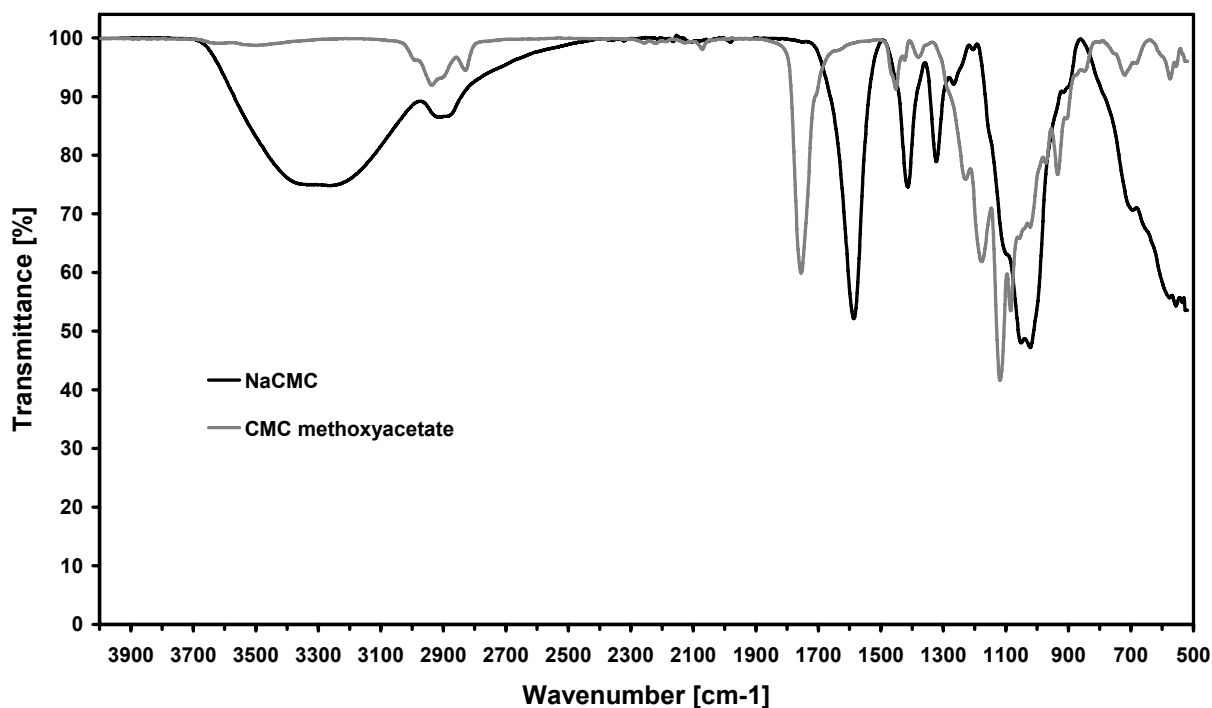


Fig. 4-18 ATR-IR spectrum of CMC 4 before and after methoxyacetylation. Wavenumbers [cm^{-1}]: 3000-2800: $\nu(\text{C-H})$,w; 1750: $\nu(\text{C=O})$,s, 1400: $\delta(\text{C-H})$,w

Therefore, the mass spectrum was in agreement with a complete acylation as indicated by ATR-IR. The pattern with m/z -values higher than DP 2 that is visible in the spectrum probably results from plasticizers (e.g. from mikrofilter or screwcap material), as it shows a Δ of 44 m/z which is typical for PEG. The results from the ESI-IT mass spectra are compared with the calculated random distribution (Fig. 4-20), the areas of $[\text{M}]$ and $[\text{M}+1]$ were considered. The influence of dilution was also investigated; two different initial weights (sample A and B) were analyzed. ESI mass spectra allowed only the analysis of DP 2. The deviation of the average DS-values of DP 2 of CMC 4 from the one obtained by CE-UV (DS 0.96) were + 31 % for sample A (DS 1.26) and + 27 % for sample B (DS 1.22) in the dilution 1:6 with methanol (measurement concentration: 0.3 mg/mL). So according to these results, methoxyacetate diminished the bias in ESI-IT-MS most effective compared to the other three acylating agents, though not completely.

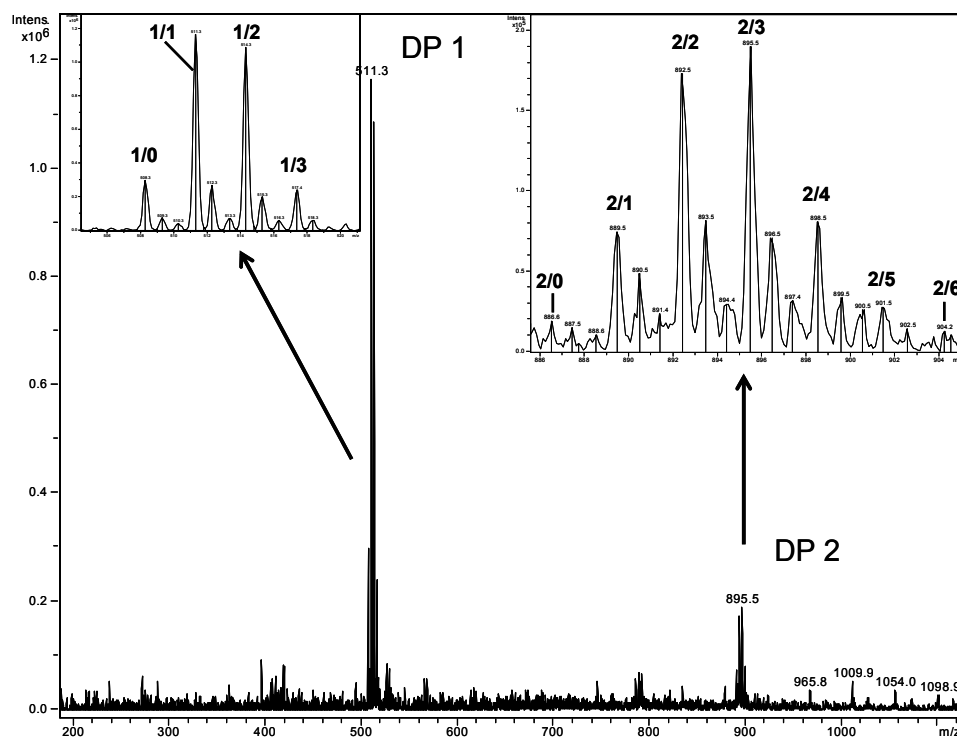


Fig. 4-19 ESI-IT-mass spectrum of the methoxyacetylated methanolizate of CMC 4 (2 mg/ mL, 8.3.5.3, 8.3.8.1), sample diluted 1:6 with methanol for measurement, peaks are assigned DP/n(CM)

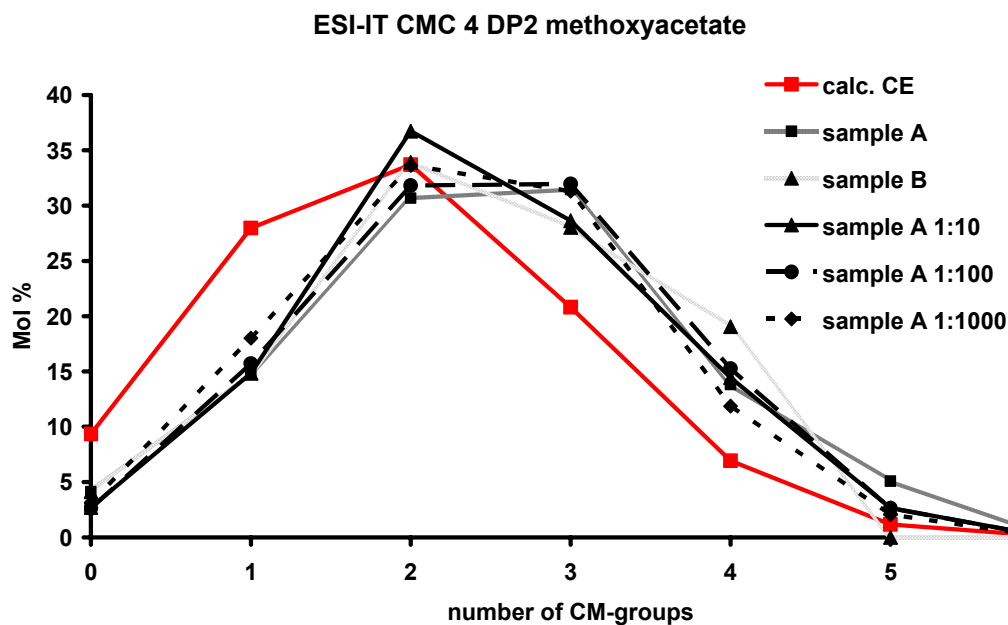


Fig. 4-20 Distribution of the CM-groups of DP 2 from CMC 4 obtained after ESI-IT-MS of the d_4 -methanolizate after methoxyacetylation (2 mg/ mL, 8.3.8.1) and different states of dilution with d_4 -methanol for measurement. Experimentally obtained data is compared with the statistical distribution calculated by Bernoulli statistics from monomer analysis by CE-UV (calc. CE, 8.3.2.1, 8.3.3).

To investigate the influence of dilution, sample A was diluted with methanol. The deviation of the DS-values for DP 2 was + 28 % (DS 1.23) for the 1:10 dilution, + 30 % (DS 1.25) for the 1:100 dilution, and + 23 % (DS 1.18) for the highest dilution, 1:1000 (see appendix Tab. 7-4). So for the methoxyacetates, the effect of dilution was not that significant as for the acetates, butyrates, and propionates. With an average DS value of 1.18, the deviation was nevertheless still too high to be interpreted with respect to a possible heterogeneity.

The methoxyacetates were also measured by MALDI-TOF in the group of Dr. Manfred Nimtz at the HZI with CHCA as matrix. The mass spectrum of CMC 4 is shown in Fig. 4-21. As for the butyrates, a pattern of underacylated compounds could be observed, though the peak intensity was not that significant. This is in disagreement with the ESI-IT-mass spectra, so this loss of acyl groups results most probably from elimination of methoxyacetic acid. MALDI-mass spectra were of much poorer quality compared to those obtained from acetates, propionates and butyrates. They allowed only the evaluation of the substitution pattern of DP 1 and 2. Fig. 4-22 shows the CM-distribution obtained in comparison with the calculated random distribution based on monomer data.

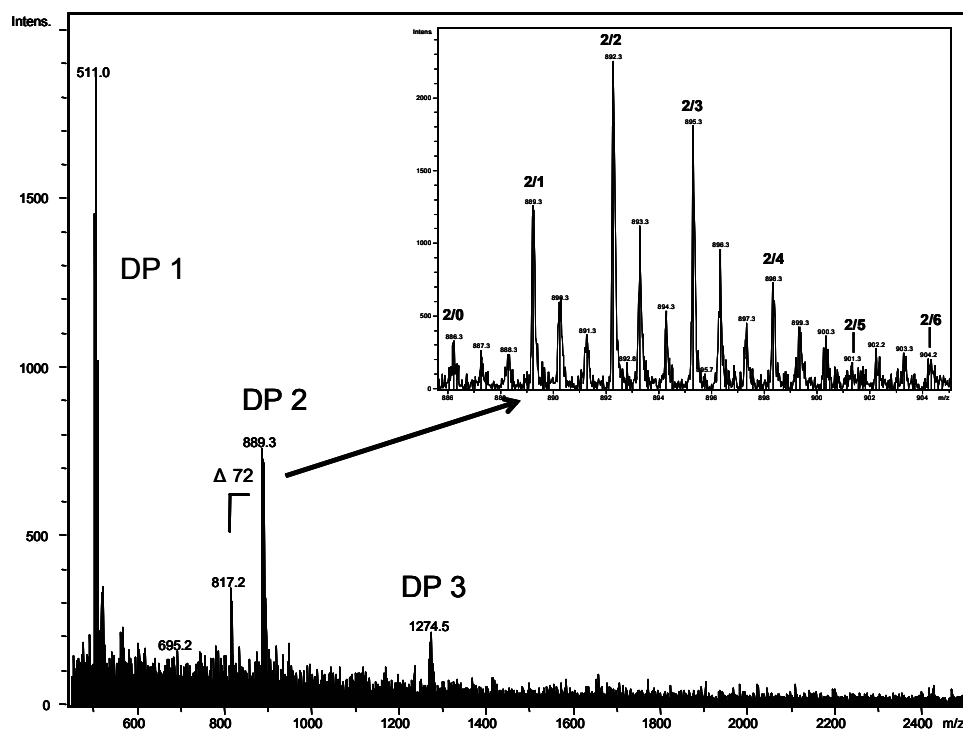


Fig. 4-21 MALDI-TOF-mass spectrum of the methoxyacetylated methanolizate of CMC 4 (8.3.8.1), peaks are assigned DP/n(CM)

The obtained DS values are lower than for the acyl derivatives discussed above and therefore closer to the average DS from titration (0.99), and CE-UV (0.96), respectively. The DS-value of sample A (0.03 mg/ mL) determined from DP 1 is 0.97 and therefore in agreement with the one obtained from CE-UV. Also the monomer distribution fits to that obtained by CE-UV. The values evaluated from CE-UV are: c_0 : 30.6 %, c_1 : 45.8 %, c_2 : 20.8 %, and c_3 : 2.8 %. Those obtained from MALDI-TOF are: c_0 : 33.3 %, c_1 : 42.6 %, c_2 : 23.4 %, and c_3 : 3.7 %. With DS 1.08, DP 2 of the same sample showed less agreement.

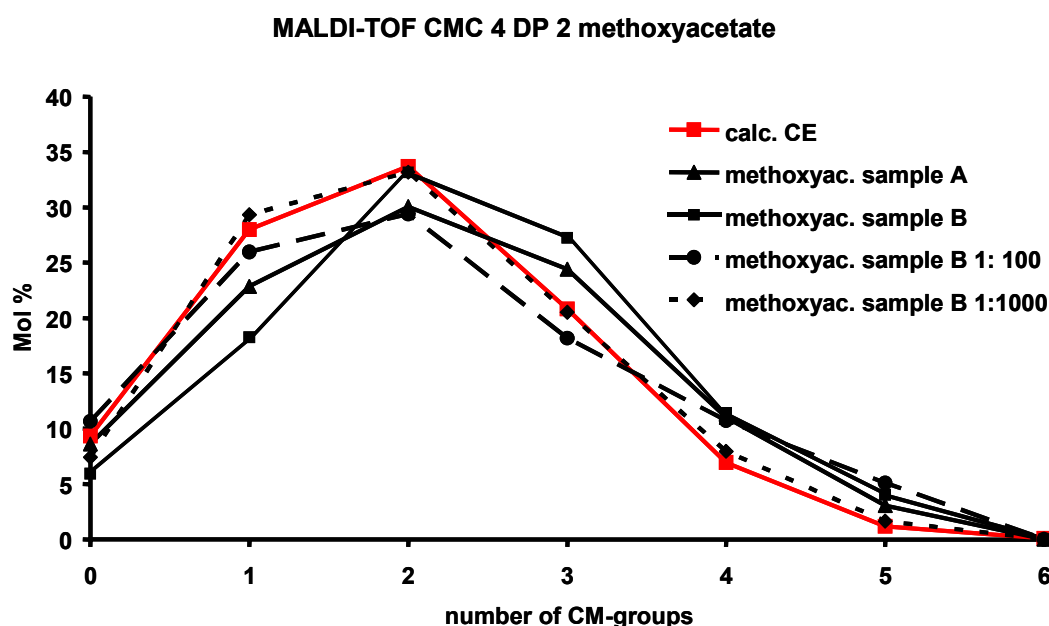


Fig. 4-22 Distribution of the CM-groups in DP 2 of CMC 4 obtained from MALDI-TOF-MS of the d_4 -methanolizate after methoxyacetylation (2 mg/ mL, 8.3.8.1) and different states of dilution with d_4 -methanol for measurement. Experimentally obtained data are compared with the statistical distribution calculated by Bernouilli statistics from monomer analysis by CE-UV (calc.CE, 8.3.2.1, 8.3.3).

Dilution with methanol influenced the quality of spectra negatively. For the highest dilution, only the MALDI mass spectrum of sample B could be evaluated, and it shows a very poor signal/noise ratio. So despite the DS 0.99 and the very good agreement with the theoretical distribution, these results have to be interpreted carefully.

The deviation from the calculated random distribution seems to be caused by the biases due to sample preparation and measurement.

The effects during ionization and ion analysis can be diminished by the methoxyacetyl group while less bias is observed in MALDI-TOF-MS than in ESI-IT-MS. It is hence assumed that the critical step is the partial degradation.

4.1.3 Variations of the acylation process

During methoxyacetylation with the acyl chloride HCl is formed (pK_a HCl: -4 to -10), while the acylations with anhydrides produce the less acidic carbonic acids (pK_a acetic acid: 4.76, propionic acid: 4.87, butanoic acid: 4.83). Since only DP 1 and 2 were observed in ESI-IT and up to DP 3 in MALDI-TOF after methoxyacetylation, it was assumed that subsequent degradation of CMC-oligomers occurred during acylation.

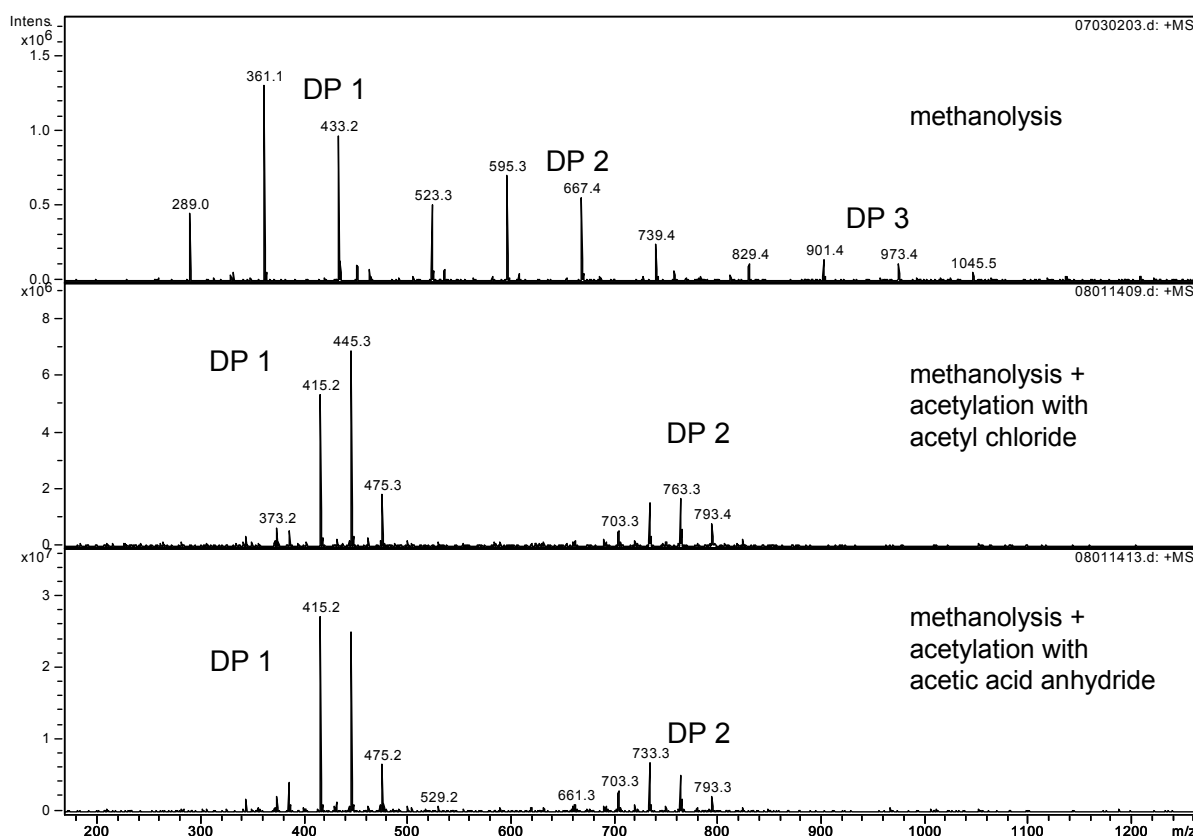


Fig. 4-23 Comparison of acetylchloride (top) and acetic acid anhydride (bottom) as acylating agents after methanolysis (CMC 4 was investigated, 8.3.8.3).

To investigate whether a subsequent degradation was responsible for the lack of higher oligomers, a direct comparison of acylchloride and acylanhydride was performed. CMC 4 (DS CE-UV: 0.96) was methanolysized (8.3.5.3 DS DP 2 methanolysate: 1.60), and acetylated with acetic anhydride, and acetyl chloride and *N*-methylimidazole as base, respectively (8.3.8.3). The ESI-IT mass spectra (Fig.

4-23) did not differ significantly with respect to their oligomer distribution. DP 3 is visible for the methanolizates, whereas in both acetylated samples only DP 1 and 2 could be detected, which is due to the different polarities of the analyte molecules. With 1.45 (acetyl chloride) and 1.24 (acetic acid anhydride), both average DS-values calculated from DP 2 of ESI-MS are too high, as already observed. Both actylations differ with respect to the substitution pattern within DP 2 and thus the average DS-values. These deviations are considered as not to be systematic, since the previous investigations showed that acetate could not reduce bias in ESI-IT (chapter 4.1.1).

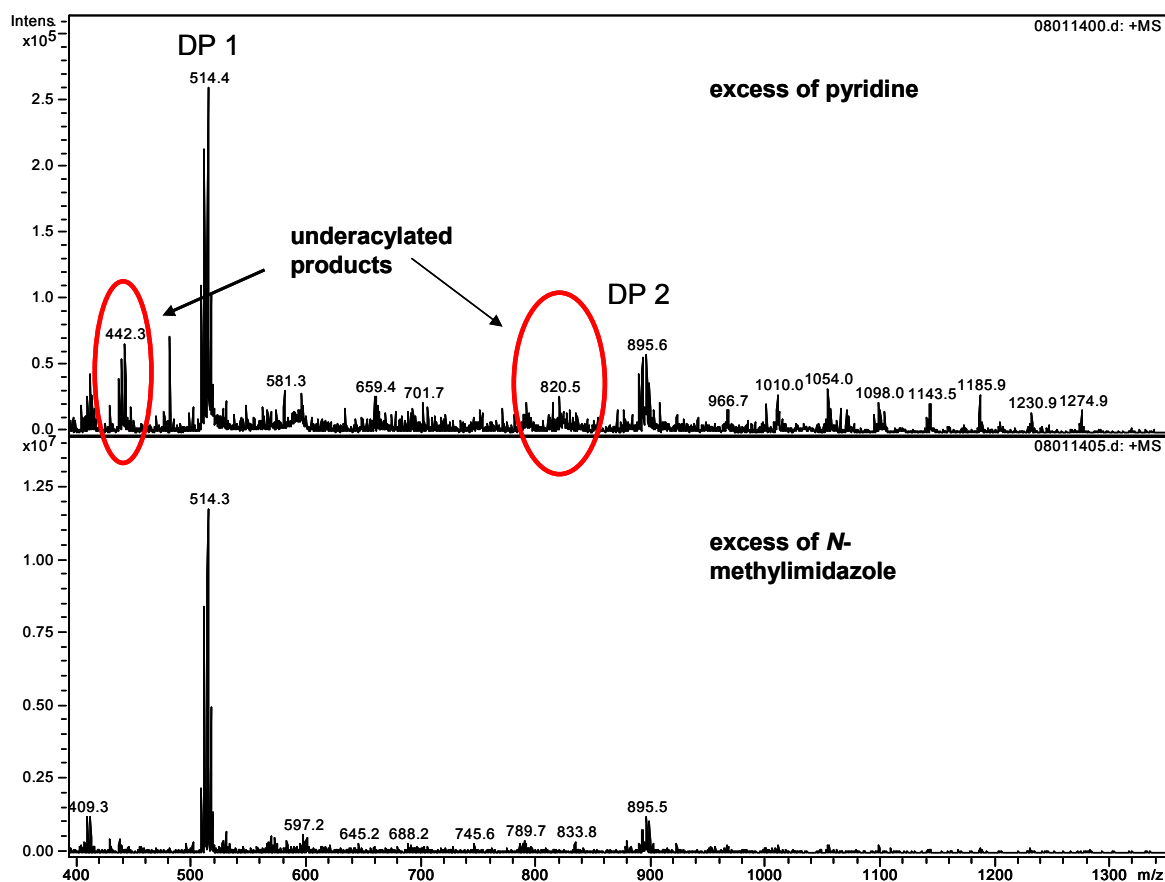


Fig. 4-24 ESI-IT mass spectra of the methanolizate of CMC 4 (2 mg/ mL), methoxyacetylated with an excess of pyridine (top, 8.3.8.2) and *N*-methylimidazole (bottom, 8.3.8.4), samples diluted 1 : 10 with MeOH/ THF (1 : 10, v/v)

As can be seen in Fig. 4-23, the differences between the methanolizates before and after acetylation are not significant. According to these results, a subsequent degradation due to the stronger acid HCl is not responsible for the lack of oligomers.

An excess of base can diminish the acyl-DS, i.e., underacylation occurs^[193,195]. Therefore, different AGU/ base ratios were investigated (Fig. 4-24). For pyridine, underacylation only occurred when 300 eq per AGU (reaction temperature: 90 °C)

were used. But even with only 75 eq pyridine the sample solutions became yellowish to brownish colored. Therefore, acylation was also performed with the more effective catalyst *N*-methylimidazole^[192]. Because of the higher reactivity compared to pyridine, the reaction requires only room temperature and the color formation could be avoided (8.3.8.3). No patterns of underacylated could be observed in the spectra when using up to 50 eq *N*-methylimidazole per AGU.

4.2 Influences during MS measurement

4.2.1 Variations of the solvent

The chosen parameters such as skimmer voltages and the properties of the solvent have a large influence on the quality of mass spectra. Acylated compounds are relatively unpolar, so they have a very poor solubility in methanol (ϵ_0 : 32.7 at 20 °C). After clean-up, the acylated compounds were dissolved in dichloromethane. This solvent is not applicable for ESI-IT. Dichloromethane has a too low boiling point (40 °C) to form a stable spray and it is aprotic. As already described, the analytes were measured after diluting the dichloromethane solution with methanol at least 1 : 6 since higher dichloromethane concentrations lead to an unstable spray. A high methanol content leads to precipitation of the analyte. Tetrahydrofuran (THF) was thus tested as an alternative for dichloromethane. With 66 °C, its boiling point is comparable to that of methanol (65 °C), and its polarity (ϵ_0 : 9.1 at 20 °C) can be compared to dichloromethane (ϵ_0 : 7.5 at 20 °C). THF is aprotic, so an addition of methanol is necessary for an appropriate ionization. Different THF/ methanol ratios were investigated. As expected, with increasing methanol content, the total intensity (i.e. signal/ noise ratio) of the mass spectra and the spray stability increased whereas the analyte solubility decreased. Finally, a ratio of methanol/ THF 10: 1 was the best compromise between analyte dissolution and spray stability/ total intensity. The variation of the solvent had no influence on the distribution of the CM-cellooligosaccharides.

4.2.2 Fractionation by column chromatography

Another approach to improve the quality of mass spectra is to cut-off DP 1 by pre-measurement fractionation. It is assumed that the peaks of higher DPs are

suppressed by the high peak intensity of the DP 1 pattern. Following assumptions have to be fulfilled for an applicable chromatographic system: first, the separation must depend only on DP, not influenced by the CM-substitution pattern. Furthermore, all compounds must elute to avoid losses due to permanent adsorption on the stationary phase. SEC with Sephadex LH-20 is not appropriate as the exclusion limit is with 4 to 5 kDa too high. The low molecular weight compounds of methoxyacetylated oligomers (DP 1 \approx 520 g/ mol, DP 2 \approx 900 g/ mol) would not be separated from each other. Sephadex G-10 has an exclusion limit of 700 Da, but even on this material no adequate separation could be achieved, and overlapping with polymer material occurred.

The conditions for an appropriate column chromatography were tested by TLC with silica. Different mixtures of chloroform/ methanol, THF/ methanol and acetone/ hexane were tested. Best results were obtained with a volume ratio of acetone/ hexane 1 : 1. According to the R_f -value ratios on TLC, an analyte/ silica ratio of 1 : 100 was chosen for column chromatography ^[196].

100 mg CMC 4 were methanolized by stirring under reflux in a 100 mL-round flask (8.3.11.1). This way, methanolysis was not performed at 90 °C as in the prior studies, but at the boiling temperature of the methanolic HCl (approx. 65 °C). Due to that a polymeric residue remained after 90 min, the time chosen for prior investigations. Even after 3 h, not all material had dissolved, so the whole sample together with the residue was further treated. During methoxyacetylation, a clear solution was obtained so a complete acylation due to sufficient accessibility was assumed and could be confirmed by ATR-IR spectroscopy (Fig. 4-25). The total yield after methoxyacetylation and clean-up was 96 % (CMC mass evaluated as AGU with 3 methoxyacetylgroups).

After methoxyacetylation, 60 mg CMC were fractionated on 8 g silica gel with acetone/ hexane 1 : 1 as eluent. Fractions 3 to 19 of 60 2 mL-fractions showed spots on TLC, and fractions 14 to 18 seemed to contain higher amounts of DP 2 (marked in Fig. 4-26).

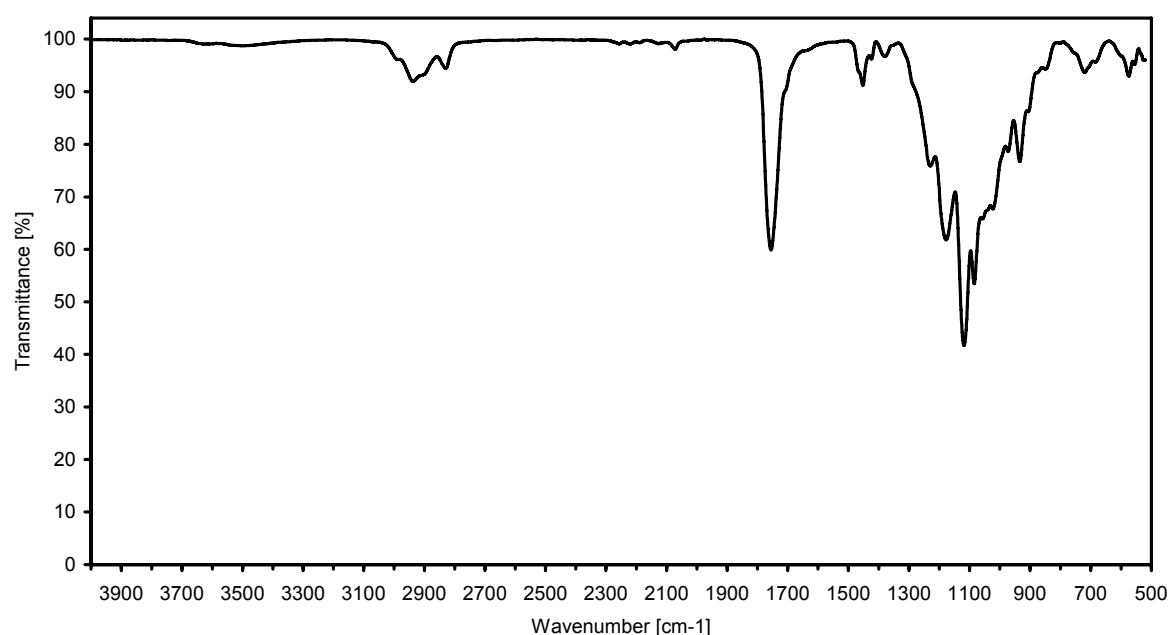


Fig. 4-25 ATR-IR spectrum of CMC 4 after methanolysis with d_4 -methanol under reflux and subsequent methoxyacetylation in larger scale (8.3.11.1). Wavenumbers [cm^{-1}]: 3000-2800: $\nu(\text{C-H})$,w; 1750: $\nu(\text{C=O})$,s, 1400: $\delta(\text{C-H})$,w

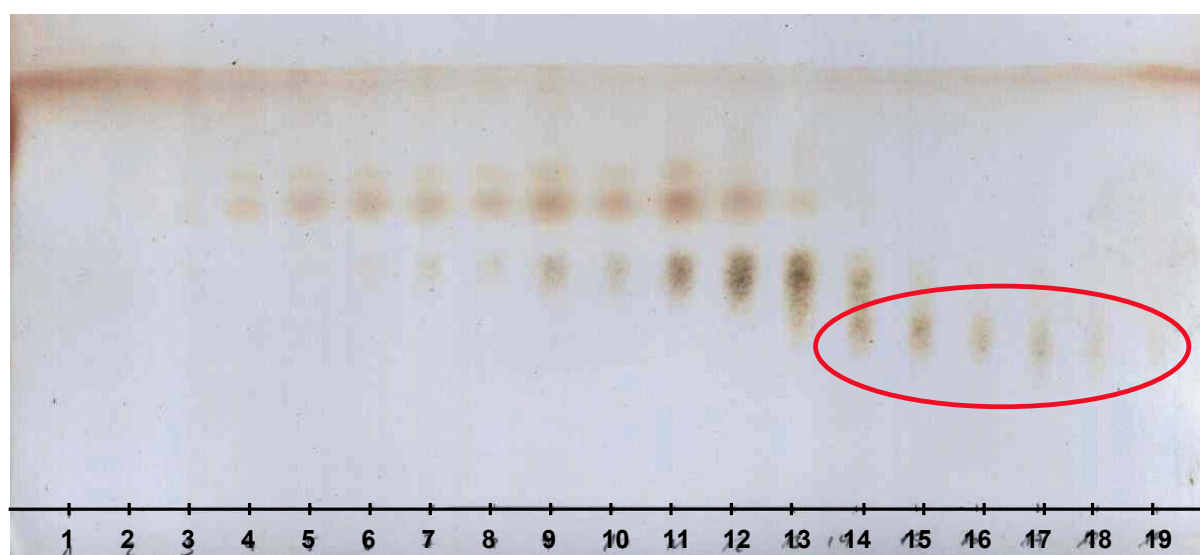


Fig. 4-26 TLC of the fractions obtained after column chromatography of methoxyacetylated, partial methanolized CMC, marked: spots according to DP 2
TLC conditions: stationary phase: silica HF 254, eluent: acetone/ hexane 1:1 v:v, detection: spraying with 10 % ethanolic H_2SO_4

The yield of each fraction was determined gravimetrically. The total yield after column chromatography was 96 % (sum of the fractions: 51 mg), in the fractions > 23 no substance could be detected by TLC. Polymer residues do not elute or show very long retention times under these conditions as can also be observed on TLC. The

fractions contained between 0.5 and 10 mg substance, most fractions contained around 2 mg. So they could be investigated by ESI-IT-MS after appropriate dilution. From fraction 13 on, dimers could be observed, the amount on monomers decreased to higher fraction numbers. Trimers could not be observed and only fractions 14 to 19 showed relatively high intensities for DP 2, which was measured with optimized parameters for this m/z -range. The obtained DS/ DP 2 of these fractions varied between 1.10 and 1.14 (Fig. 4-27), hence deviated by +15 % to +19 % from the monomer data (CE-UV DS 0.96), the weighted average of all fractions was 1.12 (+17 %). In ESI-IT-mass spectra also underacylated patterns could be observed, which is in contradiction to ATR-IR spectroscopy. These acyl losses might result from the varied sample preparation in larger scale with an excess of *N*-methylimidazole and longer reaction times at lower temperature (8.3.11.1).

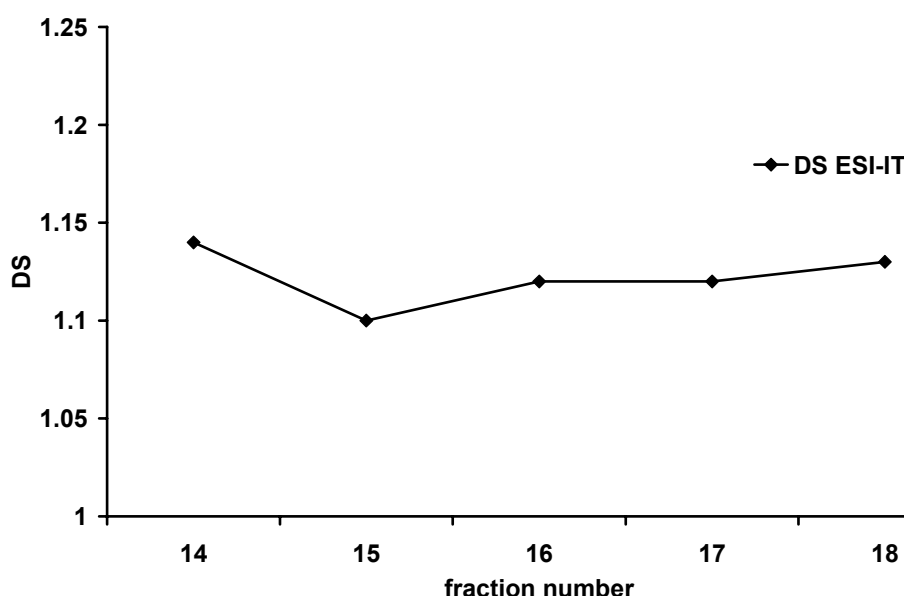


Fig. 4-27 DS values of the fractions determined by ESI-IT-MS CMC 4, DS(CE-UV 0.96, titration 0.99), average DS of all fractions: 1.12

The experimentally obtained CM-distribution for DP 2 is compared with the random distribution (Fig. 4-28). Although the deviation of the average DS (DP 2, ESI-MS, 1.12) from DS (CE, 0.96) decreased, it was still too high to be interpreted with respect to an eventual heterogeneity. However, fractionation was an improvement with respect to mass spectra quality.

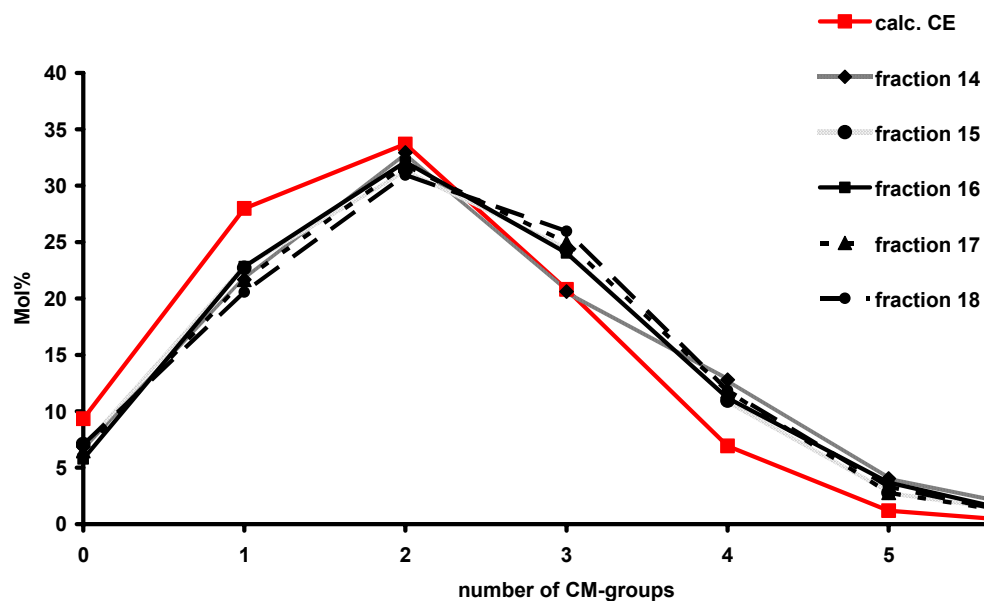


Fig. 4-28 Distribution of the CM-groups of DP 2 from methoxyacetates of CMC 4 obtained from ESI-IT-MS after fractionation (8.3.11). Experimentally obtained data is compared with the statistical distribution calculated by Bernoulli statistics from monomer analysis by CE-UV (calc.CE, 8.3.2.1, 8.3.3).

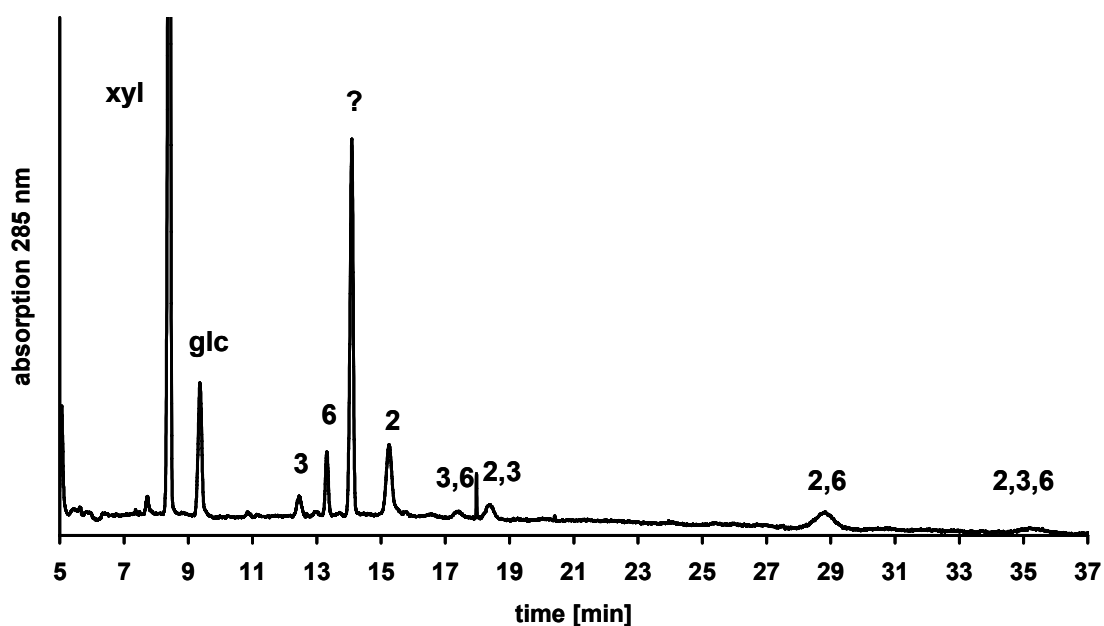


Fig. 4-29 Electropherogram of hydrolyzed (17 h, 95 °C, 1.5 M perchloric acid, 8.3.2.1) fraction 18 (0.66 mg/ mL methoxyacetylated CMC 4, DS 0.96, fractionation 8.3.11), reductively aminated with ABN (8.3.3), xylose (1.32 $\mu\text{mol/ mL}$) as internal standard, 1-(4-cyanophenyl)amino-1-deoxy-D-glucitols, peaks are assigned according to the positions of CM-substitution, CE-conditions: 175 mM borate buffer, pH 10.5, 28 kV, 25 °C (8.2.1)

The composition of the pattern remained constant during fractionation, the only exception, fraction 14, contained higher amounts on DP 1 and could therefore be neglected.

Since fractionation depends only on DP, a LC-MS method for methoxyacetylated CM-cellooligomers could be an advantageous approach. After separation based on DP, each DP could be measured in ESI-IT under individually optimized conditions without an interaction with ions from other DP patterns. To control whether the DS of the fraction was higher than the average DS of the entire sample as indicated by ESI-IT-MS, one fraction was analyzed by CE-UV. According to TLC and ESI-MS, fraction 18 (0.33 mg) contained only DP 2. This is a prerequisite to estimate a recovery rate. The fraction was totally hydrolyzed (17 h, 0.5 mL 1.5 M perchloric acid, 90 °C) reductively aminated with ABN and analyzed by CE-UV. Xylose was added as internal standard before amination to allow quantification. The electropherogram showed a large peak between 6-O- and 2-O-CM that could not be assigned to sugar components by DAD and the signal intensity was very poor.

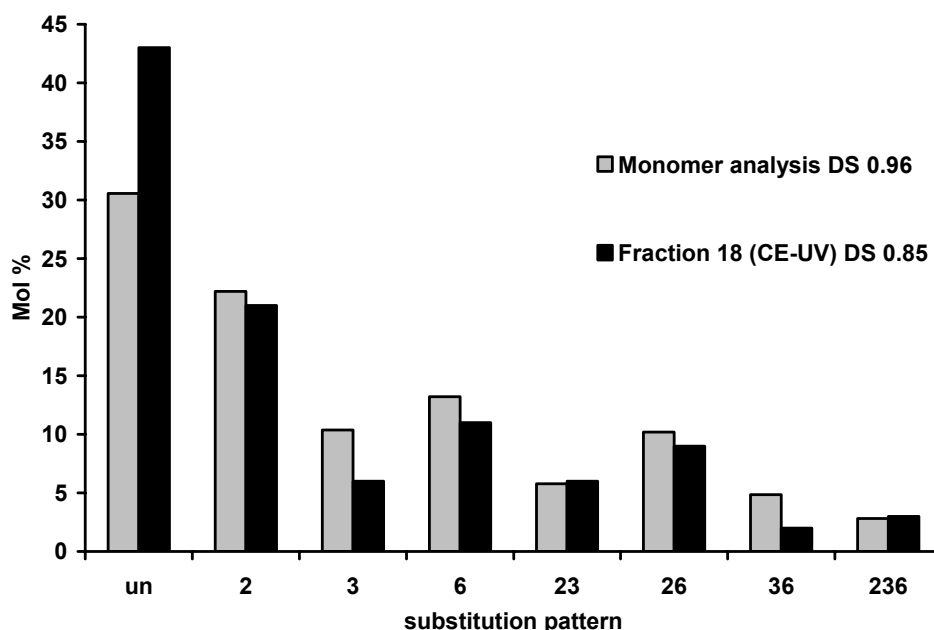


Fig. 4-30 Molar distributions of the CM-monomers obtained after hydrolysis (17 h, 0.5 mL 1.5 M HClO₄, 90 °C) of fraction 18 (methoxyacetylated CMC 4, fractionation 8.3.11), and underivatized CMC 4 (monomer analysis, 3.2, 8.3.2.1) reductive amination with ABN (8.3.3), and measurement by CE-UV (8.2.1).

The sum of CM-monomers in the fraction corresponded to a recovery rate (evaluated as methoxyacetylated 1-*d*₃-methoxy-cellobiose) of 55 %. Due to the low amount of material in the fraction a repetition was not possible. Fig. 4-30 shows the molar

distribution of the monomers of the hydrolyzed fraction and the monomer analysis (chapter 3.2). With 0.85 the average DS was much lower than calculated from ESI-IT-MS (1.12) and even lower than from monomer analysis (CE-UV: 0.96), while due to the experimental set-up, these results must not be overinterpreted. It is evident that low carboxymethylated dimers are still discriminated in MS.

4.3 Accessibility during degradation: influence on the oligomer yield

The accessibility of CMC during depolymerization is important for the course of random degradation. *Burchard*^[56] found that aliphatic cellulose ethers with a $DS < 3$ are not molecularly dispersed but form colloids. Based on his investigations he claimed the fringed micelle model (see also chapter 1.3.3).

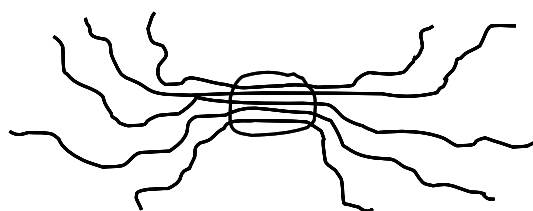


Fig. 4-31 Colloid formation of cellulose ethers in solution (fringed micelle model)^[56]

Outer parts of cellulose chains might react first/faster, yielding a non-representative mixture of degradation products. So especially for methanolysis, which is a heterogeneous process, the influence of the accessibility must be diminished. Bias that occurs from a non-random depolymerization could not be balanced by subsequent derivatization such as methoxyacetylation to form chemically uniform analytes. So the first step in oligomer analysis is also the most critical one.

4.3.1 Methoxyacetylation after hydrolysis

Heterogeneity of the system during methanolysis is a possible reason for the lack of oligomers with $DP > 3$ and for the bias observed in MS due to uneven accessibility. Therefore, an alternative for the degradation is tested. NaCMC is soluble in water, so hydrolysis is performed as degradation mechanism assuming that a homogeneous reaction would yield a broader oligomer distribution. This method has the drawback that the CM-group is not esterified, hence the products are

not neutral and can cause multiple charged ions and a mixture of sodium and proton adducts in MS. The challenge is thus to esterify the CM-groups without promoting glycosylation as a second pattern could be a new source for bias in the obtained mass spectra. Methoxyacetylation has to be performed with d_3 -methoxyacetate to allow a differentiation between the Me-CM-group and the methoxyacetate group in MS.

In summary, three steps are required: First, the degradation by hydrolysis, second, the selective methylesterification of the CM-group and at last d_3 -methoxyacetylation (Fig. 4-32).

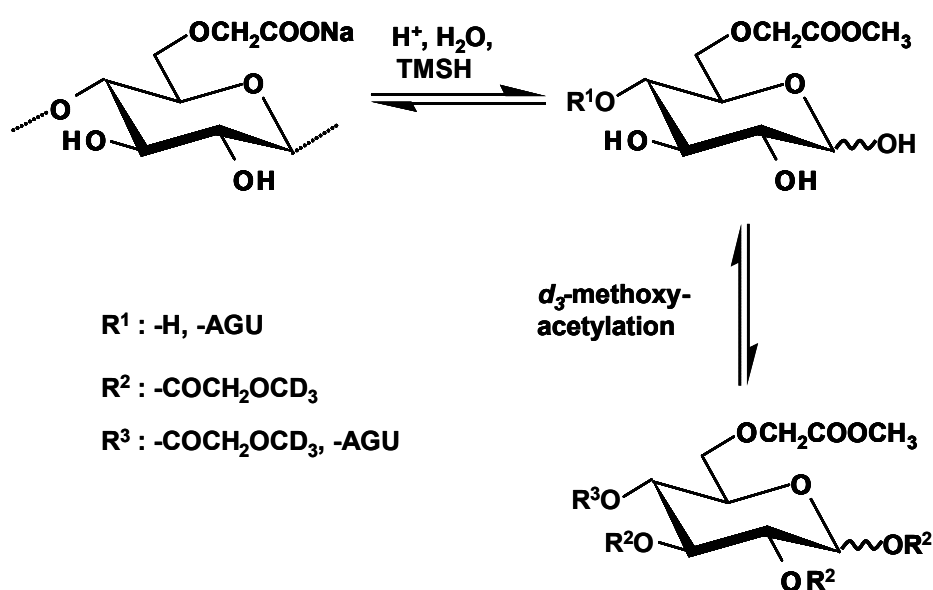


Fig. 4-32 Scheme of d_3 -methoxyacetylation after hydrolysis and selective methylesterification with trimethylsulfonium hydroxide TMSH

Trimethylsulfonium hydroxide (TMSH) was tested as selective esterifying agent (8.3.10.1). It is a less critical alternative for diazomethane, which is a common reagent for mild methylation of acidic groups but has highly toxic and cancerogenous potential. TMSH is commercially available as 0.2 M methanolic solution. A basic problem during reaction was residual undissolved material remaining at the glass wall even after 2 h of stirring at r.t.. The solution was thus heated to 50 °C for 10 min, although the probability of side reactions increases at higher temperatures. Acylation was performed as described in 8.3.8.4. The ESI-IT-mass spectrum had a very poor signal/noise ratio and a very low total intensity. No peaks could be assigned to products, so probably due to the poor accessibility of the material, the reaction was not successful.

d_3 -Methoxyacetyl- d_3 -methylester was synthesized^[128] from glycolic acid, since it is not commercially available.

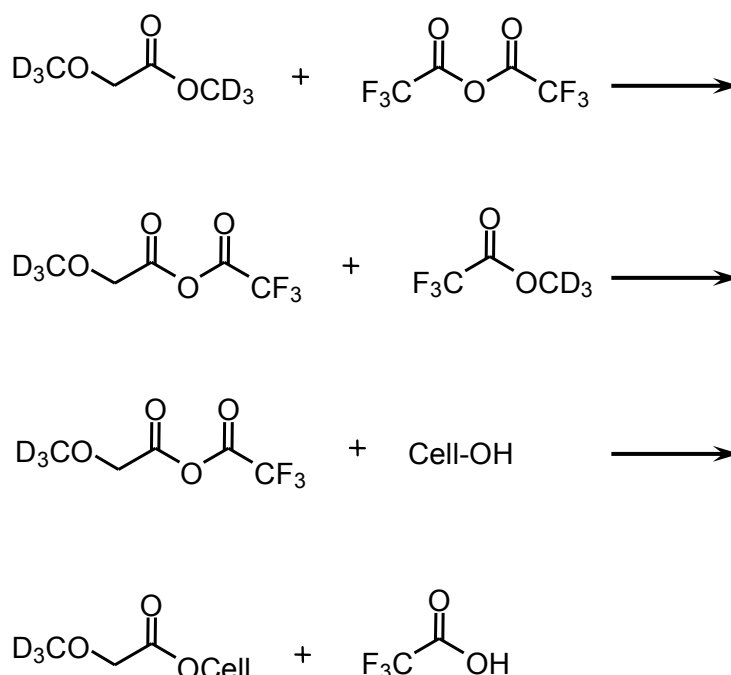


Fig. 4-33 Acylation of cellulose via reactive mixed anhydrides (impeller method), used for the acylation with d_3 -methoxyacetate

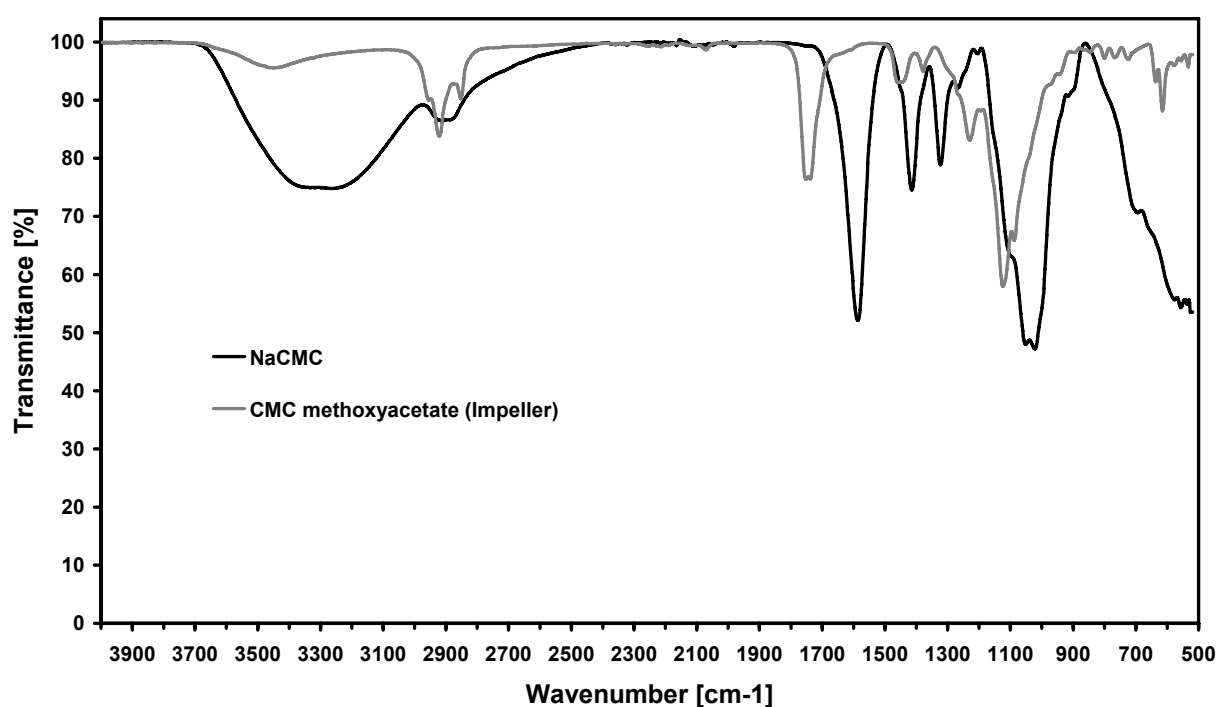


Fig. 4-34 IR spectrum of methanolyzed CMC 4 before and after methoxyacetylation (Impeller method). Wavenumbers [cm^{-1}]: 3400: $\nu(\text{O-H})$; 3000-2800: $\nu(\text{C-H})$; 1750: $\nu(\text{C=O}, \text{ester})$; 1650 $\nu(\text{C=O}, \text{COO}^-)$

The product was characterized by ^1H -NMR spectroscopy and GC-MS and no side products were observed (8.3.10.2).

To test the product, acylation of methanolized CMC 4 was performed with an adapted impeller method ^[197]. In this method d_3 -methoxyacetyl- d_3 -methylester reacts with trifluoroacetic acid anhydride (TFAA), forming the mixed anhydride. The activated mixed anhydride reacts with the free hydroxyl groups of the CMC (Fig. 4-33). The IR-spectrum (Fig. 4-34) shows that methoxyacetylation by the impeller method was not complete, but not further optimized since selective methylesterification of the CM-groups by TMSH had already failed.

The idea to use hydrolysis as degradation method is nevertheless followed further in chapter 4.4.

4.3.2 Investigation of the oligomer yield by LC-ELSD

A general problem when regarding a partial degradation is to estimate the oligomer yield. The aim is to get a broad spectrum of oligomers, especially with DP 2 to 6. To optimize the degradation method with respect to a high oligomer yield, it is necessary to have an analytical method that allows a quantitative estimation of the products. MS is not applicable, as the peak intensity does not reflect the quantitative distribution and higher oligomers and polymer residues are not detected (see also 4.4). TLC is a method that directly shows the oligomer distribution only qualitatively. Furthermore, it is not possible to differentiate between DP- and CM-substitution patterns, as the detection with ethanolic sulfuric acid is unspecific.

Therefore, based on the results obtained by fractionation, an LC method with evaporative light scattering detection (ELSD) was developed to control the oligomer yield of the degradation methods. Fractionation showed that the separation of methoxyacetylated CMC oligomers depended nearly only on DP (chapter 4.2.2); the CM-substitution pattern had no influence. ELSD is a useful direct and unspecific detection method for methoxyacetylated samples, as they have no UV-absorbing or comparable functional groups. An alternative detection method could be the measurement of the refraction index.

To apply the results from TLC, a silica HPLC column was chosen as stationary phase and acetone/hexane (1:1, v/v) as mobile phase.

Glucose, cellobiose, cellotriose, and cellotetraose were methoxyacetylated to obtain standards. During methoxyacetylation, the hydroxyl group of the anomeric carbon

atom is methoxyacetylated as well, so the standard substances are not directly comparable to the methoxyacetylated oligomers from methanolized CMC (methoxy group on C-1). The corresponding methyl glucooligomers would have been the better alternative, but they are not commercially available and/or are very expensive. According to ATR-IR- and NMR-spectroscopy, methoxyacetylation was complete.

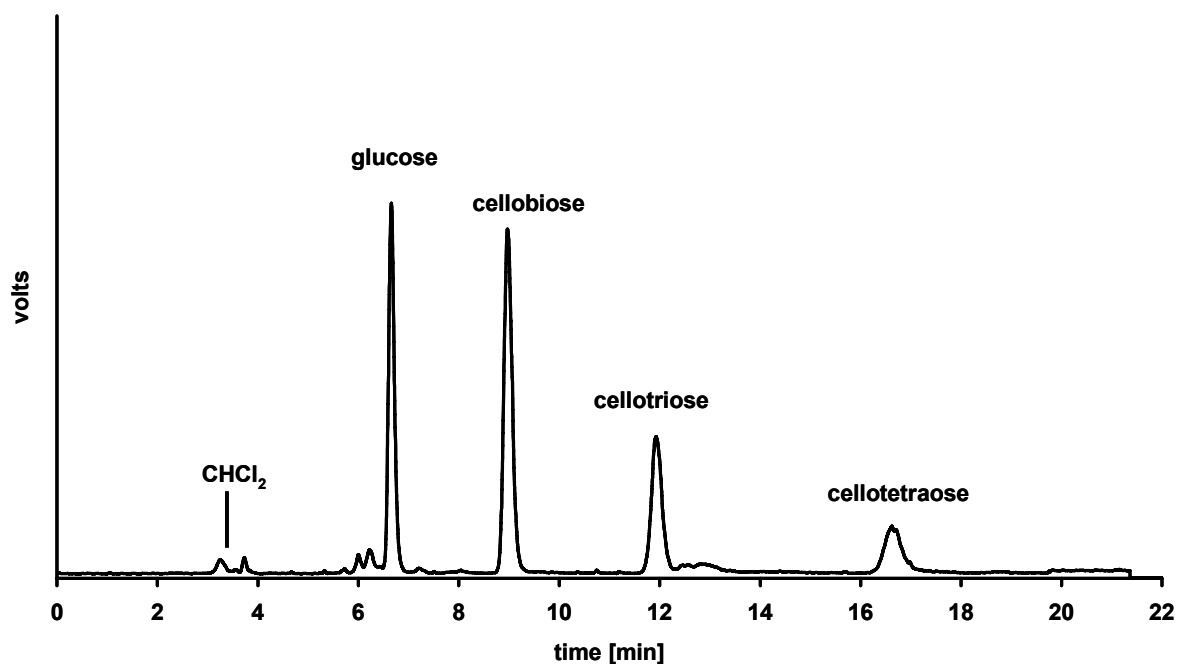


Fig. 4-35 LC-ELSD chromatogram of a standard mixture of fully methoxyacetylated celooligomers, dichloromethane was used as solvent, LC-conditions: Si-column, acetone/hexane (1/1, v/v), flow: 0.8 mL/min ELSD-conditions: nebulizer T: 50 °C, evaporator T: 70 °C

Fig. 4-35 shows the LC-ELSD chromatogram of a standard mixture of the methoxyacetylated celooligomers which were assigned by measurement of the distinct substances. An appropriate baseline separation was obtained and all substances eluted at the conditions applied. The response factors of the four standard components were determined by external calibration with the standard mixture (Fig. 4-36).

Molar response factors were evaluated for the linear range, relative to methoxyacetylated glucose (Tab. 4-1).

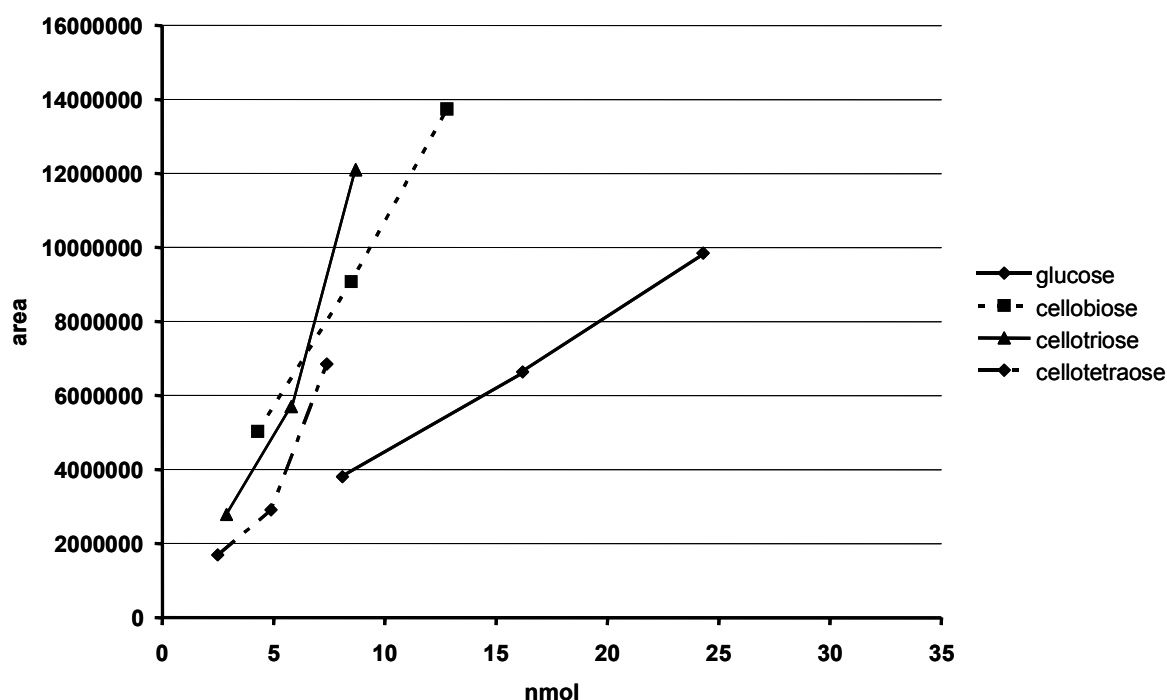


Fig. 4-36 Calibration curves obtained from a mixture of methoxyacetylated celooligomers

Tab. 4-1 Molar response factors for LC-ELSD relative to methoxyacetylated glucose

methoxyacetylated celooligomer	molar response
glucose	1.00
cellobiose	2.62
cellotriose	3.02
cellotetraose	1.98

Under the present conditions, the LC-ELSD system represents a useful tool to estimate the oligomer distribution up to DP 4 of CM-celooligomers after methoxyacetylation. This method was thus used to discuss the influence of the accessibility of CMC on methanolysis in the following chapter (4.3.3) as well as to describe the time course of hydrolysis (chapter 0).

4.3.3 Accessibility of CMC during methanolysis

As already described in the previous chapters, CMC is insoluble in methanol which might cause non-random degradation. It was therefore tried to enhance the methanol solubility of CMC to increase its accessibility. The first approach was to dissolve NaCMC in water and subsequently precipitate it, expecting that a less ordered state would be maintained (Fig. 4-37).

Schnabelrauch et al. precipitated aqueous NaCMC solution with *N,N*-dimethylformamide (DMF) and removed water from the resulting highly swollen gel by repeated distillation under reduced pressure^[198]. This procedure turned out to be inappropriate, as the required complete removal of water even after repeated distillation was not successful. Another approach was to find a non-aqueous solvent for CMC miscible with methanol. *Heinze and Heinze* reported on formic acid^[199] as derivatizing non-aqueous solvent for CMC. NaCMC dissolved within 4 to 5 h completely as formyl esters. The authors did not find evidence for the formation of mixed anhydrides between formic acid and the carboxyl groups.

This method was applied, but when adding methanol to such a formyl ester solution, also precipitation occurred spontaneously. Again, no improvement with respect to a higher oligomer yield was observed.

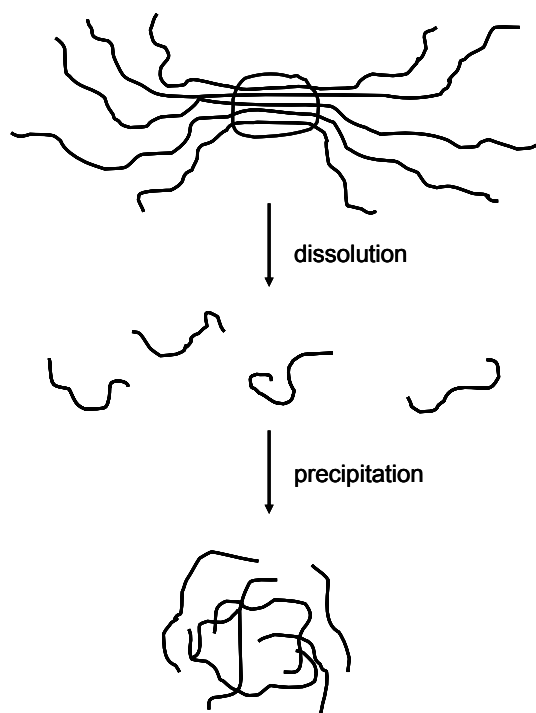


Fig. 4-37 Scheme of maintaining a less ordered state of CMC by dissolution in water and subsequent precipitation

From ATR-IR spectra of the residue remaining undissolved during methanolysis, it could not be decided whether the CMC bears COOH or COOMe groups or both, since the wavenumbers resulting from these groups differ only slightly (Fig. 4-38).

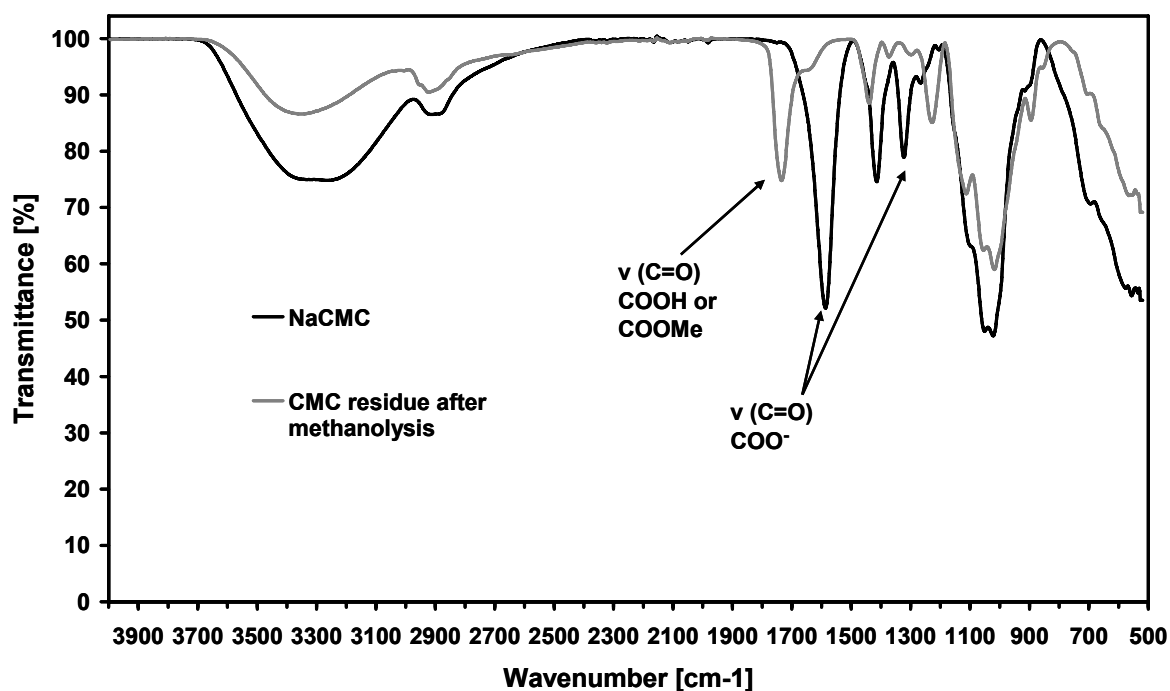


Fig. 4-38 ATR-IR spectrum of CMC 4 (sodium salt) and the residue of methanolysis (H-form or Me-ester-form). Wavenumbers [cm⁻¹]: 3400: v(O-H); 3000-2800: v(C-H); 1750: v(C=O, COOMe/ COOH); 1650 v(C=O, COO⁻)

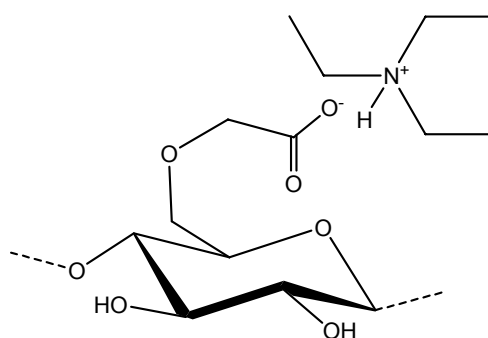


Fig. 4-39 Structure of the triethyl ammonium complex of CMC (TEA-CMC)

Alternatively, it was tried to produce a methanol soluble salt that could be acidified subsequently. Gohdes^[200] could increase the solubility of cellulose sulfate in methanol by ion exchange of the sodium salt to the triethyl ammonium (TEA) complex which should also inhibit H-bond formation. Elemental analysis and ATR-IR spectroscopy (8.3.1) showed that this was successfully applied on CMC (Fig. 4-39). TEA-CMC was dispersed in methanol, yielding a slightly turbid homogeneous suspension. As for aqueous NaCMC solutions, the viscosity of the methanolic solution was relatively high. Even after one week no precipitation occurred.

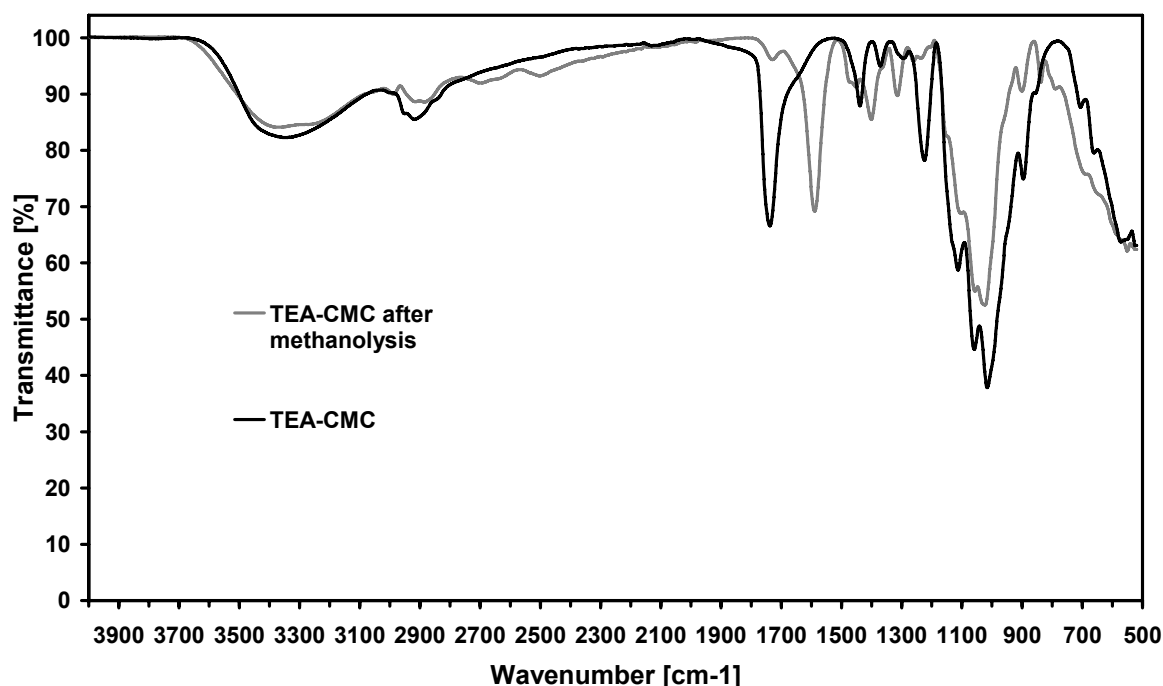


Fig. 4-40 ATR-IR spectra of CMC 4 (TEA-complex) and the precipitate from the methanolic solution after addition of acylchloride. Wavenumbers [cm^{-1}]: 3400: $\nu(\text{O-H})$; 3300: $\nu(\text{N-H})$; 3000-2800: $\nu(\text{C-H})$; 1700: $\nu(\text{C=O}, \text{COOMe}/ \text{COOH})$; 1600: $\delta(\text{N-H})$; $\nu(\text{C=O}, \text{COO}^-)$, 1300: $\nu(\text{C-N})$

During dropwise addition of acetyl chloride to form water-free methanolic HCl this suspension collapsed. The precipitate could be identified as H-CMC/ Me-CMC, respectively, by IR-spectroscopy (Fig. 4-40).

ESI-IT-MS showed no enhanced oligomer yield. Methanolizates of both, NaCMC and TEA-CMC, were investigated by LC-ELSD after methoxyacetylation. To ensure that the degradation was not too harsh, the samples were methanolized only for 30 min (1.5 M methanolic HCl, 90 °C) and the undissolved, undegraded residue was removed by microfiltration. In the chromatograms (Fig. 4-41), no peaks corresponding to oligomers could be observed, only those for DP 1 and small peaks for DP 2. The peaks were assigned with the methoxyacetylated cellooligomer standards (see chapter 4.3.2).

Quantification by external calibration showed that DP 1 represented 27 % of the original AGU. Again, an oligomer “gap” was observed, as before on TLC and in ESI-IT-MS.

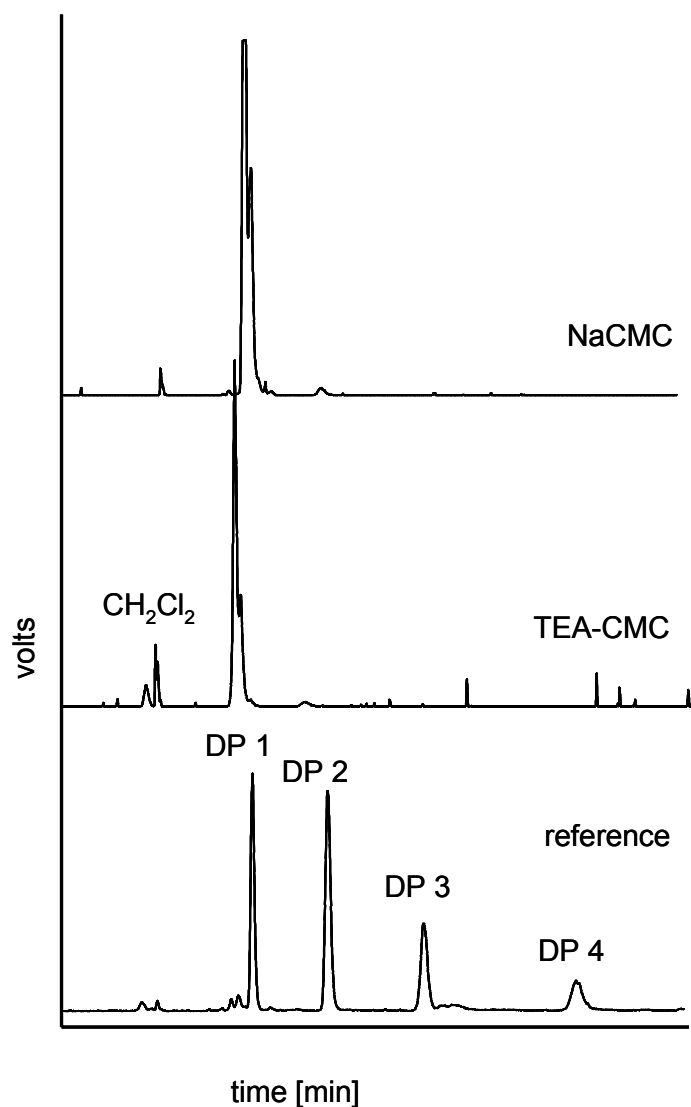


Fig. 4-41 LC-ELSD chromatograms of methoxyacetylated (8.3.8.3) methanolizates of CMC 4 (1.5 M methanolic HCl, 30 min, 90 °C). From top to bottom: NaCMC, TEA-CMC, DP- reference (methoxyacetylated glucose, cellobi-, cellotri-, and cellotetraose, see 8.3.9), HPLC conditions: eluent acetone/ hexane, 1/ 1, v/ v, see 8.2.4

In summary, prior dissolution of CMC had no positive effect on the accessibility in acidic methanol. Apparently, independent of the pretreatment, depolymerization starts in the outer, better accessible parts and proceeds like a “peeling” process. Dissolved oligosaccharides are comparably fast degraded to monomers and dimers. The result is a “gap” in the oligomer distribution. The compositions of dissolved and residual material as well as the rate constants for methanolysis are investigated and discussed more detailed in chapter 5.2.

4.4 Introduction of a permanently charged tag

The described ways to minimize bias in MS caused by differences in adduct formation with cations, were aimed to the preparation of chemically uniform analytes. Another approach is the introduction of a permanently charged tag into the analyte molecule to enable detection independent of adduct formation. Girard's T reagent (GT, 2-trimethylammonium acetic acid hydrazide chloride)^[167], is reported to increase the response of the labeled analytes in MS and therefore improve the quality and signal-to-noise-ratio of mass spectra (Fig. 4-42).

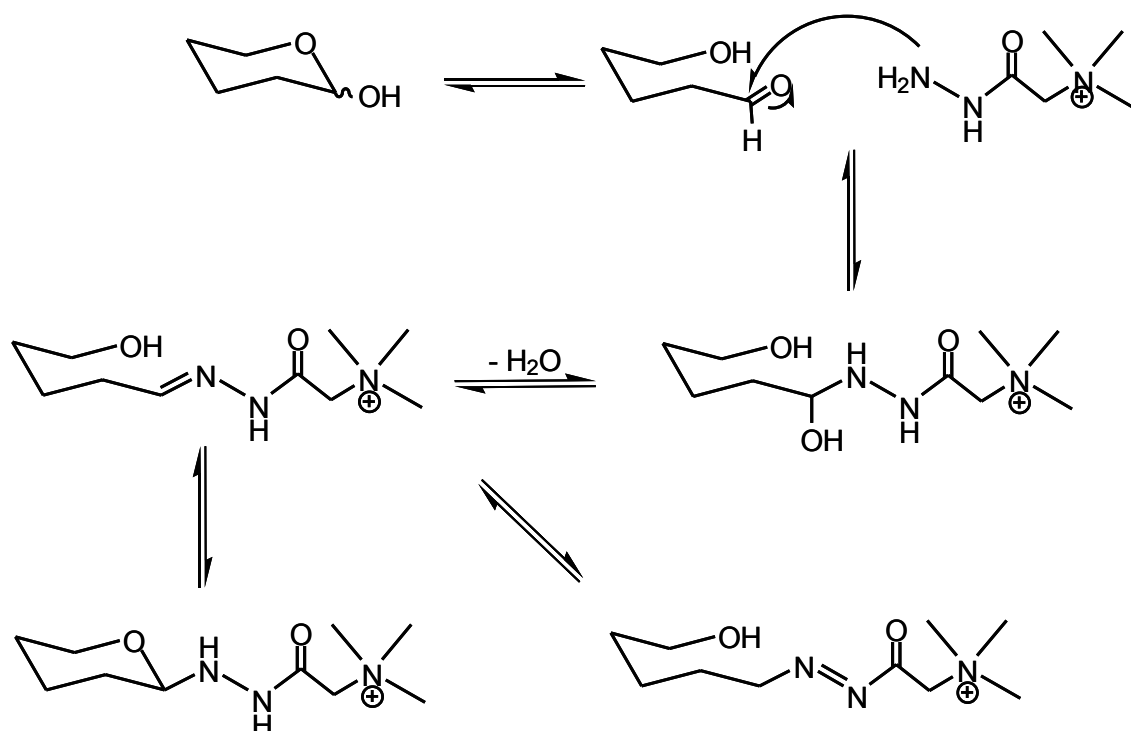


Fig. 4-42 Derivatization of the reducing end of oligosaccharides with 2-trimethylammonium acetyl hydrazide chloride (Girard's T reagent, GT), only essential functional groups are shown

The influence of GT on mass spectra of celooligomers was thus tested in dependence on DP and on CM-substitution within this work.

4.4.1 Influence on the response in MS

A celooligomer standard mixture (dried glucose to cellotetraose, nearly equimolar entry, see also 4.3.2) was investigated before and after labeling with respect to the resulting response in ESI-IT- and MALDI-TOF-MS. Tagging was performed with 2 eq GT/reducing end and the reaction was complete according to TLC (Fig. 4-43). In the ESI-IT-mass spectra of the underivatized mixture, measured

in methanol/ water 1 : 3 (total amount of carbohydrates 0.5 mg/ mL) only analyte peaks could be observed. The spectra of the labeled analytes (sample concentration 0.5 mg/ mL in methanol, Fig. 4-44) did not show any peaks from underivatized components or side products, but of non-covalent GT + Cl-poly-adducts. Against expectation, the total intensity in ESI-IT-MS was not enhanced by derivatization with GT.

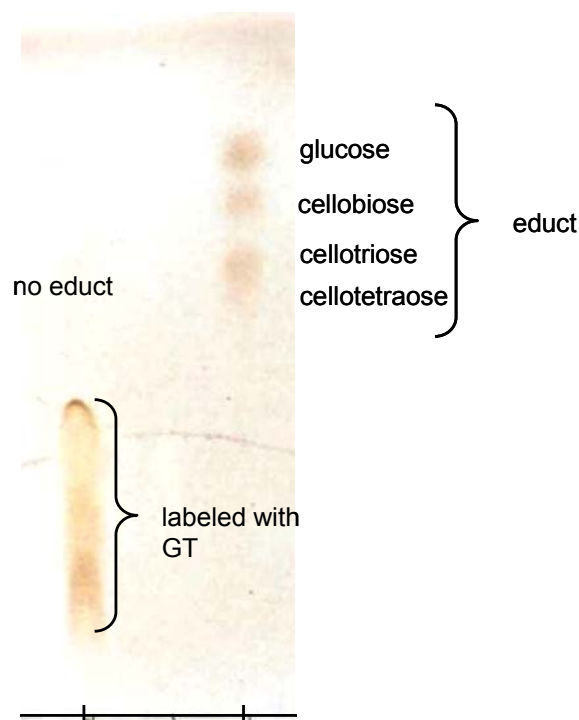


Fig. 4-43 TLC of a cellobiose standard mixture before (right) and after (left) labeling with GT (2 eq/ red. end, 8.3.4), TLC: silica, ethanol/ aq. NaClO₄ (7 g/ 100 mL) 8 : 2, v,v, detection: 10 % ethanolic H₂SO₄

In MALDI-MS, the influence of the labeling on the quality and total intensity of the mass spectrum was more significant (Fig. 4-45).

For both MS-techniques, the ratios of intensities of the cellobiose peaks differ significantly before and after amination. If all cellobioses were detected with the same response, the ratios of the peak intensities would be equal to the ratios of the equimolar entries (i.e. approx. 1 : 1 : 1 : 1).

The relative intensities of the analyte peaks in MALDI-TOF- and ESI-IT-MS, compared to the molar ratios of the standard entries and normalized to cellobiose, are shown in Fig. 4-46 and Tab. 4-2.

In ESI-IT-MS, the response for the underivatized cellobiose sodium adducts with DP > 2 was in agreement with the molar ratios of the initial inweights, but glucose

was remarkably discriminated as it showed only a tenth of the intensity of cellobiose (see also ELSD-measurements, 4.3.2).

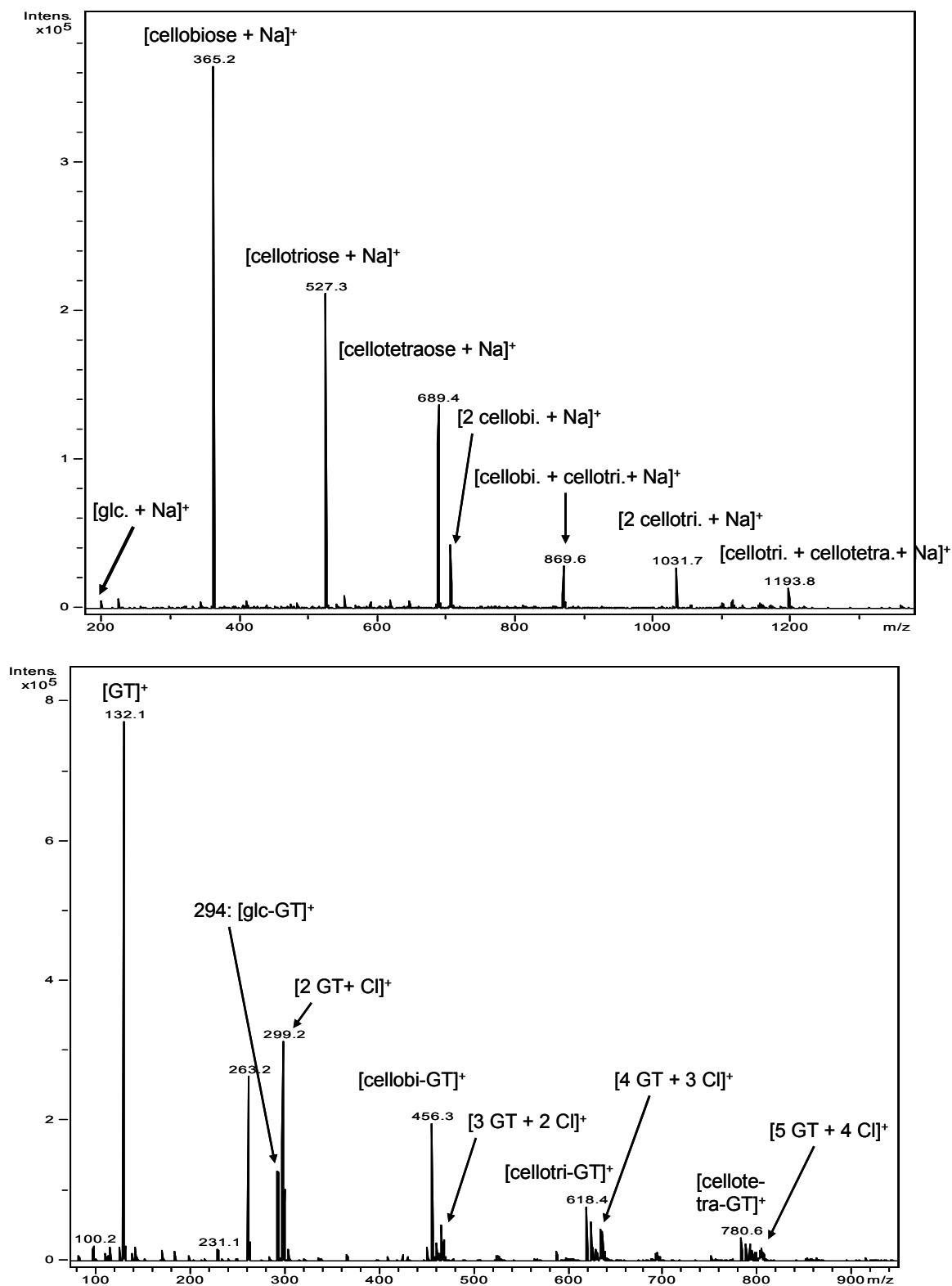


Fig. 4-44 ESI-IT mass spectra of a cellooligomer standard mixture before (top) and after (bottom) labeling with Girard's T reagent (8.3.4), 0.5 mg/ mL, respectively mass range: 50-2000 m/z , conditions: 8.2.2

After labeling of the analytes with GT, the response showed a maximum for cellobiose and decreased with increasing DP. This discrimination now probably relies on different ion selection in dependence on the selected m/z -range of the instrument.

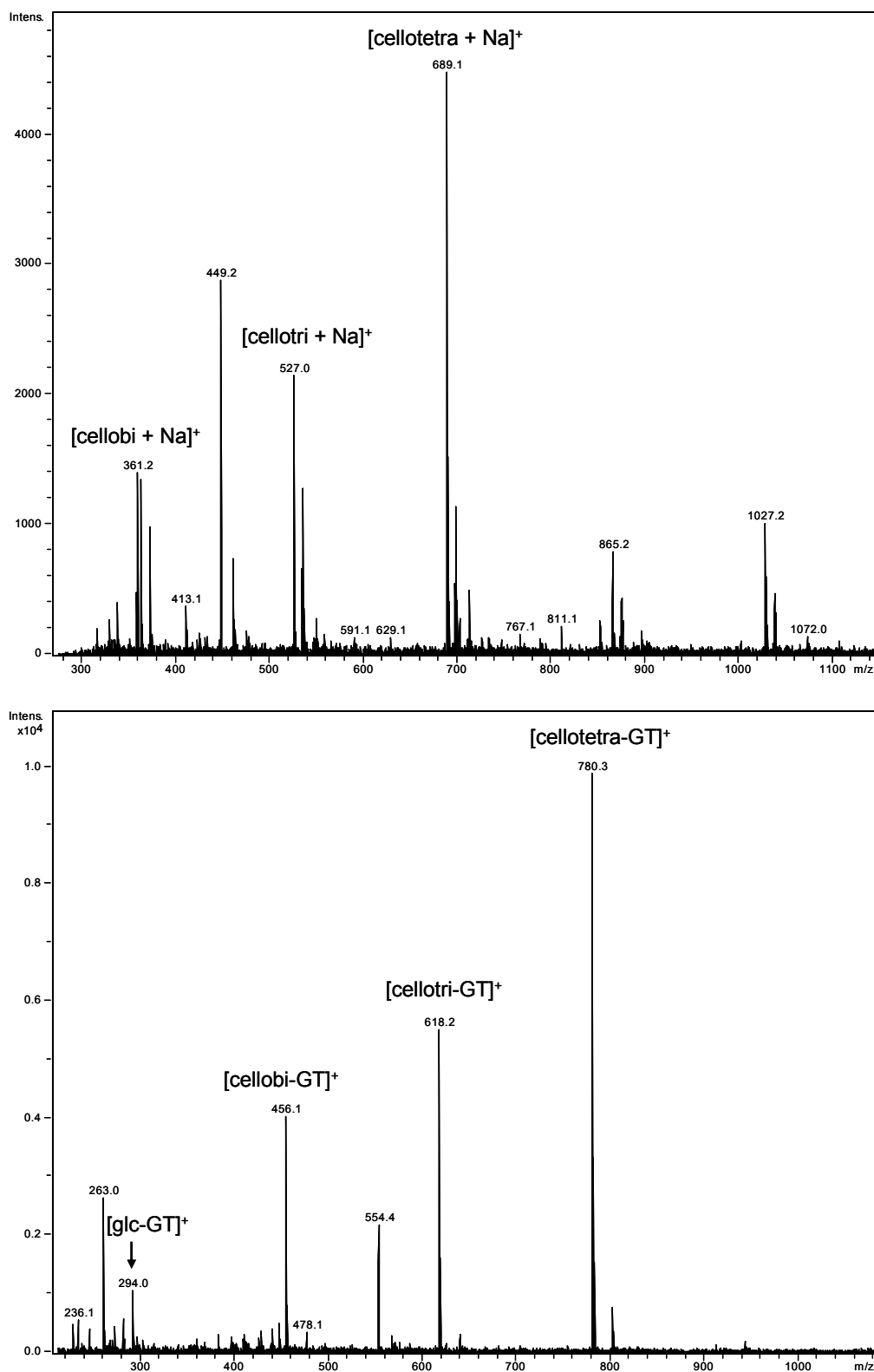


Fig. 4-45 MALDI-TOF-mass spectra of a cellobiose standard mixture before (top) and after (bottom) labeling with Girard's T reagent (8.3.4), matrix: DHB, mass range: 200-5000 m/z , conditions: 8.2.3

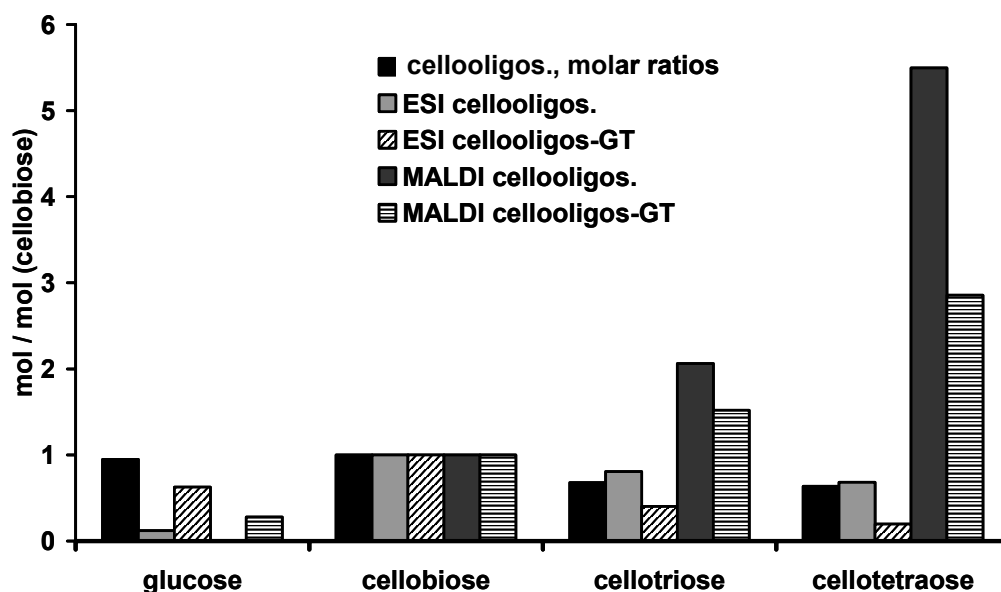


Fig. 4-46 Ratios of the relative signal intensities in MS of a cellobioses mixture before and after labeling with GT (8.3.4), measured in ESI-IT- and MALDI-TOF-MS (matrix: DHB) compared to the molar ratios of the entry, related to cellobiose

In MALDI-TOF-MS, glucose could not be detected as it was out of the minimum mass range. For the other oligosaccharides, a clear trend was visible: the response increased remarkably with increasing DP.

Tab. 4-2 Ratios of the intensities in MS and of a cellobioses mixture before and after labeling with GT (8.3.4), measured in ESI-IT- and MALDI-TOF-MS (matrix: DHB) compared to the molar ratios of the entry, normalized to cellobiose

		glucose	cellobiose	cellotriose	cellotetraose
entry	μmol	0.40	0.43	0.29	0.27
	Mol%	29.03	30.66	20.80	19.52
	molar ratio	0.95	1.00	0.68	0.64
ESI-IT	area ratio	0.12	1.00	0.81	0.68
ESI-IT (GT)	area ratio	0.63	1.00	0.40	0.20
MALDI-TOF	area ratio	n.d.	1.00	2.06	5.50
MALDI-TOF (GT)	area ratio	0.28	1.00	1.52	2.86

Cellotetraose was overrepresented nearly ten times. The labeling with GT could balance this bias to a certain extent, but the DPs > 2 still significantly predominated. For the underivatized compounds, the observed discrimination is based on the different complexation abilities for sodium. After derivatization with GT, this source for

bias was eliminated, but still discrimination could be observed, which results from the differences in ion selection depending on the preferred m/z -range of the instrument and the instrument settings. This is important knowledge for the further interpretation of mass spectra. Consequently, the instrument parameters must be optimized for each DP and calibrated with a standard mixture.

For CMC hydrolyzates or methanolizates, not only the DP affects the response in MS, but also the substitution pattern.

4.4.2 Application to CMC hydrolyzates

Since derivatization with Girard's T reagent requires the free carbonyl group on C-1, derivatization of CMC cannot be performed after methanolysis but only after hydrolysis. Perchlorate cannot be removed quantitatively, thus hydrolysis was performed with TFA instead of perchloric acid. *Enebro and Karlsson*^[201] investigated CMC hydrolyzates (4 h, 2 M TFA, 90 °C^[175]) in MALDI-TOF-MS without further derivatization. The concentration of 20 mg/ mL TFA during hydrolysis used by the authors is relatively high when aiming to avoid superstructure formation which might hinder a random degradation (see chapter 5.1). They did not remove TFA before measurement; this might cause reversion products during the evaporation of the solvent for spot preparation. They could detect peaks up to DP 8 and improve the quality of the spectra and the intensity by adding ammonium sulphate to the matrix DHB as proton source to shift the equilibrium between sodium salt and undissociated form to the latter. The authors observed a decrease of the DS-values with increasing DP, until they leveled-off at > DP 6. At the level-off limit the DS showed good agreement with the DS obtained by the supplier. The monomer composition was not determined and compared, so a possible discrimination of individual components was not discussed.

In this work, hydrolysis was performed in more diluted stage to reduce aggregate formation and a shorter reaction time was chosen (3 h, 90 °C, 5 mg/ mL 2 M TFA, see 8.3.2.4), TFA was removed by co-distillation with acetone^[202]. On TLC, beside residual polymer, only peaks for low DPs could be detected (Fig. 4-48) whereas *Enebro and Karlsson* detected up to DP 8 in MALDI-TOF for comparable hydrolytic conditions (Fig. 4-48). Since the samples still contained polymeric material and the hydrolytic conditions were even milder, the degradation could not have been too harsh.

Fig. 4-47 shows an ESI-IT-mass spectrum of partially TFA-hydrolyzed CMC 1. Since the sample was dissolved in water without an addition of methanol, the spray conditions were not optimal and the total intensities were very low. An analyte concentration of 5 mg/ mL was necessary to detect peaks. The spectra intensity was only a twentieth of those from the CMC methanolizates (chapter 4.1, Fig. 4-2), which could be measured in analyte concentrations between 0.2 and 0.002 mg/ mL with identical intensity. Addition of methanol to the aqueous sample did not improve the quality of the mass spectra. Peaks up to DP 4 could be detected as sodium adducts of the protonated CM-group $[\text{CM-H} + \text{Na}]^+$ and the sodium salt $[\text{CM-Na} + \text{Na}]^+$, so the spectrum is also very complex.

Regarding the results of the celooligomer standard (4.4.1), the DP distribution in the CMC-hydrolyzate is probably not representative, and DP 1 is discriminated. So the hydrolyzates were derivatized with GT.

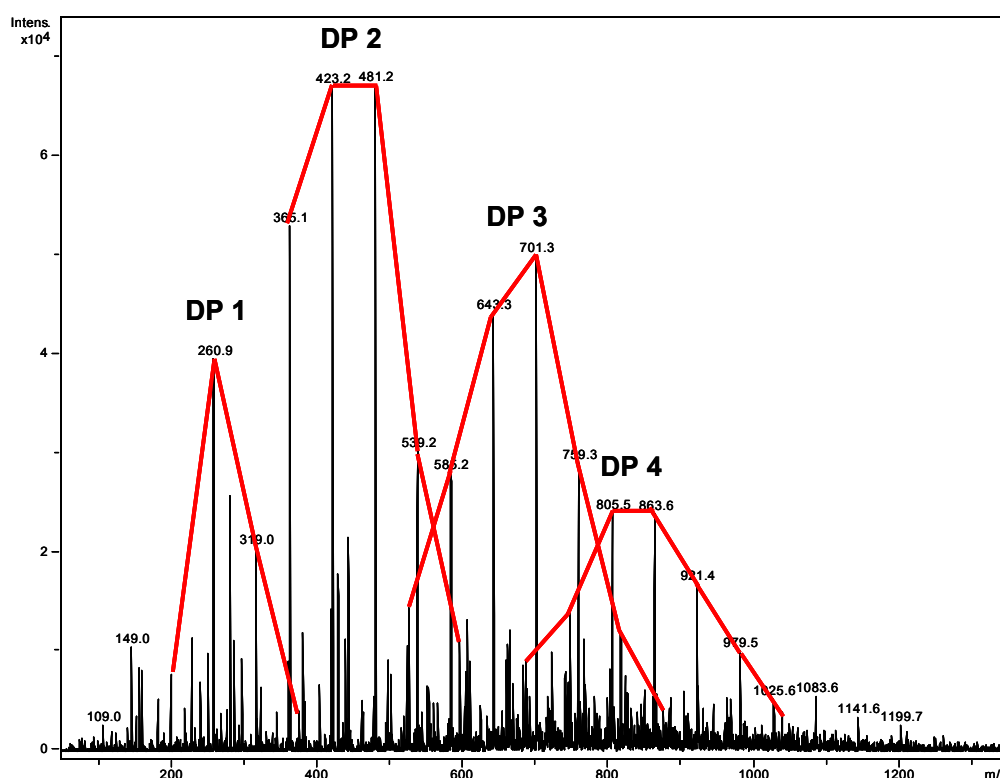


Fig. 4-47 ESI-IT mass spectrum of partially hydrolyzed (TFA, 2 M, 3 h, see 8.3.2.4) CMC 1, 5 mg/ mL H_2O , $[\text{M} + \text{Na}]^+$, protonated CM-groups ($\Delta 58 \text{ } m/z$)

First, labeling was performed according to *Naven and Harvey*^[167], with 17 eq GT/ AGU, but in the mass spectra of these samples, no product peaks could be observed. Investigations in our group of non-ionic polysaccharide ethers showed that labeling was improved when the equivalents of GT were reduced. 2 eq/ reducing end

showed well results and has also been a reasonable ratio for the celooligomer standard mixture.

As DP 2 was most prominent in the ESI-IT-mass spectra of the underivatized CMC hydrolyzates, this was assumed as average DP to calculate the amount of reducing ends in the hydrolyzate. Thus, 2 eq GT/ reducing end, i.e. 1 eq GT/ AGU, were used for derivatization. On TLC, the unlabeled celooligomer standard form 4.4.1 and partially hydrolyzed CMC 1 before and after derivatization with GT were compared. It is difficult to estimate the completeness of the reaction, since the elution behaviour of the CM-celooligomers differs from that without CM-groups.

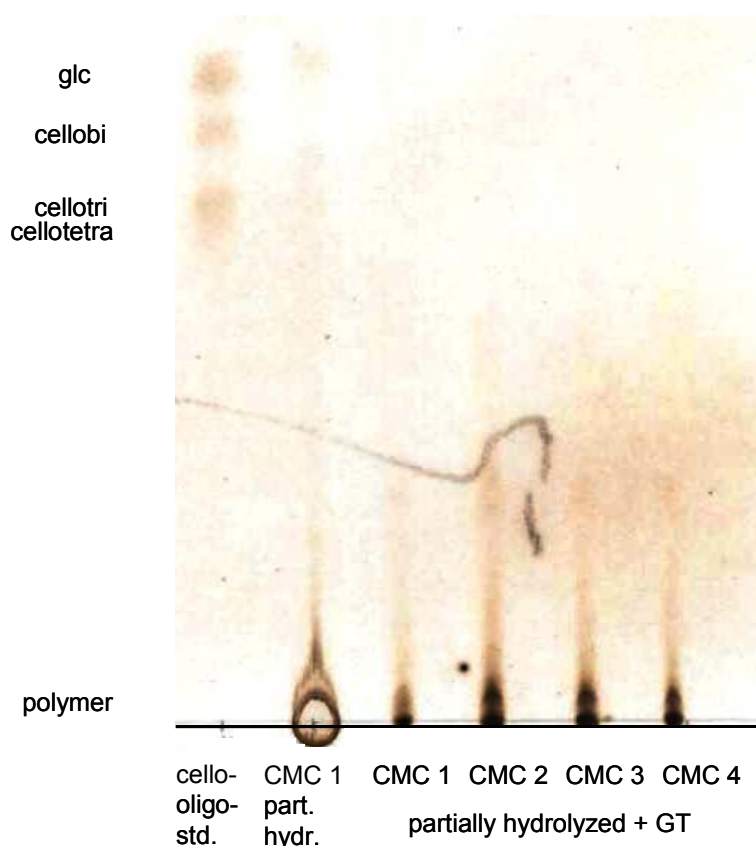


Fig. 4-48 TLC from left to right: underivatized celooligomer standard mixture, underivatized TFA-hydrolyzate of CMC 1, TFA-hydrolyzates of CMC 1 to 4 after labeling with GT (2 eq/ red. end. 8.3.4), TLC: silica, ethanol/ aq. NaClO₄ (7 g/ 100 mL) 8 : 2, v,v, detection: 10 % ethanolic H₂SO₄)

Furthermore, with increasing DP the amount of celooligomers without CM-groups in the hydrolyzates decreases. So glucose is the only indication for an insufficient reaction with GT. Glucose elutes faster than GT-glucose (see Fig. 4-43). In the derivatized hydrolyzates, no spots according to unlabeled glucose or cellobiose could be detected (Fig. 4-48).

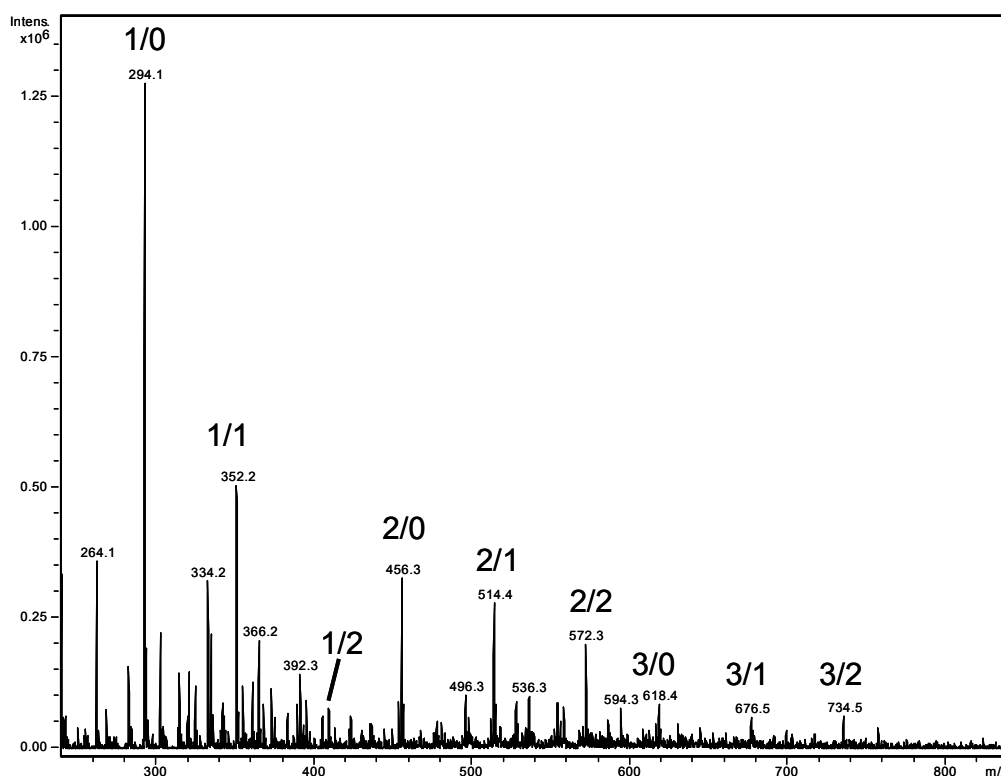


Fig. 4-49 ESI-IT mass spectrum of the partial TFA hydrolyzate of CMC 1 (8.3.2.4) shown in Fig. 4-47 after labeling with Girard's T reagent (8.3.4), 0.5 mg/ mL in methanol; peaks are assigned DP/n(CM)

The total intensity of the mass spectra after labeling was enhanced. The pattern from DP 2 and 3 predominated in the spectra of the underivatized hydrolyzate, whereas DP 1 was significantly prominent after labeling with GT. This is in agreement with Fig. 4-46 and the TLC results (Fig. 4-48) and is visualized by the relative intensities between the individual components before and after labeling displayed in Fig. 4-50. Consequently, the obtained DS was much too low. For CMC 1, the average DS evaluated from DP 2 was only 0.39 (DS CE-UV: 0.88). Although on TLC glucose as indication for insufficient labeling was not observed MS indicates that derivatization with GT could not be applied to CMC.

Since derivatization with GT did not bring the required results, the mass spectra of the underivatized partially hydrolyzed CMCs (TFA, 2 M, 3 h) were regarded with respect to eventual heterogeneity of the samples. Two prerequisites have to be fulfilled when interpreting the oligomeric substituent distribution: First, the average DS has to be constant independent of DP and secondly, the DS should be in agreement with the average DS of the entire sample.

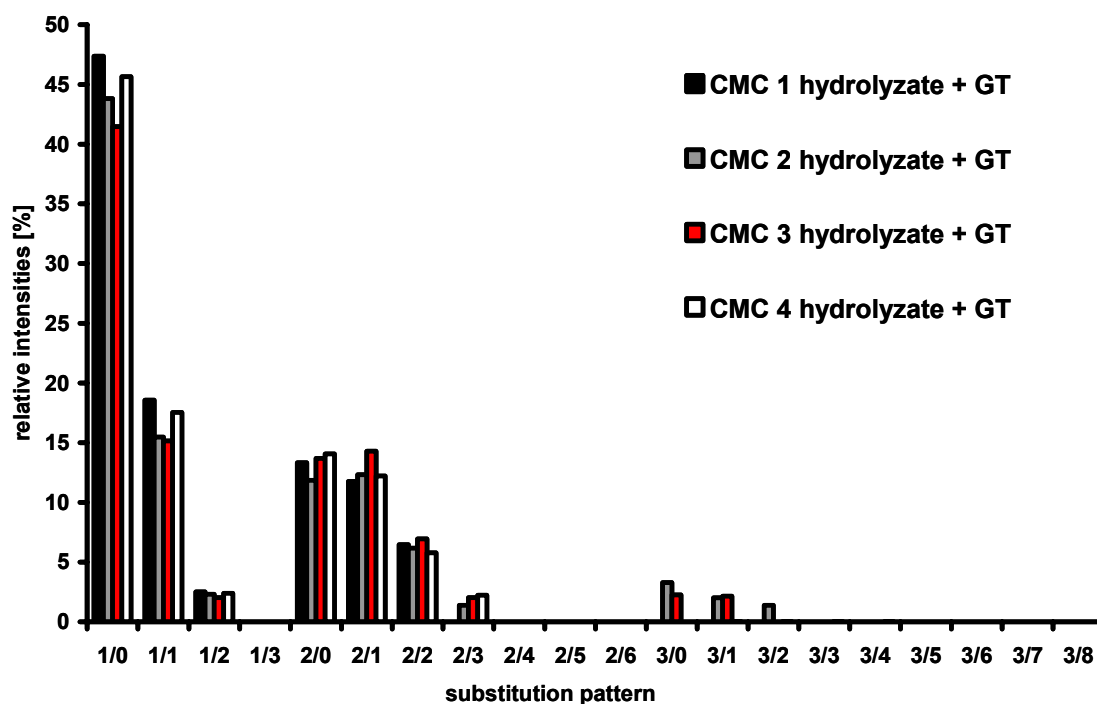
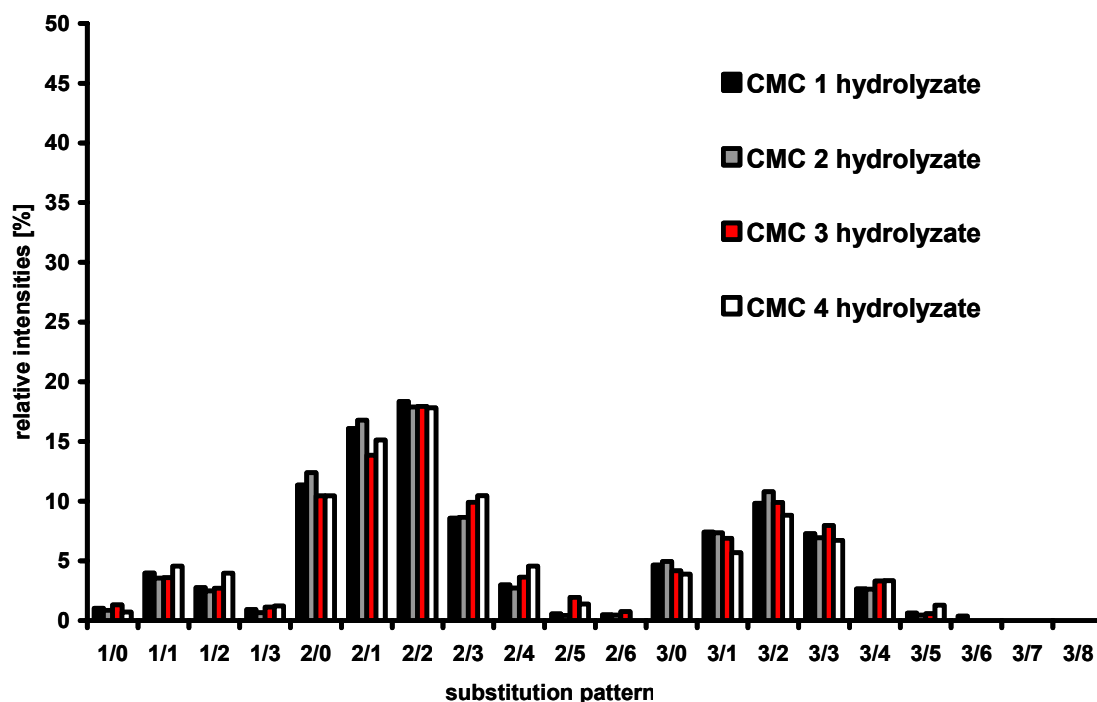


Fig. 4-50 Relative intensities of the ESI-IT spectra of the partial TFA hydrolyzates (8.3.2.4) of CMC 1 to 4 before (top) and after (bottom) labeling with Girard's T reagent (8.3.4); DP/n(CM)

The average DS values for partially hydrolyzed CMC 1 in ESI-IT-MS were 1.31 (DP 1), 0.82 (DP 2), 0.88 (DP 3), and 0.73 (DP 4). The deviations from the average DS obtained by CE-UV (0.88) were hence: + 49 % (DP 1), - 7 % (DP 2), 0 % (DP 3), and - 17 % (DP 4). It is remarkable, that the deviations were much smaller than for

the methanolizates after acylation (see chapter 4.1). The deviation increased with DP 4 due to the lower intensity and hence worse signal/noise-ratio.

The prerequisites were only partly fulfilled. The interpretation is not completely reliable since a DS trend is observed. For small DPs the DS is higher than expected, whereas the DS decreases with increasing DP to values lower than expected. This might result for one DP in a DS that agrees with the DS from monomer analysis since several discriminating effects compensate each other. The high difference in DS also influences the heterogeneity parameter which leads to false results.

The hydrolyzates were also analyzed by MALDI-TOF-MS. Only DP 3 could be evaluated as the masses of DP 2 overlapped with matrix peaks. The differences between ESI-IT and MALDI-TOF (matrix: DHB) were not that significant for the hydrolyzates as they had been for the methanolizates. Tab. 4-3 shows an overview of the determined DS-values and heterogeneity parameters. The CM-distributions for all samples are shown in Fig. 4-51 and 10.2.3.

Tab. 4-3 DS-values and heterogeneity parameters of CMC 1 to 4 determined by ESI-IT- (entry A) and MALDI-TOF-MS after TFA hydrolysis, H_i in comparison to a statistical distribution based on the monomer data from CE-UV (3.2)

	DS CE-UV	DS DP 2	Δ DS (CE)	H_2	DS DP 3	Δ DS (CE)	H_3
CMC 1 ESI	0.88	0.82	-7 %	8.8	0.88	0 %	4.9
CMC 1 MALDI			n.d.		0.84	-5 %	7.6
CMC 2 ESI	0.85	0.80	-6 %	9.4	0.88	+4 %	7.5
CMC 2 MALDI			n.d.		0.91	+7 %	10.6
CMC 3 ESI	0.94	0.94	0 %	9.3	n.d.		
CMC 3 MALDI			n.d.				
CMC 4 ESI	0.96	1.05	+9 %	13.6	1.01	+5 %	7.3
CMC 4 MALDI			n.d.			n.d.	

The DS-values evaluated for DP 3 from ESI-IT-MS show the smallest differences to the monomer analysis and hence are regarded as most reliable. MALDI-MS yielded greater deviations. For CMC 3, DP 3 could not be evaluated, such as MALDI for CMC 4. Despite the good agreement in the average DS/ DP 3, the MALDI-MS measurement of CMC 3 was not valid due to the poor signal/noise-ratio. The deviations between the entries A and B (Fig. 4-51) are relatively high. Therefore,

these should be regarded as qualitative results. For all four CMCs there are higher contributions to low and high substituted domains than expected for a random pattern.

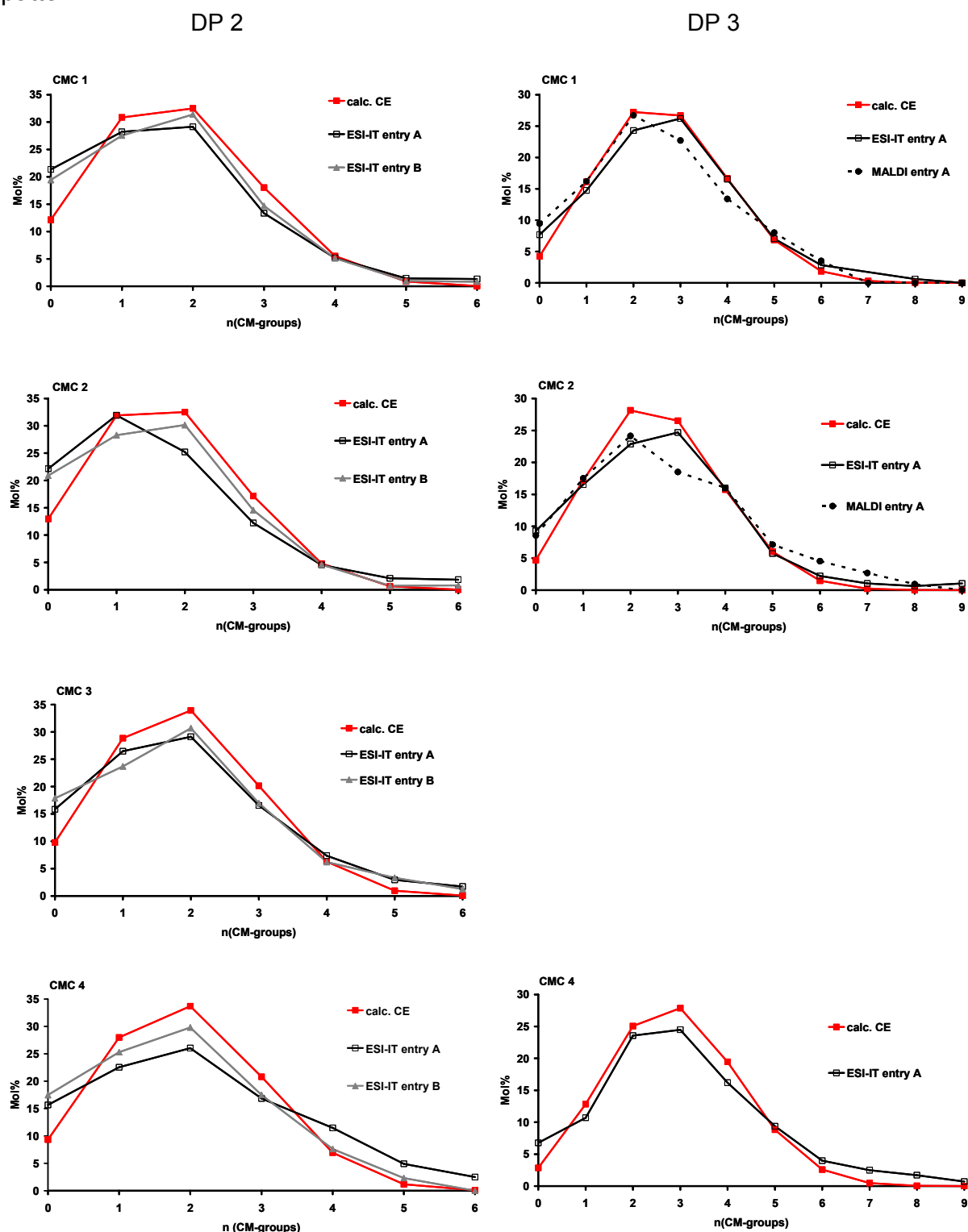


Fig. 4-51 Distribution of the CM-groups in DP 2 and 3 of TFA-hydrolyzates of CMC 1 to 4 obtained from ESI-IT- (8.3.2.4) and MALDI-TOF-MS, matrix DHB (8.2.3). Experimentally obtained data compared with the random distribution calculated by Bernoulli statistics from monomer analysis by CE-UV (calc.CE, 8.3.2.1, 8.3.3).

5 Kinetic studies of the partial degradation of CMC

Random degradation is the requirement for the investigation of CM-glucose distribution in the polymer chain by oligomer analysis. Therefore, it is necessary to study whether (or under which conditions) hydrolysis and/or methanolysis of CMC are independent of the location of the substituents in the AGU.

The rate of hydrolysis is expected to be influenced by the CM-substitution pattern in the AGU due to steric, electronic and neighbor group effects, e.g. the carboxonium ion formed as intermediate could possibly be shielded by intramolecular ring formation with a 2-O-carboxymethyl group (6-membered ring), although it is protonated under hydrolytic conditions. Articles concerning this subject are rare. To the best of our knowledge; no data are available for methanolysis of carbohydrate derivatives.

In 1987, *Rowland and Howley*^[203] investigated the influence of the location of the substituents on the hydrolysis of 2-diethylaminoethyl (DEAE)-cellulose. For their analysis, they substituted two types of cellulose: mature cotton containing typically 80 % crystalline regions (determined by X-ray diffraction), DS 0.01, and disordered cellulose prepared from ball-milling purified cotton fibres, DS 0.02. The DEAE-ethers of both types of cellulose were hydrolyzed with TFA and sulphuric acid, respectively, and the amounts of the monomers were determined after freeze-drying and TMS-derivatization by GLC-FID. *Rowland and Howley* determined the order in the releasing rate of glucose $> 3\text{-O} > 6\text{-O} \approx 2\text{-O-DEAE-glucose}$. As these results were obtained for both types of cellulose, the authors concluded that the physical state of the cellulose and factors such as accessibility and crystallinity only play a minor role for these effects. They proposed that an effect of the substituent is steric restriction of the attacking species at the glucosidic linkage, which has to be questioned in regard to the small size of the proton. The significance of their results is also limited, since the DS of their samples was very low and they did not calculate rate constants.

In an article by *Capon*^[204] from 1969 on mechanisms in carbohydrate chemistry, studies on the rates of acidic hydrolysis of methyl glucopyranosides of the late 1960s are reviewed. *De and Timell*^[205] investigated the acid catalyzed hydrolysis of O-methylated glucosides in 1966. They studied regioselectively prepared O-methyl glucosides and O-methylated gentiobiose (β -(1 \rightarrow 6)-linked diglucoside, only the AGU with the non-reducing end was methylated). The derivatives were hydrolyzed with

0.5 M sulphuric acid at 60, 70, and 80 °C, respectively, and the extent of hydrolysis was determined polarimetrically. Methylation of methyl β -D-glucosides as well as of gentiobiose was found to be slightly rate-decreasing (Tab. 5-1). Hydrolysis follows a first-order reaction. Consequently, for the methyl β -D-glucosides as well as for the 6-O-(mono-O-methyl β -D-glucopyranosyl)-D-glucoses the order in the releasing rate observed is $un > 3 > 2 \approx 4 > 6$ with respect to the methyl substituted position. The authors suggest that the lower rate of hydrolytical cleavage in methylated compounds results from the hindrance of conformational changes to carboxonium-ion formation by the methyl groups.

Tab. 5-1 First-order rate constants k and activation parameters (energy ΔE_A and entropies ΔS^\ddagger at 60 °C) for the hydrolysis of methyl-mono-O-methyl β -D-glucosides and 6-O-(mono-O-methyl β -D-glucopyranosyl)-D-glucoses in 0.5 M sulphuric acid ^[205]

Compound	$10^6 k [\text{sec}^{-1}]$ at 60 °C	$10^6 k [\text{sec}^{-1}]$ at 70 °C	$10^6 k [\text{sec}^{-1}]$ at 80 °C	$\Delta E_A [\text{kcal mol}^{-1}]$	ΔS^\ddagger at 60 °C [cal deg ⁻¹ mol ⁻¹]
methyl-mono-O-methyl β -D-glucopyranosides					
2-O-methyl	1.19	5.22	20.8	33.4	+12.9
3-O-methyl	1.27	5.66	23.8	34.2	+41.9
4-O-methyl	1.15	4.97	21.2	34.0	+41.1
6-O-methyl	0.84	3.88	16.1	34.5	+16.8
unsubstituted	1.38	6.25	24.1	33.4	+10.6
6-O-(mono-O-methyl β -D-glucopyranosyl)-D-glucose					
2-O-methyl	1.56	6.69	26.7	33.1	+12.5
3-O-methyl	1.77	7.69	32.0	33.7	+14.5
4-O-methyl	1.48	7.04	28.3	34.4	+16.4
6-O-methyl	1.37	5.46	22.3	32.6	+10.9
unsubstituted	1.87	8.25	32.9	33.3	+14.3

During hydrolysis, the intermediate carboxonium-ion is formed that is stabilized through mesomeric interactions with the ring oxygen. This stabilization is maximized when C-1, C-2, C-5, and O-5 all are in one plane, i.e., the conformation has changed from “chair” to “half-chair” (Fig. 5-1), a mechanism already postulated by *Edward* in 1955 ^[206]. The transition requires rotation around the C-2 - C-3 and C-4 - C-5 linkages. Steric factors which favour the planar conformation should thus cause an increase in reaction rates. Based on these proposed influences of sterical hindrance,

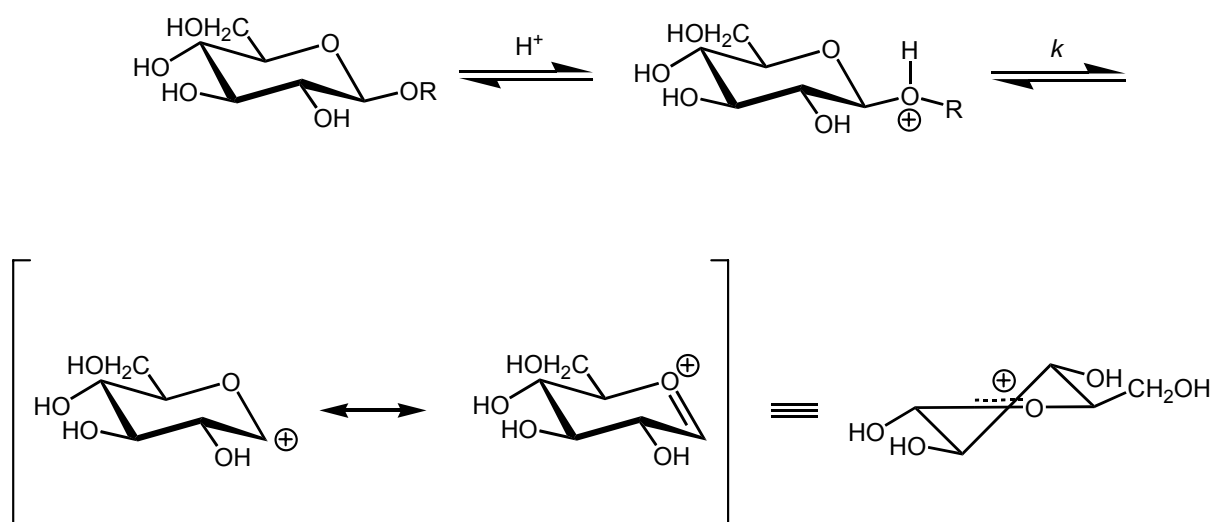


Fig. 5-1 Mechanism of the acid catalyzed hydrolysis of glycosidic bonds, including a transition of the “chair” to the “half-chair” conformation due to carboxonium-ion formation

Tab. 5-2 First-order rate constants and activation parameters for the hydrolysis of methyl O-isopropyl-D-glucopyranosides in 0.5 M sulphuric acid ^[207]

Compound	$10^6 k [\text{sec}^{-1}]$ at 70 °C	$10^6 k [\text{sec}^{-1}]$ at 80 °C	$10^6 k [\text{sec}^{-1}]$ at 93 °C	$\Delta E_A [\text{kcal mol}^{-1}]$	ΔS^\ddagger at 80 °C [eu]
methyl α -D-glucosides					
2-O-isopropyl	3.38	16.1	94.4	34.9	16.8
3-O-isopropyl	3.57	18.4	100.0	34.5	15.8
4-O-isopropyl	2.94	14.1	85.5	35.5	17.8
6-O-isopropyl	2.30	10.7	64.4	35.0	17.4
unsubstituted	2.82	13.8	76.1	33.8	13.2
methyl β -D-glucosides					
2-O-isopropyl	10.6	50.6	276.5	33.7	15.7
3-O-isopropyl	10.4	46.6	248.0	33.0	13.5
4-O-isopropyl	6.1	28.2	162.1	34.5	16.7
6-O-isopropyl	4.3	21.4	129.1	35.4	18.6
2,3-O-isopropyl	13.2	63.0	364.0	34.6	17.5
unsubstituted	6.0	25.4	141.0	33.9	14.0

Saunders and Timell ^[208] investigated the effects of substitution in position C-3 and C-5 on the hydrolysis rates.

Höök and Lindberg found in 1966 that isopropylation of the positions O-2, O-3, and O-4 increases the rate of hydrolysis of α - and β -methyl-D-glucosides^[207]. The first-order rate constants obtained are displayed in Tab. 5-2.

For the α -configured series they observed the order for rate constants of $3 > 2 > 4 \approx \text{un} > 6$. For the β -series they found the order $2,3 > 2 \approx 3 > 4 \approx \text{un} > 6$, thus deviating from the α -series with respect to the alkylated position.

A probable explanation for the rate-increasing influence of isopropylation is the stabilization of the carboxonium-ion by positive inductive effects. Jensen and Bols found in 2003^[209] in their studies of methyl glycosides that electronic rather than steric effects of remote substituents on glycosides influence the rate of hydrolysis.

According to the dependence of the rate constants on the temperature (Arrhenius-equation), the differences should become less significant with increasing temperature. For the isopropyl derivatives no such trend can be observed. Substituents in the aglycon AGU also influence the stability of the glucosidic linkage.

5.1 Kinetics of hydrolysis

To get more information about the kinetics of CMC acidic depolymerization, a method for end group analysis was developed which allows detecting possible differences in the hydrolysis rates of the various AGUs of CMC (Fig. 5-2).

First, CMC is partially hydrolyzed with 1.5 M perchloric acid (90 °C, different entries, 2 to 17 h) together with an acid-stable internal standard. The reducing ends are labeled with a chromophore which has to be stable under the conditions of the subsequent hydrolysis. The labeled partially hydrolyzed CMC can be analysed by CE-UV. To avoid overlapping of the regioisomeric glucose derivatives with oligomeric compounds, the latter can be completely degraded. Only the labeled monomers, i.e. the former end groups will be detected. The concept presented here comprises labeling of the monomers released in the second hydrolysis step with a chromophore absorbing in another UV-range and/or showing different migration behavior due to charge or size.

Monomers released at higher rates will be enriched in the early stage of hydrolysis. If the substitution pattern had no influence, the distribution of AGU from newly formed reducing ends should match the distribution of the monomer analysis at any stage of depolymerization. With this experimental set-up it cannot be differentiated between

the influences of the substituents in the glycosyl donor and those of the aglycon AGU.

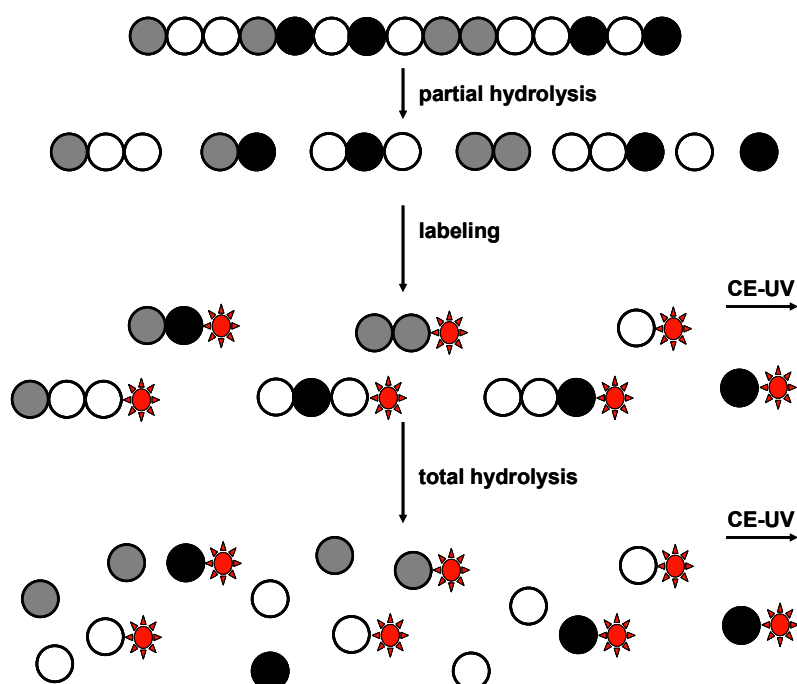


Fig. 5-2 End group analysis for CMC by CE-UV

5.1.1 Development of a CE-method for end group analysis

First step in method development was to find appropriate acid-stable chromophores and an internal standard that can be added directly to the CMC before hydrolysis. The internal standard would best to reach the cathode before glucose as it must not interfere with the migration times of the released monomers. Pentoses fulfil these requirements, so ribose, arabinose, and xylose were tested with respect to their migration behavior relative to glucose after labeling with 4-aminobenzonitrile (ABN) in the borate buffer system of the monomer analysis. From Fig. 5-3 it is obvious that xylose was best suited. According to $^1\text{H-NMR}$ (in D_2O), xylose was pure. The second problem was to find an appropriate chromophore (Tab. 5-3). ABN turned out to be not applicable as it is hydrolyzed to 4-amino benzoic acid (ABA) under acidic conditions, and an additional peak was observed in the electropherogram, as was confirmed by standard comparison and DAD spectra.

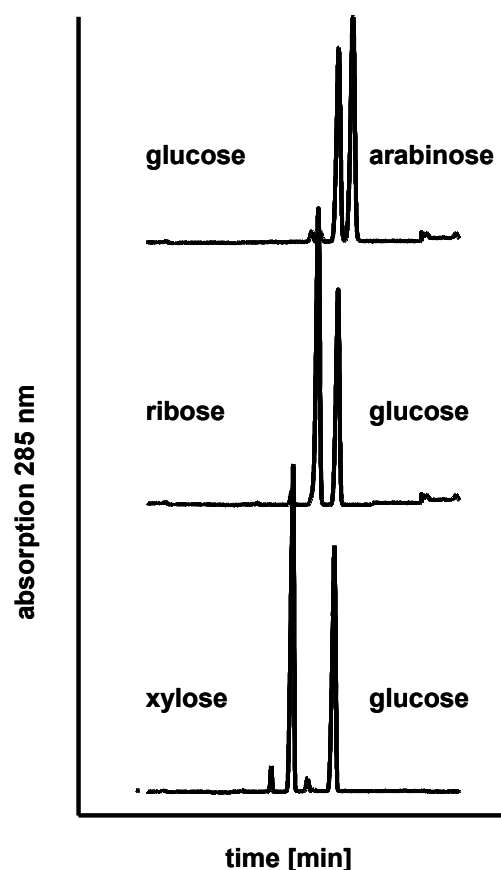
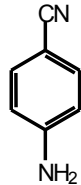
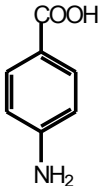



Fig. 5-3 Migration order of glucose and arabinose, ribose, and xylose, respectively, in CE-UV after labeling with ABN (175 mM borate buffer, pH 10.5, 28 kV, normal polarity)

Tab. 5-3 Overview of investigated chromophores, their charge in the applied borate buffer system and their stability during hydrolysis conditions

	Structure	Mass [g/ mol]	Absorbance max. [nm]	Charge in BGE (pH 10.5)	Stable under hydrolysis conditions
4-amino benzonitrile (ABN)		118.14	285	neutral	no
4-amino benzoic acid (ABA)		137.14	285	negative	yes
4-methyl- aniline, <i>p</i> -toluidine, (Tol)		107.17	260	neutral	yes

Therefore, ABA was investigated, which is stable under the conditions of hydrolysis. ABA-labeled analytes showed very long migration times due to the negative charge which lead to peak broadening thus reduced sensitivity. It was tried to reduce the migration times by applying an additional pressure of 5 mbar, but analytes migrating in a narrow range, such as the 3,6-O- and 2,3-O- or 2,6-O-di- and 2,3,6-O-tri-CM-glucitols were no longer baseline separated. This system was not further optimized. Instead, *p*-toluidine (4-amino-1-methylbenzene) was tested, which has a highly cancerogeneous potential. It is not negatively charged under the applied conditions and acid-stable. To test the acid stability, glucose and xylose were labeled with *p*-toluidine, and their ratios were determined before and after acidic treatment. TFA was used to avoid the elaborate removal of perchlorate. No additional peaks were obtained in the electropherograms after acidic treatment. The ratio of the peak areas glucose/ xylose (molar ratio 0.66 : 1) remained sufficiently constant with 0.66 before and 0.63 after hydrolysis (Fig. 5-4).

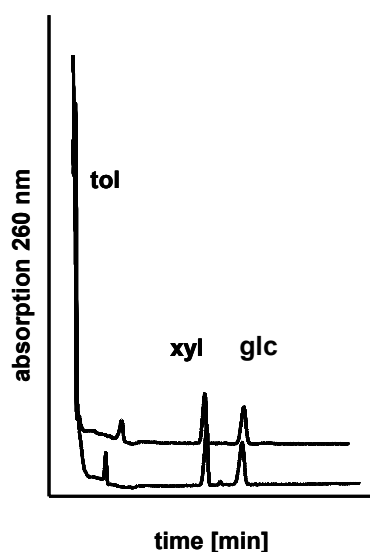


Fig. 5-4 Electropherograms of D-xylose (xyl) and D-glucose (glc) labeled with *p*-toluidine (tol) before (top) and after (bottom) TFA-hydrolysis. Glucose- to xylose-peak ratio is 0.66 before and 0.63 after hydrolysis. CE conditions: 150 mM borate buffer pH 10.5, 28 kV, 25 °C, detection at cathode (normal polarity)

5.1.2 Composition of partially hydrolyzed CMC

Five entries of 20 mg dried CMC 4 (approx. 0.08 mmol AGU) were hydrolyzed 2-17 h with 0.7 M perchloric acid (90 °C, 8.3.2.1), and reductively aminated with *p*-toluidine. Xylose (0.13 mmol, from stock solution) was added as internal standard before hydrolysis. The labeled, partially hydrolyzed samples were

subsequently hydrolyzed with perchloric acid for 17 h (total hydrolysis, see scheme in Fig. 5-2). The samples became brownish colored. Although labeled glucose and xylose were acid stable and remained colorless after hydrolysis, labeled partially hydrolyzed CMC changed color during the second hydrolysis step, and additional peaks could be observed in the electropherogram (Fig. 5-5). An assignment of these peaks was not possible. DAD spectra showed that these compounds had different absorbance maxima. The mechanism of this side reaction could not be clarified within this work.

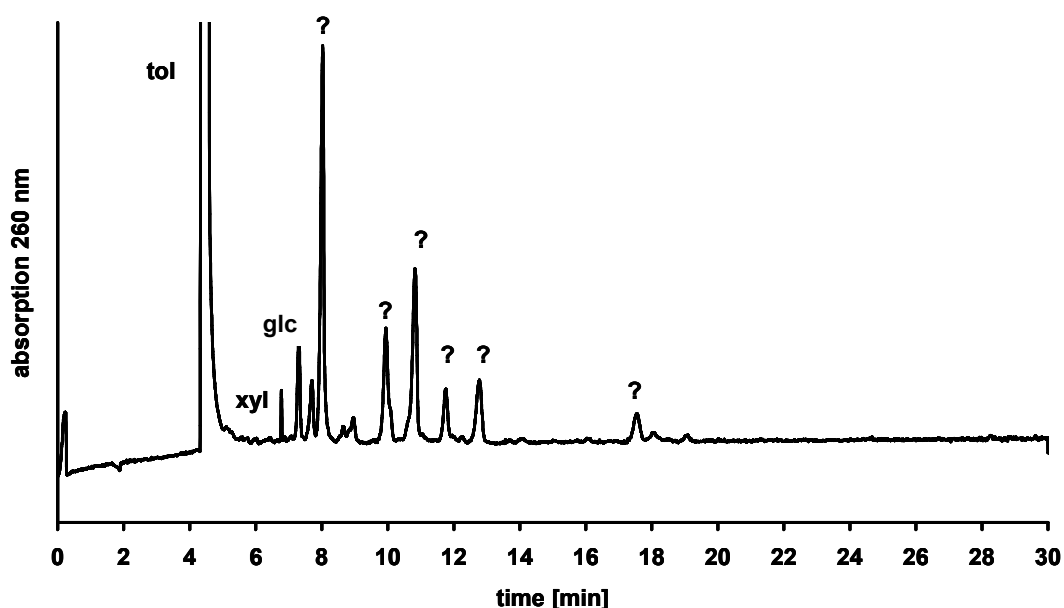


Fig. 5-5 Partially hydrolyzed (8 h) CMC 4 (20 mg, approx. 0.08 mmol AGU), reductively aminated with *p*-toluidine, completely hydrolyzed with 0.7 M perchloric acid (8.3.2.1) and measured by CE-UV. Only xylose and glucose could be assigned by co-injection and DAD-spectrum.

Since the monomer distribution after the second and complete degradation could not be determined, the results of the labeled partially hydrolyzed samples were regarded. Fig. 5-6 shows an electropherogram of CMC 4, hydrolyzed for 4 h and labeled with *p*-toluidine. The peak migrating at 6 min could be identified as cellobiose by co-injection with the standard substance, but the total amount of oligomers was unexpectedly low, since the monomer yield was only 37 % after 4 h. Thus, this electropherogram shows again the oligomer “gap” that has already been observed on TLC and in ESI-IT-MS (4.4.2). Fig. 5-7 shows the yields of the released CM-glucoses in Mol% (related to the average $M_{(AGU)}$: $162 + DS \cdot 80$ for NaCMC).

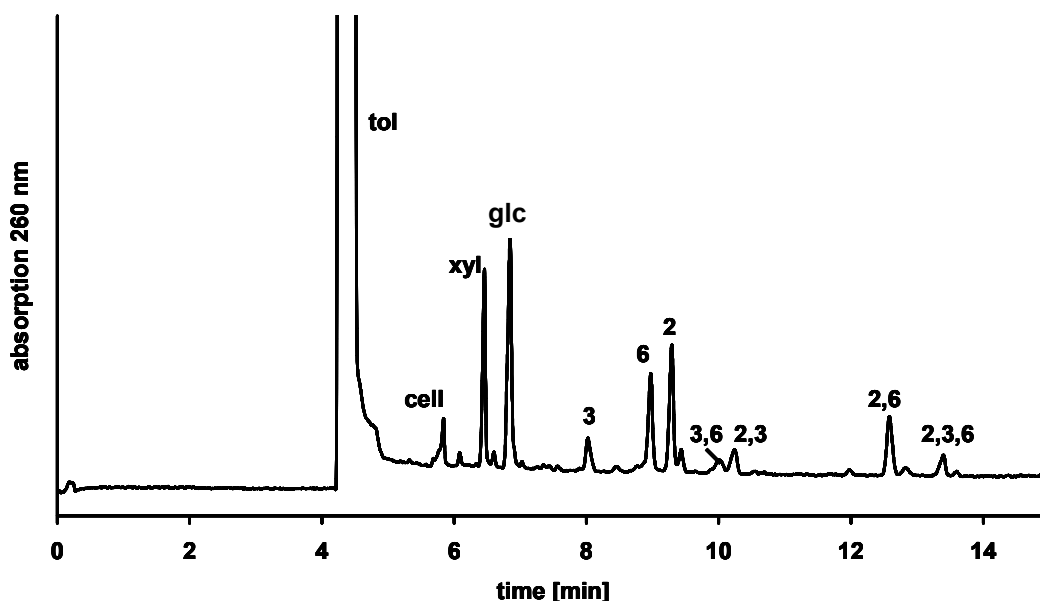


Fig. 5-6 Electropherogram of partially hydrolyzed (4 h, 0.7 M perchloric acid, 90 °C, 8.3.2.1) CMC 4 (20 mg, approx. 0.08 mmol AGU), reductively aminated with *p*-toluidine (tol), xylose (xyl) internal standard, cellobiose (cell) assigned by co-injection 1-(4-methylphenyl)amino-1-deoxy-D-glucitols, peaks are assigned according to the positions of CM-substitution
CE-conditions: 150 mM borate buffer, pH 10.5, 28 kV, 25 °C (8.2.1)

As expected, the yield of monomers increased with increasing hydrolysis time. After 2 h, 25 % monomers and after 17 h, 84 % monomers were obtained (Tab. 5-4), which is in agreement with the results from monomer analysis (chapter 3.2). Due to the relatively high amount of potassium perchlorate in the residues from hydrolysis, the corresponding ESI-IT-mass spectra were too poor to be evaluated.

TLC showed that polymeric material (and/ or gel particles or aggregates) was removed during the repeated filtration steps together with the perchlorate. To investigate the observed oligomer “gap”, partially hydrolyzed CMC 3 was methoxacetylated and investigated by LC-ELSD as described in chapter 4.3.2. Methoxyacetylation of a hydrolyzate does not eliminate the ionic character of the CM-group, so the influence of the CM-substitution pattern on the elution behavior should not be nearly levelled-off as observed for methanolizates, but from the chromatograms (Fig. 5-8) it is obvious that the differences in the retention times were small.

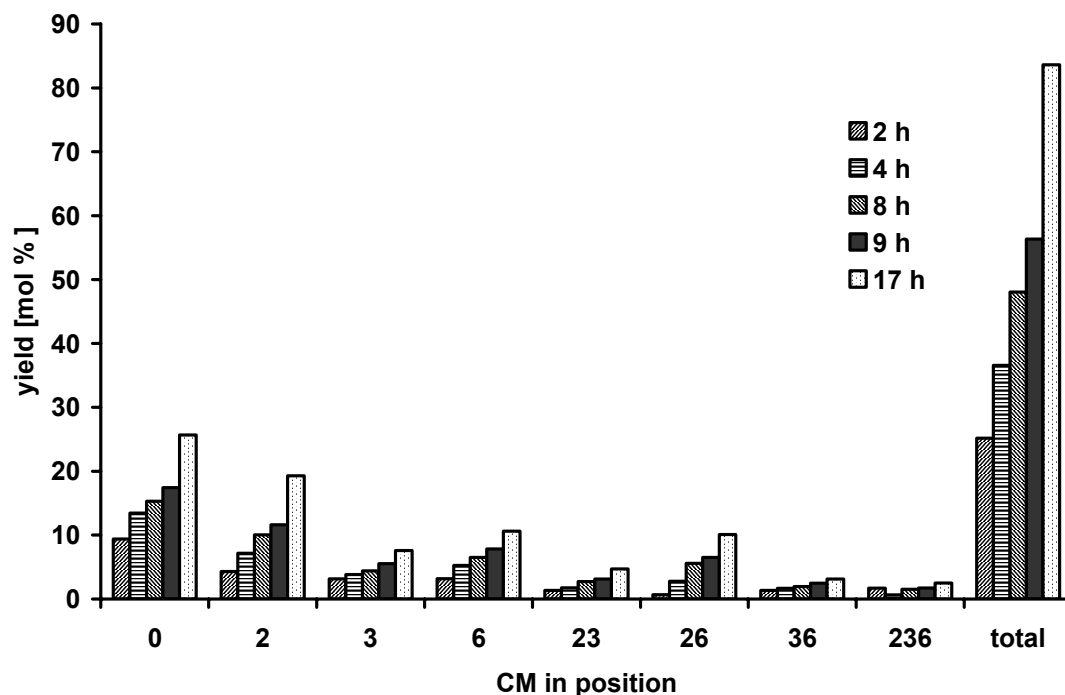


Fig. 5-7 Yields [Mol% AGU] of monomers released after partial hydrolysis (2 to 17 h with perchloric acid, 8.3.2.1) of CMC 4 (20 mg, approx. 0.08 mmol) labeling with toluidine, and analysis by CE-UV, xylose (0.133 mmol) is added as internal standard prior to hydrolysis

Tab. 5-4 Yields [Mol% AGU] of monomers released after partial hydrolysis (2 to 17 h with perchloric acid, 8.3.2.1) of CMC 4, xylose (0.133 mmol) as internal standard, CE-UV analysis

hydrolysis time [h]	2	4	8	9	17
entry dried CMC [mg]	17.87	18.07	17.99	18.52	17.93
entry CMC [μmol AGU]	74	75	75	77	74
glc	9.45	13.54	17.23	17.51	25.81
2-O-CM	4.32	7.21	11.32	11.70	19.40
3-O-CM	3.18	3.86	4.96	5.58	7.64
6-O-CM	3.23	5.30	7.32	7.89	10.69
2,3-O-CM	1.36	1.76	3.09	3.16	4.74
2,6-O-CM	0.68	2.81	6.28	6.54	10.16
3,6-O-CM	1.38	1.67	2.20	2.51	3.16
2,3,6-O-CM	1.70	0.65	1.70	1.75	2.52
total yield	25.31	36.80	54.09	56.64	84.11

No peaks of methoxyacetylated DP 1 could be assigned in the 1 h hydrolyzate. After 6 and 17 h, only DP 1, and no oligomers with higher DPs were detected. The molar yields were 36 % DP 1 in the 6 h hydrolyzed sample and 90 % DP 1 in the 17 h hydrolyzate. These results are in agreement with those obtained by CE-UV. This “gap” in the oligomer distribution, also observed on TLC (Fig. 4-48), indicates that hydrolysis has characteristics of a peeling process.

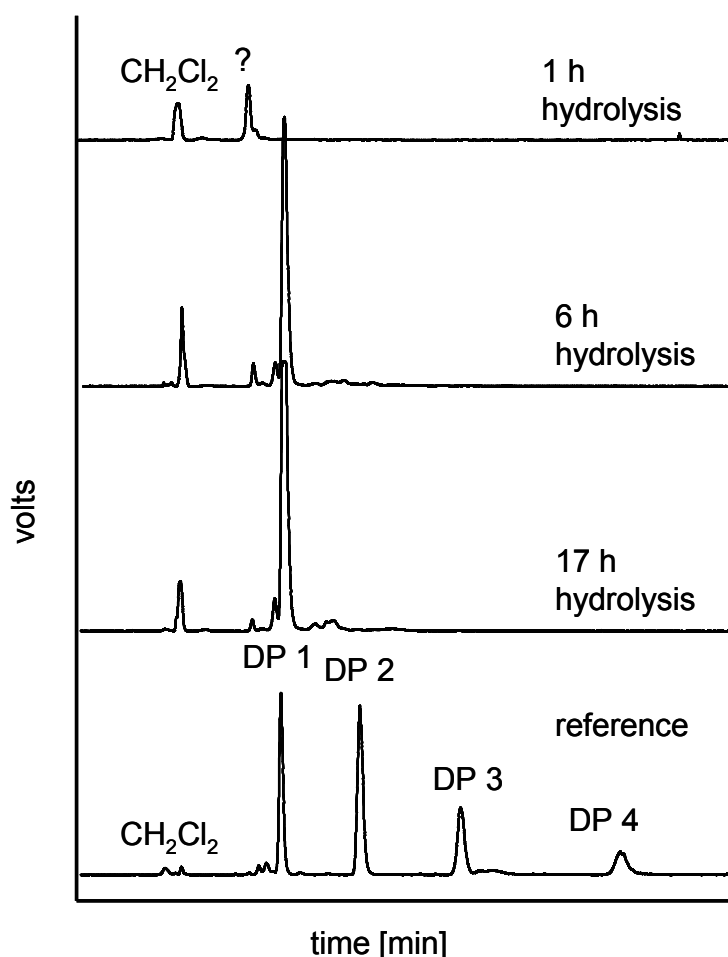


Fig. 5-8 LC-ELSD chromatograms of methoxyacetylated (8.3.8.3) hydrolyzates of CMC 3 (perchloric acid, 90 °C, 8.3.2.1). From top to bottom: 1 h hydrolysis, 6 h hydrolysis, 17 h hydrolysis, DP- reference (methoxyacetylated glucose, cellobi-, cellotri-, and cellotetraose, see 8.3.9), HPLC conditions: Si-column, acetone/hexane, 1/ 1, v/ v, see 8.2.4

5.1.3 Kinetics of the partial degradation

To get more information about the mechanism of hydrolysis, the absolute molar amounts of the released monomers (Fig. 5-7) are displayed in relation to each other in Fig. 5-9. This way, eventual trends with respect to a preferred release of distinct monomers becomes visible. According to Fig. 5-7, the monomers are not

released with the same propability. Glucose, 3-O- and 3,6-di-O-CM are enriched in the early stages of hydrolysis, whereas the yields of 2-O- and 2,6-O-CM-glucose increase with the duration of the hydrolysis. The amount 6-O- remains relatively constant over the time course. The high amount of 2,3,6-tri-O-CM-glucose in the 2 h entry is regarded as not reliable and hence neglected for further interpretations.

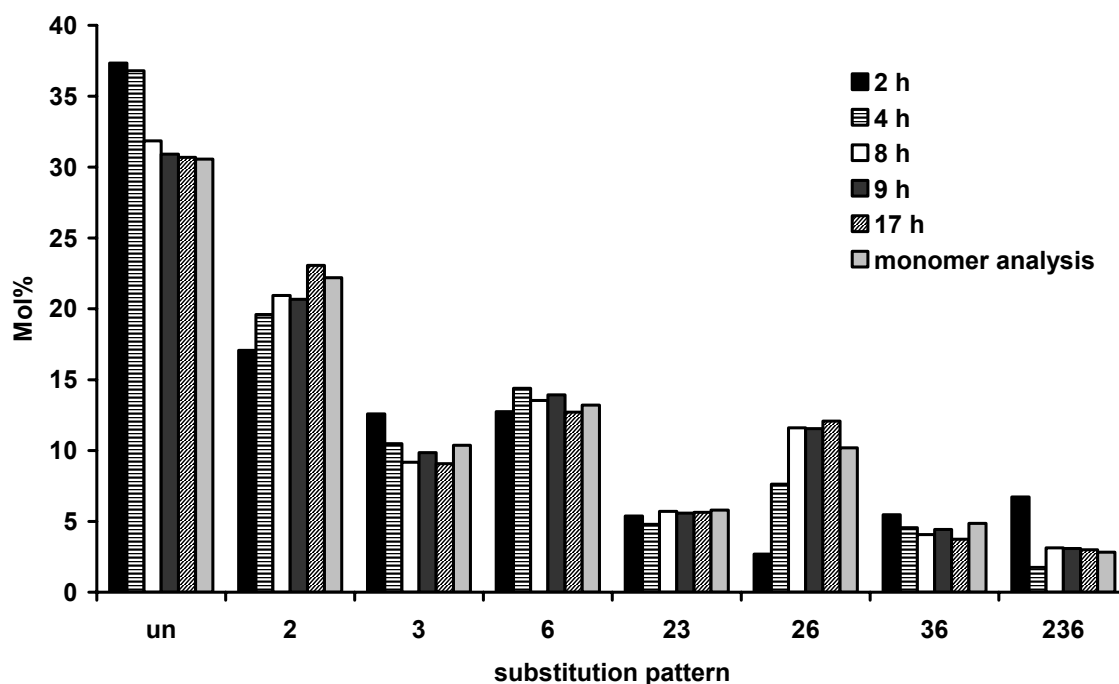


Fig. 5-9 Monomer composition [Mol%] of partially hydrolyzed CMC 4 (5 entries, 20 mg, approx. 0.08 mmol, hydrolyzed 2 to 17 h with 0.7 M perchloric acid, 90 °C, see Fig. 5-7) after labeling with *p*-toluidine and analysis with CE-UV, normalized to 100

Tab. 5-5 Monomer composition [Mol%] partially hydrolyzed CMC 4, (see Tab. 5-4)

Hydrolysis time [h]	2	4	8	9	17	Monomer analysis
glc	37.33	36.79	31.85	30.91	30.69	30.56
2-O-CM	17.06	19.59	20.93	20.66	23.07	22.20
3-O-CM	12.58	10.48	9.17	9.85	9.08	10.37
6-O-CM	12.75	14.39	13.53	13.93	12.70	13.21
2,3-O-CM	5.38	4.79	5.70	5.58	5.64	5.79
2,6-O-CM	2.70	7.63	11.61	11.55	12.08	10.19
3,6-O-CM	5.47	4.55	4.07	4.43	3.75	4.86
2,3,6-O-CM	6.72	1.76	3.14	3.09	3.00	2.82
DS	0.90	0.84	0.96	0.97	0.97	0.96

Consequently, the DS values (Tab. 5-5) of these mainly 2-O-substituted individual samples increase while hydrolysis proceeds. This effect diminishes after a hydrolysis time above 8 h and the DS values are constant at 0.97, which is in good agreement with the DS from titration (0.99) and monomer analysis (0.96).

The molar yields [μmol] of the degradation products of CMC 4 are displayed in Fig. 5-10.

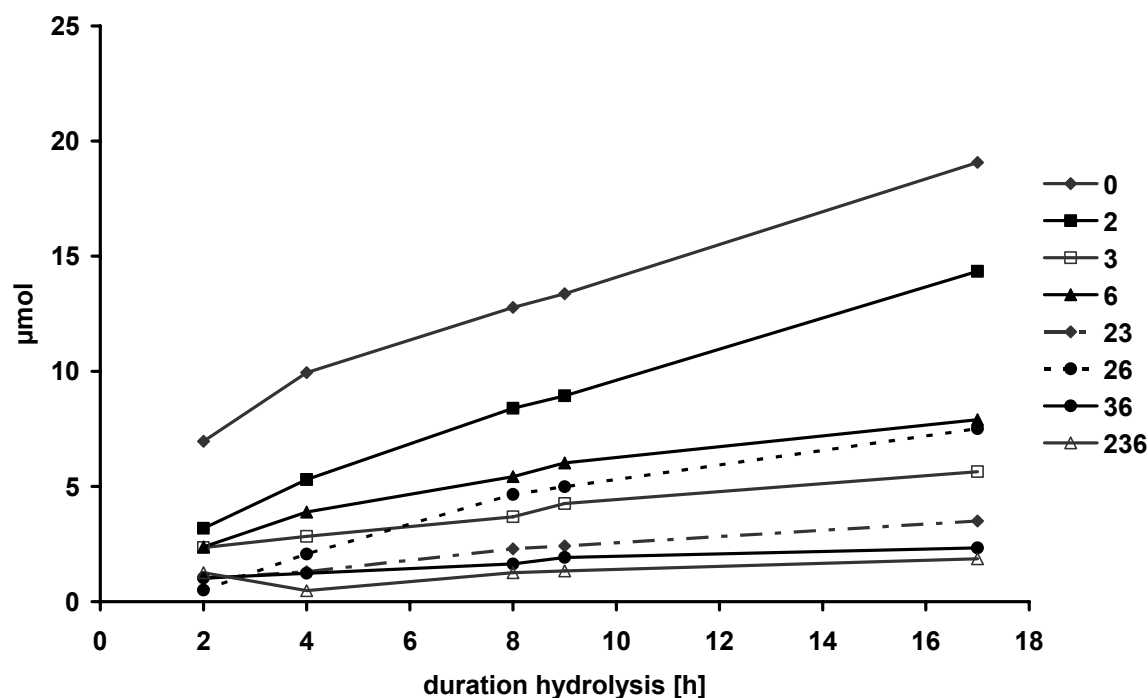


Fig. 5-10 Yields [μmol] of the degradation products of CMC 4

This graphic illustrates the trends already visible in the diagram of the relative molar distribution of the glucosides normalized to 100 in Fig. 5-9. If the acid catalyzed hydrolysis proceeded randomly, the curves would not cross. This can better be visualized by setting one of the components equal to 1 (here: glucose, Fig. 5-11) and regarding the s_i/s_0 ratios. All effects become less significant for the CMC hydrolysis products at hydrolysis times above 8 h. At this point the monomer yield is about 50 %, discriminating effects become less significant. To the end of the reaction, the curves show a more linear course (Fig. 5-10), which would indicate pseudo-zero reaction order and degradation from the outer parts of the chains. This is unexpected, since in literature for polysaccharide degradation in solution mainly first-order is assumed.

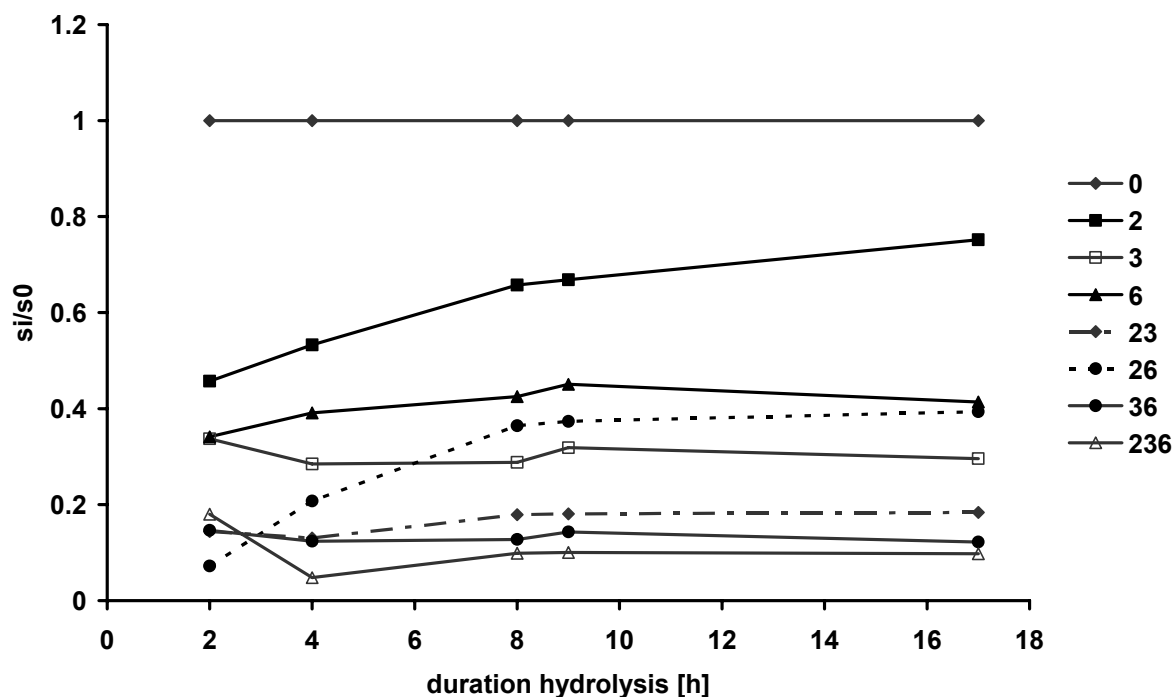


Fig. 5-11 Ratio s_i / s_0 of the absolute yields [μmol] of the CMC degradation products during partial hydrolysis

Therefore, it is investigated whether the reaction course agrees with a first-order reaction ($A \rightarrow B$) which has the general relation

$$\frac{[A]}{[A]_0} = e^{-k \cdot t} \quad (43)$$

for the consumption of educt A. The maximum monomer yield after complete degradation was 85 %, this has to be considered in the evaluation. The maximum amount of releasable monomers is given by the composition of the fully hydrolyzed sample, i.e., the hydrolyzate after 17 h. Therefore, the finally obtained molar composition of CMC is set as $[A]_0$. The decrease of CMC $[A]$ is not determined, but the molar amounts of the individual monomers, i.e., the concentrations of products B (s_i) over the time are given. Educt A is therefore expressed as $A_0 - B$, i.e. s_i in the 17 h-hydrolyzate minus s_i at hydrolysis time t . The linear relation to determine the rate constants for the release of monomers is given by

$$\ln \left(\frac{[A]_0 - [B]}{[A]_0} \right) = -k \cdot t \quad (44)$$

and k is the slope of the linear regressions obtained. Fig. 5-12 shows the corresponding logarithmic plot.

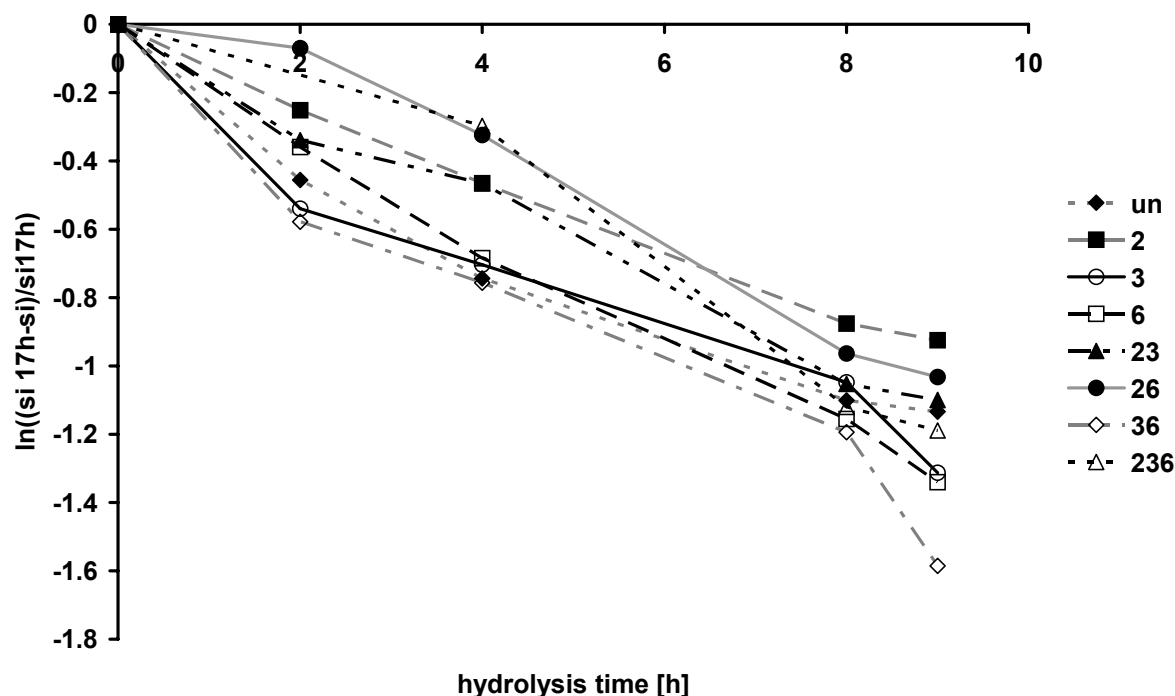


Fig. 5-12 Logarithmic plots for the eight monomers released after 2 to 9 h of perchloric acid hydrolysis of CMC 4, relative to the monomer composition of the 17 h-hydrolyzate

It is obvious from Fig. 5-12, that the logarithmic plot did not yield linear curves, consequently, the regression coefficients were relatively poor. So hydrolysis is not throughout a first-order reaction.

As can be seen from Fig. 5-10 and Fig. 5-11, hydrolysis is also not generally a pseudo-zero-order reaction, but probably a mixture of first- and zero-order. In the beginning, the reaction proceeds in dependence on concentration whereas it is independent of the amount of educt (i.e. undegraded CMC) after approx. 4 h. Since the reaction order is not consistent, no k -values can be evaluated and only a qualitative order in the releasing rates of the monomers can be estimated

In summary, for the hydrolysis of CMC with 2 M perchloric acid (90 °C) the following order of relative rates could be obtained:

$$\text{un} \approx 3 > 3,6 > 6 > 2,3,6 \approx 2,3 > 2,6 > 2$$

Tab. 5-6 Orders in the releasing rate in dependence on the substitution pattern of O-substituted glucosides.

Substituent	Glucoside	Releasing order	Acid/ temperature	Authors, year
carboxymethyl	CMC	monosub.: $un \approx 3 > 6 > 2$ total: $un \approx 3 > 3,6 > 6 > 2,3,6 \approx 2,3 > 2,6 > 2$ (no <i>k</i> -values)	0.7 M perchloric acid, 90°C	this thesis
2-diethyl- aminoethyl (DEAE)	DEAE-cellulose	$un > 3 > 6 \approx 2$ (no <i>k</i> -values)	TFA, sulphuric acid, reflux	Rowland and Howley, 1987 ^[203]
methyl	mono-O- methyl β -D- glucopyranoside	$un > 3 > 2 \approx 4 > 6$	0.5 M sulphuric acid, 60-90 °C	De and Timell, 1967 ^[205]
methyl	6-O-(mono-O- methyl β -D- glucopyranosyl)- D-glucose	$un > 3 > 2 \approx 4 > 6$	0.5 M sulphuric acid, 60-90 °C	De and Timell, 1967 ^[205]
isopropyl	O-isopropyl- methyl α -D- glucopyranoside	$3 > 2 > 4 > un > 6$	0.5 M sulphuric acid, 70-93 °C	Höök and Lindberg, 1966 ^[207]
isopropyl	O-isopropyl- methyl β -D- glucopyranoside	$2,3 > 2 > 3 > 4 > un > 6$	0.5 M sulphuric acid, 70-93 °C	Höök and Lindberg, 1966 ^[207]

The effects of the substituents are multiplicative. This supports the plausibility of the data.

From the comparison with literature data (Tab. 5-6) it is obvious that depending on the substituent (cationic like DEAE, anionic like CM, size, polarity), the influence on hydrolytic stability varies. The reaction order determined for CMC agrees with the one determined for DEAE-cellulose.

Therefore, steric effects seem to play a more important role than the charge of the substituent. Generally, substitution is rate decreasing, this is in agreement with the model proposed by Edward ^[206] (Fig. 5-1). For CMC, position 2 has a rate decreasing effect. A significant influence of position 2 due to the close proximity with the glucosidic linkage was expected. Electron withdrawing groups stabilize glycosidic linkages whereas electron donating groups (if not basic and thus protonated) reduce the stability. The glucosidic bond may be shielded by the CM-group and it might form H-bonds with the glucosidic oxygen (formation of a 8-membered ring) which would result in a decrease in the electron density at the exoglucosidic oxygen atom.

Therefore, basicity of the free electron pairs would be reduced. The negative inductive effect of the CM-group in position 2 also leads to a destabilization of the carboxonium-ion, thus a decrease of the reaction rate. Substitution in positions 3 shows least rate decreasing effects.

The prior investigations showed that hydrolysis did not follow a first-order order constantly but is most probably a mixture of first- and pseudo-zero-order courses. It is evident that CMCs with $DS < 3$ form superstructures, so-called fringed micelles, in aqueous media (see chapter 1.3.3) due to H-bonds between free OH-groups. In acidic solutions, inter- and intramolecular H-bonding between the COOH-groups support this aggregation and/or precipitation. During hydrolysis, the aqueous solution does not contain a residue of solid particles, but non-visible superstructures lead to a dependence of the degradation on the accessibility of distinct parts. H-bonds between two carboxylic acids are very strong (Fig. 1-8). With 1.64 Å the hydrogen bond $H\cdots O$ between two acetic acid molecules is in the range of the covalent C-OH bond (1.33 Å) ^[53]. Aggregates in aqueous CMC solutions that correspond to the fringed micellar model have a total size of 200 to 350 nm.

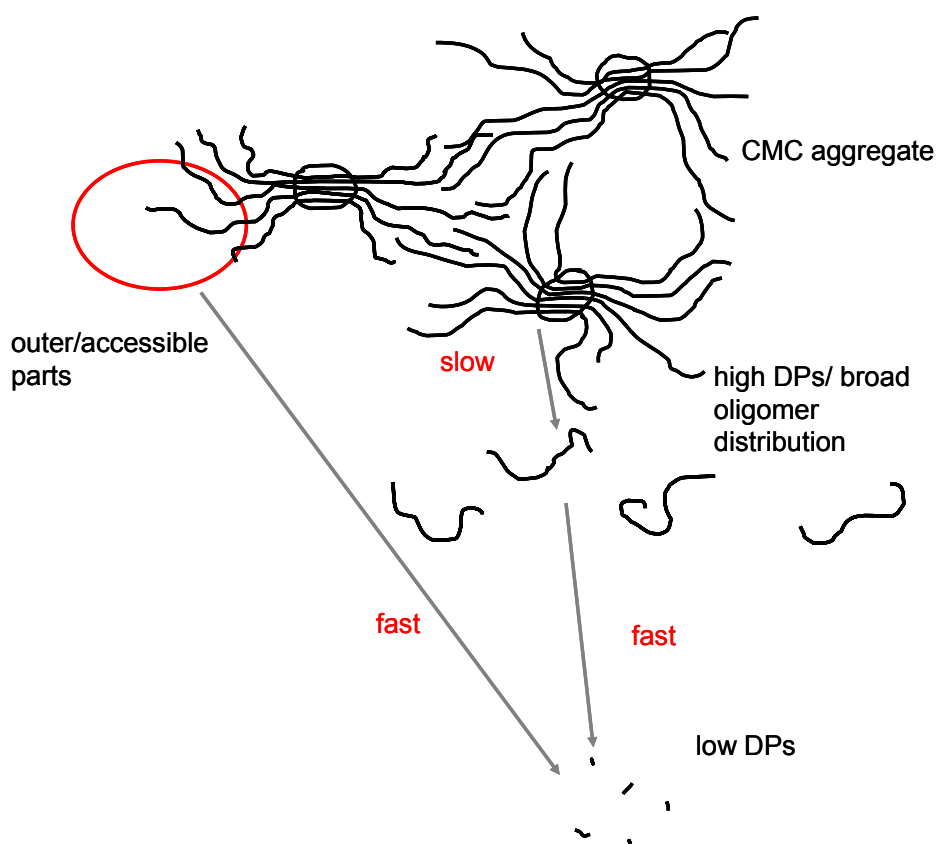


Fig. 5-13 Proposed scheme of different processes during acid hydrolysis of CMC that lead to the observed “gap” in the distribution of higher oligomers

The compact cores are in the range of 60 to 100 nm and the outer chains have lengths up to 150 nm^[58] (see chapter 1.3.3). An apparently zero-order process and the lack of oligomers could indicate that the cleavage of accessible parts from the fringed micelle to monomers is very fast (first-order, predominantly in the beginning of the reaction) whereas the disintegration of supramolecular structures is comparably slow (pseudo-zero-order in the later course, Fig. 5-13). For a broader oligomer distribution, a very short but harsh treatment (high temperature, high acid concentration, e.g. pressure disintegration) could favour the disintegration of the chains. In our group, microwave assisted hydrolysis of CM-cyclodextrins and CMS was investigated, but was also not successful in achieving a broad oligomer distribution^[210] so far. Instead, only small DPs (mainly DP 1) were obtained. So the further degradation to monomers, even when oligomers had been present, was too fast to maintain a steady oligomer concentration. To avoid the influence of the substituents it would be necessary to introduce an acid stable substituent for the free hydroxyl groups that diminishes the differences between CM- and free OH-groups already during hydrolysis, such as perdeuteromethylation for MC. The formation of H-bonds should also be inhibited.

Furthermore, it can be concluded that for each type of substituent the influence on the hydrolysis rate has to be determined individually since they have different electronic and steric effects. For cellulose ethers in general the aspect of the accessibility must be considered, therefore the significance of the comparison with methyl glucosides is limited.

5.2 Kinetics of methanolysis

As already mentioned, a random degradation is an essential prerequisite to receive results for substituent distribution from oligomer analysis that are representative. LC-ELSD analysis showed that partial methanolysis produced an oligomer “gap”, as it was observed for the partially hydrolyzed samples (chapter 4.3). Since the investigated CMCs are not soluble in methanol, methanolysis is a heterogeneous process in the beginning. Thus a peeling process is expected in which undissolved particles are degraded from outside to inside, leading to a pseudo-zero order reaction. A study is performed to investigate the methanolysis process. End group analysis as performed for the hydrolyzates (chapter 5.1) cannot be

applied for the time course study of methanolysis, since labeling with a chromophore by reductive amination requires the carbonyl function, which is protected in methyl glucosides. Therefore, instead of the terminal residues formed dependent on time, the composition of the dissolved part is investigated over the reaction course. For a random degradation, this composition should be constant over the time and in agreement the average composition of the CMC.

5.2.1 Time course study of methanolysis

20 mg dried CMC (0.08 mmol) were suspended in 5 mL of water free 1.5 M methanolic HCl in a pressure-stable V-vial and stirred at 90 °C. Each 10 to 15 min, the reaction is interrupted by cooling the vial in a NaCl-ice bath (approx. - 10 °C). When sedimentation of undissolved material was complete, an aliquot (4.5 mL) of the supernatant was removed. Fresh methanolic HCl was added to compensate the removed volume and methanolysis was continued. Seven fractions of the dissolved part were collected from 10 to 90 min methanolysis. The supernatant might contain mono- to oligosaccharides but undegraded polymer chains cannot be excluded. The removed fractions were separately hydrolysed with perchloric acid (120 °C, 2 h, 8.3.2.3), reductively aminated with ABN after addition of maltose (0.11 mmol, from stock solution) as internal standard and measured by CE-UV.

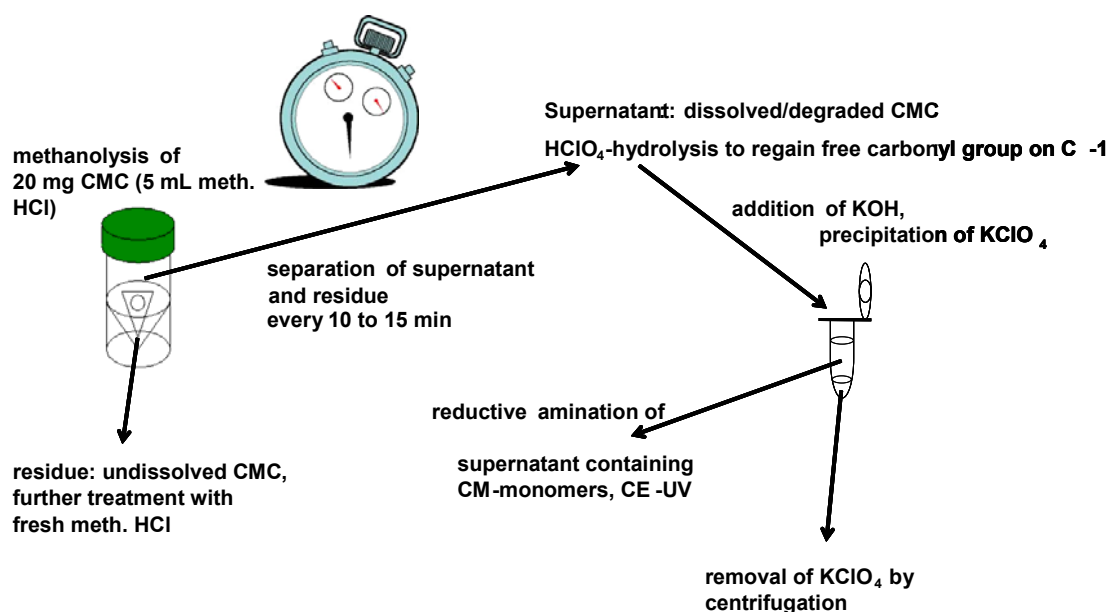


Fig. 5-14 Time course study of methanolysis

For a random process, the monomer composition in each fraction should be in agreement with the average composition of the CMC.

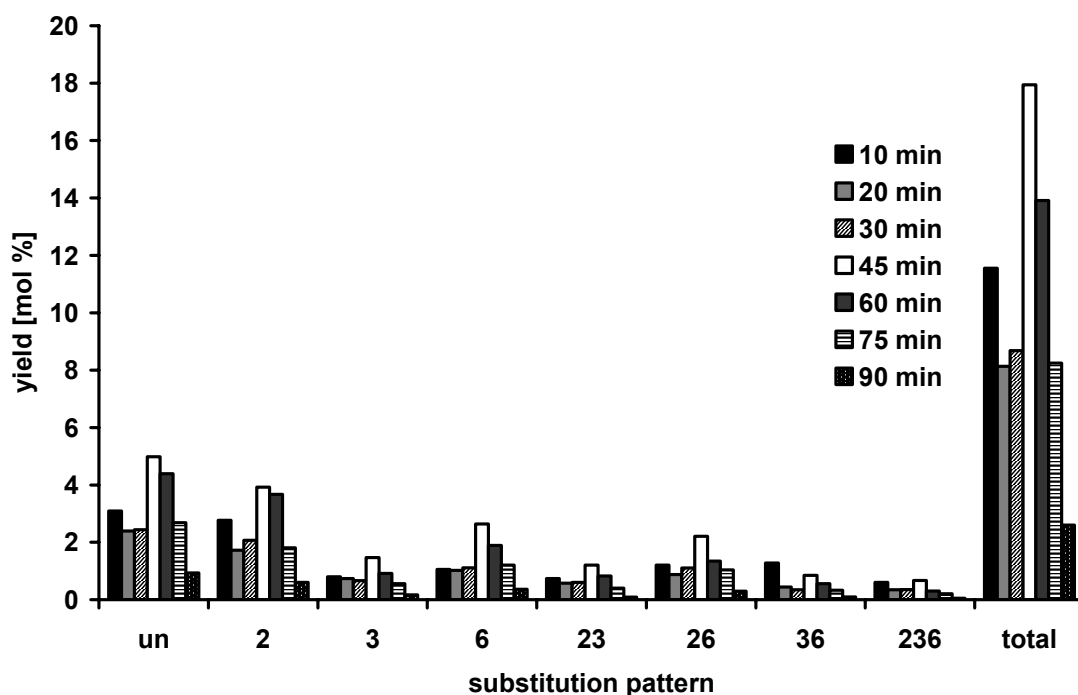


Fig. 5-15 Molar amounts of the dissolved fractions collected from CMC 4 at various times of methanolysis, maltose as internal standard, added to reductive amination.

Tab. 5-7 Molar yields (Mol%, referred to starting material) of CM-glucose derivatives obtained from the dissolved fractions collected from CMC 4 at various times of methanolysis, maltose as internal standard

Methanolysis time [min]	10	20	30	45	60	75	90
entry dried CMC [mg]	18.04						
entry CMC [μmol]	75						
glc	3.11	2.41	2.44	5.00	4.41	2.70	0.94
2-O-CM	2.78	1.73	2.08	3.93	3.68	1.82	0.60
3-O-CM	0.80	0.74	0.66	1.48	0.92	0.56	0.16
6-O-CM	1.06	1.03	1.11	2.65	1.90	1.21	0.37
2,3-O-CM	0.74	0.58	0.60	1.21	0.83	0.40	0.09
2,6-O-CM	1.21	0.88	1.11	2.21	1.35	1.04	0.30
3,6-O-CM	1.28	0.44	0.34	0.85	0.56	0.33	0.10
2,3,6-O-CM	0.60	0.34	0.36	0.67	0.30	0.21	0.05
total yield (71.29 Mol%)	11.59	8.16	8.70	18.00	13.96	8.27	2.61

The electropherogram of the first fraction after 10 min showed many peaks that did not correlate with the eight CM-glucose monomers. The peak migrating directly after glucose could be identified as mannose by co-injection, so it was assumed that the other peaks corresponded to the analogous CM-mannose derivatives or other diastereomers. They might result from hemicelluloses that are carboxymethylated during CMC manufacturing as well and are more acid labile and hence enriched in the first fraction (see chapter 3.2, Fig. 3-2). In the fraction after 20 min, these additional components were no longer observed. Although an assignment of the CM-glucose derivatives is possible due to their migration times, an overlapping of interfering peaks cannot be excluded, so the first fraction should be regarded carefully. Fig. 5-15 and

Tab. 5-7 show the molar yields of the monomers. They decreased with increasing fraction number, the summarized amounts, i.e. the final yield of monomers, was 71 % and therefore 14 % lower than found for hydrolysis, which might also result from the experimental set-up. The molar compositions of the fractions, normalized to 100, are shown in Fig. 5-16 and Tab. 5-8.

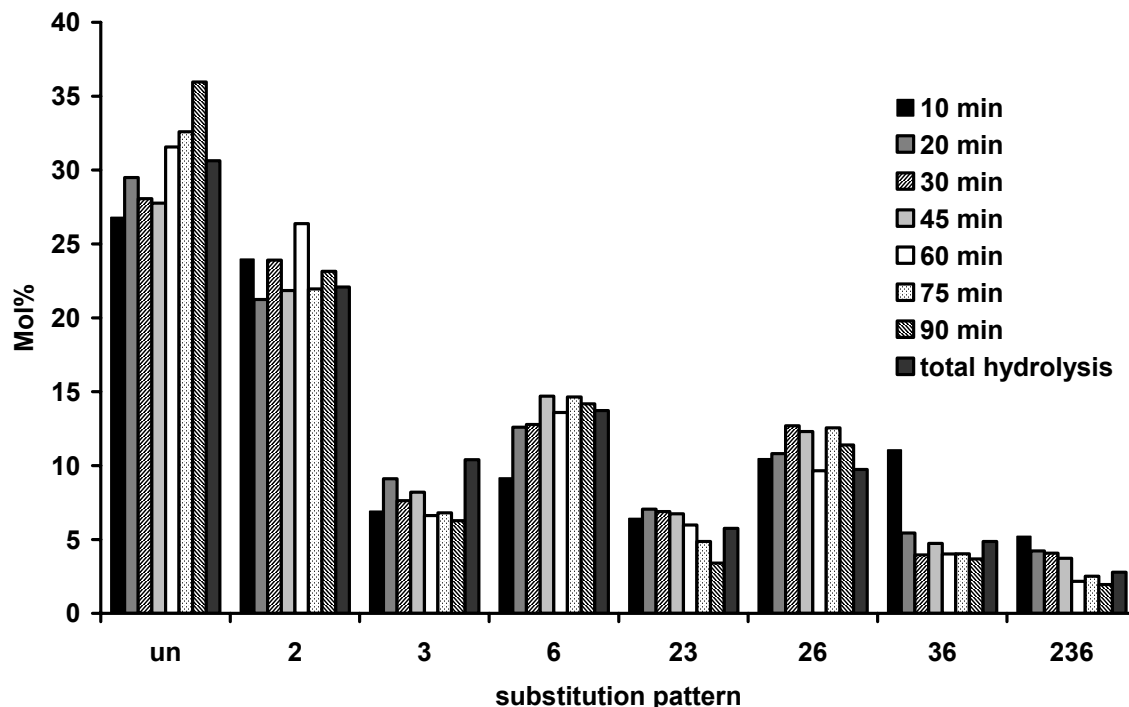


Fig. 5-16 Molar distribution of the monomers released after partial methanolysis of CMC 4 normalized to 100, fractions collected in various times of methanolysis (90 °C, 1.5 M meth. HCl) (8.3.12.1), respectively, hydrolyzed, and analyzed by CE-UV after labeling with ABN (8.3.3, 8.2.1), compared to the data from monomer analysis (CE-UV after total hydrolysis, 8.3.2.1, 8.3.3)

The composition of the total hydrolyzate (perchloric acid) from monomer analysis (see chapter 3.2) is displayed as reference. The average DS-values decreased during the course of the methanolysis. Glucose seems to be released relatively slow compared to the other monomers, but the dependence on the substitution pattern is not as significant as it was observed for the hydrolysis (chapter 5.1.3).

Tab. 5-8 Molar distribution (Mol%, normalized to 100) of the dissolved fractions collected from CMC 4 at various times of methanolysis and data from monomer analysis

Methanolysis time [min]	10	20	30	45	60	75	90	Monomer analysis
glc	26.80	29.49	28.07	27.76	31.56	32.59	35.97	30.56
2-O-CM	23.96	21.25	23.90	21.85	26.38	21.96	23.15	22.20
3-O-CM	6.92	9.12	7.62	8.20	6.62	6.81	6.28	10.37
6-O-CM	9.17	12.60	12.79	14.70	13.60	14.66	14.18	13.21
2,3-O-CM	6.42	7.05	6.89	6.74	5.98	4.87	3.40	5.79
2,6-O-CM	10.47	10.81	12.70	12.30	9.66	12.56	11.39	10.19
3,6-O-CM	11.06	5.44	3.96	4.73	4.02	4.04	3.68	4.86
2,3,6-O-CM	5.21	4.23	4.08	3.72	2.18	2.52	1.95	2.82
DS	1.12	1.02	1.04	1.03	0.92	0.94	0.86	0.96

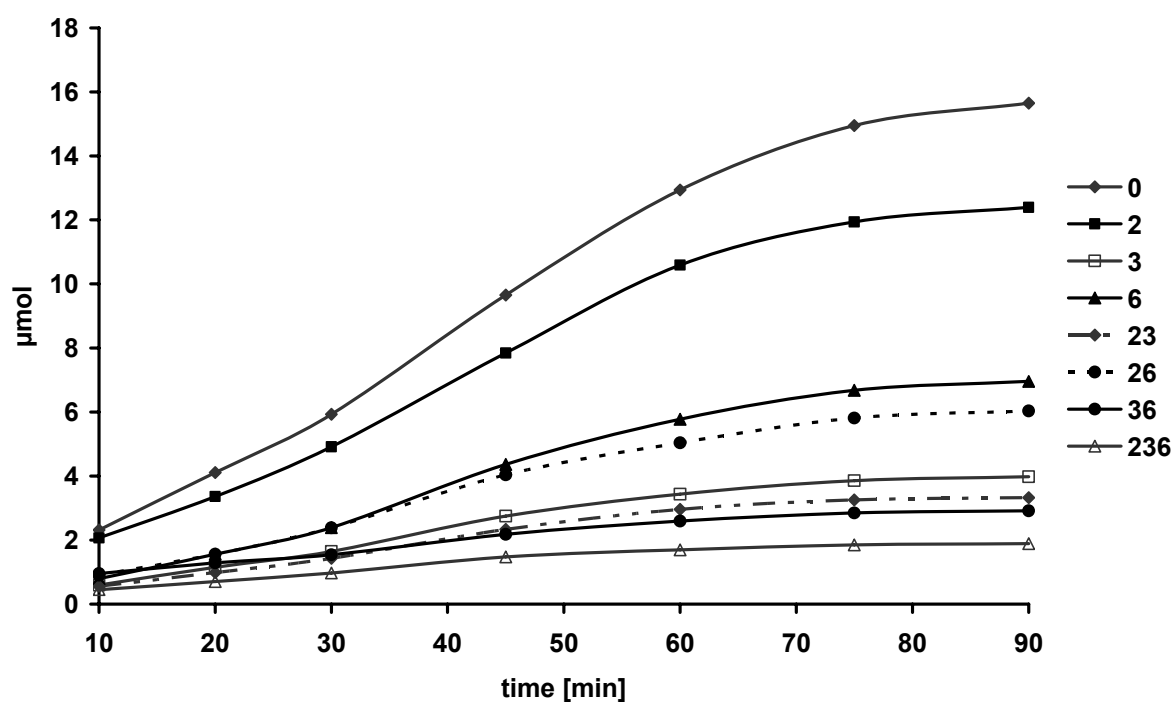


Fig. 5-17 Cumulative yields [μmol] of the degradation products of CMC 4

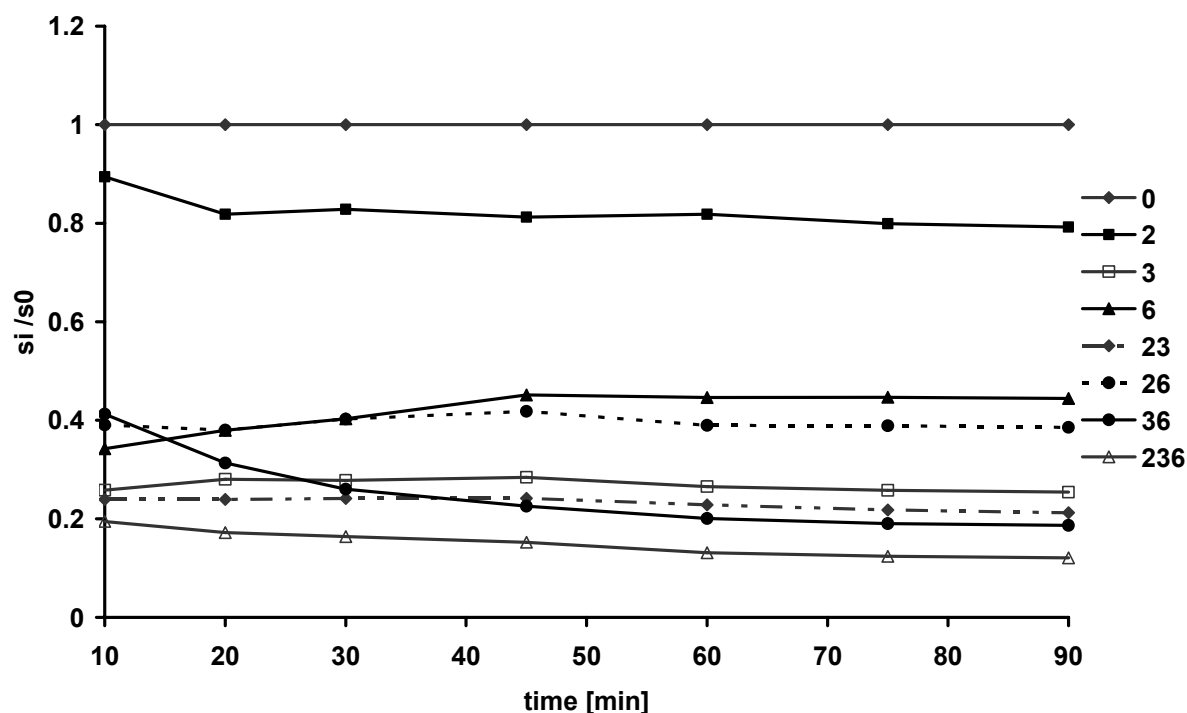


Fig. 5-18 Ratio s_i/s_0 of the accumulated yields of the CMC 4 methanolysis products

To plot the progress of methanolysis, the molar amounts are accumulated (Fig. 5-17) and referred to glucose (Fig. 5-18).

From the plot of the cumulative yields it is obvious that methanolysis is neither a pure zero- nor a pure first-order reaction. The reaction proceeds relatively fast in the beginning is then stationary and slows down in the end.

The relative rate constants cannot be evaluated, as the reaction order is obviously not consistent over the course. The drawback of this experimental set-up is that nothing is known about the DP-distribution of the dissolved part. Undegraded chains might also be in the dissolved part causing bias. The time course study is thus modified.

5.2.2 Time course study of methanolysis with removal of DP >20

Due to the hydrolysis step in the just described procedure, no differentiation between glucosyl units from the reducing ends that were formed already during methanolysis and those that were formed during hydrolysis (i.e. internal moieties) is possible. Therefore, an additional filtration step was introduced in the experimental set-up illustrated in Fig. 5-14. Before the supernatant was hydrolyzed, it was filtrated

by centrifugal filters containing a membrane with a MWCO of 5000, this corresponds with DP 20 (see 8.3.12.2).

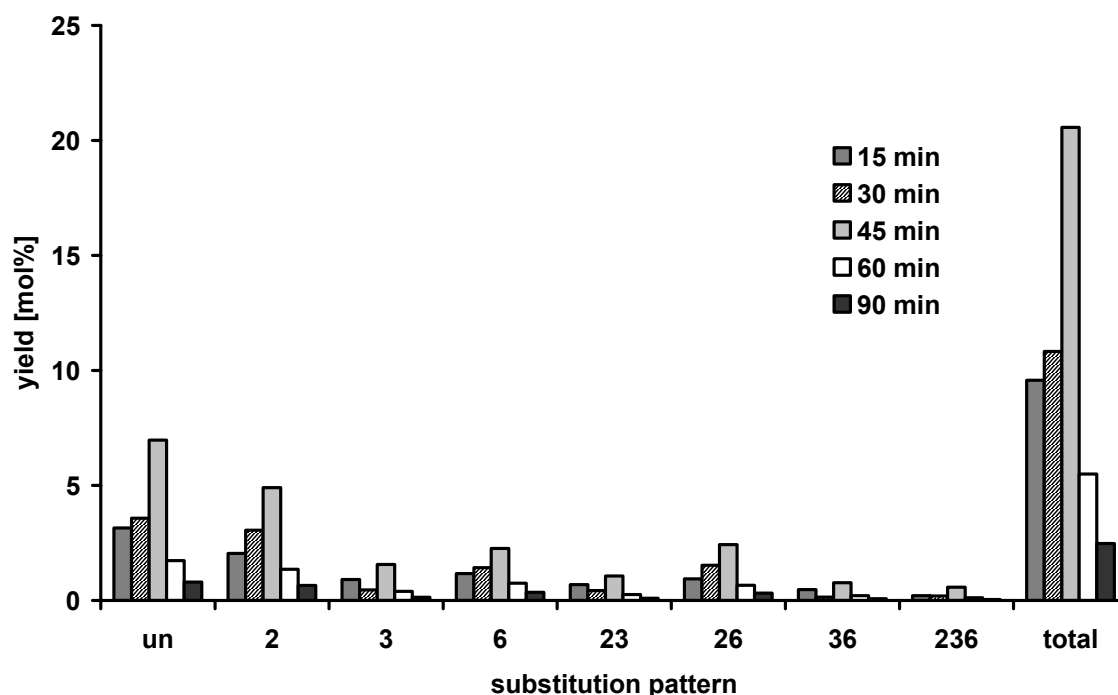


Fig. 5-19 Molar amounts of the dissolved fractions (MWCO < 5000) collected from CMC 4 at various times of methanolysis (90 °C, 1.5 M meth. HCl), xylose as internal standard added before filtration and hydrolysis.

Tab. 5-9 Molar yields (Mol%, referred to starting material) of CM-glucose derivatives obtained from the dissolved fractions (MWCO < 5000) collected from CMC 4 at various times of methanolysis, xylose as internal standard

Methanolysis time [min]	15	30	45	60	90
entry dried CMC [mg]	19.98				
entry CMC [mmol]	0.083				
glc	2.97	3.37	6.58	1.63	0.76
2-O-CM	1.93	2.89	4.63	1.28	0.62
3-O-CM	0.86	0.43	1.48	0.38	0.13
6-O-CM	1.10	1.35	2.13	0.71	0.33
2,3-O-CM	0.65	0.41	1.01	0.25	0.09
2,6-O-CM	0.88	1.44	2.29	0.63	0.30
3,6-O-CM	0.44	0.14	0.73	0.20	0.07
2,3,6-O-CM	0.19	0.19	0.54	0.11	0.04
total yield	9.03	10.21	19.40	5.18	2.34

Xylose was added as internal standard before centrifugation and subsequent hydrolysis, so possible loss due to the filtration process was considered. ESI-IT-mass spectra of the filtrates showed only DP 1 to 3, the latter with only low intensity (Fig. 5-20).

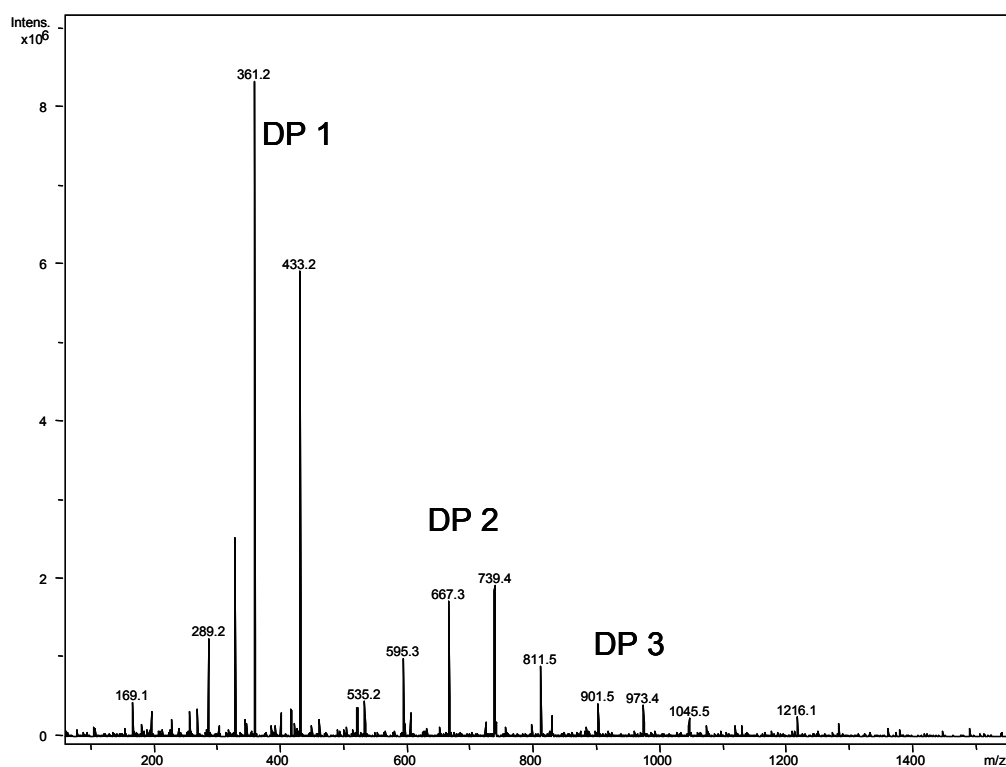


Fig. 5-20 ESI-IT mass spectrum of the filtrate (membrane filter, (MWCO < 5000) of the methanolysis-fraction after 15 min

TLC of the filtrates showed no polymer residues. The molar yields of the individual fractions are given in Fig. 5-19 and Tab. 5-9. The total monomer yield determined by CE-UV was 46 %, so the difference to the series without filtration was -25 %, most probably due to losses during centrifugal filtration. The DS-values of the individual fractions remained nearly constant (Tab. 5-10). The molar distributions of the released monomers, normalized to 100, are shown in Fig. 5-21. From these results it can be concluded that methanolysis proceeded randomly without a preference of a distinct substitution pattern after approximately 45 min, which was also indicated in the series without an additional filtration step. The cumulative molar amounts of the monomers in the fractions and their plot relative to glucose are displayed in Fig. 5-22 and Fig. 5-23. Like for the series without filtration, no rate constants could be evaluated for this reaction, since the order was not consistent. The courses of both series are very similar.

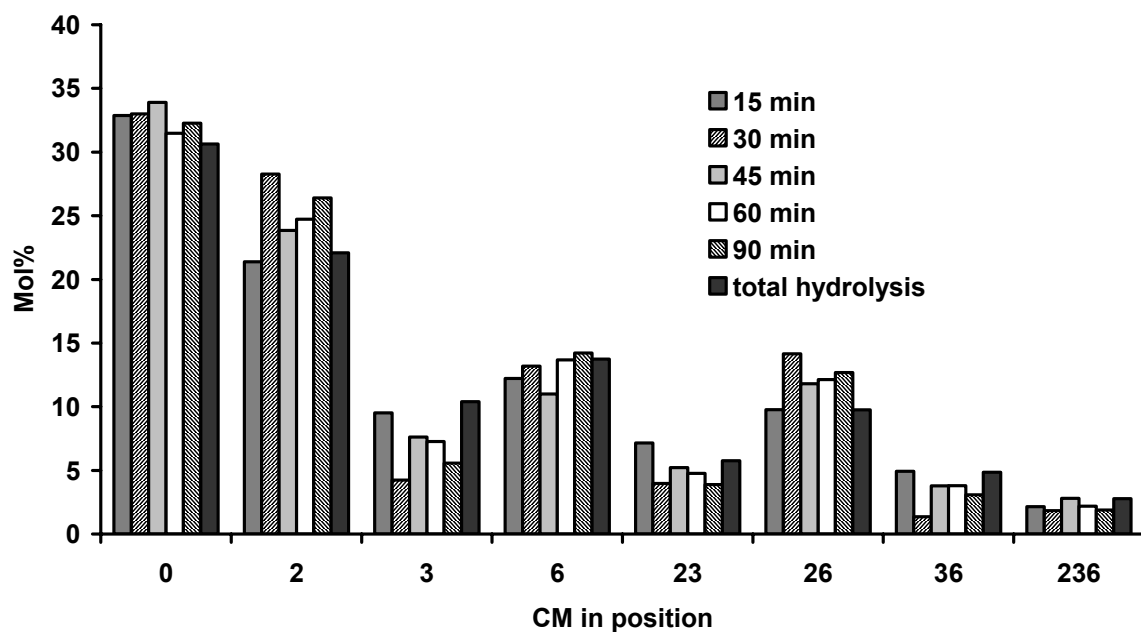


Fig. 5-21 Monomer distribution of the fractions of CMC 4 (MWCO < 5000) at various times of methanolysis (90 °C, 1.5 M meth. HCl)

Tab. 5-10 Molar distribution (Mol%, normalized to 100) of the dissolved fractions (MWCO < 5000) collected from CMC 4 at various times of methanolysis and data from monomer analysis

Methanolysis time [min]	15	30	45	60	90	monomer analysis
glc	32.88	33.00	33.91	31.47	32.27	30.56
2-O-CM	21.38	28.27	23.85	24.72	26.40	22.20
3-O-CM	9.53	4.23	7.63	7.26	5.57	10.37
6-O-CM	12.21	13.19	11.00	13.67	14.22	13.21
2,3-O-CM	7.15	3.97	5.20	4.77	3.90	5.79
2,6-O-CM	9.77	14.15	11.81	12.13	12.68	10.19
3,6-O-CM	4.93	1.35	3.78	3.80	3.08	4.86
2,3,6-O-CM	2.15	1.83	2.80	2.19	1.89	2.82
DS	0.93	0.90	0.93	0.94	0.91	0.96

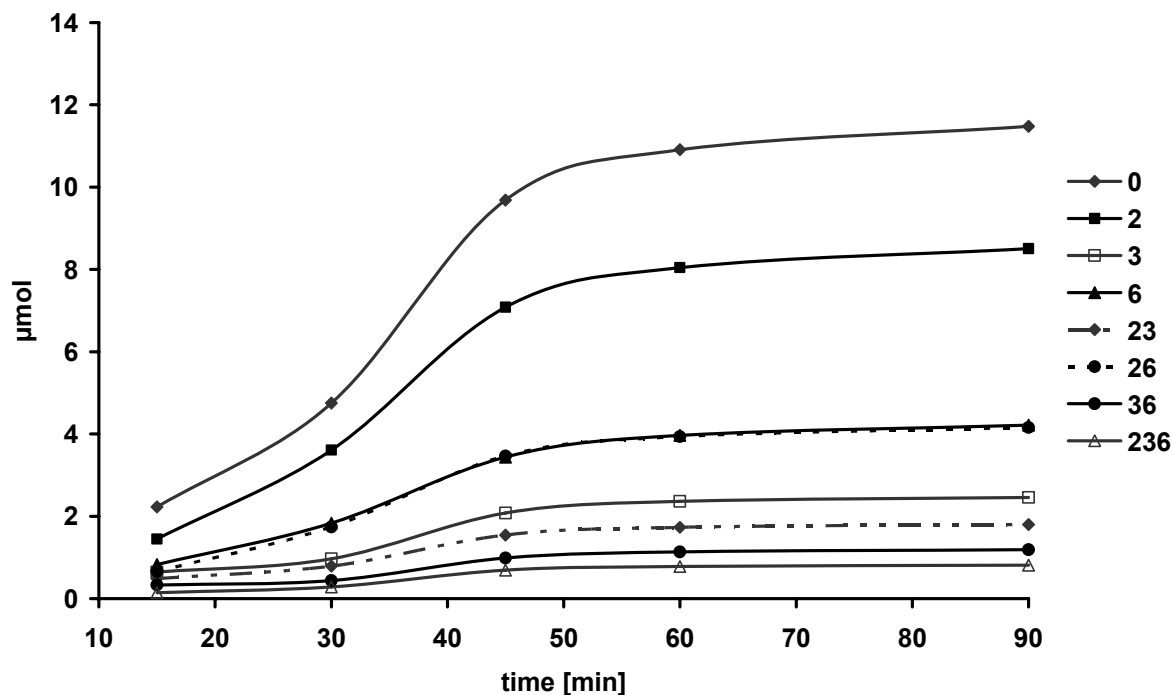


Fig. 5-22 Cumulative yields [μmol] of the dissolved methanolysis products of CMC 4 (MWCO < 5000)

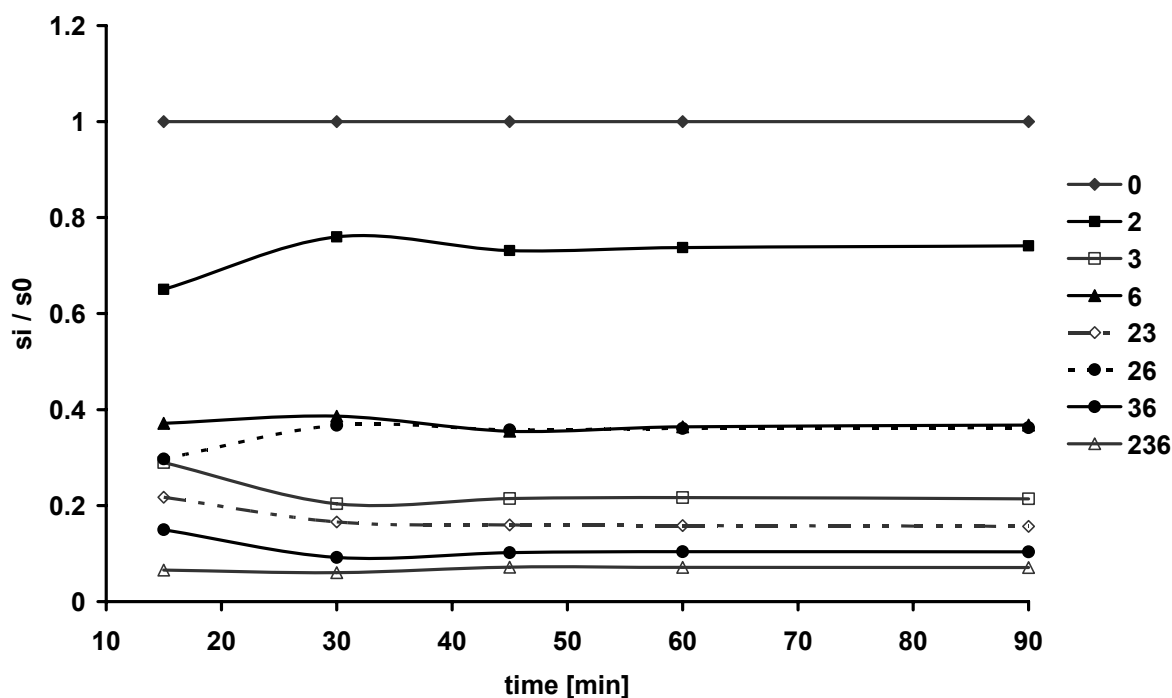


Fig. 5-23 Ratio s_1 / s_0 of the accumulated yields [μmol] of the dissolved methanolysis products of CMC 4 (MWCO < 5000)

The time course of CMC-methanolysis can be explained with a peeling-like mechanism (Fig. 5-24). In the beginning of the reaction, the rate of depolymerization is almost constant, because the concentration of outer parts (the particle surface)

does not change significantly. This leads to a pseudo-zero reaction order in the starting state. When particles disintegrate, the amount of new surface is enhanced spontaneously; the reaction rate is thus increased in the middle of the reaction course. In the end of degradation, the material is decomposed and the reaction rate slows down again.

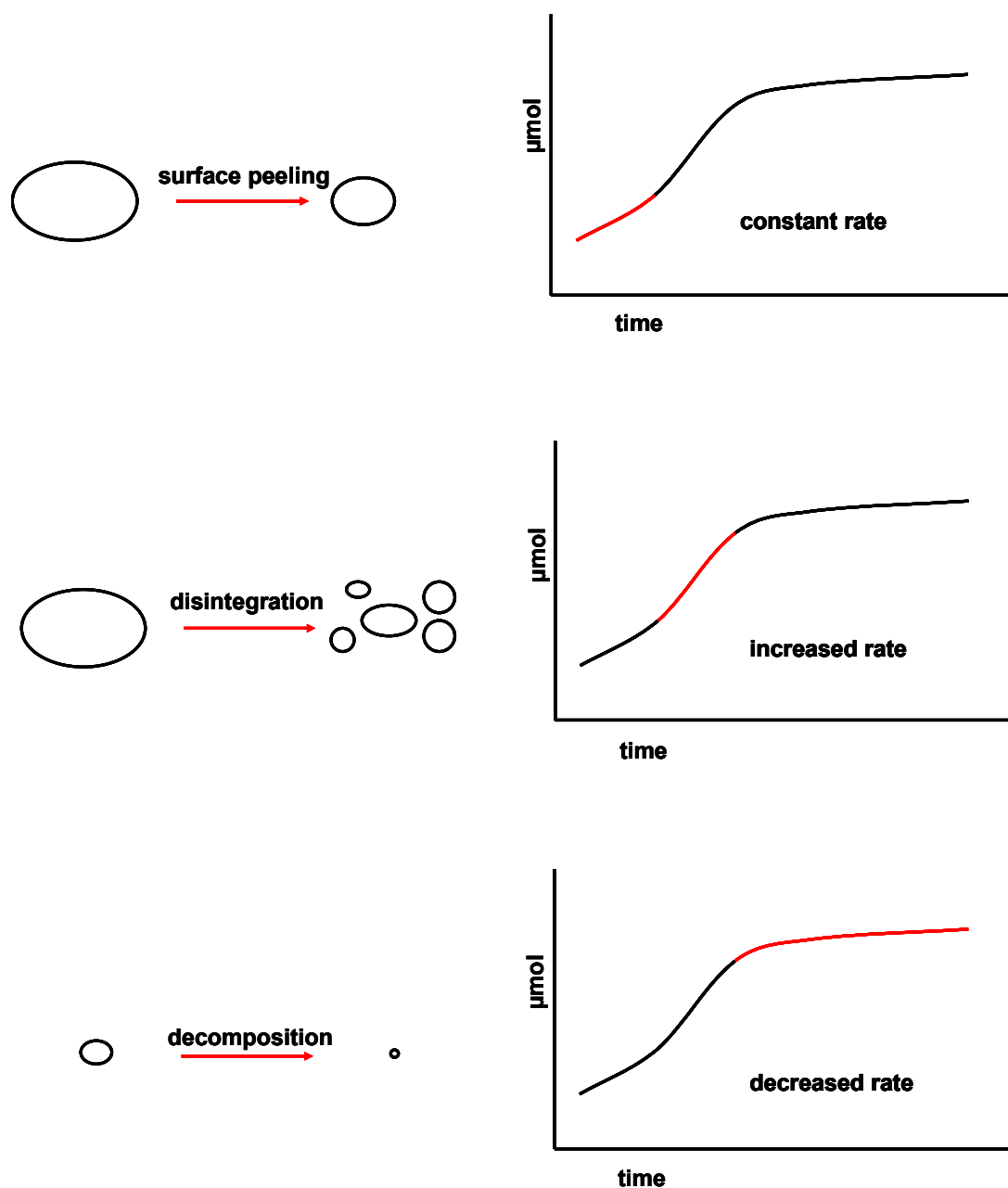


Fig. 5-24 Proposed processes during heterogeneous methanolysis of undissolved CMC particles and their influences on the reaction rates (cumulative amounts of glucose from Fig. 5-22)

Compared to hydrolysis (5.1.3), methanolysis is a more static process in such way that less influence of the substituents on the reaction course is possible. For aggregation of CMC in water due to the better solvatization, at least a small amount of self-organisation of the chains is expected. Thus, the influence of CM-groups on the process is higher for hydrolysis. In contrast, methanolysis proceeds from outside to inside of the solid particle and the chains have no time to order themselves in the medium. Methanolysis thus displays the distribution of the chains in the particle. If the substitution pattern over the polymer chains is random and the chains are ordered randomly in the solid particle, methanolysis yields a random distribution of the monomers, i.e. no trends in the release of distinct monomers are observed. The transformation of NaCMC to the TEA-salt did not improve the oligomer yield (see 4.3.3), so this approach has to be developed in future works. However, the prior investigation showed that methanolysis proceeds without a preference with respect to a distinct substitution pattern. For the conditions used within this work, a random process was achieved after approx. 45 min. Methanolysis requires optimization to get a broader oligomer distribution but this degradation method in general seems applicable for the demands of oligomer analysis.

6 Summary

The aim of this work was to determine the distribution of glucosyl units and its mono- to tri-*O*-carboxymethylated derivatives in the cellulose chain by application of the so-called “oligomer analysis” [74,77] on CMC. This strategy comprises a random degradation of the polymer to oligomeric sequences and the quantitative mass spectrometric analysis of the substituent distribution within a distinct DP (mainly 2, 3 and 4) after appropriate sample preparation [179]. Four CMCs with DS-values between 0.84 and 0.99 (determined by titration) were investigated (all supplied by DOW Wolff Cellulosics, Bomlitz, Germany).

Critical points which had to be addressed were:

1. The *partial degradation process* (hydrolysis, methanolysis)
 - 1.1. *Accessibility*: CMC is soluble in water, but depending on DS and substitution pattern it can form gel-like/swollen particles and aggregates, which also might cause bias in accessibility of the cellulose molecules. Methanolysis is a heterogeneous process right from the start, so CMC is even less accessible and a broad oligomer distribution might be difficult to achieve. But methanolysis has the advantage to form neutral products and hence to minimize the peak complexity in MS (see 2).
 - 1.2. *Influence of substituents*: The rate of hydrolysis is expected to be influenced by CM-substituents due to steric, ionic and neighbour-group effects
2. In *mass spectrometry* the following parameters can cause discrimination of the lower substituted analytes when measured by ESI-Ion Trap-MS:
 - the mass difference, e.g. due to bias caused by skimmer voltage selection
 - the polarity of analytes influences their distribution in the droplets formed by electrospraying and thus their ion yield
 - the number of CM-groups influences the complexation properties of analytes and thus formation of pseudomolecular ions (sodium adducts)

Monomer analysis: The determination of the CM-group distribution in the AGU is the basis for the interpretation of the substitution pattern on higher structural levels. Three methods for monomer analysis after complete acidic depolymerization were applied and compared with each other: Capillary Electrophoresis after labeling with a UV-active compound (CE-UV, 3.2), High-pH-Anion Exchange Chromatography

(HPEAC, 3.3), and Gas Liquid Chromatography after reduction of the CMC and subsequent preparation of glucitol acetates (GLC-FID, 3.4). HPAEC-analysis was not reliable due to detector problems. The reduction of CMC to HEC for GLC-FID analysis was insufficient even after manifold repeatings. The results of CE-UV analysis were thus most reliable and therefore referred to when discussing substituent distribution.

Mass spectrometry: To prepare analytes chemically as uniform as possible and thus eliminate discriminating influences during ionization, the free hydroxyl groups of oligomeric methyl glucosides/methyl esters obtained by partial methanolysis were subsequently acylated. Different reagents of increasing mass and decreasing polarity were used to find an appropriate compromise to suppress discriminating effects (4.1). The extent of discrimination was controlled by comparison of the DS calculated for a certain DP with the average DS of the CMC determined from monomer analysis (3.2). Acetylation, propionylation, and butyrylation could reduce discriminating effects, though not complete. Propionates were most effective in diminishing bias of these three agents, so it was concluded that similarity in polarity and sodium complexation ability was more important than similarity in mass (4.1.1). Thus, methoxyacetate, isomeric to the methoxycarbonyl-methyl-group, was tested (4.1.2), which showed the best results of all acylating agents. With + 23 % for methoxyacetate, the deviation to the average DS determined by monomer analysis was nevertheless still too high to be interpreted with respect to a possible heterogeneity. So the sodium complexation ability of the esters compared to the CM-ether was not sufficient to avoid discrimination.

Other approaches were the removal of DP 1 by column-chromatography (4.2.2) before MS measurement or the introduction of a permanently charged tag to the analyte molecule by derivatization of the partially hydrolyzed CMC with Girard's T reagent (4.4). Both efforts were insufficient, but the introduction of a permanent charge showed that against expectations high DPs were significantly overrepresented in MALDI-TOF-MS. So from MS, it is not possible to conclude on the oligomer distribution of the partial degradation.

Partial degradation: Since we were not able to completely protect the free hydroxyl groups of CMC with acid stable substituents in order to prepare chemically uniform

products on the polymeric level, partial degradation was performed directly either by hydrolysis or methanolysis. Since this is a critical step partial methanolysis and partial hydrolysis were investigated with respect to their oligomer yields (4.3). A Liquid Chromatography-method was developed (LC-ELSD, 4.3.2). Both degradation methods did not yield the required broad DP distribution, instead, an “oligomer gap” was observed: only DP 1 to 3 and polymer were obtained. In this context, efforts were made to improve the solution state of CMC in the reaction media, e.g. by ion exchange to the triethyl ammonium salt (TEA-CMC, 4.3.3). These efforts could not improve the oligomer yield. Methanolysis and hydrolysis of CMC were also studied with respect to their randomness (5). Against expectations, hydrolysis did not follow a first-order reaction constantly, but showed characteristics of a peeling-process (i.e. a pseudo-zero order reaction) in the further reaction course (5.1.3), which is a probable explanation for the observed “oligomer gap”. This is assumed to be caused by aggregates of CMC that are degraded primarily at their “dissolved ends”. In the beginning of hydrolysis, cleavage of the glucosidic bonds was also influenced by the substitution pattern in the AGU. A release order of $un \approx 3 > 3,6 > 6 > 2,3,6 \approx 2,3 > 2,6 > 2$ was obtained. After 8 h hydrolysis time (17 h total reaction time) the reaction proceeded randomly, but the degree of degradation then was with 54 % monomers already too high.

Methanolysis starts as a heterogeneous process. The reaction course thus showed characteristics of a peeling process, i.e. pseudo-zero order in the beginning and fastened in the further course (5.2). Methanolysis proceeded randomly after 45 min (90 min total reaction time). At that time, the amount of monomers was 46 %.

The current investigations showed that oligomer analysis could not be applied directly on CMC, since the individual steps still require improvement. First, partial degradation needs to be optimized with respect to the oligomer yield. For hydrolysis, aggregation needs to be suppressed, e.g. by effective H-bond breaking agents. This was tested for methanolysis with the formation of TEA-CMC to improve the solubility, but the tendencies of CMC to form H-bonds between CM-groups were stronger. As result, HCMC precipitated spontaneously after addition of acid. During MS-measurement, the optimization of the instrument settings for a distinct DP is necessary. A chromatographic separation depending on DP before MS-measurement is a useful step that could be further developed. Another approach

would be the DP- and DS-depending separation of CM-oligomers by CE due to the anionic substitution pattern. Detection could be performed UV-based after labeling with a chromophore or by MS. The consistent molar response of the labeled analytes allows quantification.

7 Zusammenfassung

Ziel dieser Arbeit war die Bestimmung der Verteilung von Glukosyleinheiten und deren mono- bis trisubstituierten O-Carboxymethylderivaten in der Cellulosekette. Dabei sollte die sogenannte „Oligomeranalytik“ auf CMC angewendet werden^[74,77]. Diese beinhaltet einen statistischen Abbau des Polymers in Oligomereinheiten und die anschließende quantitative massenspektrometrische Analyse der Substituentenverteilung innerhalb eines bestimmten DP (hauptsächlich 2, 3 und 4) nach geeigneter Probenvorbereitung^[179]. In dieser Arbeit wurden vier CMCs mit DS-Werten zwischen 0.84 und 0.99 (Bestimmung über Titration) untersucht (von DOW Wolff Cellulosics, Bomlitz, Deutschland, zur Verfügung gestellt). Kritische Punkte, die bei der Entwicklung einer Methode für CMC beachtet werden mussten, sind:

1. Der *partielle Abbau* (Hydrolyse, Methanolyse):
 - 1.1. *Zugänglichkeit*: CMC ist wasserlöslich, kann aber abhängig vom DS und dem Substitutionsmuster gelähnliche gequollene Partikel und Aggregate bilden. Diese können zu einer unterschiedlichen Zugänglichkeit der Cellulosemoleküle und damit zu Diskriminierung führen. Die Methanolyse von CMC ist von Beginn an ein heterogener Prozess, damit ist die CMC noch weniger zugänglich als bei der Hydrolyse, was eine gewünschte breite Oligomerverteilung weiter erschweren kann (siehe Punkt 2).
 - 1.2. *Einfluss der Substituenten*: Der Verlauf der Hydrolyse/Methanolyse kann durch die sterischen und ionischen Eigenschaften der CM-Substituenten sowie durch Nachbargruppeneffekte beeinflusst werden.
2. In der *Massenspektrometrie* können die folgenden Parameter zu einer Verzerrung des Bildes durch Diskriminierung niedriger substituierter Analyten bei Verwendung eines ESI-IT-MS führen:
 - Die Massendifferenzen, hervorgerufen z.B. durch die Wahl unterschiedlicher Linsenspannungen
 - Die Polarität der Analyten beeinflusst deren Verteilung innerhalb der Tröpfchen im Elektrospray und somit deren Ionenausbeute
 - Die Anzahl der CM-Gruppen beeinflusst die Fähigkeit des Analyten zur Komplexierung u.a. von Natrium (Bildung von Pseudo-Molekülonen)

Monomeranalytik: Die Ermittlung der CM-Gruppenverteilung in der AGU ist die Basis für Interpretationen des Substitutionsmuster höherer struktureller Ebenen. In dieser Arbeit wurden drei Methoden nach saurer Totalhydrolyse untersucht und anschließend miteinander verglichen: Die Kapillarelektrophorese nach Derivatisierung mit einem UV-aktiven Chromophor (CE-UV, 3.2), Anionenaustauscher-Chromatographie (HPAEC, 3.3) und Gaschromatographie nach Reduktion der CMC und anschließender Bildung von Alditolacetaten (GC-FID, 3.4). Die Ergebnisse der HPAEC-Methode konnten aufgrund von Detektorproblemen nicht verwendet werden. Bei der GC-FID Methode war die Reduktion der CMC zu HEC auch nach mehreren Wiederholungen nicht vollständig. Daher stellte sich CE-UV als zuverlässigste Methode heraus und diente als Referenz bei der Diskussion der Substituentenverteilung.

Massenspektrometrie: Um chemisch möglichst einheitliche Analyten zu erhalten und dadurch Einflüsse während der Ionisierung zu eliminieren, wurden die freien Hydroxygruppen der oligomeren Methylglukoside/Methylester nach partieller Methanolyse mit verschiedenen Acylierungsmitteln umgesetzt. Dabei wurden Anhydride mit ansteigender Masse und abnehmender Polarität eingesetzt, um einen angemessenen Kompromiss zur Unterdrückung diskriminierender Einflüsse zu erzielen (4.1). Der Einfluss auf die Diskriminierung wurde durch Vergleich des DS-Werts eines bestimmten DP_s mit dem durchschnittlichen DS der Monomeranalytik verfolgt.

Acetylierung, Propionylierung und Butyrylierung konnten die Diskriminierung zwar verringern, aber nicht vollständig unterdrücken. Dabei zeigten die Propionate die größten Effekte. Daraus konnte gefolgert werden, dass eine Ähnlichkeit zur Polarität und zur Komplexfähigkeit des CM-Methylesters wichtiger ist als eine Massenähnlichkeit (4.1.1). Daher wurde schließlich das zum CM-Methylester isomere Methoxyacetat verwendet. Aber auch bei dieser Derivatisierung zeigte sich, dass die Abweichung der massenspektrometrisch ermittelten DS-Werte zum durchschnittlichen DS der Monomeranalytik zwar von allen Acylierungsmitteln am geringsten, jedoch mit + 23 % immer noch zu hoch war, um Aussagen hinsichtlich einer eventuellen Heterogenität der CMC zu treffen. Die Komplexeigenschaften des CM-Ethers konnten demnach mit einem Ester nicht nachgestellt werden.

Es wurde auch versucht, Bevorzugungen in der Ionisierung durch Abtrennung der Monomerfraktion durch Säulenchromatographie vor der Messung zu verhindern (4.2.2). Ein anderer Ansatz nutzte die Einführung einer permanenten Ladung in das Analytmolekül durch Derivatisierung mit Girard's T (4.4). Beide Ansätze waren jedoch nicht erfolgreich. Allerdings zeigten die Versuche mit Girard's T, dass höhere DPs in MALDI-TOF-MS signifikant überrepräsentiert werden.

Partieller Abbau: Da es uns nicht möglich war, die freien OH-Gruppen mit säurestabilen Substituenten zu schützen um chemisch einheitliche Produkte auf der Polymerebene zu erhalten, wurden die CMCs direkt partiell hydrolysiert bzw. methanolysiert. Wie schon diskutiert ist dies ein kritischer Schritt. Daher wurden beide Methoden in Hinblick auf die Oligomerausbeute untersucht (4.3). Dazu wurde eine Flüssigchromatographiemethode entwickelt (LC-ELSD, 4.3.2). Bei der Hydrolyse wie auch der Methanolyse wurde eine „Lücke“ in der Oligomerverteilung beobachtet: nur DP 1 bis 3 und Polymer lagen vor. Beide Methode lieferten nicht die gewünschte breite Verteilung. In diesem Zusammenhang wurde versucht, die Löslichkeit von NaCMC in den Reaktionsmedien zu erhöhen, u. a. durch Ionenaustausch zum Triethylammoniumsalz (TEA-CMC, 4.3.3). Die Oligomerausbeute konnte dadurch allerdings nicht erhöht werden.

Methanolyse und Hydrolyse wurden auch hinsichtlich ihrer Zufälligkeit untersucht (5). Entgegen der Erwartung verlief die Hydrolyse nicht durchgehend erster Ordnung, sondern zeigte im späteren Verlauf Merkmale eines Peelingprozesses, d.h. sie verlief pseudo-nullter Ordnung (5.1.3). Dies kann mit dem Vorhandensein von Aggregaten erklärt werden, die von den „losen Enden“ her abgebaut werden, was eine wahrscheinlich Erklärung für die beobachtete „Oligomer-Lücke“ darstellt. Zu Beginn der Reaktion wird die Geschwindigkeit der Spaltung der glukosidischen Bindung auch vom Substitutionsmuster in der AGU bestimmt. Dabei wurde eine Reihenfolge von $un \approx 3 > 3,6 > 6 > 2,3,6 \approx 2,3 > 2,6 > 2$ beobachtet. Nach 8 h Reaktionszeit (bei einer Gesamtzeit von 17 h) verlief die Hydrolyse statistisch. Zu diesem Zeitpunkt betrug der Anteil an Monomeren allerdings schon 54 %, damit war der Abbau schon zu weit fortgeschritten.

Die Methanolyse von CMC ist im Gegensatz dazu von Anfang an ein heterogener Prozess. Der Reaktionsverlauf war demzufolge zu Beginn nullter Ordnung. Im weiteren Verlauf beschleunigte die Reaktion, vermutlich durch den Zerfall der

Partikel. Die Methanolyse verlief ab 45 min statistisch (bei einer Gesamtreaktionszeit von 90 min). An diesem Punkt betrug der Anteil an Monomeren 46 %.

Die Untersuchungen dieser Arbeit zeigten, dass die auf neutrale Celluloseether vielfach erfolgreich angewandte Oligomeranalytik nicht direkt auf CMC übertragen werden konnte. Die einzelnen Schritte müssen in zukünftigen Arbeiten noch weiter ausgearbeitet werden. Zuerst müssten die Abbaureaktionen in Hinblick auf eine höhere Oligomerausbeute optimiert werden. Insbesondere für die Hydrolyse könnte beispielsweise der Einsatz effektiver H-Brückenbrecher eine sinnvolle Maßnahme sein. Für den massenspektrometrischen Teil ist die jeweilige Optimierung der instrumentellen Einstellungen auf den zu untersuchenden DP-Bereich sinnvoll. Auch die chromatographische Vortrennung nach DP sollte weiter verfolgt werden.

Ein anderer Ansatz wäre die DS- und DP-abhängige Trennung von CM-Oligomeren aufgrund des anionischen Substitutionsmusters mittels Kapillarelektrophorese. Die Detektion könnte nach entsprechender Derivatisierung mittels UV oder aber über MS erfolgen. Aufgrund des einheitlichen molaren Response der gelabelten Analyten wäre eine Quantifizierung möglich.

8 Experimental

8.1 Chemicals

4-aminobenzoic acid (ABS)	> 99 %, <i>Riedel-de-Haën</i>
4-aminobenzonitrile (ABN)	purum, > 97 %, <i>Fluka</i>
acetic anhydride	puriss, p.a., <i>Fluka</i>
acetonitrile	Chromasolv >99.9 %, <i>Riedel-de-Haën</i>
acetyl chloride	puriss., p.a., > 99 %, <i>Fluka</i>
boric acid	puriss., p.a., <i>Fluka</i>
butyric acid anhydride	> 98 %, <i>Sigma-Aldrich</i>
CD ₃ I	99.5 %, <i>Deutero</i>
cellobiose	for biochemistry, <i>Merck</i>
cellotetraose	<i>Carbosynth</i>
cellotriose	<i>Carbosynth</i>
D ₂ O	99.95 %, <i>Deutero</i>
d ₄ -methanol	99.8 %, <i>Deutero</i>
D-glucose	water free for biochemistry, > 99.5 %, <i>Merck</i>
dichloromethane	for HPLC, <i>Fisher Scientific</i>
dry methanol	Seccosolv > 99.5 %, max. H ₂ O: 0.005 %, <i>Merck</i>
D-xylose	> 99 %, water < 0.2 %, <i>Fluka Biochemica</i>
glacial acetic acid	p.a., 99.8 %, <i>Riedel-de-Haën</i>
KOH	p.a., <i>Carl Roth</i>
maltose	monohydr., <i>Sigma-Aldrich</i>
methanol	for HPLC, <i>Fisher Scientific</i>
methoxyacetyl chloride	purum, > 97.0 %, <i>Fluka</i>
Na ₂ SO ₄	water free, p.a., <i>Fluka</i>
NaCNBH ₃	p.a., <i>Merck-Schuchardt</i>
NaHCO ₃	> 99.5 %, <i>Acros Organics</i>
NaOH	puriss., p.a., <i>Fluka</i>
N-methylimidazole	puriss., > 99.0 %, <i>Fluka</i>
perchloric acid	puriss., p.a., > 69 %, <i>Fluka</i>
propionic acid anhydride	> 98 %, <i>Fluka</i>
p-toluidine	> 99 %, <i>Riedel-de-Haën</i>

pyridine	puriss., absolute, max. H ₂ O: 0.0005 %, crown cap, <i>Fluka</i>
triethylamine	puriss., p.a., > 99.5 %, <i>Fluka</i>
trifluoro-acetic acid (TFA)	p.a., <i>Riedel-de-Haën</i>
trimethyl sulfonium hydroxide	0.2 M methanolic solution for GLC, <i>M&N</i>
water	HPLC quality, Nanopure®, <i>Werner</i>

All reagents used were from highest purity available.

Amberlite IR-120	H ⁺ -form, 16-45 mesh, <i>Fluka</i>
Dialysis tube	MWCO12,000-14,000, <i>Carl Roth</i>
Membrane filter	Minisart SRP15, pore size: 0.45 µm, <i>Sartorius</i>
Paper filter	Blue ribbon, <i>M & N</i>
TLC plates	Silica 60 F254,20x20,, <i>Merck</i>

Carboxymethylcelluloses

Four CMC samples were provided from Dow Wolff Cellulosics (DWC). The average DS (determined by titration) and the NaCl content were determined by DWC. The water content was determined gravimetrically (80 °C, 8 h).

Tab. 8-1 DS values, dry mass and NaCl content of the investigated CMC samples provided by DWC

	DS (DWC)	dry mass [w %]	NaCl [%] (DWC)	M(AGU, Na salt)
CMC 1	0.86	88.77	< 0.05	231
CMC 2	0.84	89.06	< 0.05	229
CMC 3	0.92	90.62	< 0.05	236
CMC 4	0.99	89.55	< 0.05	241

8.2 Instrumentation

8.2.1 Capillary Electrophoresis

Instrument:	P/ACE MDQ (<i>Beckman</i> , Munich, Germany)
Capillary:	fused silica, L: 60 cm, I.D.: 50 μm , O.D.: 375 μm
Voltage:	28 kV
Temperature:	25 °C
Detection:	ABN, ABS: 285 nm, <i>p</i> -toluidine: 260 nm, sulfanilic acid: 217 nm (DAD)
Software:	P/ACE-MDQ version 2.3 (<i>Beckman</i> , Munich, Germany)

8.2.2 ESI-Ion Trap-Mass Spectrometer

Instrument:	Esquire LC 00081 (<i>Bruker Daltonics</i> , Bremen, Germany)
Software:	<i>Bruker Data Analysis Esquire LC</i> , <i>Bruker Daltonics</i> , Bremen
Syringe Pump Flow:	190-220 $\mu\text{L/h}$
Mode:	ESI, positive ion mode
Number of Scans:	200
Capillary Voltage:	4500 V
End Plate Offset:	-500 kV
Capillary Exit:	120 V
Skim 1:	40.0 V
Skim 2:	10.0 V
Dry Gas:	nitrogen, 4 L/min, 300 °C
Nebulizer Gas:	nitrogen, 10 p.s.i.
Sample Preparation:	0.002-0.2 mg/mL sample diluted in methanol, methanol/dichloromethane, and methanol/THF in various ratios, respectively, membrane filtration
Membrane filter:	Minisart SRP15, <i>Sartorius</i> , poresize 0.45 μm

8.2.3 MALDI-TOF-MS (Helmholtz centre for Infection research, HZI)

Instrument:	Ultraflex TOF-TOF (<i>Bruker Daltonics</i> , Bremen, Germany) with delayed extraction and reflectron system
Inlet:	direct
Laser:	nitrogen, 337 nm
Pulse Width:	3 ns
Irridiance:	10^7 - 10^8 W/cm ²
Spot size:	0.2 mm ²
Matrix:	CHCA or DHB
Capillary Voltage:	4000 V
End Plate Offset:	-3500 kV
Skim 1:	20.0 V
Sample prep.:	1 µL-portion containing equal volumes of sample solution (~10 pmol/µL) and matrix are spotted on the stainless steel target and dried at r.t.
Accelerating Voltage:	25 kV

8.2.4 HPLC-ELSD

Column:	Eurosphere 100 Si, 4 mm I.D., <i>Knauer</i>
Pump:	System Gold 126 Solvent Module, <i>Beckman Coulter</i>
Eluent A:	acetone, 50 %
Eluent B:	hexane, 50 %
Flow:	0.6 mL/min
Autosampler:	System Gold LC 508, <i>Beckman Coulter</i>
Tray Temperature:	25 °C
Injection Volume:	20 µL
ELSD:	PL-ELS 2100, <i>Polymer Laboratories</i>
Evaporator Temp.:	70 °C
Nebuliser Temp.:	50 °C
Gas Flow:	1.6 SLM

Software: System Gold Nouveau, version 1.7,
Beckman Coulter

8.2.5 GLC-FID

Instrument: GC 6000 Vega Series 2, *Carlo-Erba*, Italy
Column: CP Sil 8 CB, Chrompak, The Netherlands,
25 m, I.D.: 0.25 mm with retention gap
Injection: on column, volume: 1 μ L
Carrier: hydrogen
Pressure: 80 kPa
Detector: FID
Integrator: Merck-Hitachi D-2000 Chromatointegrator,
Hitachi Ltd. Tokyo

8.2.6 GLC-MS

Instrument: Agilent 6890/ JMS-T 100GC
Software: GC AccoTOF, JOEL
Column: J&W HP-5, 30 m x 0.32 mm ID
Injection: split (10:1)
Injection Temp.: 250 °C
Injection Volume: 1 μ L
Carrier: He (1.0 mL/min)
Transfer Line: 270 °C
Detector Voltage: 2000 V
Gas: Ammonia 3.8 (0.5 mL/min)

8.2.7 HPAEC-PAD

Instrument: Dionex 500
Column: Carbopac PA1 (Dionex), 250 x 9 mm
Eluent: NaOH-gradient system (Tab. 8-2)
Flow: 3 mL/ min
Channel A: Water
Channel B: 100 mM NaOH

Channel C:	100 mM NaOH in 1 M sodium acetate
Channel D:	500 mM NaOH
Detection:	PAD ED 50 (<i>Dionex</i>), gold electrode, after addition of 300 mM NaOH (0.7 mL/ min, channel A and D, Tab. 8-3)

Tab. 8-2 Gradient system for the separation of CMC monomers, Carbpak PA 1

Time [min]	B [%] 100 mM NaOH	C [%] 100 mM NaOH in 1 M NaOAc
0.0	95	5
15.0	0	100
17.0	0	100
17.1	95	5
40.0	new start	new start

Tab. 8-3 Potentials PAD ED 50 (*Dionex*) for CMC monomer analysis

Time [s]	Potential [V] vs Ag/AgCl	Integration
0.00	0.1	
0.20	0.1	begin
0.40	0.1	end
0.41	-2.0	
0.42	-2.0	
0.43	0.6	
0.44	-0.1	
0.50	-0.1	

8.2.8 ATR-IR

Instrument:	<i>Bruker</i> Tensor 27
Technique:	Diamond ATR
Number of Scans:	32
Scan Range:	600-4000 cm ⁻¹

8.2.9 ¹H-NMR

Instrument: AV II 300x
Frequency: 300 MHz

8.2.10 Column chromatography

Stationary phase: silica gel 60, particle size: 0.063-0.2 mm (70-230 mesh), *Fluka*
Analyte/Silica gel: 1:100
Eluent: acetone/hexane 1/1, v/v
Drop speed: 0.4 mL/ min
Fraction size: 2 mL
Detection: TLC, spraying with 10 % ethanolic sulphuric acid, 115 °C (brown spots)

8.2.11 Ion exchange (triethylammonia salt)

Ion exchanger: Amberlite IR-120, H⁺-form, *Merck*
Analyte/Exchanger: 50-100 mg/15 mL
Activation: saturated aqueous triethylamine solution and washing (water) till neutrality
Regeneration: 20fold volume of 1 M aqueous HCl
Eluent: water

8.2.12 Heating block

Instrument: Reacti-Therm Heating/Stirring Module No 18971, *Pierce*
Evaporating Unit: Reacti-Vap Evaporating Unit, Model 18780, *Pierce*
Vials: 0.5 mL, 1 mL, 2 mL, 5 mL-V-vials, *Supelco*

8.2.13 Lyophilization

Instrument: Alpha 2-4-LOC-1 M, *Christ GmbH*

8.3 Methods

8.3.1 Ion exchange to triethylammonium-(TEA)-CMC ^[79]

The ion exchanger Amberlite IR-120 (75 mL) is treated with saturated aqueous triethyl amine solution and washed with water until neutrality (8.2.11). Then 500 mg dialysed (MWCO dialysis tube 12000 to 14000), lyophilized, and dried Na-CMC (approx. 2 mmol) are dissolved in water and added to the exchanger. The triethyl ammonium salt of CMC (TEA-CMC) is eluted with water and freeze dried afterwards (8.2.13). Regeneration of the ion exchanger is performed with the 20fold volume of 1 M aqueous HCl. TEA-CMC is dispersed in methanol, yielding a slightly turbid solution with enhanced viscosity. It is characterized by elementary analysis and ATR-IR spectroscopy (8.2.8).

ATR-IR: Wavenumbers [cm^{-1}]: 3400: $\nu(\text{O-H})$,s; 3300: $\nu(\text{N-H})$,s; 3000-2800: $\nu(\text{C-H})$,m; 1600: $\delta(\text{N-H})$,s, 1300: $\nu(\text{C-N})$,w; Yield (weight%): 130 %, corresponding to an ion exchange of 97 % in case of 100% recovery of AGU.

Tab. 8-4 Elementary analysis of TEA-CMC

atom	%	%
N	3.27	3.07
C	44.72	44.72
H	8.10	8.07
weight [mg]	1.16	1.37

8.3.2 Hydrolysis

8.3.2.1 Perchloric acid hydrolysis (complete depolymerization, method A ^[62,109])

To 500 μL 70 % HClO_4 (approx. 7 M) 20 mg NaCMC (approx. 0.08 mmol AGU) is added in a pressure stable 5 mL-V-vial and stirred 15 min at r.t.. After addition of 4.5 mL dist. water (\rightarrow 0.7 M acid), the reaction is stirred at 95 °C for 17 h in a heating block (8.2.12). The pH of the cooled clear hydrolyzate is adjusted to 2 to 3 with 2 M KOH (p.a. quality), afterwards the solution is stirred over night at r.t.. The pH is adjusted to 7 with aqueous KOH and precipitated KClO_4 is removed by filtration (blue ribbon paper filter). The filtrate is cooled over night at 4 °C to support further precipitation of perchlorate. Filtration and cold storage over night are repeated until

no more KClO_4 precipitates. Then, samples are lyophilized (8.2.13), the residue is dissolved in 5 mL dist. water and filtrated (membrane filter).

8.3.2.2 Perchloric acid hydrolysis (complete depolymerization, method B^[188])

In a pressure stable 100-mL-flask, 100 mg CMC (approx. 0.4 mmol) are wetted as completely as possible with 2 mL 70 % HClO_4 (approx. 7 M) and are allowed to swell for 10 min at r.t. without stirring. Afterwards, the mixture is diluted with 20 mL dist. Water and stirred for 60 min at 120 °C. The cool, clear hydrolyzate is neutralized with 2 M KOH. The mixture is cooled over night at 4 °C, afterwards precipitated KClO_4 is removed by centrifugation under cooling to 4 °C (10000 U min^{-1}). The clear supernatant is decanted into a 100-mL-volumetric flask, residue is slurried with cold, dist. Water and centrifuged again. Supernatants are pooled and filled-up to 100 mL with dist. water.

8.3.2.3 Perchloric acid hydrolysis (complete depolymerization, method C)

The fractions from 8.3.12.1 and 8.3.12.2, respectively, are transferred into a 0.5 mL V-vial and are dried under nitrogen flow. Then, 20 μL perchloric acid and 200 μL water (HPLC quality) are added. The reaction is stirred and heated to 120 °C in a heating block for 1 to 2 h. After the reaction mixture is cooled to r.t., 120 μL 2 M KOH (p.a.quality) are added and the solution is stored at 4 °C (refrigerator) over night to support precipitation of potassium perchlorate. If necessary, more KOH is added afterwards until pH 7 is obtained. The neutralized sample is filled into a 1.5 mL Eppendorf centrifugal cap. The sample is centrifuged at 4 °C at 15000 Umin^{-1} until all solid material is sedimented (approx. 5 to 20 min). The supernatant is removed, filled into a 0.5 mL V-vial, and reductively aminated for CE-UV measurement (8.3.3).

8.3.2.4 Partial TFA hydrolysis

CMC (25 mg, approx. 0.10 mmol) is stirred and heated to 90 °C in a 5 mL-V-vial with 5 mL 2 M aqueous TFA for 3 h. The sample is co-distilled with acetone to remove TFA and evaporated to dryness under a stream of nitrogen.

8.3.2.5 Total TFA hydrolysis

CMC (25 mg, approx. 0.10 mmol) is stirred at 90 °C in a 5 mL-V-vial with 5 mL 2 M aqueous TFA for 17 h. The sample is codistilled with acetone to remove TFA and evaporated to dryness under a stream of nitrogen.

8.3.3 Reductive amination ^[109]

The CMC hydrolyzate from 8.3.2.1 (100 µL, 0.4 mg, approx. 0.02 mmol AGU) are aminated with 50 µL of a 1.5 M methanolic ABN (ABS or 1.5 M ethanolic *p*-toluidine) solution (approx. 0.075 mmol, 3-4 eq/ AGU), 50 µL of a 1 M methanolic solution of sodium cyanoborohydride (approx. 0.05 mmol, 3 eq/ AGU) and 20 µL glacial acetic acid (0.3 µmol). The mixture is stirred and heated for 30 min at 60 °C and subsequently evaporated to dryness under a stream of dry nitrogen. The residue is dissolved in 500 to 1000 µL of a methanol-water-mixture (1:4, v/v) and filtered through a membrane filter. Finally, 100 µL of this solution are used for CE measurement (8.2.1).

8.3.4 Labeling with Girard'sT reagent

Methanolic GT-solution (350 µL containing 17 to 2 eq/ reducing end) and 150 µL glacial acetic acid (2.25 mmol) are added to 500 µL of the neutral aq. TFA-hydrolyzate from 8.3.2.4 (10 mg/ mL CMC, approx. 0.02 mmol in 500 µL) in a 1-mL-V-vial. The reaction is stirred and heated for 30 min at 40 °C in a heating block, then evaporated to dryness with nitrogen. For measurement with MS, the sample is dissolved in 1 mL methanol.

8.3.5 Methanolysis

8.3.5.1 Preparation of dry methanol ^[196]

To prepare 50 mL of dry methanol or *d*₄-methanol, 250 mg magnesium and 25 mg iodide are added to 2,5 mL methanol/*d*₄-methanol in a dried 100 mL round bottom flask. The reagents are heated under reflux until all magnesium is used. Then, the residual methanol is added. After 3 h heating under reflux, dry methanol is distilled on activated (3 h, 300 °C) molsiev (3 Å).

8.3.5.2 Preparation of waterfree methanolic/ d_4 -methanolic HCl

For 100 mL 1.5 M methanolic HCl, 10.7 mL acetyl chloride (0.15 mmol) are added dropwise to cooled dry methanol/ d_4 -methanol.

8.3.5.3 Partial methanolysis/ d_4 -methanolysis

In a 1 mL V-vial, 2 mg CMC (8 μ mol AGU) are depolymerized with 1 mL 1.5 M waterfree methanolic/ d_4 -methanolic hydrochloric acid (8.3.5.1; 8.3.5.2) by stirring at 90 °C for 60 to 90 min in a heating block (8.2.12), until all CMC has dissolved. After cooling to room temperature, HCl is removed by co-distillation with methanol/ d_4 -methanol under a stream of dry nitrogen. The solution is dissolved afterwards in 1 mL methanol/ d_4 -methanol.

8.3.5.4 Methanolysis/ d_4 -methanolysis of TEA-CMC

TEA-CMC (2 mg, approx. 7.5 μ mol AGU) is dispersed in a 1-mL-V-vial in 0.5 mL methanol/ d_4 -methanol, yielding a slightly turbid solution with increased viscosity. Acetyl chloride (0.107 mL) is added to the cooled solution to obtain 1.5 M methanolic/ d_4 -methanolic HCl after the reaction mixture was filled up to 1 mL. Methanolysis is proceeded by stirring at 90 °C for 15 to 60 min (partial methanolysis, 8.3.5.3).

8.3.6 CMC monomer analysis with GLC-FID after reduction to HEC

8.3.6.1 CMC reduction to HEC

100 mg of CMC (approx. 0.4 mmol AGU) are dissolved in 30 mL dist. water. During the addition of 320 mg EDC hydrochloride (1.67 mmol, 4 eq/ CM-group) the pH value is held constant at 4.75 with 0.1 M aqueous HCl. The reaction mixture is stirred at r.t. for 2 h. For the reduction, 250 mg NaBH₄ (7.14 mmol, 17 eq/ CM-group) are added, pH is kept at 7.00 with 4 M HCl during the addition. The sample is cleaned-up by dialysis over night. The reduction step is repeated up to four times. The sample is dialysed and freeze-dried after the last reduction step, the completeness is controlled by ATR-IR spectroscopy (8.2.8).

Yield (weight%): CMC 1: 65 %, CMC 2: 73 %, CMC 3: 58 %, CMC 4: 61 %

8.3.6.2 *Permethylation with Li-dimsyl*

100 mg polysaccharide (HEC from 8.3.6.1, approx. 0.5 mmol AGU) are dissolved in 10 mL DMSO in a dried Schlenk-flask. The base Li-dimsyl is freshly prepared by adding 5 % MeLi in diethylether to 10 mL dry DMSO and evaporating methane and ether under nitrogen. A 1.5 M solution of $\text{Li}^+\text{CH}_3\text{SOCH}_2^-$ is obtained. 10 eq/ OH of the Li-dimsyl solution are added to the polymer under nitrogen atmosphere, the reaction mixture is stirred for 1 h. Then 10 eq/ OH methyl lithium are added and the reaction is stirred for approx. 24 h at r.t. The sample is cleaned-up by dialysis (MWCO 12-14000) and freeze-dried.

8.3.6.3 *Preparation for GLC-FID/-MS analysis*

2 mg polysaccharide (HEC from, 8.3.6.1 approx. 0.01 mmol AGU) were hydrolyzed in a 1-mL-V-vial with 1 mL 2 M TFA for 120 min at 120 °C. After cooling to r.t., the aqueous acid was removed in a stream of dry nitrogen by co-distillation with toluene. The hydrolyzed sample was reduced with a solution of 0.5 mL 0.25 M NaBD_4 in 2 M NH_3 at 60 °C for 120 min. Residues of borate were removed by co-distillation with 15 % methanolic acetic acid in a stream of nitrogen at 40 °C. The residue was dissolved in 50 μL pyridine (0.62 mmol, approx. 60 eq/ AGU) and 200 μL acetic acid anhydride (2.12 mmol, approx. 200 eq/ AGU) and heated at 90 °C for 3 h. Acetylated sample was extracted with dichloromethane, the organic phase is washed with aq. sat. NaHCO_3 , 0.1 M cold HCl and distilled water. Afterwards the sample is dried with CaCl_2 , the solvent is removed under a stream of dry nitrogen and the residue is dissolved in 4 mL CH_2Cl_2 . This solution was measured in GLC-FID/-MS (see appendix 10.1)

8.3.7 **Acetylation, propionylation, butyrylation**

8.3.7.1 *Acetylation, propionylation after partial methanolysis* ^[126]

CMC (2 mg, approx. 8 μmol AGU) is degraded with 1 mL 1.5 M dry methanolic HCl (8.3.5.3). After cooling to r.t., HCl is removed by codestillation with methanol under a stream of dry nitrogen.

Yield (weight%): 105 %

Then 200 μL of the corresponding anhydrides of acetic acid (2.12 mmol, approx. 80 eq/ OH, 250 eq/ AGU) and propionic acid (1.55 mmol, approx. 65 eq/ OH,

200 eq/ AGU), respectively (300 μ L of butyric acid anhydride, 1.83 mmol, approx. 75 eq/ OH, 220 eq/ AGU) are added to the sample together with 50 μ L pyridine (0.62 mmol, approx. 25 eq/ OH, 75 eq/ AGU). The reaction mixture is stirred for 3 h at 90 °C. The sample is cleaned-up by washing the organic phase (CH_2Cl_2) with aq. sat. NaHCO_3 , 0.1 M cold HCl and distilled water. Afterwards the sample is dried with CaCl_2 , the solvent is removed under a stream of dry nitrogen and the residue is dissolved in 1 mL CH_2Cl_2 . Completeness of the reaction is controlled by ATR-IR spectroscopy (8.2.8).

Acetates: ATR-IR: Wavenumbers [cm^{-1}]: 3000-2800: $\nu(\text{C-H})$,w; 1750: $\nu(\text{C=O})$,s, 1400: $\delta(\text{C-H})$,w, 1250: $\nu(\text{C-O-C})$,s;

Propionates: ATR-IR: Wavenumbers [cm^{-1}]: 3000-2800: $\nu(\text{C-H})$,w-m; 1750: $\nu(\text{C=O})$,m-s, 1400: $\delta(\text{C-H})$,w, 1250: $\nu(\text{C-O-C})$,w;

Butyrates: ATR-IR: Wavenumbers [cm^{-1}]: 3000-2800: $\nu(\text{C-H})$,m; 1750: $\nu(\text{C=O})$,m-s, 1400: $\delta(\text{C-H})$,w, 1250: $\nu(\text{C-O-C})$,w

Yield (weight%) for all acylations related to yield after methanolysis: 80-85 %

Before measurement with ESI-MS-Ion Trap (8.2.2) and MALDI-TOF-MS (8.2.3) samples are diluted with methanol 1:6. To investigate the influence of dilution on the spectra quality, a series of dilutions of 1: 10, 1: 100 and 1: 1000 is prepared.

MALDI-MS measurements are performed by Dr. Manfred Nimtz, Helmholtz-Zentrum für Infektionsforschung (HZI), Braunschweig with α -cyano-4-hydroxycinnaminic acid (CHCA) as matrix without further derivatization (8.2.3).

No peaks corresponding to underacylated compounds in ESI-IT-MS (Tab. 8-5).

8.3.8 Methoxyacetylation

8.3.8.1 Preparation with methoxyacetyl chloride and pyridine

CMC (2 mg, approx. 8 μ mol AGU) is degraded with water-free 1.5 M d_4 -methanolic HCl (8.3.5.3). In the beginning the reaction proceeds heterogeneously, the residue dissolves after 60 min. Acylation is performed by adding 150 μ L methoxyacetyl chloride (1.65 mmol, approx. 200 eq/ AGU, 65 eq/ OH) and 50 μ L pyridine (0.62 mmol, approx. 25 eq/ OH, 75 eq/ AGU) and stirring for 3 h at 90 °C. Clean-up was performed by extraction with dichloromethane and washing of the organic phase with aq. sat. NaHCO_3 , 0.1 M cold HCl and distilled water. Afterwards

the sample is dried with CaCl_2 , the solvent is removed under a stream of dry nitrogen and the residue is dissolved in 1 mL CH_2Cl_2 .

Before measurement with ESI-IT-MS (8.2.2), the samples are diluted with d_4 -methanol 1 : 10, 1 : 100 and 1 : 1000, respectively, to investigate the influence of different states of dilution. ATR-IR: Wavenumbers [cm^{-1}]: 3000-2800: $\nu(\text{C-H})$,w; 1750: $\nu(\text{C=O})$,s, 1400: $\delta(\text{C-H})$,w,

8.3.8.2 Preparation with methoxyacetyl chloride an excess of pyridine

CMC (2 mg, approx. 8 μmol AGU) is degraded with 1 mL water free 1.5 M d_4 -methanolic HCl (8.3.5.3). After removing the HCl by codestillation with d_4 -methanol under nitrogen flow, 200 μL pyridine (2.48 mmol, approx. 100 eq/ OH, 300 eq/ AGU) and 30 μL methoxyacetyl chloride (0.33 mmol, 40 eq/ AGU, 13 eq/ OH) are added. The mixture is stirred for 3 h at 90 °C. The sample is cleaned-up by washing the organic phase with aq. sat. NaHCO_3 , 0.1 M cold HCl, and distilled water. Afterwards the sample is dried with CaCl_2 , the solvent is removed under a stream of dry nitrogen and the residue is dissolved in 1 mL CH_2Cl_2 .

8.3.8.3 Preparation with methoxyacetyl chloride and N-methylimidazole

CMC (2 mg, approx. 8 μmol AGU) is degraded with 1 mL water free 1.5 M d_4 -methanolic HCl (8.3.5.3). After removing the HCl by codestillation with d_4 -methanol under nitrogen flow, 200 μL CHCl_3 are added under nitrogen atmosphere to exclude humidity. After addition of 50 μL methoxyacetyl chloride (0.55 mmol, approx. 65 eq/ AGU, 20 eq/ OH) and 30 μL N-methylimidazole (0.33 mmol, approx. 45 eq/ AGU, 15 eq/ OH), the mixture is stirred for 1 h at r. t.. The sample is cleaned-up by washing the organic phase with aq. sat. NaHCO_3 , 0.1 M cold HCl and distilled water. Then, the sample is dried with CaCl_2 , the solvent is removed under a stream of dry nitrogen and the residue is dissolved in 1 mL CH_2Cl_2 .

8.3.8.4 Preparation with methoxyacetyl chloride and an excess of N-methylimidazole

CMC (20 mg, 0.08 mmol AGU) is degraded with 5 mL waterfree 1.5 M d_4 -methanolic HCl (8.3.5.3). After removing the HCl by codestillation with

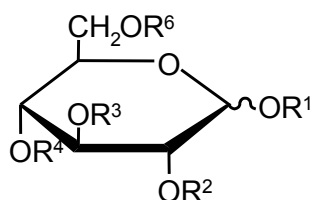
d_4 -methanol under dry nitrogen flow, 320 μ L *N*-methylimidazole (4.05 mmol, approx. 50 eq/ AGU, 15 eq/ OH) and 100 μ L methoxyacetyl chloride (1.09 mmol, approx. 15 eq/ AGU, 5 eq/ OH) are added. The mixture is stirred for 1 h at r.t. The sample is cleaned-up by washing the organic phase with aq. sat. NaHCO_3 , 0.1 M cold HCl and distilled water. Afterwards the sample is dried with CaCl_2 , the solvent is removed under a stream of dry nitrogen and the residue is dissolved in 1 mL CH_2Cl_2 .

Yield (weight%) related to yield after methanolysis: 85 %

8.3.8.5 Preparation from TEA-CMC with methoxyacetyl chloride and an excess of *N*-methylimidazole

TEA-CMC (20 mg, approx. 0.075 mmol AGU) is dissolved in 4.46 mL d_4 -methanol and the solution is stirred at r.t. over night. Afterwards, 0.52 mL acetylchloride are added to the cold mixture yielding 1.5 M d_4 -methanolic HCl. Methanolysis is performed by stirring at 90 °C for 60 min. After removing the HCl by codestillation with d_4 -methanol under dry nitrogen flow, 320 μ L *N*-methylimidazole (4.05 mmol, approx. 50 eq/ AGU, 15 eq/ OH) and 100 μ L methoxyacetyl chloride (1.09 mmol, approx. 15 eq/ AGU, 5 eq/ OH) are added. The mixture is stirred for 1 h at r.t.. Clean-up is performed by washing the organic phase with aq. sat. NaHCO_3 , 0.1 M cold HCl and distilled water. Then, the sample is dried with CaCl_2 , the solvent is removed under a stream of dry nitrogen and the residue is dissolved in 1 mL CH_2Cl_2 .

Yield (weight%) related to yield after methanolysis: 80 %



R^1 : CH_3 , $\text{R}^{2,3,4,6}$: Acetate, Propionate, Butyrate, Methoxyacetate

Tab. 8-5 M/z values for acylated CM-cellooligosaccharides, evaluated as sodium adducts $[M+Na]^+$

R ¹ DP/n(CM)	Methanolizate	Acetate		Propionate		Butyrate		Methoxyacetate	
	CH ₃	CH ₃	COCH ₃	CH ₃	COCH ₂ CH ₃	CH ₃	COCH ₂ CH ₂ CH ₃	CD ₃	COCH ₂ OCH ₃
1/0	217	385	413	441	483	497	553	508	563
1/1	289	415	443	457	499	499	555	511	566
1/2	361	445	473	473	515	501	557	514	569
1/3	433	475	503	489	531	503	559	517	572
2/0	379	673	701	771	813	869	925	886	941
2/1	451	703	731	787	829	871	927	889	944
2/2	523	733	761	803	845	873	929	892	947
2/3	595	763	791	819	861	875	931	895	950
2/4	667	793	821	835	877	877	933	898	953
2/5	739	823	851	851	893	879	935	901	956
2/6	811	853	881	867	909	881	937	904	959
3/0	541	961	989	1101	1143	1241	1297	1264	1319
3/1	613	991	1019	1117	1159	1243	1299	1267	1322
3/2	685	1021	1049	1133	1175	1245	1301	1270	1325
3/3	757	1051	1079	1149	1191	1247	1303	1273	1328
3/4	829	1081	1109	1165	1207	1249	1305	1276	1331
3/5	901	1111	1139	1181	1223	1251	1307	1279	1334
3/6	973	1141	1169	1197	1239	1253	1309	1282	1337
3/7	1045	1171	1199	1213	1255	1255	1311	1285	1340
3/8	1117	1201	1229	1229	1271	1257	1313	1288	1343
3/9	1189	1231	1259	1245	1287	1259	1315	1291	1346
4/0	703	1249	1277	1431	1473	1613	1669	1642	1697
4/1	775	1279	1307	1447	1489	1615	1671	1645	1700
4/2	847	1309	1337	1463	1505	1617	1673	1648	1703
4/3	919	1339	1367	1479	1521	1619	1675	1651	1706
4/4	991	1369	1397	1495	1537	1621	1677	1654	1709
4/5	1063	1399	1427	1511	1553	1623	1679	1657	1712
4/6	1135	1429	1457	1527	1569	1625	1681	1660	1715
4/7	1207	1459	1487	1543	1585	1627	1683	1663	1718
4/8	1279	1489	1517	1559	1601	1629	1685	1666	1721
4/9	1351	1519	1547	1575	1617	1631	1687	1669	1724
4/10	1423	1549	1577	1591	1633	1633	1689	1672	1727
4/11	1495	1579	1607	1607	1649	1635	1691	1675	1730
4/12	1567	1609	1637	1623	1665	1637	1693	1678	1733

8.3.9 Cellooligomer standards for LC-ELSD

3 mg of dried glucose (16.7 μ mol, 83 μ mol OH), cellobiose (8.8 μ mol, 70 mmol OH), cellotriose (6.0 μ mol, 65 μ mol OH), and cellotetraose (4.5 μ mol, 63 μ mol OH), respectively, are methoxyacetylated with 30 μ L methoxyacetyl chloride (0.33 mmol, 4-5 eq/ OH), 100 μ L *N*-methylimidazole (1.27 mmol, 15-20 eq/ OH) in 200 μ L dichloromethane. Samples are cleaned-up by liquid extraction with dichloromethane and washing of the organic phase with aq. sat. NaHCO₃, 0.1 M cold HCl and distilled water. The sample is dried with CaCl₂, the solvent is removed under

a stream of dry nitrogen and the residue is dissolved in 1 mL CH₂Cl₂. For ELSD measurement, standard celooligomers are diluted with acetone/hexane.

Methoxyacetylated celooligomers are characterized by ESI-IT-MS (8.2.2), ATR-IR-spectroscopy (8.2.8), and ¹H-NMR-spectroscopy (8.2.9).

Methoxyacetylated glucose (1,2,3,4,5-penta-O-methoxyacetylglucose): ESI-IT-MS *m/z*: 563.2 [M+ Na]⁺, ¹H-NMR (CDCl₃): δ [ppm] = 3.2-3.65 (5s, 15H, R-OC(O)CH₂-O-CH₃), 3.8-4.15 (m, 10H, R-OC(O)CH₂-O-CH₃), 4.2-4.4 (m, 3H, H-5, H-6a, H-6b), 5.1-5.2 (m, 2H, H-2, H-4), 5.47 (dd, 1H, H-3, ³J_{2,3}= 10 Hz, ³J_{3,4}= 10 Hz), 6.37 (d, 1H, H-1, ³J_{1,2}= 3.5 Hz), ATR-IR: Wavenumbers [cm⁻¹]: 3000-2800: ν(C-H),w; 1750: ν(C=O),s, 1450: δ(C-H),w, 1250: ν(C-O-C, ester),w, 1100: ν(C-O-C, ether),s; Yield (weight%): 80 %

Methoxyacetylated cellobiose: ESI-IT-MS *m/z*: 941.6 [M+ Na]⁺, ATR-IR: Wavenumbers [cm⁻¹]: 3000-2800: ν(C-H),w; 1750: ν(C=O),s, 1450: δ(C-H),w, 1250: ν(C-O-C, ester),w, 1120: ν(C-O-C, ether),s; Yield (weight%): 75 %

Methoxyacetylated cellotriose: ESI-IT-MS *m/z*: 1319.9 [M+ Na]⁺, ATR-IR: Wavenumbers [cm⁻¹]: 3000-2800: ν(C-H),w; 1750: ν(C=O),s, 1450: δ(C-H),w, 1250: ν(C-O-C, ester),w, 1120: ν(C-O-C, ether),s

Methoxyacetylated cellotetraose: ESI-IT-MS *m/z*: 1697.9 [M+ Na]⁺, ATR-IR: Wavenumbers [cm⁻¹]: 3000-2800: ν(C-H),w; 1750: ν(C=O),s, 1450: δ(C-H),w, 1250: ν(C-O-C, ester),w, 1100: ν(C-O-C, ether),s

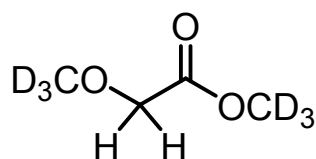
8.3.10 Methoxyacetylation after hydrolysis

8.3.10.1 Methyl esterification with TMSH

1 mL TMSH solution (0.2 M in methanol) is added to the dry residue of 20 mg partially hydrolyzed CMC (0.08 mmol AGU, see 8.3.2.4) and stirred at r.t. for 2 h, until a homogeneous suspension is obtained which is heated to 50 °C for 10 min. The reaction mixture is evaporated to dryness under a stream of dry nitrogen. The residue is methoxyacetylated with 50 µL methoxyacetyl chloride (0.55 mmol, approx. 65 eq/ AGU, 20 eq/ OH) and 30 µL *N*-methylimidazole (0.33 mmol, approx.

45 eq/ AGU, 15 eq/ OH), by stirring for 1 h at r. t.. The sample is cleaned-up by washing the organic phase with aq. sat. NaHCO_3 , 0.1 M cold HCl and distilled water. The sample is dried with sodium sulfate, the solvent is removed under a stream of dry nitrogen and the residue is dissolved in 1 mL CH_2Cl_2 . After dilution with methanol (0.5 mg/ mL), the sample is measured in ESI-IT-MS.

8.3.10.2 Synthesis of d_3 -methoxyacetyl- d_3 -methylester^[197]



1.000 g glycolic acid (13.15 mmol, 2 OH) is dissolved in a dried 100-mL-Schlenck flask under dry nitrogen atmosphere in 40 mL dry DMSO. First, 2.6 g NaOH (65.0 mmol, 5 eq, 2.5 eq/ OH) is added under nitrogen, then 4.08 mL CD_3I (64.15 mmol, 5 eq, 2.5 eq/ OH). The reaction mixture is stirred at r.t. for 6 h, then the half amount of base and nucleophile is added and the mixture is stirred over night. The solution is diluted with water and extracted with dichloromethane three times. The organic phase is washed with aq. sat. NaHCO_3 , cold 0.1 M HCl, and water and subsequently dried with sodium sulphate. The solvent is removed under a stream of dry nitrogen and the residue is dissolved in 10 mL CH_2Cl_2 . Characterization of the product was performed by GLC-MS (8.2.6) and ^1H -NMR-spectroscopy (8.2.9).

^1H -NMR (CDCl_3): δ 4.05 (s), GLC-MS ($m/z > 50$): R_t : 4.46 min, m/z : 78 (McLafferty product), 62 (α -cleavage); Yield (weight%): 95 %,

8.3.10.3 Acylation via an adapted impeller method^[197]

224 μL TFAA and 1.638 mL of the d_3 -methoxyacetyl- d_3 -methylester (8.3.10.2) are dissolved in CH_2Cl_2 (molar ratio TFAA/ ester: 1.2) are mixed and stirred at 50 °C for 5 h forming the reactive mixed anhydride. The solution is added to the dried methanolizate of 20 mg CMC (8.3.5.3). The product is cleaned-up by extraction with dichloromethane and washing of the organic phase with, aq. sat. NaHCO_3 , 0.1 M cold HCl, and water and subsequently dried with CaCl_2 . The solvent is removed under a stream of dry nitrogen and the residue is dissolved in 1 mL CH_2Cl_2 .

The product is controlled by ATR-IR-spectroscopy (8.2.8).

ATR-IR: Wavenumbers [cm^{-1}]: 3400: $\nu(\text{O-H})$,s; 3000-2800: $\nu(\text{C-H})$,w; 1750: $\nu(\text{C=O}$, ester),s

8.3.11 Fractionation

8.3.11.1 Methanolysis and methoxyacetylation in 100 mg-scale

To 22.3 mL d_4 -methanol in a 100-mL-round flask 2.7 mL acetyl chloride are added under ice cooling, yielding 75 mL 1.5 M d_3 -methanolic HCl. Then, 100 mg (appr. 0.4 mmol AGU) CMC are added and the mixture is stirred under reflux for 90 min. A residue of undissolved material remains which is further treated together with the dissolved sample. Methanol is partly removed by the rotary evaporator. HCl is removed by codestillation with d_4 -methanol, and the reaction mixture is dried under nitrogen. Then, an excess of 10 mL *N*-methylimidazole and 1.5 mL methoxyacetyl chloride (16 mmol, approx. 40 eq/ AGU, 13 eq/OH) are added, yielding a clear solution that is stirred for 1 h at r.t..

The products are extracted with CH_2Cl_2 and the organic phase is washed with sat. aq. NaHCO_3 , 0.1 M cold HCl, and distilled water. The organic phase is dried with sodium sulphate, the solvent is removed under a stream of dry nitrogen and the residue is subsequently dissolved in 5 mL CH_2Cl_2 (0.08 mmol methoxyac. CMC/ mL).

Yield (weight%): 85 %

8.3.11.2 Column chromatography

4 mL of the solution obtained from 8.3.11.1 (0.064 mmol methoxyac. CMC) are used for column chromatography (silica gel) with a drop speed of 0.4 mL/ min (eluent: acetone/ hexane, 1 : 1, v/v). 2 mL-fractions are collected and controlled by TLC (8.2.10). Recovery (weight%): 96 %

8.3.12 Time course study of methanolysis

8.3.12.1 *Separation of undissolved material and dissolved products in the supernatant*

Waterfree methanolic HCl (2 mL, 1.5 M, 8.3.5.1, 8.3.5.2) is added to 20 mg dry NaCMC (approx. 0.075 mmol) in a 2 mL-V-vial. To start methanolysis, the reaction mixture is stirred and heated to 90 °C in a heating block (8.2.12). In intervals of 10 to 15 min until a total reaction time of 90 min, the reaction is interrupted by cooling the vial into a NaCl/ice bath (approx. - 10 °C). When the undissolved residue is sedimented, an aliquot (1.7 mL) of the the supernatant is taken. The corresponding volume of fresh methanolic HCl is added to the residue and the reaction is continued. After 90 min of summarized reaction intervals, all material is dissolved. The removed fractions are completely hydrolyzed in a 1 mL V-vial with perchloric acid at 120 °C. HClO₄ is removed by addition of KOH and centrifugation of the precipitate (8.3.2.3). 40 µL of an aqueous maltose solution of 1.000 g maltose monohydrate (2.78 mmol water free maltose) in 100 mL water (HPLC quality) are added to the supernatant as internal standard prior to reductive amination and measurement by CE-UV (8.3.3). Molar response factors of labeled maltose and glucose are experimentally proven to be 1.

8.3.12.2 *Separation of undissolved material and dissolved products in the supernatant with an additional filtration step*

Waterfree methanolic HCl (2 mL, 1.5 M, 8.3.5.1, 8.3.5.2) is added to 20 mg dry NaCMC (approx. 0.075 mmol) in a 2 mL-V-vial. To start methanolysis, the reaction mixture is stirred and heated to 90 °C in a heating block (8.2.12). In intervals of 10 to 15 min until a total reaction time of 90 min, the reaction is interrupted by cooling the vial into a NaCl/ice bath (approx. - 10 °C). When the undissolved residue is sedimented, an aliquot (4.7 mL) of the the supernatant is taken. The corresponding volume of fresh methanolic HCl is added to the residue and the reaction is continued. After 90 min of summarized reaction intervals, all material is dissolved. To allow filtration in 0.5 mL-Eppendorf centrifugal membrane filters (MWCO 5000), the volume of the sample solution needs to be decreased. Therefore, the fractions of the dissolved part are co-distilled with methanol to remove HCl, and then they are evaporated to dryness under nitrogen. The dry residues are dissolved in 0.5 mL and

transferred to the Eppendorf centrifugal membrane filters. To allow quantification, 80 μL of a xylose standard solution (535.4 mg xylose/ 50 mL methanol/ H_2O 1 : 4, v/v, corresponding to 0.07 mmol/ mL) are added to each filter. The samples are centrifuged at 4 °C at 15000 Umin^{-1} . The filtrates are transferred to 1 mL-V-vials, evaporated to dryness and then totally hydrolyzed with 1 mL perchloric acid at 120 °C. HClO_4 is removed by addition of KOH and centrifugation of the precipitate (8.3.2.3). The supernatants are reductively aminated with ABN and measured by CE-UV (8.3.3). Molar response factors of labeled xylose and glucose are experimentally proven to be 1.

9 References

- [1] Hess, K., *Die Chemie der Zellulose und Ihrer Begleiter*. Akad. Verlagsges., Leipzig, Germany, **1928**.
- [2] Thielking, H. and Schmidt, M., *Cellulose Ethers*. Ullmann's Encyclopedia of Industrial Chemistry, Wiley-VCH, Weinheim, Germany, **2006**.
- [3] Payen, A., *Troisième mémoire sur le développement des Végétaux*. Extrait des Mémoires de l'Académie Royale des Sciences, Imprimerie Royale, Paris, France, **1842**.
- [4] Staudinger, H., *Die hochmolekularen organischen Verbindungen - Kautschuk und Cellulose*. Springer Verlag, **1932**.
- [5] Freudenberg, K., *Cellulose*. Ber., **1921**, 54B, 767-72.
- [6] Herzog, R.O. and Jancke, W., *X-ray spectroscopic investigations on cellulose*. Z. Phys., **1920**, 3, 196-198.
- [7] Herzog, R.O., Jancke, W., and Polanyi, M., *X-Ray spectroscopic investigations on cellulose II*. Z. Phys., **1920**, 3, 343-348.
- [8] Michell, A.J. and Higgins, H.G., *Conformation and intramolecular hydrogen bonding in glucose and xylose derivatives*. Tetrahedron, **1965**, 21(5), 1109-20.
- [9] Ellefsen, O. and Toennesen, B.A., *Structure of cellulose and its derivatives. X-ray and electron diffraction. Polymorphic forms*. High Polym., **1971**, 5(4), 151-80.
- [10] Toennesen, B.A. and Ellefsen, O., *Structure of cellulose and its derivatives. Submicroscopical investigations*. High Polym., **1971**, 5(4), 265-304.
- [11] Fink, H.-P. and Phillipp, B., *Models of Cellulose Physical Structure from the Viewpoint of the Cellulose I to II Transition*. J. Appl. Polym. Sci., **1985**, 30, 3779-3790.
- [12] Fink, H.-P., Hofmann, D., and Purz, H.J., *Zur Fibrillarstruktur nativer Cellulose*. Acta Polym., **1990**, 41, 131-137.
- [13] Krässig, H. and Schurz, J., *Cellulose*. Ullmann's Encyclopedia of Industrial Chemistry, Wiley-VCH, Weinheim, Germany, **1986**.
- [14] Hon, D.N.S., *Cellulose: a random walk along its historical path*. Cellulose (Dordrecht, Netherlands), **1994**, 1(1), 1-25.
- [15] Vander Hart, D.L. and Atalla, R.H., *Studies of Microstructure in Native Cellulose Using Solid-State ¹³C-NMR*. Macromolecules, **1984**, 17, 1465-1472.
- [16] Horii, F., Yamamoto, H., Kitamaru, R., Tanahashi, M., and Higuchi, T., *Transformation of Native Cellulose Crystals Induced by Saturated Steam at High Temperatures*. Macromolecules, **1987**, 20, 2946-2949.
- [17] Koyama, M., Helbert, W., Imai, T., Sugiyama, J., and Henrissat, B., *Parallel-up structure evidences the molecular directionality during biosynthesis of bacterial cellulose*. P. Natl. Acad. Sci. USA, **1997**, 94, 9091-9095.
- [18] Marchessault, R.H. and Liang, C.Y., *Infrared spectra of crystalline polysaccharides. III. Mercerized cellulose*. J. Polym. Sci., **1960**, 43, 71-84.
- [19] Gardner, K.H. and Blackwell, J., *The Structure of Native Cellulose*. Biopolymers, **1974**, 13, 1975-2001.
- [20] Meyer, K.H. and Misch, L., *Positions des atomes dans le nouveau modèle spatial de la cellulose*. Helv. Chim. Acta, **1937**, 20(1), 232-244.
- [21] O'Neill, M.A. and York, W.S., *The composition and structure of plant primary cell wall*. The Plant Cell Wall, Blackwell Publishing, Oxford, UK, **2003**.
- [22] Obembe, O.O., Jacobsen, E., Visser, R.G.F., and Vincken, J.-P., *Cellulose-hemicellulose networks as target for in planta modification of the properties of natural fibres*. Biotechnol. Mol. Biol. Rev., **2006**, 1(3), 76-86.
- [23] Hon, D.N.S., *Chemical modification of cellulose*. Chemical modification of lignocellulosic materials, Marcel Dekker, New York, Basel, Hongkong, **1996**.
- [24] Krässig, H., Schurz, J., Steadman, R.G., Schliefer, K., and Albrecht, W., *Cellulose*. Industrial Polymers Handbook, **2001**, 3, 1423-1500.

- [25] **Machell, G. and Richards, G.**, *The Alkaline Degradation of Polysaccharides. Part II. The Alkali-stable Residues from the Action of Sodium Hydroxide on Cellulose.* J. Chem. Soc., **1957**, 4500-4506.
- [26] **Johansson, M.H. and Samuelson, O.**, *The Formation of End Groups in Cellulose during Alkali Cooking.* Carbohydr. Res., **1974**, 34, 33-43.
- [27] **Roehrling, J., Potthast, A., Rosenau, T., Lange, T., Ebner, G., Sixta, H., and Kosma, P.**, *A novel method for the determination of carbonyl groups in cellulose by fluorescence labeling. 1. Method development.* Biomacromolecules, **2002**, 3(5), 959-968.
- [28] **Roehrling, J., Potthast, A., Rosenau, T., Lange, T., Borgards, A., Sixta, H., and Kosma, P.**, *A novel method for the determination of carbonyl groups in cellulose by fluorescence labeling. 2. Validation and applications.* Biomacromolecules, **2002**, 3(5), 969-975.
- [29] **Bohrn, R., Potthast, A., Rosenau, T., Kosma, P., and Sixta, H.**, *A novel diazo reagent for fluorescence labeling of carboxyl groups in pulp.* Lenz. Berichte, **2004**, 83, 84-91.
- [30] **Bohrn, R., Potthast, A., Rosenau, T., Sixta, H., and Kosma, P.**, *Synthesis and testing of a novel fluorescence label for carboxyls in carbohydrates and cellulose.* Synlett, **2005**, 20, 3087-3090.
- [31] **Aspinall, G.O.**, *The Polysaccharides.* New York Academic Press, **1983**.
- [32] **Klemm, D., Heublein, B., Fink, H.-P., and Bohn, A.**, *Cellulose: Fascinating biopolymer and sustainable raw material.* Angew. Chem. Int. Edit., **2005**, 44(22), 3358-3393.
- [33] **Suida, W.**, *Influence of active groups in the textile fibres on the process of dyeing.* Monatsh. Chem., **1905**, 26, 413-427.
- [34] **DE332203C1**, *Verfahren zur Herstellung von Celluloseverbindungen*, Jansen, E., Deutsche Celluloid Fabrik, **1918**, Germany.
- [35] **Klemm, D., Philipp, B., Heinze, T., Heinze, U., and Wagenknecht, W.**, *Comprehensive Cellulose Chemistry, Volume 2.* Wiley VCH, Weinheim, Germany, **1998**.
- [36] **Heinze, T.**, *New ionic polymers by cellulose functionalization.* Macromol. Chem. Phys., **1998**, 199(11), 2341-2364.
- [37] **Heinze, T., Schwikal, K., and Barthel, S.**, *Ionic liquids as reaction medium in cellulose functionalization.* Macromol. Biosci., **2005**, 5(6), 520-525.
- [38] **Alderman, D.A.**, *A review of cellulose ethers in hydrophilic matrices for oral controlled-release dosage forms.* Int. J. Pharm. Technol. Prod. Manuf., **1984**, 3(5), 1-9.
- [39] **Ranga Rao, K., Padmalatha Devi, K., and Buri, P.**, *Influence of molecular size and water solubility of the solute on its release from swelling and erosion controlled polymeric matrices.* J. Controlled Release, **1990**, 12, 133-141.
- [40] **Doelker, E.**, *Water-swollen cellulose derivatives in pharmacy.* Hydrogels in Medicine and Pharmacy Polymers, CRC Press, Boca Raton, Florida, USA, **1987**.
- [41] **Stigsson, V., Kloow, G., and Germgard, U.**, *Historical overview of CMC production on an industrial scale.* Paper Asia, **2001**, 16-21.
- [42] **Posey-Dowty, J.D., Watterson, T.L., Wilson, A.K., Edgar, K.J., Shelton, M.C., and Lingerfeld Jr., L.R.**, *Zero-order release formulation using a novel cellulose ester.* Cellulose, **2007**, 14, 73-83.
- [43] **Scherz, H.**, *Hydrokolloide: Stabilisatoren, Dickungs- und Geliermittel in Lebensmitteln.* Behr, Hamburg, Germany, **1996**.
- [44] **Hader, R.N., Waldeck, W.F., and Smith, F.W.**, *Carboxymethylcellulose.* J. Ind. Eng. Chem., **1952**, 44, 2803-2812.
- [45] **Dönges, R.**, *Developments in the production and application of cellulose ethers.* Papier, **1997**, 12, 653-670.
- [46] **Yokota, H.**, *The mechanism of cellulose alkalization in the isopropyl alcohol - water - sodium hydroxide - cellulose system.* J. Appl. Polym. Sci., **1985**, 30, 263-277.

- [47] Cheng, F., L., G., Jianxin, F., and Jingwu, Z., *Characterisation of carboxymethyl cellulose synthesized in two phase medium C_6H_6 - C_2H_5OH . I. Distribution of substituent groups in the anhydroglucose unit*. J. Appl. Polym. Sci., **1996**, 61, 1831-1838.
- [48] Olaru, N., Olaru, O., Stoleriu, A., and Timpu, D., *Carboxymethylcellulose synthesis in organic media containing ethanol and/or acetone*. J. Appl. Polym. Sci., **1998**, 67, 481-486.
- [49] Heinze, T., Liebert, T., Klüfers, P., and Meister, F., *Carboxymethylation of cellulose in unconventional media*. Cellulose, **1999**, 6, 153-165.
- [50] Fink, H.P., Walenta, E., Kunze, J., and Mann, G., *Wide angle X-ray and solid state ^{13}C -NMR studies of cellulose alkalization*. Cellulose and Cellulose Derivatives, Woodhead Publications, **1995**.
- [51] Dapía, S., Santos, V., and Parajó, J.C., *Carboxymethylcellulose from totally chlorine free-bleached Milox pulps*. Bioresour. Technol., **2003**, 89, 289-293.
- [52] Trivedi, H.C., Patel, C.K., and Patel, R.D., *Studies on Carboxymethylcellulose: Potentiometric Titrations*, 3. Macromol. Chem. Phys., **1981**, 182, 243-245.
- [53] Jeffrey, G.A. and Saenger, W., *Hydrogen Bonding in Biological Structures*. Springer-Verlag, Berlin, Heidelberg, New York, **1994**.
- [54] Käuper, P., *Natriumcarboxymethylcellulose: Bestimmung der chemischen Struktur, der Lösungsstruktur und der Elektrolytwechselwirkungen*. Berichte aus der Chemie, Shaker, Aachen, Germany, **1998**.
- [55] Schulz, L., Seger, B., and Burchard, W., *Structures of cellulose in solution*. Macromol. Chem. Phys., **2000**, 201(15), 2008-2022.
- [56] Burchard, W., *Solubility and Solution Structure of Cellulose Derivatives*. Cellulose, **2003**, 10, 213-225.
- [57] Francis, P.S., *Solution Properties of Water-Soluble Polymers. I. Control of Aggregation of Sodium Carboxymethylcellulose (CMC) by Choice of Solvent and/or Electrolyte*. J. Appl. Polym. Sci., **1961**, 5(15), 261-270.
- [58] Liebert, T., Hornig, S., Hesse, S., and Heinze, T., *Microscopic Visualization of Nanostructures of Cellulose Derivatives*. Macromol. Symp., **2005**, 223, 253-266.
- [59] Salmi, T., Valtakari, D., Paatero, E., Holmbom, B., and Sjöholm, R., *Kinetic study of the carboxymethylation of cellulose*. Ind. Eng. Chem. Res., **1994**, 33, 1454-1459.
- [60] Germgard, U. and Hedlund, A., *Some aspects on the kinetics of etherification in the preparation of CMC*. Cellulose, **2007**, 14, 161-169.
- [61] Baar, A., Kulicke, W.-M., Szablikowski, K., and Kieseewetter, R., *Nuclear Magnetic Resonance Spectroscopic Characterization of Carboxymethylcellulose*. Macromol. Chem. Phys., **1994**, 195, 1483-1492.
- [62] Kragten, E.A., Kamerling, J.P., and Vliegenthart, J.F.G., *Composition analysis of carboxymethylcellulose by high-pH anion-exchange chromatography with pulsed amperometric detection*. J. Chromatogr., **1992**, 623(1), 49-53.
- [63] Zeller, S.G., Griesgraber, G.W., and Gray, G.R., *Analysis of positions of substitution of O-carboxymethyl groups in partially O-carboxymethylated cellulose by the reductive-cleavage method*. Carbohydr. Res., **1991**, 211(1), 41-45.
- [64] Abdel-Malik, M.M. and Yalpani, M., *Determination of substituent distribution in cellulose ethers by means of carbon-13 NMR spectroscopy*. Cellulose, **1990**, 263-268.
- [65] Niemelä, K. and Sjöström, E., *Characterization of hardwood-derived carboxymethyl cellulose by gas-liquid chromatography and mass spectrometry*. Polym. Commun., **1989**, 30(8), 254-6.
- [66] Reuben, J. and Conner, H.T., *Analysis of the carbon-13 NMR spectrum of hydrolyzed O-(carboxymethyl)cellulose: monomer composition and substitution patterns*. Carbohydr. Res., **1983**, 115(1), 1-13.
- [67] Ho, F.F.L. and Klosiewicz, D.W., *Proton NMR Spectrometry for Determination of Substituents and their Distribution in Carboxymethylcellulose*. Anal. Chem., **1980**, 52, 913-916.

- [68] **Buytenhuys, F.A. and Bonn, R.**, *Distribution of substituents in CMC*. Papier, **1977**, 31(12), 525-7.
- [69] **Croon, I. and Purves, C.B.**, *The distribution of the substituents in partially substituted carboxymethyl cellulose*. Sven. Papperstid., **1959**, 62, 876-82.
- [70] **Timell, T.E. and Spurlin, H.M.**, *Carboxymethylcelluloses II. The distribution of the substituents in partially substituted carboxymethylcelluloses*. Sven. Papperstid., **1952**, 55, 700-8.
- [71] **Spurlin, H.M.**, *Arrangement of substituents in cellulose derivatives*. J. Am. Chem. Soc., **1939**, 61, 2222-7.
- [72] **Reuben, J.**, *Analysis of the carbon-13 NMR spectra of hydrolyzed and methanolized O-methylcelluloses: monomer compositions and models for their description*. Carbohydr. Res., **1986**, 157, 201-13.
- [73] **Ott, E., Spurlin, H.M., and Grafflin, M.W.**, *Cellulose and Cellulose Derivatives, Part II*. New York Interscience, 904, **1963**.
- [74] **Arisz, P.W., Kauw, H.J.J., and Boon, J.J.**, *Substituent distribution along the cellulose backbone in O-methylcelluloses using GC and FAB-MS for monomer and oligomer analysis*. Carbohydr. Res., **1995**, 271(1), 1-14.
- [75] **Mischnick, P., Heinrich, J., Gohdes, M., Wilke, O., and Rogmann, N.**, *Structure analysis of 1,4-glucan derivatives*. Macromol. Chem. Phys., **2000**, 201(15), 1985-1995.
- [76] **Wilke, O.**, *Thesis: Bestimmung der Substituentenverteilung in kationischen Stärkeethern*. **1998**, University of Hamburg.
- [77] **Mischnick, P. and Kuehn, G.**, *Model studies on methyl amyloses: correlation between reaction conditions and primary structure*. Carbohydr. Res., **1996**, 290(2), 199-207.
- [78] **Heinrich, J. and Mischnick, P.**, *Determination of the substitution pattern in the polymer chain of cellulose acetates*. J. Polym. Sci. Pol. Chem., **1999**, 37(15), 3011-3016.
- [79] **Gohdes, M. and Mischnick, P.**, *Determination of the substitution pattern in the polymer chain of cellulose sulfates*. Carbohydr. Res., **1998**, 309(1), 109-115.
- [80] **Adden, R., Müller, R., Brinkmalm, G., Ehrler, R., Mischnick, P.**, *Comprehensive Analysis of the Substituent Distribution in Hydroxyethyl Celluloses by Quantitative MALDI-ToF-MS*. Macromol. Biosci., **2006**, 6(6), 435-444.
- [81] **Adden, R., Niedner, W., Müller, R., and Mischnick, P.**, *Comprehensive Analysis of the Substituent Distribution in the Glucosyl Units and along the Polymer Chain of Hydroxyethylmethyl Celluloses and Statistical Evaluation*. Anal. Chem., **2006**, 78(4), 1146-1157.
- [82] **Adden, R., Müller, R., and Mischnick, P.**, *Analysis of the substituent distribution in the glucosyl units and along the polymer chain of hydroxypropylmethyl cellulose and statistical evaluation*. Cellulose, **2006**, 13, 459-476.
- [83] **Heinrich, J.**, *Thesis: Strukturaufklärung von Cellulosederivaten und Galactanen mittels chemischer, chromatographischer und massenspektrometrischer Methoden*. **1999**, University of Hamburg.
- [84] **Gordon, H.T., Thornburg, W.W., and Wrum, L.N.**, *Rapid paper chromatographic fractionation of complex mixtures of water soluble-substances*. J. Chromatogr., **1962**, 9, 44-59.
- [85] **Ghebregzabher, M., Rufini, S., Monaldi, B., and Lato, M.**, *Thin-layer chromatography of carbohydrates*. J. Chromatogr., **1976**, 127, 133-162.
- [86] **Honda, S.**, *High-performance liquid chromatography of mono- and oligosaccharides*. Anal. Biochem., **1984**, 140, 1-47.
- [87] **Lee, Y.C.**, *Carbohydrate analysis with high-performance anion-exchange chromatography. A review*. J. Chromatogr. A, **1996**, 720, 137-149.
- [88] **Cataldi, T.R.I., Campa, C., and De Benedetto, G.E.**, *Carbohydrate analysis by high-performance anion-exchange chromatography with pulsed amperometric detection: The potential is still growing*. Fresenius J. Anal. Chem., **2000**, 368(8), 739-758.

- [89] **Hanko, V.P. and Rohrer, J.S.**, *Determination of carbohydrates, sugar alcohols, and glycols in cell cultures and fermentation broths using high-performance anion-exchange chromatography with pulsed amperometric detection*. Anal. Biochem., **2000**, 283, 192-199.
- [90] **Rohrer, J.S.**, *Analyzing sialic acids using high-performance anion-exchange chromatography with pulsed amperometric detection*. Anal. Biochem., **2000**, 283, 3-9.
- [91] **Al-Hakim, A. and Linhardt, R.J.**, *Isolation and recovery of acidic oligosaccharides from polyacrylamide gels by semi-dry electrotransfer*. Electrophoresis, **1990**, 11, 23-28.
- [92] **Scherz, H.**, *Thin-layer electrophoretic separation of monosaccharides, oligosaccharides and related compounds on reverse phase silica gel*. Electrophoresis, **1990**, 11, 18-22.
- [93] **Novotny, M.V. and Sudor, J.**, *High-performance capillary electrophoresis of glycoconjugates*. Electrophoresis, **1993**, 14, 373-389.
- [94] **El Rassi, Z.**, *Capillary Electrophoresis of Carbohydrates*. Adv. Chromatogr., **1994**, 34, 177-250.
- [95] **Campa, C., Coslovi, A., Flamigni, A., and Rossi, M.**, *Overview on advances in capillary electrophoresis-mass spectrometry of carbohydrates: A tabulated review*. Electrophoresis, **2006**, 27, 2027-2050.
- [96] **Jorgenson, J.W. and Lukacs, K.D.**, *Zone electrophoresis in open tubular glass capillaries*. Anal. Chem., **1981**, 53, 1298-1302.
- [97] **Landers, J.P.**, *Introduction to Capillary Electrophoresis*. 3 ed. *Handbook of Capillary and Mikrochip Electrophoresis and associated Microtechniques*, CRC Press, Boca Raton, Florida, USA, **2008**.
- [98] **Foster, A.B.**, *Zone Electrophoresis of Carbohydrates*. Adv. Carbohydr. Chem., **1957**, 12, 81-116.
- [99] **van Duin, M., Peters, J.A., Kieboom, A.P.G., and van Bakkum, H.**, *Studies on Borate Esters II*. Tetrahedron, **1985**, 41, 3411-3421.
- [100] **Khandurina, J.**, *Analysis of Carbohydrates by Capillary Electrophoresis*. 3 ed. *Handbook of Capillary and Mikrochip Electrophoresis and associated Microtechniques*, CRC Press, Boca Raton, Florida, USA, **2008**.
- [101] **Honda, S., Iwase, S., Makino, A., and Fujiwara, S.**, *Simultaneous Determination of Reducing Monosaccharides by Capillary Zone Electrophoresis as the Borate Complexes of N-2-Pyridylglycamines*. Anal. Biochem., **1989**, 176, 72-77.
- [102] **Honda, S.**, *Separation of neutral carbohydrates by capillary electrophoresis*. J. Chromatogr. A, **1996**, 720, 337-351.
- [103] **Suzuki, S. and Honda, S.**, *A tabulated review of capillary electrophoresis of carbohydrates*. Electrophoresis, **1998**, 19, 2539-2560.
- [104] **Bazzanella, A. and Bächmann, K.**, *Separation and direct UV-detection of sugars by capillary electrophoresis*. J. Chromatogr. A, **1998**, 799, 283-288.
- [105] **Hoffstetter-Kuhn, S., Paulus, A., Gassmann, E., and Widmer, H.M.**, *Influence of borate complexation on the electrophoretic behavior of carbohydrates in capillary electrophoresis*. Anal. Chem., **1991**, 63(15), 1541-1547.
- [106] **Oudhoff, K.A., Buijtenhuijs, F.A., Wijnen, P.H., Schoenmakers, P.J., and Kok, W.T.**, *Determination of the degree of substitution and its distribution of carboxymethylcelluloses by capillary zone electrophoresis*. Carbohydr. Res., **2004**, 339, 1917-1924.
- [107] **Stefanson, M.**, *Characterization of cellulose derivatives and their migration behavior in capillary electrophoresis*. Carbohydr. Res., **1998**, 312, 45-52.
- [108] **Horner, S., Puls, J., Saake, B., Klohr, E.A., and Thielking, H.**, *Enzyme-aided characterization of carboxymethyl cellulose*. Carbohydr. Polym., **1999**, 40(1), 1-7.
- [109] **Tüting, W., Albrecht, G., Volkert, B., and Mischnick, P.**, *Structure analysis of carboxymethyl starch by capillary electrophoresis and enzymic degradation*. Starch/Stärke, **2004**, 56(7), 315-321.
- [110] **Faustmann, B.**, *Thesis: Analytik von amphiphilen Stärkederivaten mittels Kapillarelektrophorese*. **2008**, University of Braunschweig.

- [111] Ruiz-Calero, V., Puignou, L., and Galceran, M.T., *Use of reversed polarity and a pressure gradient in the analysis of disaccharide composition of heparin by capillary electrophoresis*. J. Chromatogr. A, **1998**, 828, 497-508.
- [112] Ruiz-Calero, V., E., M., Puignou, L., and Galceran, M.T., *Pressure-assisted capillary electrophoresis-electrospray ion trap mass spectrometry for the analysis of heparin depolymerised disaccharides*. J. Chromatogr. A, **2001**, 914, 277-291.
- [113] Liang, A., Chao, Y., Liu, X., Du., Y., Wang, K., Qian, S., and Lin, B., *Separation, identification, and interaction of heparin oligosaccharides with granulocyte-colony stimulating factor using capillary electrophoresis and mass spectrometry*. Electrophoresis, **2005**, 26, 3460-3467.
- [114] Ramasamy, I., Kennedy, J., and Tan, K., *Capillary Electrophoresis for Characterization of Low Molecular Weight Heparins*. Lab. Hematol., **2003**, 9, 64-66.
- [115] Larsson, M., Sundberg, R., and Folestad, S., *On-line capillary electrophoresis with mass spectrometry detection for the analysis of carbohydrates after derivatization with 8-aminonaphthalene-1,3,6-trisulfonic acid*. J. Chromatogr. A, **2001**, 934(1-2), 75-85.
- [116] Gennaro, L.A., Delaney, J., Vouros, P., Harvey, D.J., and Domon, B., *capillary electrophoresis/ electrospray ion trap mass spectrometry for the analysis of negatively charged derivatized and underivatized glycans*. Rapid Commun. Mass Spectrom., **2002**, 16, 192-200.
- [117] Rocklin, R.D. and Pohl, C.A., *Determination of carbohydrates by anion exchange chromatography with pulsed amperometric detection*. J. Liq. Chromatogr., **1983**, 6(9), 1577-90.
- [118] Townsend, R.R., Hardy, M.R., and Lee, Y.C., *Separation of oligosaccharides using high-performance anion-exchange chromatography with pulsed amperometric detection*. Methods Enzymol., **1989**, 179, 65-79.
- [119] Lee, Y.C., *High-performance anion-exchange chromatography for carbohydrate analysis*. Anal. Biochem., **1990**, 189, 151-162.
- [120] Koizumi, K., Kubota, Y., Ozaki, H., Shigenobu, K., Fukuda, M., and Tanimoto, T., *J. Chromatogr.*, **1992**, 595, 340-345.
- [121] Pfeiffer, G., Geyer, H., Geyer, R., Kalsner, I., and Wendorf, P., *Seperation of glycoprotein-N-glycans by high-pH anion-exchange chromatography*. Biomed. Chromatogr., **1990**, 4, 193-199.
- [122] Pfeiffer, G., Strube, K.H., Schmidt, M., and Geyer, R., *Glycosylation of two recombinant human uterine tissue plasminogen activator variance carrying an additional N-glycosylation side in the epidermal-growth-factor-like domain*. Eur. J. Biochem., **1995**, 219, 331-348.
- [123] Ammeraal, R.N., Delgado, G.A., Tenbarge, F.L., and Friedman, R.B., *High-performance anion-exchange chromatography with pulsed amperometric detection of linear and branched glucose oligosaccharides*. Carbohydr. Res., **1991**, 215(1), 179-92.
- [124] Koizumi, K., Fukuda, M., and Hizukuri, S., *Estimation of the distributions of chain length of amylopectins by high-performance liquid chromatography with pulsed amperometric detection*. J. Chromatogr., **1991**, 585(2), 233-8.
- [125] Heinrich, J. and Mischnick, P., *Rapid method for the determination of the substitution pattern of O-methylated 1,4-glucans by high-pH anion-exchange chromatography with pulsed amperometric detection*. J. Chromatogr. A, **1996**, 749(1+2), 41-45.
- [126] Björndal, H., Lindberg, B., and Svensson, S., *Gas-liquid chromatography of partially methylated alditols as their acetates*. Acta Chem. Scand., **1967**, 21(7), 1801-4.
- [127] Björndal, H., Lindberg, B., and Svensson, S., *Mass spectrometry of partially methylated alditol acetates*. Carbohydr. Res., **1967**, 5(4), 433-40.
- [128] Ciucanu, I. and Kerek, F., *A simple and rapid method for the permethylation of carbohydrates*. Carbohydr. Res., **1984**, 131(2), 209-17.

- [129] **Hakomori, S.**, *A Rapid Permethylation of Glycolipid, and Polysaccharide Catalyzed by Methylsulfinyl Carbanion in Dimethyl Sulfoxide*. J. Biochem., **1964**, 55, 205-8.
- [130] **Larm, O., Larsson, K.K., and Theander, O.**, *Gas chromatographic analysis of the substitution pattern of hydroxyethyl starch*. Starch/Staerke, **1981**, 33(7), 240-244.
- [131] **Ukai, S., Honda, A., Nagai, K., and Kiho, T.**, *Gas-liquid chromatographic analysis of carboxymethyl cellulose and carboxymethyl starch*. J. Chromatogr., **1990**, 513, 338-343.
- [132] **Taylor, R.L. and Conrad, H.E.**, *Stoichiometric depolymerization of polyuronides and glycosaminoglucans to monosaccharides following reduction to their carbodiimide-activated carboxyl groups*. Biochemistry, **1972**, 11(8), 1383-8.
- [133] **Taylor, R.L., Shively, J.E., and Conrad, H.E.**, *Stoichiometric reduction of uronic acid carboxyl groups in polysaccharides*. Methods in Carbohydrate Chemistry, **1976**, 6, 149-151.
- [134] **Niemelä, K. and Sjöström, E.**, *Identification of the products of hydrolysis of carboxymethylcellulose*. Carbohydr. Res., **1988**, 180, 43-52.
- [135] **Rolf, D. and Gray, G.R.**, *Reductive cleavage of glycosides*. J. Am. Chem. Soc., **1982**, 104(12), 3539-3541.
- [136] **Ackman, R.G.**, *Fundamental groups in the response of flame ionization detectors to oxygenated aliphatic hydrocarbons*. J. Gas Chromatogr., **1964**, 2, 173-179.
- [137] **Addison, R.F. and Ackman, R.G.**, *Flame ionization detector molar responses for methyl esters of some polyfunctional metabolic acids*. J. Gas Chromatogr., **1968**, 6, 135-138.
- [138] **Mares, P., Skorepa, J., and Friedrich, M.**, *Computerized quantitative analysis of methyl and ethyl esters of long chain fatty acids by gas-liquid chromatography using relative molar response*. J. Chromatogr., **1969**, 42(4), 435-441.
- [139] **Sweet, D.P., Shapiro, R.H., and Albersheim, P.**, *Quantitative analysis by various GLC [gas-liquid chromatography] response-factor theories for partially methylated and partially ethylated alditol acetates*. Carbohydr. Res., **1975**, 40(2), 217-225.
- [140] **Blakeney, A.B. and Stone, B.A.**, *Methylation of carbohydrates with lithium methylsulphinyll carbanion*. Carbohydr. Res., **1985**, 140, 319-324.
- [141] **D'Ambra, A.J., Rice, M.J., Zeller, S.G., Gruber, P.R., and Gray, G.R.**, *Analysis of positions of substitution of O-methyl or O-ethyl groups in partially methylated or ethylated cellulose by the reductive-cleavage method*. Carbohydr. Res., **1988**, 177, 111-16.
- [142] **Barber, M., Bordoli, R.D., Elliot, G.J., Sdgwick, R.D., and Tyler, A.N.**, *Fast Atom Bombardment of Solids as an Ion Source in Mass Spectrometry*. Nature, **1981**, 293, 270-5.
- [143] **Taylor, G.I.**, *Disintegration of Water Drops in an Electric Field*. Proc. R. Soc. London, Sect. A, **1964**, 280, 383-397.
- [144] **Wilm, M. and Mann, M.**, *Electrospray and Taylor-Cone Theory, Dole's Beam of Makromolecules at Last?* Int. J. Mass Spectrom. Ion Processes, **1994**, 136, 167-180.
- [145] **Rayleigh, L.**, *On the Equilibrium of Liquid Conducting Masses Charged with Electricity*. Phil. Mag. J. Sci., **1882**, 14, 184-186.
- [146] **Gomez, A. and Tang, K.**, *Charge and Fission of Droplets in Electrostatic Sprays*. Phys. Fluids, **1994**, 6, 404-414.
- [147] **Duft, D., Achtzehn, T., Müller, R., Huber, B.A., and Leisner, T.**, *Coulomb Fission. Rayleigh Jets from Levitated Microdroplets*. Nature, **2003**, 421, 128.
- [148] **Dole, M., Mack, L.L., Hines, R.L., Mobley, R.C., Ferguson, L.D., and Alice, M.B.**, *Molecular beams of macroions*. J. Chem. Phys., **1968**, 49(5), 2240-9.
- [149] **Iribarne, J.V. and Thomson, B.A.**, *On the evaporation of small ions from charged droplets*. J. Chem. Phys., **1976**, 64(6), 2287-94.
- [150] **Fenn, J.B.**, *Ion Formation From Charged Droplets: Roles of Geometry, Energy, and Time*. J. Am. Soc. Mass Spectr., **1993**, 4, 524-535.
- [151] **Tanaka, K., Waki, H., Ido, Y., Akita, S., Yoshida, Y., and Yohida, T.**, *Protein and polymer analyses up to m/z 100,000 by laser ionization time-of-flight mass spectrometry*. Rapid Commun. Mass Spectrom., **1988**, 2(8), 151-3.

- [152] Karas, M. and Hillenkamp, F., *Laser desorption ionization of proteins with molecular masses exceeding 10,000 daltons*. Anal. Chem., **1988**, 60(20), 2299-301.
- [153] Karas, M. and Krueger, R., *Ion formation in MALDI: The cluster ionization mechanism*. Chem. Rev., **2003**, 103(2), 427-439.
- [154] Paul, W. and Steinwedel, H.A., *A new Mass Spectrometer without Magnetic Field*. Z. Naturforsch., **1953**, 8A, 448-450.
- [155] Mamyrin, B.A., Karataev, V.I., Shmikk, D.V., and Zagulin, V.A., *Mass reflectron. New nonmagnetic time-of-flight high-resolution mass spectrometer*. Zh. Eksp. Teor. Fiz., **1973**, 64(1), 82-9.
- [156] Pasch, H. and Schrepp, W., *MALDI-TOF Mass Spectrometry of Synthetic Polymers*. Springer, Berlin, Heidelberg, New York, Hongkong, London, Milano, Paris, Tokio, **2003**.
- [157] Bahr, U., Pfenniger, Karas, M., and Stahl, B., *High-Sensitive Analysis of Neutral Underivatized Oligosaccharides by Nanoelectrospray Mass Spectrometry*. Anal. Chem., **1997**, 69, 4530-4535.
- [158] Reinhold, V.N., Reinhold, B.B., and Chan, S., *Carbohydrate Sequence Analysis by Electrospray Ionization-Mass Spectrometry*. Methods Enzymol., **1996**, 271, 377-402.
- [159] Reinhold, V.N., Reinhold, B.B., and Costello, C.E., *Carbohydrate Molecular Weight Profiling, Sequence, Linkage, and Branching Data: ES-MS and CID*. Anal. Chem., **1995**, 67, 1772-1784.
- [160] Harvey, D.J., *Electrospray mass spectrometry and fragmentation of N-linked carbohydrates derivatized at the reducing terminus*. J. Am. Soc. Mass Spectr., **2000**, 11(10), 900-15.
- [161] Stahl, B., Thurl, S., Zeng, J., Karas, M., Hillenkamp, F., Steup, M., and Sawatzki, G., *Oligosaccharides from human milk as revealed by matrix-assisted laser-desorption/ionization mass spectrometry*. Anal. Biochem., **1994**, 223, 218-226.
- [162] Stahl, B., Steup, M., Karas, M., and Hillenkamp, F., *Analysis of neutral oligosaccharides by by matrix-assisted laser desorption/ionization*. Anal. Chem., **1991**, 63, 1463-1466.
- [163] Harvey, D.J., *Matrix-assisted laser desorption/ionization mass spectrometry of carbohydrates*. Mass Spectrom. Rev., **1999**, 18(6), 349-450.
- [164] Harvey, D.J., *Structural determination of N-linked glycans by matrix-assisted laser desorption/ionization and electrospray ionization mass spectrometry*. Proteomics, **2005**, 5(7), 1774-1786.
- [165] Zaia, J., *Mass spectrometry of oligosaccharides*. Mass Spectrom. Rev., **2004**, 23(3), 161-227.
- [166] Domon, B. and Costello, C.E., *A systematic nomenclature for carbohydrate fragmentations in FAB-MS/MS spectra of glycoconjugates*. Glycoconjugate J., **1988**, 5(4), 397-409.
- [167] Naven, T.J.P. and Harvey, D.J., *Cationic Derivatization of Oligosaccharides with Girard's T Reagent for Improved performance in Matrix-assisted Laser Desorption/Ionization and Electrospray Mass Spectrometry*. Rapid Commun. Mass Spectrom., **1996**, 10, 829-834.
- [168] Gouw, J.W., Burgers, P.C., Trikoupi, M.A., and Terlouw, J.K., *Derivatization of small oligosaccharides prior to analysis by matrix-assisted laser desorption/ionization using glycidyltrimethylammonium chloride and Girard's reagent T*. Rapid Commun. Mass Spectrom., **2002**, 16(10), 905-912.
- [169] Harvey, D.J., *Fragmentation of Negative Ions from Carbohydrates: Part 1. Use of Nitrate and Other Anionic Adducts for the Production of Negative Ion Electrospray Spectra from N-linked Carbohydrates*. J. Am. Soc. Mass Spectr., **2005**, 16(5), 622-630.
- [170] Harvey, D.J., *Fragmentation of Negative Ions from Carbohydrates: Part 2. Fragmentation of High-Mannose N-Linked Glycans*. J. Am. Soc. Mass Spectr., **2005**, 16(5), 631-646.

- [171] Harvey, D.J., *Fragmentation of Negative Ions from Carbohydrates: Part 3. Fragmentation of Hybrid and Complex N-Linked Glycans*. J. Am. Soc. Mass Spectr., **2005**, 16(5), 647-659.
- [172] Tüting, W., Wegemann, K., and Mischnick, P., *Enzymatic degradation and electrospray tandem mass spectrometry as tools for determining the structure of cationic starches prepared by wet and dry methods*. Carbohydr. Res., **2004**, 339(3), 637-648.
- [173] Tüting, W., Adden, R., and Mischnick, P., *Fragmentation pattern of regioselectively O-methylated malto-oligosaccharides in electrospray ionization-mass spectrometry/collision induced dissociation*. Int. J. Mass Spectrom., **2004**, 232(2), 107-115.
- [174] Adden, R. and Mischnick, P., *A novel method for the analysis of the substitution pattern of O-methyl-a- and b-1,4-glucans by means of electrospray ionisation-mass spectrometry/collision induced dissociation*. Int. J. Mass Spectrom., **2005**, 242(1), 63-73.
- [175] Momcilovic, D., Wittgren, B., Wahlund, K.-G., Karlsson, J., and Brinkmalm, G., *Sample preparation effects in matrix-assisted laser desorption/ionisation time-of-flight mass spectrometry of partially depolymerised methyl cellulose*. Rapid Commun. Mass Spectrom., **2003**, 17(11), 1116-1124.
- [176] Momcilovic, D., Wittgren, B., Wahlund, K.-G., Karlsson, J., Brinkmalm, G., *Sample preparation effects in matrix-assisted laser desorption/ionisation time-of-flight mass spectrometry of partially depolymerised carboxymethyl cellulose*. Rapid Commun. Mass Spectrom., **2003**, 17(11), 1107-1115.
- [177] Momcilovic, D., Schagerloef, H., Wittgren, B., Wahlund, K.-G., and Brinkmalm, G., *Improved Chemical Analysis of Cellulose Ethers Using Dialkylamine Derivatization and Mass Spectrometry*. Biomacromolecules, **2005**, 6(5), 2793-2799.
- [178] Momcilovic, D., Schagerloef, H., Roeme, D., Joerten-Karlsson, M., Karlsson, K.-E., Wittgren, B., Tjerneld, F., Wahlund, K.-G., and Brinkmalm, G., *Derivatization Using Dimethylamine for Tandem Mass Spectrometric Structure Analysis of Enzymatically and Acidically Depolymerized Methyl Cellulose*. Anal. Chem., **2005**, 77(9), 2948-2959.
- [179] Mischnick, P. and Hennig, C., *A New Model for the Substitution Patterns in the Polymer Chain of Polysaccharide Derivatives*. Biomacromolecules, **2001**, 2(1), 180-184.
- [180] Lazik, W., Heinze, T., Pfeiffer, K., Albrecht, G., and Mischnick, P., *Starch derivatives of a high degree of functionalization. VI. Multistep carboxymethylation*. J. Appl. Polym. Sci., **2002**, 86(3), 743-752.
- [181] Tüting, W., Albrecht, G., Volkert, B., and Mischnick, P., *Structure analysis of carboxymethyl starch by capillary electrophoresis and enzymic degradation*. Starch/Staerke, **2004**, 56(7), 315-321.
- [182] Heinze, T., Erler, U., Nehls, I., and Klemm, D., *Determination of the substituent pattern of heterogeneously and homogeneously synthesized carboxymethyl cellulose by using high-performance liquid chromatography*. Angew. Makromol. Chem., **1994**, 215, 93-106.
- [183] Saake, B., Horner, S., Puls, J., Heinze, T., and Koch, W., *A new approach in the analysis of the substituent distribution of carboxymethyl celluloses*. Cellulose, **2001**, 8(1), 59-67.
- [184] Nehls, I., Wagenknecht, W., Philipp, B., and Stscherbina, D., *Characterization of cellulose and cellulose derivatives in solution by high resolution carbon-13 NMR spectrometry*. Prog. Polym. Sci., **1994**, 19(1), 29-78.
- [185] Heinze, T., *Habilitationsschrift: Ionische Funktionspolymere aus Cellulose: Neue Synthesekonzepte, Strukturaufklärung und Eigenschaften*. **1997**, University of Jena.
- [186] Kasulke, U., Philipp, B., and Metzner, K., *Hydrolytic degradation of water-soluble cellulose derivatives under homogeneous reaction conditions. 3. Total hydrolysis of anionic cellulose ethers with sulfuric acid and trifluoroacetic acid*. Acta Polym., **1985**, 36(12), 662-5.

- [187] **Belitz, H.-D., Grosch, W., and Schieberle, P.**, *Lehrbuch der Lebensmittelchemie*. Springer, Berlin, Heidelberg, New York, **2001**.
- [188] **Horner, S.**, *Thesis: Enzymunterstützte Charakterisierung von Carboxymethylcellulose*. **2000**, University of Hamburg.
- [189] **Jorgensen, A.D., Picel, K.C., and Stamoudis, V.C.**, *Prediction of gas chromatography flame ionization detector response factors from molecular structures*. *Anal. Chem.*, **1990**, 62(7), 683-689.
- [190] **Scanlon, J.T. and Willis, D.E.**, *Calculation of flame ionization detector relative response factors using the effective carbon number concept*. *J. Chromatogr. Sci.*, **1985**, 23(8), 333-340.
- [191] **Reuben, J.C., Herbert T.**, *Analysis of the carbon-13 NMR spectrum of hydrolyzed O-(carboxymethyl)cellulose: monomer composition and substitution patterns*. *Carbohydr. Res.*, **1983**, 115(1), 1-13.
- [192] **Connors, K.A. and Pandit, N.K.**, *N-Methylimidazole as a catalyst for analytical acetylations of hydroxy compounds*. *Anal. Chem.*, **1978**, 50(11), 1542-5.
- [193] **Heinze, T., Liebert, T., and Koschella, A.**, *Esterification of Polysaccharides*. Springer Verlag, **2006**.
- [194] **Sircar, A.K., Stanonis, D.J., and Conrad, C.M.**, *Cellulose Propionylpropionate as a Side Product in the reaction of Cotton Cellulose with Propionyl Chloride*. *J. Appl. Polym. Sci.*, **1967**, 11, 1683-1692.
- [195] **Malm, C.J., Mench, J.W., Kendall, D.L., and Hiatt, G.D.**, *Properties*. *J. Ind. Eng. Chem.*, **1951**, 43, 688-91.
- [196] **Leonard, J., Lygo, B., and Procter, G.**, *Praxis der Organischen Chemie - Ein Handbuch*. Wiley-VCH, Weinheim, Germany, **1996**.
- [197] **Morooka, T., Norimoto, M., Yamada, T., and Shiraishi, N.**, *Dielectric properties of cellulose acylates*. *J. Appl. Polym. Sci.*, **1984**, 26(11), 3981-3990.
- [198] **Schnabelrauch, M., Heinze, T., Klemm, D., Nehls, I., and Kötz, J.**, *Investigations on synthesis and characterization of carboxy-groups containing cellulose sulfates*. *Polym. Bull.*, **1991**, 27, 147-153.
- [199] **Heinze, T. and Heinze, U.**, *The first approach to non-aqueous solutions of carboxymethylcellulose*. *Macromol. Rapid Commun.*, **1997**, 18, 1033-1040.
- [200] **Gohdes, M.**, *Thesis: Substituentenverteilung von Cellulosesulfaten in der Monomereinheit und entlang der Polymerkette*. **1997**, University of Hamburg.
- [201] **Enebro, J. and Karlsson, S.**, *Improved matrix-assisted laser desorption/ionisation time-of-flight mass spectrometry of carboxymethyl cellulose*. *Rapid Commun. Mass Spectrom.*, **2006**, 20(24), 3693-3698.
- [202] **Ulbricht, A.**, *Diploma work: Analytik von O-Carboxymethylglucosen und -cellooligomeren mittels Kapillarelektrophorese nach reduktiver Aminierung*. **2007**, University of Braunschweig.
- [203] **Rowland, S.P. and Howley, P.S.**, *Influence of the location of substituents in substituted celluloses on solution hydrolysis of the D-glucosidic linkages*. *Carbohydr. Res.*, **1987**, 165, 69-76.
- [204] **Capon, B.**, *Mechanism in Carbohydrate Chemistry*. *Chem. Rev.*, **1969**, 69, 407-498.
- [205] **De, K.K. and Timell, T.E.**, *Acid hydrolysis of glycosides. III. Hydrolysis of O-methylated glucosides and disaccharides*. *Carbohydr. Res.*, **1967**, 4(1), 72-77.
- [206] **Edward, J.T.**, *Stability of glycosides to acid hydrolysis*. *Chem. Ind. (London)*, **1955**, 1102-1104.
- [207] **Höök, J.E. and Lindberg, B.**, *Acid hydrolysis of the monoisopropyl ethers of methyl alpha- and beta-D-glucopyranoside*. *Acta Chem. Scand. (1947-1973)*, **1966**, 20(9), 2363-2369.
- [208] **Saunders, M.D. and Timell, T.E.**, *The acid hydrolysis of glycosides. VI. Effect of substitution at C-3 and C-5*. *Carbohydr. Res.*, **1968**, 6(1), 12-17.
- [209] **Jensen, H.H. and Bols, M.**, *Steric Effects Are Not the Cause of the Rate Difference in Hydrolysis of Stereoisomeric Glycoides*. *Org. Lett.*, **2003**, 5(19), 3419-3421.

- [210] Orth, T., *Diploma work: DS- und DP-abhängige Trennung von O-Carboxymethyloligosacchariden mittels Kapillarelektrophorese - Vergleich mit der massenspektrometrischen Analyse*. 2008, University of Braunschweig.

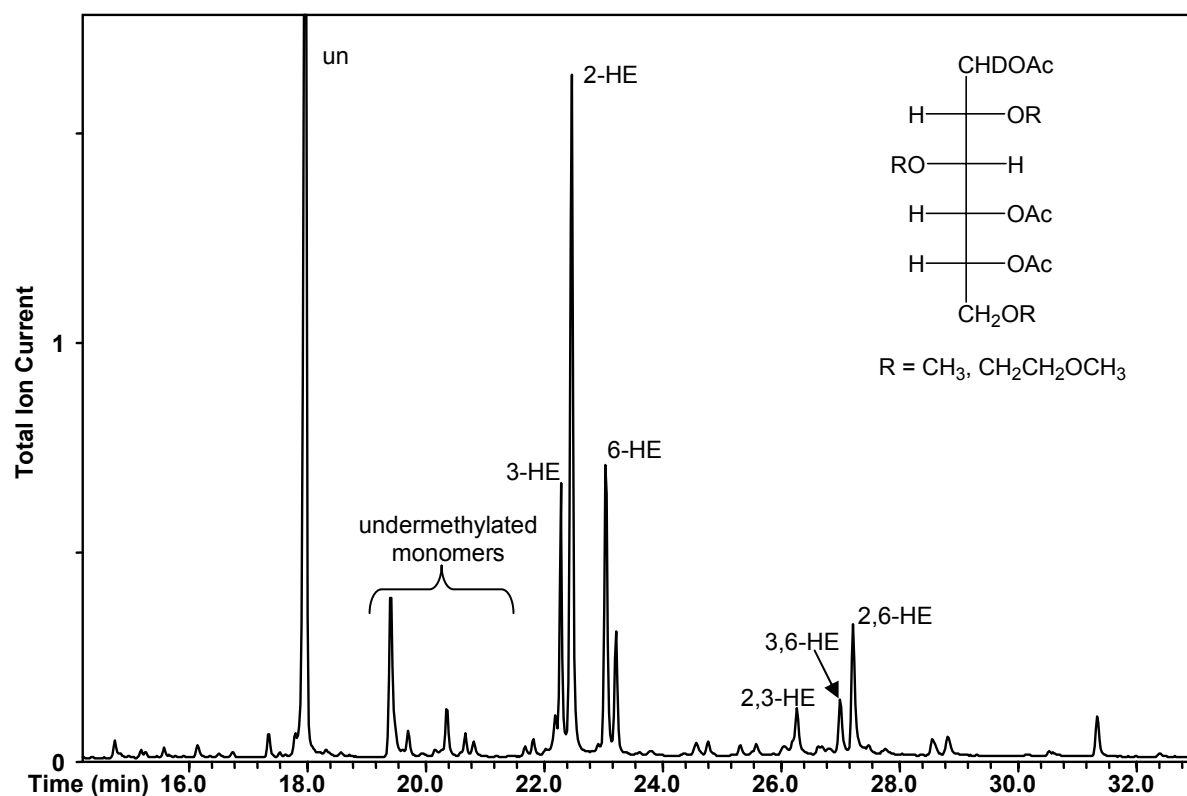
10 Appendix

10.1 GLC-MS spectra of alditol acetates obtained from CMC 1 after reduction to HEC (total ion current chromatogram)

Temperature profile for settings described in 8.2.5 and 8.2.6:

Start at 60 °C for 1 min followed by heating up to 130 °C at 20 °C/min.

Subsequently heated up at 4 °C/min to 290 °C and keeping isothermic for 30 min.

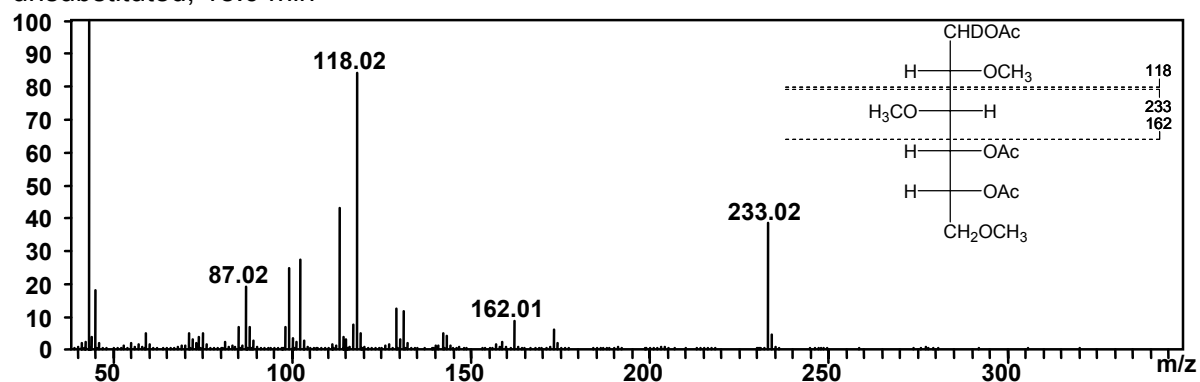


Assignment	Pattern	Retention time [min]	ECR	Response factor
un	2,3,6-Me	18.0	745	1.000
3-HE	2,6-Me-3-HEMe	22.3	845	0.882
2-HE	3,6-Me-2-HEMe	22.5	845	0.882
6-HE	2,3-Me-6-HEMe	23.1	845	0.882
2,3-HE	6-Me-2,3-HEMe	26.3	945	0.788
3,6-HE	2-Me-3,6-HEMe	27.0	945	0.788
2,6-HE	3-Me-2,6-HEMe	27.2	945	0.788
2,3,6-HE	236-HEMe	-	1045	0.713

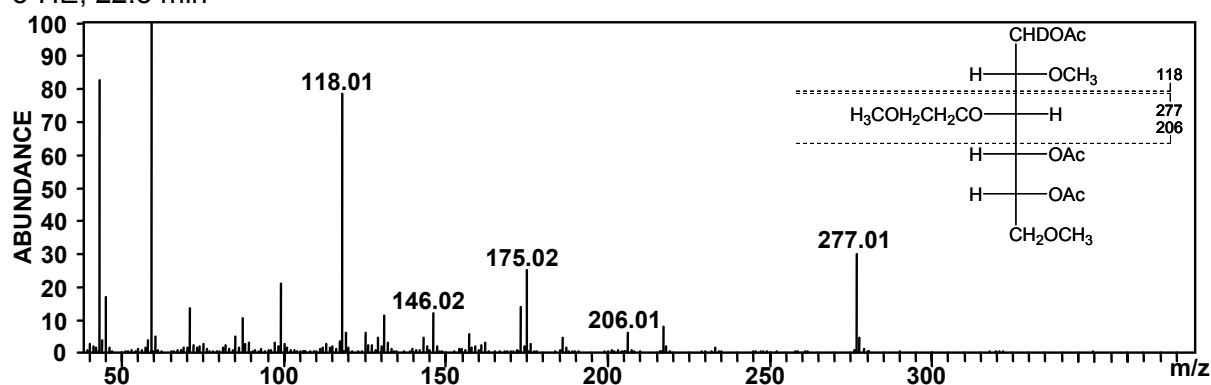
Increments used for calculation of ECR:

CH _n OCH ₃	100	CHOAc	145
CH ₂ OAc	155	O-CH ₂ -CH ₂ -	100

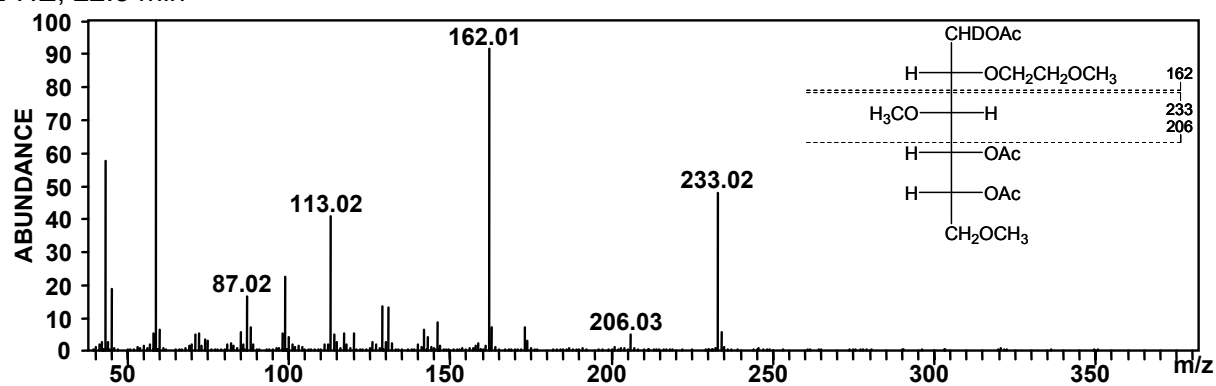
unsubstituted, 18.0 min



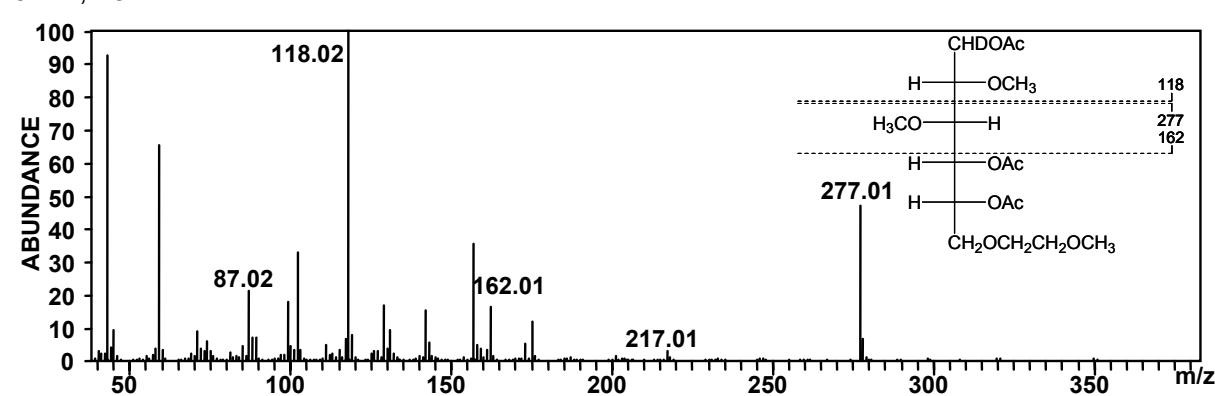
3-HE, 22.3 min



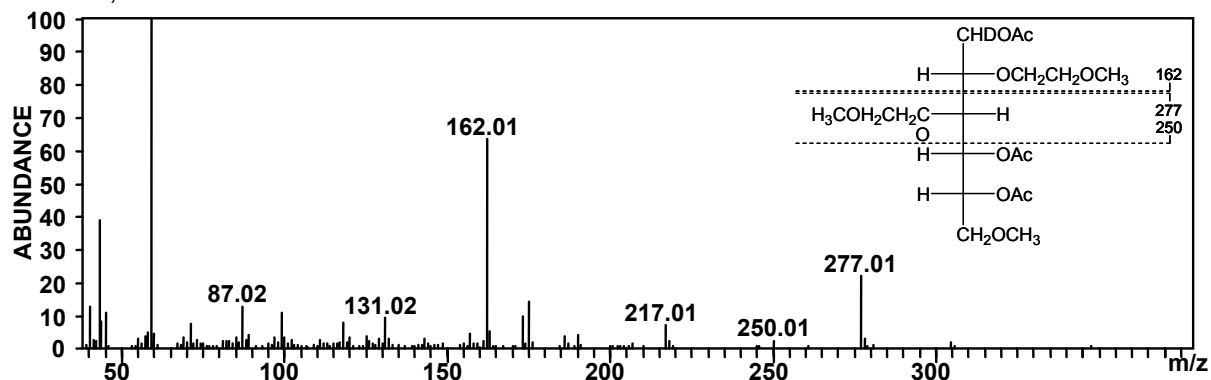
2-HE, 22.5 min



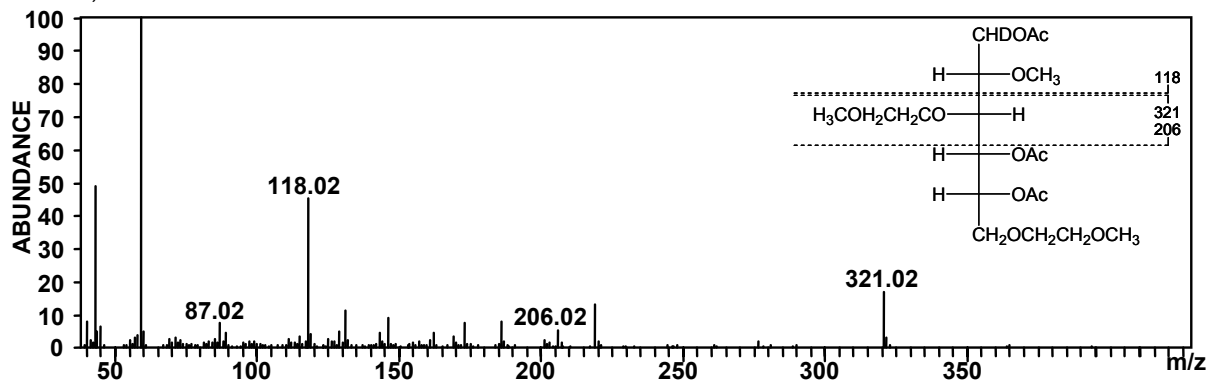
6-HE, 23.1 min



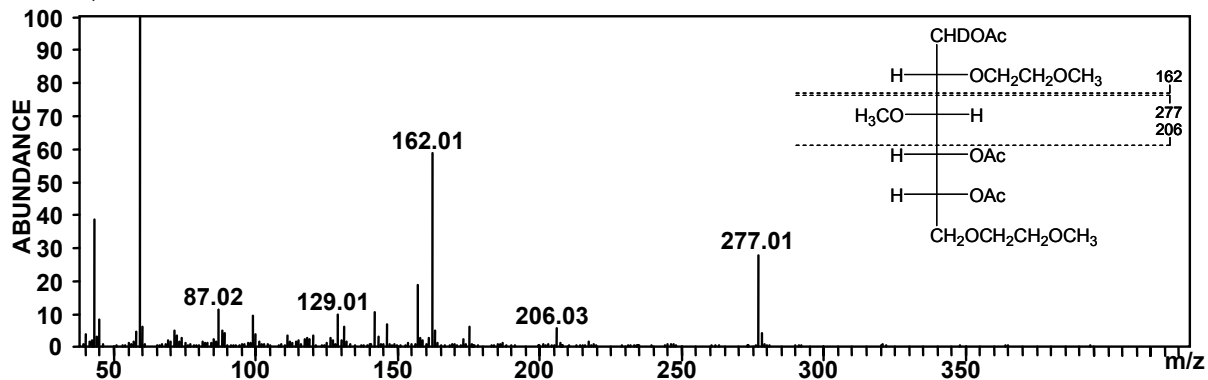
23-HE, 26.3 min



36-HE, 27.0 min



26-HE, 27.2 min



CMC 2 DP 2 n(CM)	Methanolysis 1: 10		Acetylation 1: 10	Propionyl. 1: 10	Butyrylation 1:10
	calc. CE	exp.	exp.	exp.	exp.
0	12.96	1.26	0.76	0.00	0.61
1	31.89	9.95	13.33	7.50	7.66
2	32.52	30.63	33.04	27.11	26.06
3	17.16	31.96	34.10	34.08	34.92
4	4.80	17.89	15.70	23.10	22.12
5	0.64	6.52	2.69	8.21	6.96
6	0.03	1.80	0.38	0.00	1.67
DS	0.85	1.41	1.30	1.49	1.49

DP3 n(CM)	Methanolysis 1: 10		Acetylation 1: 10	Propionyl. 1: 10	Butyrylation 1:10
	calc. CE	exp.	exp.	exp.	exp.
0	4.67	0.00	0.00	0.00	0.43
1	17.22	0.00	5.97	0.00	1.07
2	28.15	7.61	14.09	7.59	8.05
3	26.53	21.08	26.69	20.80	18.73
4	15.73	28.56	21.24	30.48	29.40
5	6.01	24.25	15.99	26.26	22.01
6	1.46	14.85	14.99	11.52	14.25
7	0.21	3.65	1.03	3.34	4.51
8	0.02	0.00	0.00	0.00	1.56
9	0.00	0.00	0.00	0.00	0.00
DS	0.85	1.43	1.25	1.41	1.44

CMC 3 DP 2 n(CM)	Methanolysis 1: 10		Acetylation 1: 10	Propionyl. 1: 10	Butyrylation 1: 10
	calc. CE	exp.	exp.	exp.	exp.
0	9.78	0.00	1.69	0.67	0.00
1	28.86	7.91	10.73	4.83	6.38
2	33.93	28.94	26.68	24.38	19.57
3	20.13	29.75	35.45	38.52	30.39
4	6.28	23.21	20.62	25.97	24.77
5	0.96	7.89	4.01	5.63	12.87
6	0.06	2.30	0.82	0.00	6.02
DS	0.94	1.51	1.39	1.51	1.68

DP 3 n(CM)	Methanolysis 1: 10		Acetylation 1: 10	Propionyl. 1: 10	Butyrylation 1: 10
	calc. CE	exp.	exp.	exp.	exp.
0	3.06	0.00	0.00	0.00	0.00
1	13.54	0.00	1.53	3.71	0.00
2	25.90	7.69	7.27	6.02	0.00
3	28.01	14.68	24.48	21.80	0.00
4	18.79	25.18	32.09	21.64	0.00
5	8.07	26.45	23.93	27.67	0.00
6	2.21	16.10	8.19	14.34	0.00
7	0.37	8.41	2.51	4.82	0.00
8	0.03	1.49	0.00	0.00	0.00
9	0.00	0.00	0.00	0.00	0.00
DS	0.94	1.53	1.35	1.42	0.00

CMC 4 DP 2 n(CM)	Methanolysis		Acetylation		Propionyl.		Butyrylation		Methoxyvac.		Methoxyvac..		Methoxyvac.		Methoxyvac.	
	calc.	CE	exp.	exp.	1: 10	exp.	1: 10	exp.	A 1: 6	exp.	A 1: 10	exp.	A 1: 100	exp.	A 1: 1000	exp.
0	9.34		0.00	0.92	0.00	0.00	1.18	4.13	4.11	2.70	2.62	3.12				
1	27.98		3.99	0.51	7.29	10.45	14.86	14.87	14.87	14.84	15.71	18.02				
2	33.69		22.87	22.80	25.08	27.51	30.68	33.91	33.91	36.74	31.81	33.63				
3	20.81		33.23	37.31	36.34	31.64	31.44	28.04	28.04	28.63	31.96	31.30				
4	6.93		26.15	27.78	24.68	22.09	13.81	19.06	19.06	14.44	15.27	11.86				
5	1.18		12.20	9.06	6.61	5.50	5.09	0.00	0.00	2.65	2.63	2.06				
6	0.08		1.56	1.63	0.00	1.63	0.00	0.00	0.00	0.00	0.00	0.00				
DS	0.96		1.62	1.62	1.49	1.43	1.26	1.22	1.23	1.25	1.18					

DP 3 n(CM)	Methanolysis		Acetylation		Propionyl.		Butyrylation		Methoxyvac.		Methoxyvac..		Methoxyvac.		Methoxyvac.	
	calc.	CE	exp.	exp.	1: 10	exp.	1: 10	exp.	A 1: 6	exp.	A 1: 10	exp.	A 1: 100	exp.	A 1: 1000	exp.
0	2.85		0.00	0.00	0.00	0.00	2.13	4.13	4.11	2.70	2.62	3.12				
1	12.82		0.00	0.00	0.00	0.00	5.59	14.86	14.87	14.84	15.71	18.02				
2	25.05		4.67	4.79	5.32	9.83	30.68	33.91	33.91	36.74	31.81	33.63				
3	27.88		9.25	20.16	20.29	18.31	31.44	28.04	28.04	28.63	31.96	31.30				
4	19.45		22.27	26.91	29.77	19.61	31.44	28.04	28.04	28.63	31.96	31.30				
5	8.82		28.50	25.62	28.13	19.92	13.81	19.06	19.06	14.44	15.27	11.86				
6	2.59		22.86	17.62	16.49	12.41	5.09	0.00	0.00	2.65	2.63	2.06				
7	0.48		12.44	4.91	0.00	7.45	0.00	0.00	0.00	0.00	0.00	0.00				
8	0.05		0.00	0.00	0.00	3.43	0.00	0.00	0.00	0.00	0.00	0.00				
9	0.00		0.00	0.00	0.00	1.32	0.00	0.00	0.00	0.00	0.00	0.00				
DS	0.96		1.64	1.49	1.43	1.41	1.26	1.22	1.23	1.25	1.18					

10.2.2 Results of MALDI-TOF-MS analysis of CMC 1-4 after methanolysis and acylation (8.3.7 and 8.3.8)

Results compared with the theoretical monomer distribution in Mol% (calculated by Bernoulli statistics based on the monomer analysis by CE-UV, calc.CE).

CMC 1 DP 2 n(CM)	calc. CE	Methanolysis exp.	Acetylation 1: 6 exp.	Propionyl. 1: 6 exp.	Butyrylation 1: 6 exp.
0	12.15		3.29	2.10	0.00
1	30.86		15.61	21.34	12.25
2	32.51		31.46	41.33	31.32
3	18.04		21.10	25.30	33.62
4	5.52		16.85	7.27	17.22
5	0.87		9.22	1.68	4.40
6	0.06		2.48	0.98	1.20
DS	0.88		1.35	1.12	1.37

DP 3 n(CM)	calc. CE	exp.	exp.	exp.	exp.
0	4.23	0.00	1.55	0.00	0.00
1	16.13	2.74	3.04	2.33	1.18
2	27.24	9.65	11.64	10.17	6.48
3	26.68	17.68	23.66	29.09	16.24
4	16.66	29.49	26.84	33.26	22.84
5	6.86	22.19	21.09	17.79	28.88
6	1.85	14.46	9.72	6.15	17.63
7	0.32	3.80	2.46	1.20	5.41
8	0.03	0.00	0.00	0.00	1.33
9	0.00	0.00	0.00	0.00	0.00
DS	0.88	1.39	1.29	1.26	1.51

DP 4 n(CM)	calc. CE	exp.	exp.	exp.	exp.
0	1.48	0.00	0.00	2.04	0.00
1	7.50	0.00	0.89	0.00	0.00
2	17.42	0.00	2.75	0.00	0.00
3	24.44	5.02	8.84	7.53	4.16
4	23.04	15.28	17.65	13.89	12.33
5	15.35	23.27	25.33	24.65	16.70
6	7.39	24.98	20.62	27.28	24.65
7	2.59	15.56	14.96	14.82	18.49
8	0.66	11.99	6.23	7.41	13.73
9	0.12	3.90	1.95	2.38	9.95
10	0.01	0.00	0.79	0.00	0.00
11	0.00	0.00	0.00	0.00	0.00
12	0.00	0.00	0.00	0.00	0.00
DS	0.88	1.46	1.33	1.37	1.55

DP 5 n(CM)	calc. CE	exp.	exp.	exp.
0	0.51	0.00	0.00	2.98
1	3.27	0.00	0.00	0.00
2	9.66	0.00	2.21	0.00
3	17.65	0.00	4.45	0.00
4	22.25	8.40	9.74	10.70
5	20.49	14.58	19.03	12.76
6	14.21	17.81	21.96	18.21
7	7.56	13.14	16.25	19.41
8	3.11	18.68	15.70	21.36
9	0.99	15.51	6.43	8.10
10	0.24	11.87	4.23	6.49
11	0.04	0.00	0.00	0.00
12	0.01	0.00	0.00	0.00
13	0.00	0.00	0.00	0.00
14	0.00	0.00	0.00	0.00
15	0.00	0.00	0.00	0.00
DS	0.88	1.43	1.25	1.32

CMC 2 DP 2 n(CM)	Methanolysis		Acetylation 1: 6	Propionyl. 1: 6	Butyrylation 1: 6
	calc. CE		exp.	exp.	exp.
0	12.96		0.00	3.07	0.00
1	31.89		0.00	26.68	12.10
2	32.52		38.87	38.26	31.00
3	17.16		39.86	22.86	35.87
4	4.80		21.27	8.14	15.84
5	0.64		0.00	0.99	4.26
6	0.03		0.00	0.00	0.94
DS	0.85		1.41	1.05	1.36

DP 3 n(CM)	calc. CE	exp.	exp.	exp.	exp.
0	4.67	0.00	0.00	0.00	0.00
1	17.22	0.00	0.00	1.71	0.00
2	28.15	9.51	7.81	12.85	10.02
3	26.53	24.96	28.66	27.31	20.01
4	15.73	32.81	35.28	31.49	27.29
5	6.01	21.37	22.00	18.34	24.21
6	1.46	11.35	6.26	6.35	14.05
7	0.21	0.00	0.00	1.95	4.41
8	0.02	0.00	0.00	0.00	0.00
9	0.00	0.00	0.00	0.00	0.00
DS	0.85	1.33	1.30	1.26	1.42

DP 4 n(CM)	calc. CE	exp.	exp.	exp.
0	1.68	0.00	0.00	0.00
1	8.27	0.00	0.00	0.00
2	18.60	0.00	3.02	0.00
3	25.19	12.85	6.61	9.78
4	22.76	14.99	14.85	19.94
5	14.39	16.77	25.37	23.16
6	6.48	19.82	23.67	22.60
7	2.08	21.92	17.82	15.95
8	0.47	7.91	7.10	8.56
9	0.07	5.74	1.57	0.00
10	0.01	0.00	0.00	0.00
11	0.00	0.00	0.00	0.00
12	0.00	0.00	0.00	0.00
DS	8.85	1.42	1.37	1.35

DP 5 n(CM)	calc. CE	exp.	exp.	exp.
0	0.61	0.00	0.00	0.00
1	3.72	0.00	0.00	0.00
2	10.66	2.21	0.00	0.00
3	18.82	4.45	0.00	0.00
4	22.83	9.74	0.00	0.00
5	20.11	19.03	16.03	23.55
6	13.23	21.96	25.47	28.51
7	6.60	16.25	24.62	24.54
8	2.51	15.70	20.61	14.85
9	0.72	6.43	13.26	8.55
10	0.16	4.23	0.00	0.00
11	0.02	0.00	0.00	0.00
12	0.00	0.00	0.00	0.00
13	0.00	0.00	0.00	0.00
14	0.00	0.00	0.00	0.00
15	0.00	0.00	0.00	0.00
DS	0.85	1.25	1.38	1.64

CMC 3 DP 2 n(CM)	Methanolysis		Acetylation 1: 6	Propionyl. 1: 6	Butyrylation 1: 6
	calc. CE		exp.	exp.	exp.
0	9.78		4.37	2.81	0.70
1	28.86		7.47	24.36	9.96
2	33.93		26.34	38.26	30.56
3	20.13		32.79	25.62	35.44
4	6.28		19.62	6.99	17.64
5	0.96		7.07	1.96	5.09
6	0.06		2.33	0.00	0.61
DS	0.94		1.43	1.08	1.39

DP 3 n(CM)	calc. CE	exp.	exp.	exp.	exp.
0	3.06	0.00	0.00	0.00	0.00
1	13.54	0.00	1.55	1.79	0.00
2	25.90	5.56	8.16	11.13	5.52
3	28.01	15.63	20.75	29.09	17.77
4	18.79	24.17	26.99	29.58	27.08
5	8.07	27.98	23.95	20.53	28.07
6	2.21	19.82	13.30	6.41	15.32
7	0.37	6.84	4.10	1.47	5.37
8	0.03	0.00	0.76	0.00	0.88
9	0.00	0.00	0.43	0.00	0.00
DS	0.94	1.54	1.42	1.27	1.50

DP 4 n(CM)	calc. CE	exp.	exp.	exp.	exp.
0	0.96	0.00	0.00	0.00	0.00
1	5.65	0.00	0.54	0.00	0.00
2	14.97	0.00	2.64	2.07	0.00
3	23.52	4.41	6.13	5.91	4.60
4	24.36	9.11	15.53	12.22	12.17
5	17.47	13.77	24.78	22.36	20.07
6	8.88	17.86	22.75	25.01	23.10
7	3.21	24.48	16.46	18.29	19.12
8	0.82	17.38	7.45	8.99	12.94
9	0.14	10.44	2.57	3.46	6.23
10	0.02	2.55	1.16	1.70	1.77
11	0.00	0.00	0.00	0.00	0.00
12	0.00	0.00	0.00	0.00	0.00
DS	0.94	1.64	1.39	1.45	1.53

DP 5 n(CM)	calc. CE	exp.	exp.	exp.	exp.
0	0.30	0.00	0.00	0.00	0.00
1	2.21	0.00	0.00	0.00	0.00
2	7.48	0.00	0.00	0.00	0.00
3	15.43	0.00	3.35	0.00	0.00
4	21.63	3.12	6.03	0.00	0.00
5	21.81	4.34	15.45	9.27	0.00
6	16.32	10.34	19.70	9.95	23.33
7	9.21	18.24	20.24	29.57	23.44
8	3.95	22.95	15.85	21.79	33.73
9	1.28	21.21	10.86	29.43	19.51
10	0.31	13.85	6.60	0.00	0.00
11	0.06	5.94	1.92	0.00	0.00
12	0.01	0.00	0.00	0.00	0.00
13	0.00	0.00	0.00	0.00	0.00
14	0.00	0.00	0.00	0.00	0.00
15	0.00	0.00	0.00	0.00	0.00
DS	0.94	1.60	1.37	1.50	1.87

CMC 4 DP 2 n(CM)	Methanolysis calc. CE	Acetylation exp.	Propionyl. exp.	Butyrylation exp.	Methoxyac. entry A exp.	Methoxyac. entry B exp.	Methoxyac. B 1:100 exp.
0	9.34	0.00	2.07	0.79	8.61	5.92	7.41
1	27.98	9.56	22.88	12.89	22.86	18.26	29.32
2	33.69	29.87	37.50	33.91	30.04	33.14	33.19
3	20.81	34.37	27.99	38.61	24.41	27.24	20.52
4	6.93	22.40	8.47	11.41	11.02	11.42	7.93
5	1.18	3.81	1.10	2.39	3.05	4.02	1.63
6	0.08	0.00	0.00	0.00	0.00	0.00	0.00
DS	0.96	1.41	1.11	1.27	1.08	1.16	0.99

DP 3 n(CM)	calc. CE	exp.	exp.	exp.	exp.	exp.	exp.	exp.
0	2.85	0.00	0.00	0.00	0.00	0.00	7.70	0.00
1	12.82	0.64	1.62	1.76	0.96	11.00	9.88	9.00
2	25.05	4.15	10.00	10.44	6.02	22.06	14.31	21.44
3	27.88	11.89	21.39	26.02	15.21	25.12	20.13	34.04
4	19.45	23.71	30.63	34.90	26.07	21.11	19.02	22.76
5	8.82	25.38	22.64	18.63	28.29	12.49	11.92	12.76
6	2.59	18.64	10.20	6.92	16.32	8.21	8.46	0.00
7	0.48	11.60	3.52	1.34	5.68	0.00	8.58	0.00
8	0.05	3.45	0.00	0.00	1.45	0.00	0.00	0.00
9	0.00	0.54	0.00	0.00	0.00	0.00	0.00	0.00
DS	0.96	1.64	1.36	1.28	1.51	1.09	1.15	1.03

DP 4 n(CM)	calc. CE	exp.	exp.	exp.	exp.
0	0.87	0.00	0.00	1.28	0.00
1	5.23	0.00	0.40	0.86	0.00
2	14.12	0.00	2.28	1.76	1.35
3	22.74	2.54	8.39	6.85	4.59
4	24.29	10.23	16.93	16.40	10.16
5	18.12	15.11	22.34	22.78	17.61
6	9.67	20.21	23.59	21.54	22.63
7	3.72	23.03	15.56	16.59	20.09
8	1.02	18.41	7.39	8.41	14.91
9	0.20	6.89	2.72	2.81	8.66
10	0.02	3.57	0.41	0.72	0.00
11	0.00	0.00	0.00	0.00	0.00
12	0.00	0.00	0.00	0.00	0.00
DS	0.96	1.63	1.37	1.37	1.55

DP 5 n(CM)	calc. CE	exp.	exp.
0	0.27	0.00	9.13
1	2.00	0.00	7.24
2	6.89	0.68	2.96
3	14.53	3.19	0.00
4	20.92	7.61	3.01
5	21.79	14.03	13.27
6	16.95	18.62	14.97
7	10.03	21.10	17.65
8	4.54	16.85	14.67
9	1.58	9.91	11.78
10	0.42	5.05	5.31
11	0.08	1.88	0.00
12	0.01	1.09	0.00
13	0.00	0.00	0.00
14	0.00	0.00	0.00
15	0.00	0.00	0.00
DS	0.96	1.36	1.16

10.2.3 Results of ESI-IT- and MALDI-TOF-MS analysis of CMC 1-4 after TFA-hydrolysis and derivatized with Girard'sT reagent (8.3.4)

Results of hydrolyzates (ESI-IT) and derivatized hydrolyzates (ESI-IT + GT) are compared with the theoretical monomer distribution in Mol% (calculated by Bernoulli statistics based on the monomer analysis by CE-UV, calc.CE).

CMC 1 DP 2 n(CM)	calc. CE	ESI-IT entry A exp.	ESI-IT entry B exp.	ESI-IT+ GT entry B exp	MALDI-TOF entry A
0	12.15	21.35	19.43	42.27	
1	30.86	28.21	27.55	37.22	
2	32.51	29.14	31.40	20.51	
3	18.04	13.34	14.69	0.00	
4	5.52	5.17	5.13	0.00	
5	0.87	1.46	0.97	0.00	
6	0.06	1.32	0.84	0.00	
DS	0.88	0.81	0.82	0.39	

DP 3 n(CM)	calc. CE	exp.	exp.	exp.
0	4.23	7.69	14.16	9.46
1	16.13	14.75	22.59	16.18
2	27.24	24.30	29.90	26.72
3	26.68	26.20	22.15	22.71
4	16.66	16.55	8.12	13.40
5	6.86	7.05	1.93	8.02
6	1.85	2.85	1.15	3.51
7	0.32	0.61	0.00	0.00
8	0.03	0.00	0.00	0.00
9	0.00	0.00	0.00	0.00
DS	0.88	0.88	0.66	0.84

DP 4 n(CM)	calc. CE	exp.	exp.
0	1.48	5.74	10.24
1	7.50	13.89	14.13
2	17.42	22.79	14.39
3	24.44	23.94	30.14
4	23.04	16.72	13.51
5	15.35	10.66	10.75
6	7.39	4.38	4.63
7	2.59	0.79	2.21
8	0.66	1.09	0.00
9	0.12	0.00	0.00
10	0.01	0.00	0.00
11	0.00	0.00	0.00
12	0.00	0.00	0.00
DS	0.88	0.73	0.71

CMC 2 DP 2 n(CM)	calc. CE	ESI-IT entry A exp.	ESI-IT entry B exp.	ESI-GT entry B exp.	MALDI-TOF entry A
0	12.96	22.15	20.88	37.37	
1	31.89	31.93	28.30	38.85	
2	32.52	25.21	30.14	19.45	
3	17.16	12.22	14.56	4.34	
4	4.80	4.55	4.60	0.00	
5	0.64	2.09	0.72	0.00	
6	0.03	1.85	0.79	0.00	
DS	0.86	0.79	0.80	0.45	

DP 3 n(CM)	calc. CE	exp.	exp.	exp.	exp.
0	4.67	9.28	14.97	49.27	8.55
1	17.22	16.53	22.19	30.05	17.50
2	28.15	22.88	32.57	20.69	24.14
3	26.53	24.69	20.92	0.00	18.51
4	15.73	15.98	7.93	0.00	16.02
5	6.01	5.73	1.41	0.00	7.13
6	1.46	2.22	0.00	0.00	4.53
7	0.21	1.03	0.00	0.00	2.68
8	0.02	0.64	0.00	0.00	0.94
9	0.00	1.03	0.00	0.00	0.00
DS	0.86	0.88	0.63	0.24	0.91

DP 4 n(CM)	calc. CE	exp.	exp.
0	1.68	7.23	11.58
1	8.27	12.30	17.08
2	18.60	22.87	14.82
3	25.19	24.48	17.12
4	22.76	17.60	14.54
5	14.39	9.63	6.68
6	6.48	4.43	5.17
7	2.08	1.46	2.41
8	0.47	0.00	2.58
9	0.07	0.00	1.16
10	0.01	0.00	2.81
11	0.00	0.00	2.65
12	0.00	0.00	1.40
DS	0.86	0.72	0.86

CMC 3		ESI-IT	ESI-IT	ESI-IT GT	MALDI-TOF
DP 2		entry A	entry B	entry B	entry A
n(CM)	calc. CE	exp.	exp.	exp.	
0	9.78	15.85	17.86	37.04	
1	28.86	26.47	23.69	38.68	
2	33.93	29.11	30.69	18.79	
3	20.13	16.56	16.95	5.49	
4	6.28	7.36	6.21	0.00	
5	0.96	2.94	3.33	0.00	
6	0.06	1.72	1.27	0.00	
DS	0.94	0.94	0.93	0.46	

DP 3					
n(CM)	calc. CE	exp.	exp.	exp.	exp.
0	3.06	7.02	12.73	51.39	9.34
1	13.54	11.60	21.02	48.61	21.74
2	25.90	18.97	30.14	0.00	19.08
3	28.01	24.58	24.26	0.00	17.64
4	18.79	16.24	10.07	0.00	10.62
5	8.07	12.79	1.78	0.00	6.61
6	2.21	3.65	0.00	0.00	7.66
7	0.37	2.72	0.00	0.00	5.98
8	0.03	1.30	0.00	0.00	1.33
9	0.00	1.11	0.00	0.00	0.00
DS	0.94	1.05	0.68	0.16	0.96

DP 4			
n(CM)	calc. CE	exp.	exp.
0	0.96	2.80	7.10
1	5.65	9.51	11.96
2	14.97	16.67	19.07
3	23.52	21.14	17.40
4	24.36	20.13	14.05
5	17.47	13.09	7.66
6	8.88	7.61	5.52
7	3.21	3.69	5.07
8	0.82	1.41	4.69
9	0.14	0.89	1.71
10	0.02	1.03	3.57
11	0.00	1.20	0.00
12	0.00	0.82	2.19
DS	0.94	0.94	0.95

CMC 4 DP 2 n(CM)	calc. CE	ESI-IT entry A exp.	ESI-IT entry B exp.	MALDI entry A	ESI-IT GT entry B exp.
0	9.34	15.67	17.47		41.01
1	27.98	22.55	25.30		35.62
2	33.69	26.05	29.81		16.86
3	20.81	16.85	17.48		6.50
4	6.93	11.47	7.62		0.00
5	1.18	4.90	2.31		0.00
6	0.08	2.50	0.00		0.00
DS	0.96	1.05	0.90		0.44

DP 3 n(CM)	calc. CE	exp.	exp.	exp.
0	2.85	6.76	13.05	0.00
1	12.82	10.70	19.12	21.86
2	25.05	23.57	29.67	31.08
3	27.88	24.48	22.58	21.86
4	19.45	16.20	11.23	25.20
5	8.82	9.38	4.35	0.00
6	2.59	3.98	0.00	0.00
7	0.48	2.50	0.00	0.00
8	0.05	1.72	0.00	0.00
9	0.00	0.71	0.00	0.00
DS	0.96	1.01	0.71	0.83

DP 4 n(CM)	calc. CE	exp.
0	0.87	6.82
1	5.23	10.23
2	14.12	21.50
3	22.74	22.67
4	24.29	18.61
5	18.12	10.40
6	9.67	6.83
7	3.72	2.94
8	1.02	0.00
9	0.20	0.00
10	0.02	0.00
11	0.00	0.00
12	0.00	0.00
DS	0.96	0.77

10.3 Cellooligomerstandards for LC-ELSD

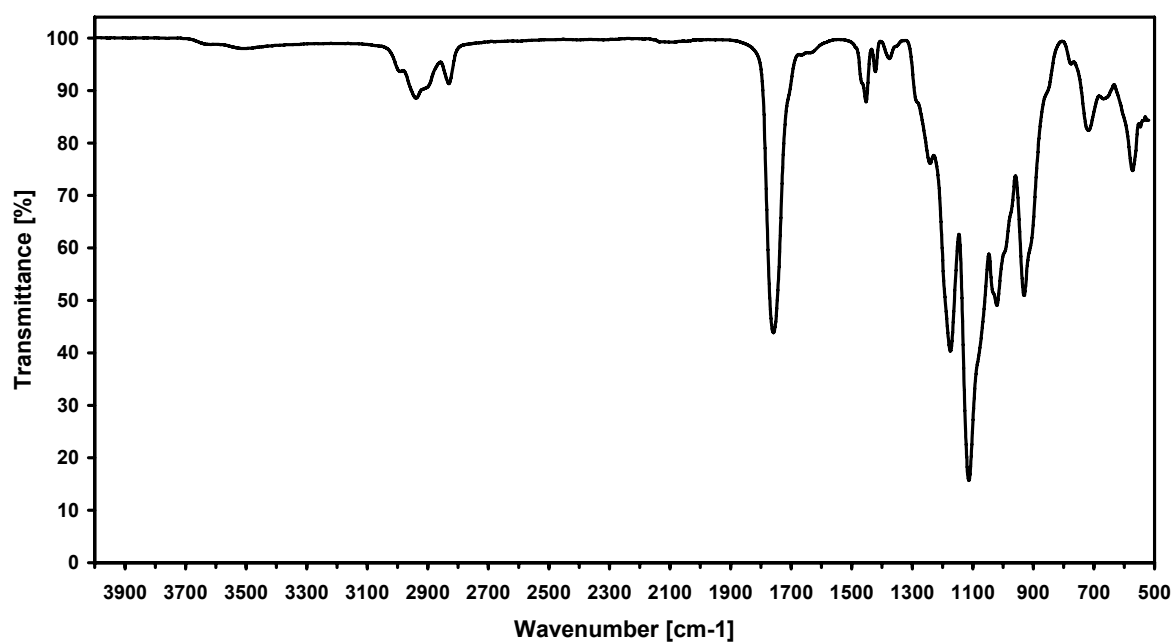


Fig. 10-1 ATR-IR spectrum of methoxyacetylated glucose

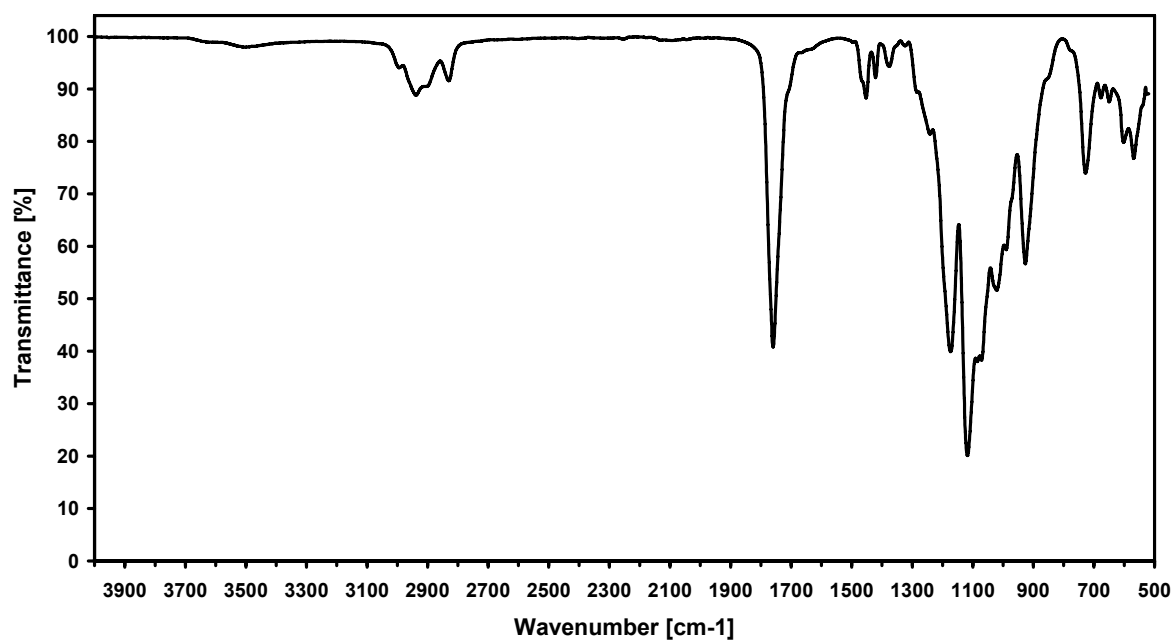


Fig. 10-2 ATR-IR spectrum of methoxyacetylated cellobiose

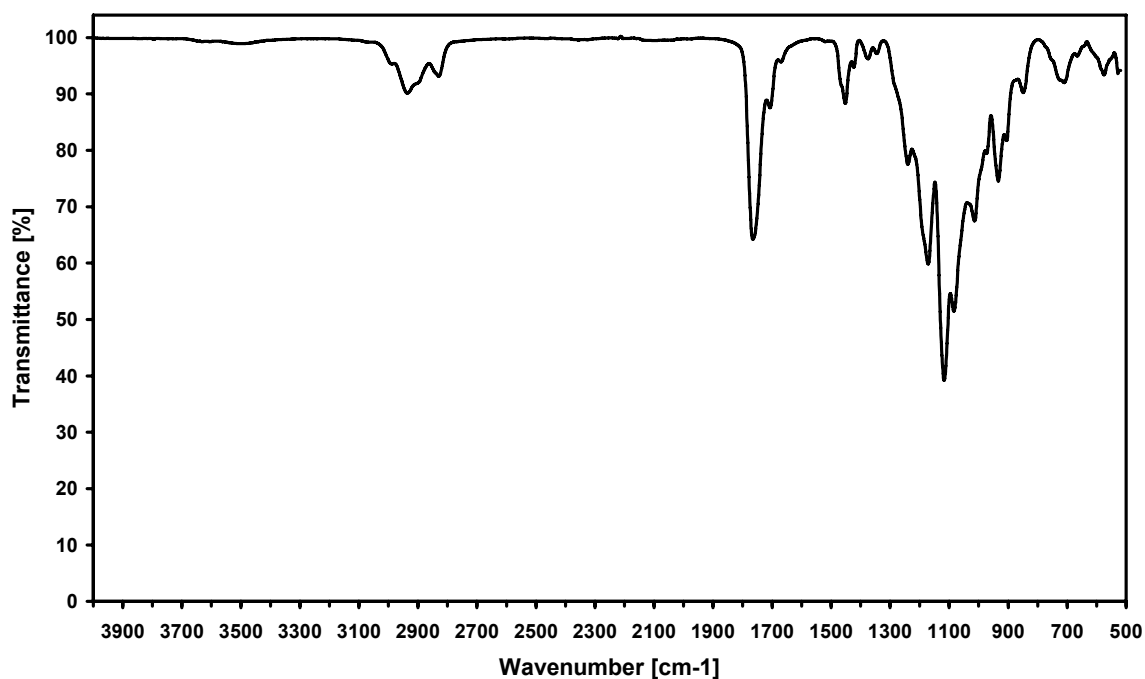


Fig. 10-3 ATR-IR spectrum of methoxyacetylated cellotriose

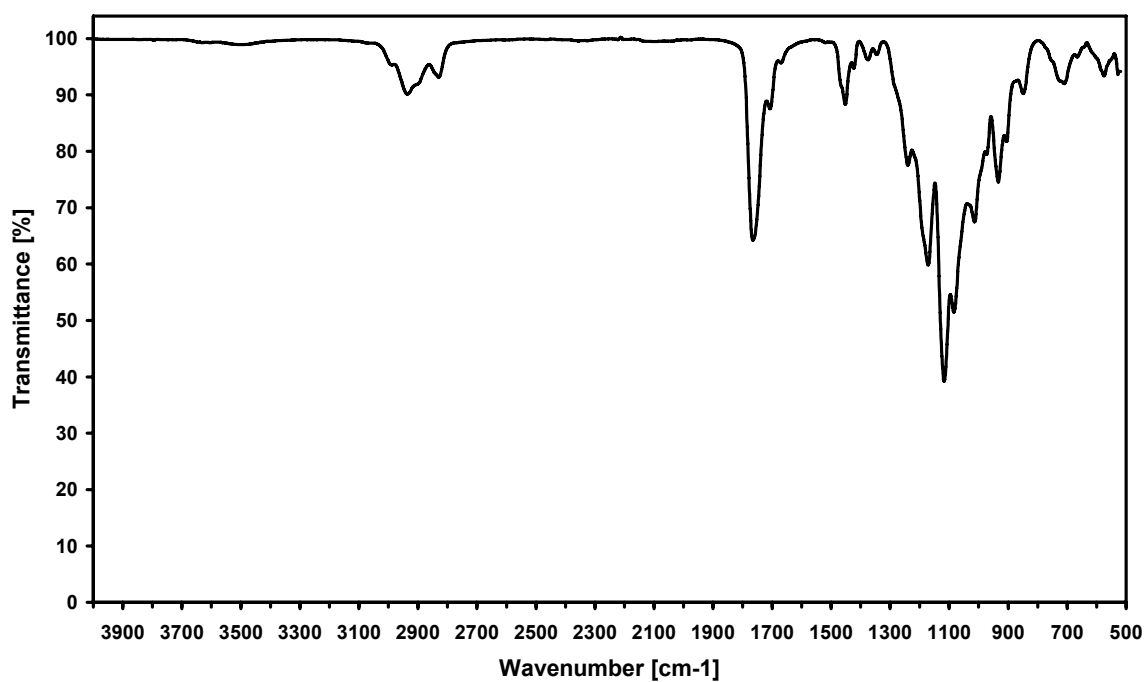


Fig. 10-4 ATR-IR spectrum of methoxyacetylated cellotetraose